THE UNIVERSITY
of EDINBURGH

White matter connectivity, cognition, symptoms and genetic risk factors in Schizophrenia

Clara Alloza Romero

Doctor of Philosophy

College of Medicine and Veterinary Medicine

The University of Edinburgh

2018

"Nothing describes the function of a neuron better than its connections"

Marsel Mesulam

Declaration and acknowledgements

I declare that this thesis is composed by myself and, except where otherwise stated, is entirely my own work. The presented work has not been submitted for any other degree or professional qualification. This thesis includes three published articles and as part of a larger research group, I have acknowledged in detail the contribution of myself and each co-author below:

Chapter 4: Alloza, C., Cox, S.R., Duff, B., Semple, S.I., Bastin, M.E., Whalley, H.C., Lawrie, S.M., 2016. Information processing speed mediates the relationship between white matter and general intelligence in schizophrenia. Psychiatry Res. 254, 26–33. https://doi.org/10.1016/j.pscychresns.2016.05.008

This study was conceived by CA, SRC, MEB, HCW and SML. CA processed and analysed the data and wrote the manuscript. SRC, MEB, HCW and SML were the main supervisors of this project. BD and SIS collected the cognitive and imaging data. All authors reviewed the manuscript for publication.

Chapter 5: Alloza, C., Bastin, M.E., Cox, S.R., Gibson, J., Duff, B., Semple, S.I., Whalley, H.C., Lawrie, S.M., 2017. Central and non-central networks, cognition, clinical symptoms, and polygenic risk scores in schizophrenia. Hum. Brain Mapp. https://doi.org/10.1002/hbm.23798

This study was conceived by CA, SRC, MEB, HCW and SML. CA analysed the data and wrote the manuscript. SRC, MEB, HCW and SML were the main supervisors of this project. MEB processed the imaging data. JG created the polygenic risk scores. BD and SIS collected the cognitive and imaging data. All authors reviewed the manuscript for publication.

Chapter 6: Alloza, C., Cox, S.R., Blesa Cábez, M., Redmond, P., Whalley, H.C., Ritchie, S.J., Muñoz Maniega, S., Del C Valdés Hernández, M., Tucker-Drob, E.M., Lawrie, S.M., Wardlaw, J.M., Deary, I.J., Bastin, M.E., 2018. Polygenic risk score for schizophrenia and structural brain connectivity in older age: A longitudinal connectome and tractography study. NeuroImage. https://doi.org/10.1016/j.neuroimage.2018.08.075

This study was conceived by CA, SRC and MEB. CA analysed the data and wrote the manuscript. SRC and MEB were the main supervisors of this project with co-supervision provided by HCW and SML. MEB, SMM and MDC processed the imaging data. SJR created the polygenic risk scores. PR provided all the data. MBC and EMT-D aided with the interpretation of the results. JMW and IJD are the Principal Investigators of this cohort. All authors reviewed the manuscript for publication.

Chapter 7: Alloza, C., Blesa Cábez, M., Bastin, M.E., Cox, S.R., Gibson, J., Whalley, H.C., Lawrie, S.M. Neurostructural properties of the salience network and polygenic risk scores for schizophrenia in UKBiobank (*in preparation*).

This study was conceived by CA, SRC and MEB. CA analysed the data and wrote the manuscript. SRC and MEB were the main supervisors of this project with co-supervision provided by HCW and SML. MBC aided with the imaging analysis. JG created the polygenic risk scores.

Abstract

Schizophrenia is a highly heritable complex neuropsychiatric disorder with a lifetime prevalence of around 1%. It is often characterised by impaired white matter structural dysconnectivity. In vivo and post-mortem alterations in white matter microstructure have been reported, along with differences in the topology of the structural connectome; overall these suggest a reduced communication between distal brain regions. Schizophrenia is characterised by persistent cognitive impairments that predate the occurrence of symptoms and have been shown to have a neural foundation reflecting aberrant brain connectivity. So far, 179 independent genome-wide significant single nucleotide polymorphisms (SNPs) have been associated with a diagnosis of schizophrenia. The high heritability and polygenicity of schizophrenia, white matter parameters and cognitive functions provides a great opportunity to investigate the potential relationships between them due to the genetic overlap shared among these factors.

This work investigates the psychopathology of schizophrenia from a neurobiological, psychological and genetic perspective. The datasets used here include data from the Scottish Family Mental Health (SFMH) study, the Lothian Birth Cohort 1936 (LBC1936) and UK Biobank. The main goal of this thesis was to study white matter microstructure in schizophrenia using diffusion MRI (dMRI) data. Our first aim was to examine whether processing speed mediated the association between white matter structure and general intelligence in patients diagnosed with schizophrenia in the SFMH study. Secondly, we investigated specific networks from the structural connectome and their topological properties in both healthy controls and patients diagnosed with schizophrenia in the SFMH study. These networks were studied alongside cognition, clinical symptoms and polygenic risk factor for schizophrenia (szPGRS). The third aim of this thesis was to study the effects of szPGRS on the longitudinal trajectories of white matter connectivity (measured using tractography and graph theory metrics) in the LBC1936 over a period of three-years. Finally, we derived the

salience network which has been previously associated with schizophrenia and examined the effect of szPGRS on the grey matter nodes associated with this network and their connecting white matter tracts in UK Biobank.

With regards to the first aim, we found that processing speed significantly mediates the association between a general factor of white matter structure and general intelligence in schizophrenia. These results suggest that, as in healthy controls, processing speed acts as a key cognitive resource facilitating higher order cognition by allowing multiple cognitive processes to be simultaneously available. Secondly, we found that several graph theory metrics were significantly impaired in patients diagnosed with schizophrenia compared with healthy controls. Moreover, these metrics were significantly associated with intelligence. There was a strong tendency towards significance for a correlation between intelligence and szPGRS that was significantly mediated by graph theory metrics in both healthy controls and schizophrenia patients of the SFMH study. These results are consistent with the hypothesis that intelligence deficits are associated with a genetic risk for schizophrenia, which is mediated via the disruption of distributed brain networks. In the LBC1936 we found that higher szPGRS showed significant associations with longitudinal increases in MD in several white matter tracts. Significant declines over time were observed in graph theory metrics. Overall these findings suggest that szPGRS confer risk for ageing-related degradation of some aspects of structural connectivity. Moreover, we found significant associations between higher szPGRS and decreases in cortical thickness, in particular, in a latent factor for cortical thickness of the salience network.

Taken together, our findings suggest that white matter connectivity plays a significant role in the disorder and its psychopathology. The computation of the structural connectome has improved our understanding of the topological characteristics of the brain's networks in schizophrenia and how it relates to the microstructural level. In particular, the data suggests

that white matter structure provides a neuroanatomical substrate for cognition and that structural connectivity mediates the relationship between szPGRS and intelligence. Additionally, these results suggest that szPGRS may have a role in age-related changes in brain structural connectivity, even among individuals who are not diagnosed with schizophrenia. Further work will be required to validate these results and will hopefully examine additional risk factors and biomarkers, with the ultimate aims of improving scientific knowledge about schizophrenia and conceivably of improving clinical practice.

Lay abstract

Schizophrenia is a devastating disorder and affects around 1% of the world's population. As schizophrenia is a complex and heterogeneous disease, and because its underlying causes remain relatively unknown, the development of more effective treatments is hindered. Currently, the treatment of schizophrenia is mostly symptomatic. Cognitive functions are persistently impaired in schizophrenia and usually appear before clinical symptoms. Cognitive functions are believed to be have a neural foundation, pointing towards impaired functional and structural brain connectivity in the disorder. It is well established that schizophrenia, brain connectivity and intelligence are very heritable; further, these factors share a genetic overlap between them, providing a great opportunity to investigate the potential associations between these factors.

This thesis examines structural imaging data from patients diagnosed with schizophrenia and healthy controls. We derived quantitative data from individual white matter tracts and computed networks describing the characteristics of the whole brain. Thus, the work presented here focuses on examining the relationships between brain connectivity, intelligence and genetic risk factors for schizophrenia. For instance, we found that processing speed, which describes how the brain receives and responds to information, mediates the association between white matter and intelligence, suggesting that processing speed has a key role in facilitating important cognitive abilities by allowing multiple processes to be simultaneously available. Moreover, we found that white matter connectivity supports the association between a genetic risk factor for schizophrenia and cognitive functions. We found that even among healthy participants, a higher genetic risk for schizophrenia has an adverse effect on brain connectivity over time.

Acknowledgements

This work has been supervised by Prof Stephen Lawrie, Dr Mark Bastin, Dr Simon Cox and Dr Heather Whalley, to whom I am most grateful for their support, advice and guidance during these years. Stephen, thank you for your trust, our heated discussions and your attempts to make me see the bright side of science when I most needed it. Mark, I am extremely indebted for your constant support, not only professional but also personally, and for all those debating hours of "muchos buenos" gastronomy, politics and brain networks. Simon, with your enthusiasm and thoroughness, you have made me aspire to be a better scientist and find every step of this project amusing, thanks maintain my inquiring spirit. Heather, thank you for your kindness, valuable discussions and suggestions during these years. Thanks to all my colleagues at Kennedy Tower for your company and laughs.

I would also like to thank my friends who have made these years so much better. From trips to the highlands to the pubs and from Scotland to Madrid; Ally, Manu, Sara, Irene, Mario, Maroto, Chiara, Daisy, Cal, Julius, Eleni, Mairi, Dave, Emily, Sanziana, Villarejo, Moya, Lara and to all the people that I have met during these years; I could not have been more delighted to have met all of you, thanks for all the adventures and for putting up with me during these years, specially Yassodara.

Finally, I would like to thank my family for their infinite love and understanding, without their support this work would have never been finished, I dedicate this thesis to them.

Table of Contents

Glossary

22q12DS	22q11.2 deletion syndrome
ATR	Anterior thalamic radiation
B-SNIP	Bipolar Schizophrenia Network on Intermediate Phenotypes
CAC	Caudal anterior cingulate
CHR	Clinical high risk
CNS	Central Nervous System
CSD	Constrained spherical deconvolution
CSF	Cerebrospinal fluid
dMRI	Diffusion MRI
DSI	Diffusion Spectrum Imaging
DSM	Diagnostic and Statistical Manual of Mental Disorders
DTI	Diffusion Tensor Imaging
DWI	Diffusion-weighted Imaging
FA	Fractional anisotropy
FEP	First episode of psychosis
fMRI	Functional MRI
g	General cognitive ability
gFA	General factor of fractional anisotropy
gMD	General factor of mean diffusivity
g_{speed}	General factor of processing speed
GWAS	Genome-wide association study
HARDI	High-angular resolution diffusion imaging
ICD	International Classification of Diseases and Related Health Problems
ILF	Inferior longitudinal fasciuli
IQ	Intelligence Quotient
LBC36	Lothian Birth Cohort 1936
MD	Mean diffusivity
MRI	Magnetic resonance imaging
MST	Minimum spanning tree
PANS	Positive and Negative Syndrome Scale
PCA	Principal Component Analysis
PGRS	Polygenic risk score
pve	Partial volume effect
QBI	Q-Ball Imaging
QSI	Q-Space Imaging
RD	Radial diffusivity
RF	Radio frequency
ROI	Region of interest
SANS	Scale for the Assessment of Negative Symptoms

SEM	Structural equation modelling
SFMH	Scottish Family Mental Health
SIFT	Spherical-deconvolution informed filtering of tractograms
SNP	Single nucleotide polymorphism
szPGRS	Polygenic risk score for schizophrenia
TBSS	Tract-based Spatial Statistics
VBA	Voxel based analysis

Chapter 1 Schizophrenia

1.1. Introduction

Schizophrenia is a highly heritable and complex neuropsychiatric disorder with a lifetime prevalence around 1%. It is positioned as one of the leading causes of disability worldwide and its morbidity and mortality rates are noteworthy (Gurung and Prata, 2015). The onset generally manifests during adolescence or early adulthood, and its symptoms are usually chronic and devastating. In general, the understanding of a disease and its corresponding diagnosis is based on the identification of aetiological factors (such as genetic and environmental risks) and pathogenesis (the mechanisms by which the etiologic agents produce the disorder). However, the aetiology and pathogenesis of most psychiatric disorders have not yet been determined and therefore, the diagnosis still relies on the patient's description of symptoms and the examiner's observations. Schizophrenia has a multiple and varied phenotypic expression which hinders an adequate definition; thus, the lack of appropriate clinical descriptions that relate to the underlying pathophysiology impedes an improved treatment or prognosis for the patients. Thus, increasing effort is being directed to define an adequate biological construct of schizophrenia. Moreover, the disorder is characterized by severe neurocognitive impairments that precede the onset of positive and negative symptoms. The cognitive deficits have been suggested to reflect both general intellectual decline and domain-specific impairments (Ahmed and Bhat, 2014). Cognitive impairments have a neural foundation, suggesting that they may reflect structural and functional abnormalities in connectivity and neurotransmission; with increasing evidence proposing that cognitive impairments contribute to symptom severity, relapse, and disability (Chen et al., 2005; Lipkovich et al., 2009), clinical research has focused on improving neurocognition from pharmacological, therapeutic and brain stimulation perspectives. Therefore, schizophrenia can be recognised and diagnosed with much agreement; however, its aetiology and pathophysiology are yet uncertain. With progress in the fields of genetics

and neuroimaging, it should eventually be possible to diagnose schizophrenia objectively and validly.

1.2. General overview

Emil Kraepelin (1919-1971) was the first clinician to comprehensively study schizophrenia and termed the disorder *dementia praecox,* describing the disorder as "a series of states, the common characteristic of which is a peculiar destruction of the internal connection of the psychic personality" (Kraepelin and Robertson, 1919). This terminology refers to its early onset ("praecox") and the severe cognitive and behavioural decline described in the patients ("dementia"); stressing also the importance of the chronicity and poor outcome as the defining characteristics of the disorder. Moreover, Kraepelin distinguished schizophrenia from manic depression as two forms of psychosis and contributed to the development of a mental illness classification guideline.

The work of the psychiatrist Bleuler (1911-1950) was complementary to Kraepelin, integrating the symptomatology and signs found in his patients. Due to the intrinsic heterogeneity of the disorder, he conceptualized schizophrenia as "the group of schizophrenias". For Bleuler, the core aspect of the disorder was the presence of a fragmentation of thought, which he referred to as a "loosening of associations". It was he who termed the disorder as we currently know, "schizophrenia", deriving the concept from the Greek verb *schizein* to the split ("schizo") of the mind ("phrene"). Bleuler was the first clinician to introduce the classification of symptomatology into primary and secondary symptoms, suggesting that the four fundamental symptoms of schizophrenia included associational disturbances, ambivalence, affective disturbances, and autistic behaviour (now considered negative symptoms), whereas hallucinations and delusions were classified as secondary (or accessory) symptoms of the disorder.

Another great contribution to the understanding of schizophrenia came from the work of Kurt Schneider (Schneider, 1959), who attempted to identify specific features that were characteristic of schizophrenia. He emphasised diagnostically discriminating symptoms that could be observed and be present enough to be useful to classify different diagnoses. He identified certain delusional and hallucinatory symptoms that he believed were exclusive of schizophrenia, such as thought insertion, voices in third person, thought broadcasting, etc., while the rest of hallucinations and delusions were present in a broader range of psychotic disorders. Schneider's work has been very influential at the level of diagnosis as his conceptualizations were incorporated in structured interviews and diagnostic algorithms.

1.3. Diagnosis and clinical description

The work of Kraepelin, Bleuer, and Schneider have been the foundation of our current conceptualization of schizophrenia, establishing the importance of first-rank symptoms which now have been found to best describe the positive symptoms in schizophrenia (Schneider, 1959). Nowadays, the diagnosis of schizophrenia is generally obtained through a structured interview and meeting the criteria of the Diagnostic and Statistical Manual of Mental Disorders (DSM-I, DSM-II, DSM-III, DSM-III-R, DSM-IV, DSM-IV-TR and DSM-V; American Psychiatric Association, 1952, 1968, 1980, 1987, 1994, 2000, 2013) or the International Classification of Diseases and Related Health Problems (ICD), established by the World Health Organization (WHO, 1994). For instance, the DSM diagnostic criteria across editions is based on three principals resulting from the early work on schizophrenia. Three main roots are reflected in DSM: (1) Kraepelin's work on avolition, chronicity, and poor outcome (Kraepelin, 1971), (2) Bleuler's view on the relevance of negative symptoms and dissociative pathology (Bleuler, 1950), and (3) Schneider's focus on positive symptoms (Schneider, 1959).

Characteristic symptoms of schizophrenia include a range of cognitive, behavioural, and emotional impairments; however, no single symptom is pathognomonic of the disorder. The adequate diagnosis involves the recognition of a variety of signs and symptoms associated with occupational or social functioning. Prodromal symptoms often precede the active phase and subthreshold symptoms may be observable in the residual phase. Negative symptoms are frequently described in the prodromal and residual phases and can be severe. Lack of social interactions may occur also in the prodromal phase and be an indication of the development of the disorder. Psychotic symptoms tend to decrease over the life course, likely to be associated with reduced dopamine activity with age. On the other hand, negative symptoms are more closely related to prognosis and tend to be more persistent. Additionally, cognitive impairments may not improve over the course of the disorder. Figure 1 represents the clinical and pathophysiological course of schizophrenia.

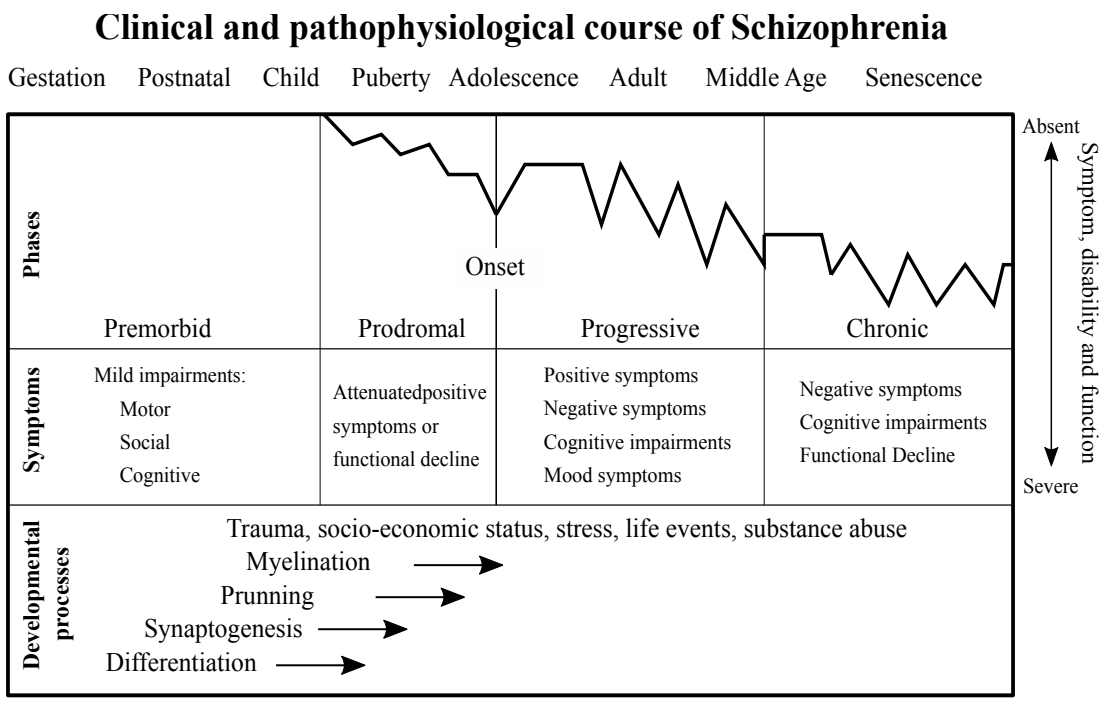

Figure 1 Clinical and pathophysiological course of schizophrenia. Adapted from Lieberman et al. 2001 and Tandon et al. 2008.

There are five symptomatic domains characteristic of psychotic disorders: delusions, hallucinations, disorganised thinking, abnormal motor behaviour (including catatonia), and negative symptoms. Delusions are fixed beliefs that are not responsive to change even with conflicting evidence against them. Their subject may include different themes, such as persecutory, somatic, grandiose, etc., and they can be classified as bizarre or non-bizarre depending on the understanding by same-culture peers. Hallucinations are perception-like experiences that appear without an external stimulus. They can occur in any sensory modality; however, auditory hallucinations are the most prevalent in the disorder. They can appear as voices and are perceived differently from the individual's own thoughts. Disorganised thinking is usually inferred from the individual's speech; it can be presented as constant changes of topic, answers tangentially related or completely unrelated to the question, and sometimes speech may be severe enough to be completely incomprehensible. Abnormal motor behaviour can range from child-like behaviours to erratic agitation. This also includes catatonic behaviour, where the patient presents a decrease in reactivity to the environment. Negative symptoms account for a great portion of morbidity in schizophrenia. Diminished emotional expression and avolition are the most prominent negative symptoms found in the disorder. Diminished emotional expression includes reductions of facial expressions, eye contact, body movements, etc. Avolition refers to a decrease in self-motivation activities. Other negative symptoms comprise alogia (diminished speech output), anhedonia (decreased ability to experience pleasure or positive stimuli), and asociality (lack of interest in social interactions).

1.3.1. Diagnostic tools

Both the DSM-V and ICD-10 classifications are the result of clinical observation and scientific research providing a reliable diagnosis of schizophrenia. Tables 1 and 2 provide a summary of the criteria needed for the diagnosis. The DSM and ICD are intentionally different

in purpose, use, and function. ICD is a nomenclature that is used by different professionals, not only in the clinical practice. For that reason, its format is easier to use, less detailed, and more useful in a practical manner. On the other hand, DSM was designed to cover scientific and academic challenges and for clinical professionals. Therefore its contents and diagnostic assessments are more comprehensive (Biedermann and Fleischhacker, 2016). Furthermore, both criteria require that other diagnoses should be first ruled out: mood disorders with psychotic symptoms, schizoaffective disorders, and drug-induced psychoses. Despite their discrepancies, DSM and ICD are sufficiently similar in order to promote cross-site validity.

Despite the apparent reliability of diagnosis, schizophrenia manifests itself with a highly complex and heterogeneous profile with most of its core characteristics being inferential and where subjective experiences play a significant role. Additionally, patients usually manifest other psychiatric comorbidities, varied longitudinal course, and difficulties adhering to treatment. A number of studies have begun to examine social, cultural, and demographic differences in the pathogenesis of psychotic symptoms and conceptualization of the disorder (Bauer et al., 2011; Pérez-Álvarez, 2012).

Table 1 DSM V

Criterion A. Two (or more of the following), each present for a significant period of time during a 1-month period (or less if successfully treated). At least one of these should include 1-3. 1. Delusions 2. Hallucinations 3. Disorganised speech 4. Grossly disorganized or catatonic behaviour 5. Negative symptoms, e.g. avolition, alogia, diminished emotional expression Criterion B. Social/ Occupational Dysfunction Criterion C. Duration of at least six months, with at least one month of active symptoms.

Table 2 ICD 10

Either *at least one* of the syndromes, symptoms, and signs listed under (1) below, *or* at least two of the symptoms and signs listed under (2) should be present for most of the time during an episode of psychotic illness lasting for at least 1 month (or at some time during most of the days).

(1) At least one of the following must be present:

(a) thought echo, thought insertion or withdrawal, or thought broadcasting;

(b) delusions of control, influence, or passivity, clearly referred to body or limb movements or specific thoughts, actions, or sensations; delusional perception;

(c) hallucinatory voices giving a running commentary on the patient's behavior, or discussing the patient among themselves, or other types of hallucinatory voices coming from some part of the body;

(d) persistent delusions of other kinds that are culturally inappropriate and completely impossible (e.g., being able to control the weather, or being in communication with aliens from another world).

(2) *Or* at least two of the following:

(a) persistent hallucinations in any modality, when occurring every day for at least 1 month, when accompanied by delusions (which may be fleeting or half-formed) without clear affective content, or when accompanied by persistent overvalued ideas;

(b) neologisms, breaks, or interpolations in the train of thought, resulting in incoherence or irrelevant speech;

(c) catatonic behavior, such as excitement, posturing or waxy flexibility, negativism, mutism, and stupor;

(d) negative symptoms, such as marked apathy, paucity of speech, and blunting or incongruity of emotional responses (it must be clear that these are not due to depression or to neuroleptic medication).

1.4. Cognitive impairments

In recent years, the study of cognitive deficits in schizophrenia and their neural foundation has gained much attention, as they are essential predictors of impairments in functional domains and potential therapeutic targets. Historically, cognitive deficits were thought to be present exclusively in older patients diagnosed with schizophrenia. However, this conceptualization has been challenged as it has become evident that cognitive deficits are present and often precede the onset of the disorder. Many attempts have been made to elucidate the prevalence, degree, and nature of these impairments. It has been suggested that cognitive deficits may be independent of the long-term course of symptoms and contribute to relapses and remissions (Falkai et al., 2015). Thus, understanding the underlying process is essential to provide a better treatment and improve the outcome of patients.

One of the biggest meta-analyses carried out to investigate the cognitive impairments in schizophrenia was conducted by Heinrichs and Zakzanis (1998). Their dataset comprised 204 studies, consisting of 7420 patients with schizophrenia and 5865 controls. Effect sizes were obtained for several neurocognitive tests which included domains of memory, motor, attention, general intelligence, spatial ability, executive, and language functions. The greatest impairment was observed in global verbal memory. However, as multiple specific domains were significantly impaired, this may reflect a widespread reduction in general cognitive functioning. As reviewed in O'Carroll (2000), several studies found evidence indicating that clinical features and cognitive deficits may have a different underlying pathophysiology. For instance, Goldberg et al. (1993) showed a symptomatic improvement in patients with schizophrenia using clozapine that was not accompanied by an improvement in cognitive functions, suggesting that certain cognitive functions may be independent of psychotic symptoms and enduring features of schizophrenia.

There are several lines of thought regarding the course of cognitive impairments in the disorder. The term 'dementia praecox' was termed to highlight the continuing cognitive decline observed in patients. Nonetheless, as previously mentioned, recent studies on prodromal phases and clinical high risk have garnered more support for the idea that cognitive decline predates the onset of the illness (Bora et al., 2014; Erlenmeyer-Kimling et al., 2000; Gottesman and Erlenmeyer-Kimling, 2001). This is in line with recent studies reporting the high hereditability and polygenicity of intelligence (Davies et al., 2011). In general, cognitive deficits are stable across time; however, recent evidence has suggested that these deficits may not follow a normal pattern of age-related decline in the disorder (Bora and Murray, 2014). A longitudinal study investigated the rate of decline using the Mini-Mental State Examination (MMSE), which measures cognitive impairment, in a dataset that comprised 107 institutionalised patients with schizophrenia (aged 25-80 years) and 132 healthy controls (aged 50-80 years) (Friedman et al., 2001). They concluded that the greatest rate in cognitive decline was observed in the subgroup aged above 65, with the greatest decline at that age. Two main conclusions can be drawn from the numerous studies carried out: first, that there are two key points where cognitive decline is greatest, around the first psychotic episode and around 65 years old, and second, that these two points may be the most suitable for cognitive rehabilitation (Bora et al., 2014).

Specific cognitive domains have been associated with the disorder, such as attention, working memory, learning, memory, and executive function (Elvevåg and Goldberg, 2000). On average, the Intelligence Quotient (IQ) scores for schizophrenia patients are one standard deviation below healthy controls with an overlap of distribution of scores of 41.1% (Burdick et al., 2009). First episode patients also show early cognitive deficits, suggesting that this impairment is not entirely dependent on symptoms or medication, but possibly an endophenotype of the disorder. As suggested above, intelligence deficits are found in the premorbid period before psychotic symptoms appear (Woodberry et al., 2008). However, not

all the patients present significant cognitive impairments when compared to controls. In this line, it has been proposed that these patients may not show significant reductions in cognitive performance but may have suffered decrement when compared with their own premorbid level (Keefe et al., 2005; Reichenberg et al., 2009). The implications of impaired cognitive functions for these patients are tremendous, hindering an optimal adaptation in life by having consequences in functional social problem solving, social skill acquisition, etc. (Green, 1996). Consequently, neurocognition has become a fundamental target for treatment of schizophrenia.

1.5. Genetic risk factors

It is well established that genetic predisposition is a major risk factor for developing schizophrenia. Familial, adoption and twin studies have contributed greatly to the understanding of genetic risk factors in the disorder (see Figure 2). Several adoption studies examined the risk for schizophrenia in offspring of parents with schizophrenia adopted by healthy parents and healthy offspring adopted by parents with schizophrenia. Results showed that there was an increased risk for schizophrenia that was related to the presence of the disorder in the biological parents (Heston, 1966; Kety et al., 1976). Twin studies have been useful to calculate the heritability of schizophrenia, which measures how much variation in phenotypic expression can be attributable to genetic variation in the same population. It has been estimated that genetic effects and its interactions with environmental factors contribute to around 80% of the liability for schizophrenia (Cannon et al., 1998; Cardno et al., 1999; Sullivan et al., 2003). Monozygotic twin studies have shown an increase of at least three-fold more concordance for the disorder compared to dizygotic twins (Gottesman and Shields, 1976; Sullivan et al., 2003). Dizygotic studies showed that if one twin develops schizophrenia, the other has a risk of between 10-15%, very similar to that found in siblings. However,

monozygotic twins show a greater risk of about 40-50% if one of the twins presents the disorder (Tandon et al., 2008).

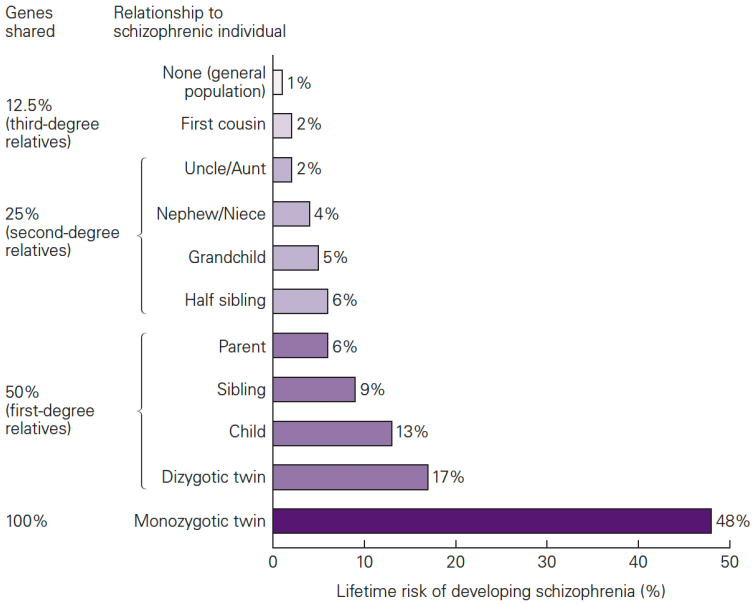

Figure 2 Lifetime risk for developing schizophrenia as a function of genetic relatedness to a patient diagnosed with schizophrenia. Note that the risk increases with increasing relatedness. However, variation within categories may be caused by epigenetic effects or mutations. Reproduced from Gottesman (1991) and Schwartz et al. (2013).

Several chromosomal regions have been associated with the disorder; however, no single gene variation has been consistently shown to increase the likelihood of developing schizophrenia (Tandon et al., 2008). In the last years, large-scale genomic studies have contributed to the discovery of specific DNA variants and several risk alleles to the disorder. The latest schizophrenia genome-wide association study (GWAS) – which included a meta-analysis with 40675 cases and 64643 controls – identified 179 schizophrenia-associated genetic loci that were enriched among genes expressed in the brain and tissues involved in the immune system (Pardiñas et al., 2018; Schizophrenia Working Group of the Psychiatric Genomics Consortium, 2014), determining that schizophrenia is highly polygenic. This study also highlighted that the distribution of associations was not random, but specific to genes that

were expressed in certain tissues and cellular types that may potentially serve as therapeutic targets.

Based on this aspect of high polygenicity, Sullivan (2012) proposed that the most parsimonious way of integrating this aspect is considering schizophrenia as a pathway disease, where variation in one or several genetic pathways contribute to the risk of the disorder. As genetic studies have already shown, reductionist approaches that focus on a single gene variant and usually are not able to integrate all the features of schizophrenia. However, an approach based on the combination of hundreds of genes and their interactions may be able to better capture the nature of the disorder. Moreover, the genetic risk for schizophrenia seems to be highly pleiotropic, referring to the mechanism where one gene or allele can affect multiple phenotypic traits that appear unrelated. In the case of psychiatric disorders, for instance, schizophrenia and bipolar disorder share some risk factors. In this conceptualization of schizophrenia as a pathway disorder, disruption of a genetic node in a pathway may result in a different clinical expression rather than a gradual presentation of schizophrenia.

Therefore, we can conclude that schizophrenia is a highly heritable disorder, characterised not only by putative genetic variations but by a more segregated expression of hundreds of genes that ultimately contribute to the risk for the disorder. However, the development of schizophrenia is not exclusively the result of genetic risk factors but of the interactions between genetic and environmental risk factors, such as migration, urbanicity, gender, and trauma.

1.6. Neurobiology of white matter

Human white matter accounts for approximately 40% of Central Nervous System (CNS) tissue (Morell and Norton, 1980). In the mammalian CNS, neurons only represent 10% of the total number of cells, while astrocytes, microglia, and oligodendrocytes account for most of

the remaining 90%. Oligodendrocytes, a type of glial cell, arise in the late stages of development once most neurons have appeared, upon which they migrate towards the grey and white matter and subsequently differentiate into myelin-forming cells. Oligodendrocytes form the myelin sheath that insulates the axons, enhancing signal conduction, and their damage can potentially impair sensory, motor, and cognitive functions. The diameter of the axon and the thickness of the myelin sheath are therefore proportionally related to conduction velocity along the axon. The other type of glial cells found in the white matter, the astrocytes, have numerous functions relating to insulation, signalling regulation, and nourishment of neurons. Although glial cells are not directly involved in the generation of action potentials, it has been shown that they participate in neuro-glial signalling processes. The microstructure heterogeneity in the white matter is evident: axons of different diameters, glial cells of different shapes and sizes, and irregular distribution of extra-cellular space all contribute to the different biophysical properties of the white matter. Figure 3 shows a representation of the principal glial cells.

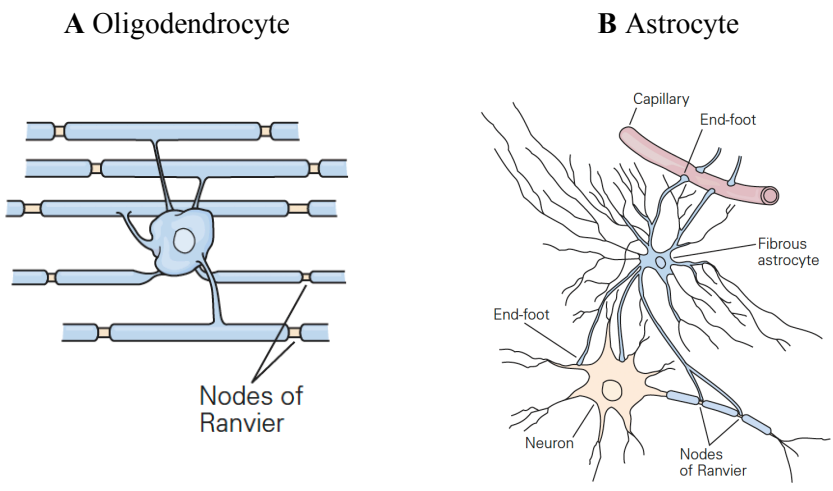

Figure 3 Principal types of glial cells in the Central Nervous System. Adapted from Alberts et al. (2002) and Schwartz et al. (2013).

A surprisingly diverse number of psychiatric and nervous system diseases are linked to abnormalities in white matter or in myelin genes. Polymorphisms for several myelin genes have been discovered as risk factors for schizophrenia, depression, and obsessive-compulsive disorder, suggesting that white matter deficiencies are a contributing cause for many psychiatric diseases (reviewed in Fields, 2008). Even though abnormalities at the synapse level are the cellular basis for most psychiatric disorders, impaired communication between distant brain regions can affect numerous neurological processes. It has been suggested that impaired cognitive abilities, mood changes, hallucinations, and disorganised thinking which accompany many neuropsychiatric disorders may be the result of desynchronised brain connectivity. Evidence from neuroimaging studies, similarities with demyelinating diseases (such as metachromatic leukodystrophy and multiple sclerosis), age-related changes in white matter, abnormalities in myelin-related genes, and morphologic abnormalities in oligodendroglia have now converged to support the implication of white matter in schizophrenia (Davis et al., 2003).

1.7. The dysconnection hypothesis

Cognitive functions and their underlying neurodynamics have been studied from two different perspectives: to consider the brain as a set of segregated areas, each of them serving a specific function, or to consider cognitive functions the result of the integration between distant brain regions. The former perspective was first proposed by Wernicke (1906), who postulated that psychoses were the result of the anatomical disruption of association fibres. In addition, Bleuer's *disintegration of the psyche* (Bob and Mashour, 2011) suggested that the phenomenal aspects of dissociation and disintegration of the consciousness may be related to an underlying impaired neural integration and a disruption in brain's connectivity. Taken all together, these perspectives provide complementary evidence to support the conceptualization of schizophrenia as a failure in brain's integration. Therefore, the difficulty of understanding

schizophrenia as a circumscribed brain deficit, accompanied by the evidence that supports the existence of impairments in brain connectivity, indicates that the integrative perspective may be able to better encapsulate the heterogeneous and complex presentation of the disorder.

For instance, hallucinations and delusions can be better explained as a result of impaired brain integration rather than as a deficit in a specific brain region. Moreover, abnormal integration of prefrontal neural activity in subcortical, limbic, and temporal brain regions have been consistently described in the disorder (Friston and Frith, 1995). Overall, the dysconnection hypothesis suggests that schizophrenia may be understood in terms of cognition and pathophysiology as a brain integration failure (Friston, 1998).

1.8. Aims and outline of the thesis

This work investigates the psychopathology of schizophrenia from a neurobiological, psychological, and genetic perspective. The second chapter is dedicated to white matter imaging and it captures both Magnetic Resonance Imaging (MRI) – in particular, Diffusion Tensor Imaging (DTI) – and the structural connectome. Chapter 3 summarises main findings of white matter connectivity in schizophrenia and its associations with symptoms, cognitive functions, and genetic risk factors, and provides a brief discussion on accelerated white matter ageing in the disorder. Chapters 4, 5, 6 and 7 present the results from the different projects undertaken; each of these chapters is briefly introduced and discussed. The datasets used here include data from the Scottish Family Mental Health (SFMH) study, the Lothian Birth Cohort 1936 (LBC1936), and UK Biobank. The main goal of this thesis was to study white matter microstructure in schizophrenia using diffusion MRI (dMRI) data. Our first aim was to examine whether processing speed mediated the association between white matter structure and general intelligence in patients diagnosed with schizophrenia in the SFMH study. Secondly, we investigated specific networks from the structural connectome and their

topological properties in both healthy controls and patients diagnosed with schizophrenia in the SFMH study. These networks were studied alongside cognition, clinical symptoms and polygenic risk factor for schizophrenia (szPGRS). The third aim of this thesis was to study the effects of szPGRS on the longitudinal trajectories of white matter connectivity (measured using tractography and graph theory metrics) in the LBC1936 over a period of three-years. Finally, we derived the salience network which has been previously associated with schizophrenia and examined the effect of szPGRS over the nodes and edges involved in this network using data from UK Biobank. Chapter 8 comprises an overall summary of the main findings presented in this thesis and a general discussion of limitations and considerations for future work.

Chapter 2 Magnetic resonance imaging

2.1 Introduction

Recent advancements in neuroimaging have enable scientists the possibility of observing the human brain *in vivo* and develop methods to study its function and structure. This work aimed to study the water diffusion parameters in white matter and organizational properties of brain's networks. Therefore, in this chapter, I will describe the basics of Magnetic resonance imaging (MRI) with particular interest on diffusion MRI (dMRI) and the tensor fitting model, discussing it strengths and limitations in the context of this work. Finally, this chapter is dedicated to the description of the connectome, graph theory metrics, and network thresholding options.

2.2 Magnetic Resonance Imaging

Magnetic resonance imaging (MRI) uses the magnetic properties of the hydrogen atom to produce comprehensive images of internal body structures and other tissues. The hydrogen nucleus is used due to its abundance in water and fat. Under normal circumstances, the hydrogen protons spin with their axes randomly aligned. However, when the body is placed under a static magnetic field (B_0), the proton's axes are aligned parallel or anti-parallel to the direction of the magnetic field and rotate along the axis. The quality of the images is dependent on the strength of the magnetic field and currently it can range from 0.5 to 7 Tesla. When additional energy in the form of radio frequency (RF) is introduced, protons are excited and jump to a higher energy state (anti-parallel to B_0) and the magnetic vector (sum of proton spin axes) is deflected. When the RF is switched off, the protons release their previously absorbed energy and the magnetic vector returns to its resting state (relaxation phase), causing a signal to be emitted. Two relaxation times can be measured: the first is the time taken for the magnetic vector to return to its resting state (T1) and the second for the axial spin to return to its resting state (T2*).

The construction of contrast images is based on the differing T1 and T2* relaxation properties of different brain tissues. In most structural MRI studies, a T1 contrast is used to obtain the images, while a T2* contrast is used for functional MRI. For a more thorough description of MRI one can refer to Hashemi et al. (2004). The work presented in this thesis will focus on structural MRI, specifically in diffusion MRI (dMRI).

Since the introduction of MRI, fMRI has been widely used, partly due to the numerous advantages it offers regarding studies relating behavior and function. Most typically, the method applied is based on Blood Oxygenation Level-dependence (BOLD). It is based on the magnetic susceptibilities of deoxyhemoglobin; when the brain is activated under a task, there is a net increase in signal intensity, which is attributed to a greater increase in regional oxygenated blood flow that exceeds regional oxygen consumption. Although the implications derived from fMRI studies have been of great interest in the field, it is out of the scope of this thesis to comprehensibly review all fMRI literature. Therefore, I will highlight the importance of such studies only in relation to schizophrenia. There have been numerous fMRI studies in schizophrenia, with results suggesting impaired brain activity in dorsal and ventral prefrontal, anterior cingulate and posterior cortical regions (Minzenberg et al., 2009); and across several cognitive tasks: motor, working memory, attention, word fluency, emotion processing, and decision making (reviewed in Gur and Gur, 2010). However, much inconsistency is observed in the literature, with studies reporting increases in functional connectivity within the default mode network (Whitfield-Gabrieli et al., 2009) while others finding both impairments and mixed connectivity between nodes of this network (for a review see Fornito et al., 2012). More support for the hypothesis of impaired functional connectivity in schizophrenia comes from resting state fMRI studies (Fornito and Bullmore, 2010; Jafri et al., 2008; Lynall et al., 2010; Salvador et al., 2010), defined as the statistical correlation between spatially distributed neurophysiological time-series (Friston, 1994). For instance, Damaraju et al., (2014) showed that during resting state, patients with schizophrenia showed hypoconnectivity within sensory

regions (auditory, motor and visual) and hyperconnectivity between the thalamus and these sensory regions. Taken together, fMRI studies offer valuable information about the relationship between brain and behaviour; however, as with any MRI modality, much inconsistency is found in the literature, probably indicating the use of different methodological techniques and heterogeneity of the disease.

2.3. Diffusion MRI

Diffusion MRI (dMRI, Johansen-Berg and Behrens, 2009; Jones, 2011; Le Bihan et al., 2006, 1986) is currently the only technique capable of mapping *in vivo* fibre architecture of tissue – such as nervous and muscle tissue, hence triggering enormous interest in the medical field. Ultimately, dMRI measures the dephasing of water proton spins due to diffusion when a strong magnetic field is applied. The longer the protons are allowed to diffuse ("diffusion time") and the higher the displacement per unit time, the more molecules will be displaced from their origin with different phase shifts. This dispersion leads to a loss of signal amplitude or signal attenuation. The portion of dephasing – resulting from the protons' motion – can be derived by comparing the signal amplitude with and without the diffusion gradient applied. Therefore, signal attenuation reflects generally the mobility of water molecules depending on temperature, viscosity, the presence of other molecules, and other factors (Jones et al., 2013). However, it is also dependent on biological microstructures, *e.g.* cell membranes, myelin sheaths, and microtubules (Beaulieu, 2002). Therefore, dMRI measures the amount of restriction experienced by water molecules moving along the axis of the gradient applied and averaged over the voxel. One of the several functionalities of dMRI is the ability to study the microstructural properties of tissues.

2.3.1. Diffusion Tensor Imaging

In this thesis, dMRI data were modelled using the diffusion tensor. While dMRI refers to the contrast of acquired images, Diffusion Tensor Imaging (DTI) is one of the methods to model dMRI data. The diffusion of water molecules in biological environments is characterised by Brownian motion. If diffusion is not hindered, the position of each water molecule will be random and describe a Gaussian distribution over time (Pfefferbaum et al., 2000). White matter tracts consist of densely packed axons, different types of neuroglia, and other cells (Mori and van Zijl, 2002). The brain's white matter is highly organised into discrete fibre bundles that have a complex geometry in the brain. Therefore, diffusion of water molecules in white matter tracts is hindered, restricting the movement across the long axis of axons. The degree of restriction in diffusion is called anisotropy. As shown by Basser et al. (1994a) the outcomes obtained from DTI not only provide measures of diffusion anisotropy, but also the predominant direction of water molecules in each voxel (Mori and van Zijl, 2002).

The introduction of DTI allowed the non-invasive indirect study of the degree of anisotropy and structural orientation of white matter tracts (Basser et al., 1994a, 1994b; Pierpaoli et al., 1996). Based on the assumption that water diffusion in white matter is hindered along the axon resulting in higher anisotropy than in grey matter or in cerebral-spinal fluid (CSF); Basser et al. (1994b, 1994a) modelled the diffusion process as an ellipsoid which mathematically can be represented as a 3x3 symmetric matrix or tensor:

$$g = \begin{bmatrix} g_x \\ g_y \\ g_z \end{bmatrix} \qquad D = \begin{bmatrix} D_{xx} & D_{xy} & D_{xz} \\ D_{xy} & D_{yy} & D_{yz} \\ D_{xz} & D_{yz} & D_{zz} \end{bmatrix}$$

where the vector g is the applied gradient and D the apparent diffusion tensor. The diagonal elements of D (D_{xx}, D_{yy} and D_{zz}) represent the diffusion along those directions, while the off-

diagonal elements represent the covariance between each pair of axes. The process of eigen-decomposition of the tensor provides the *eigenvectors* (ε_1, ε_2, ε_3) and *eigenvalues* (λ_1, λ_2, λ_3). Both *eigenvectors* and *eigenvalues* are paired in what are called *eigenpairs*, so that ε_1 is paired with λ_1. The eigenvalue (e.g., λ_2) represents the diffusion value of the tensor in the direction of the corresponding eigenvector (e.g., ε_2). The eigenvector ε_1 that is associated with the largest eigenvalue is also designed as the principal eigenvector and indicates the predominant orientation of the axon, while its associated eigenvalue (λ_1) denotes the maximum value of diffusion. Figure 4 represents different diffusion cases and their associated ellipsoid models and eigenvalues.

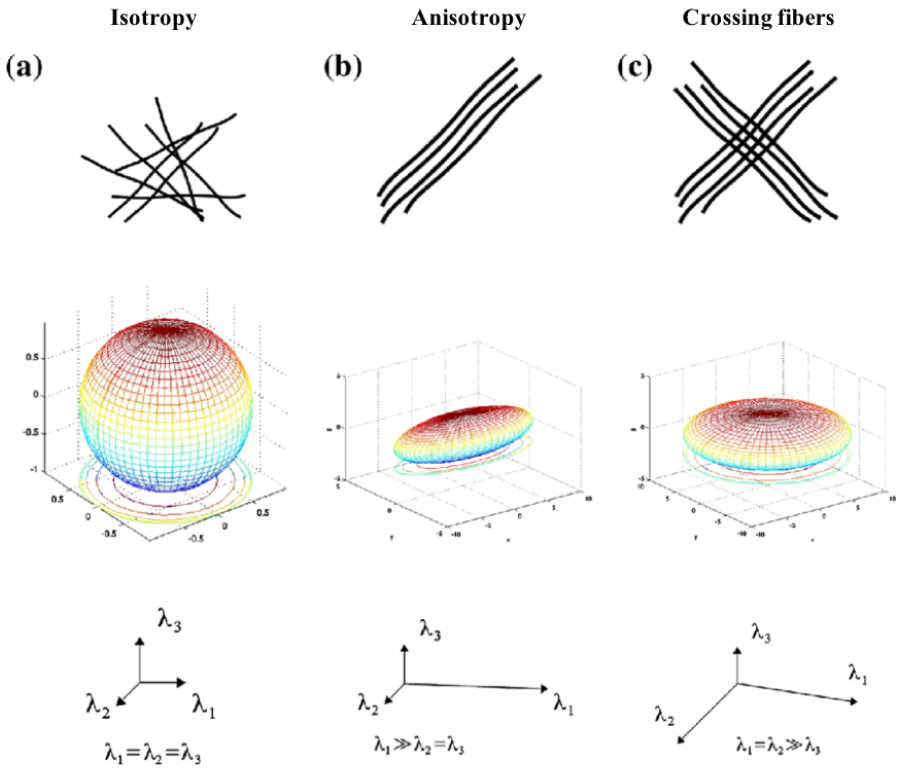

Figure 4 This figure represents tissue architecture (top row), ellipsoid models (medium row) and associated eigenvalues (bottom row). Figure A) represents an isotropic case, where water diffusion is not hindered and describes a Gaussian function over time, its associated diffusion

ellipsoid is spherical, and its eigenvalues are of equal order. B) Highly anisotropic case, where diffusion is restricted along the long axis, represented by an ellipsoid with a principal eigenvalue indicating main direction of diffusion. C) Two crossing fibres, two main directions of diffusion are present and therefore two leading eigenvalues, this case is particularly difficult to model using DTI as it can only represent a single fibre population. Figure adapted from Engwer et al. (2015).

Common quantitative measures that are obtained from DTI include fractional anisotropy (FA), mean diffusivity (MD), and radial and axial diffusivity (RD, AD), which are calculated in each voxel and can be sensitive to different tissue properties, such as axonal ordering and density, degree of myelination, etc., without being specific to any of them (Basser et al., 1994a; Jones et al., 2013; Song et al., 2002).

FA estimates the degree of anisotropy of a diffusion process and can vary between 0 (isotropic diffusion) and 1 (anisotropic diffusion):

$$FA = \sqrt{\frac{3}{2}} \frac{\sqrt{(\lambda_1 - \overline{\lambda})^2 + (\lambda_2 - \overline{\lambda})^2 + (\lambda_3 - \overline{\lambda})^2}}{\sqrt{\lambda_1^2 + \lambda_2^2 + \lambda_3^2}}$$

where $\bar{\lambda}$ is the average between the three eigenvalues.

On the other hand, MD is a scalar measure that estimates the average diffusion within a specific voxel:

$$MD = \frac{\lambda_1 + \lambda_2 + \lambda_3}{3}$$

AD corresponds to the diffusion in the first eigenvalue and RD to the average between the second and third eigenvalues. RD is a measure that represents the perpendicular diffusion to the principal diffusivity direction.

Changes in these estimates, specifically increases in MD and decreases in FA, are usually interpreted as deficits in the microstructure of white matter tracts.

2.3.2. Neurobiological interpretation of diffusion parameters

Several attempts have been made to study the relationship between dMRI parameters and their biological interpretation within white matter microstructure. Discrete associations have been reported; for instance, FA has been linked to axonal loss after stroke (Pierpaoli et al., 2001), and MD with tissue cellularity in a brain tumour patient (Gauvain et al., 2001). However, none of the dMRI parameters are a direct measure of white matter compartments and are highly influenced by a number of factors (Wozniak and Lim, 2006). The presence of macromolecules, cellular membranes, organelles, degree of myelination, internal axonal structure, axon packing, membrane permeability, and tissue water content may also affect the quantification of microstructural properties. The degree of anisotropy has often been associated with axon count and density while the degree of myelination has been linked with FA (Beaulieu, 2011). However, FA does not determine tissue anisotropy as it has also been shown in non-myelinated axons (Hecke et al., 2015). Moreover, as axon count and degree of myelination are strongly correlated, it becomes impossible to disentangle them when observing FA changes (Curran et al., 2016).

MD measures the average diffusivity in a particular voxel independently of its direction. Hence, it will be higher in areas where water molecules are not restricted, such as in the ventricles, and lower in areas with a high tissue complexity, such as in the grey matter. MD has been repeatedly investigated within neurodevelopmental frameworks; as brain water content decreases with maturation, due to the extracellular spaces present in unmyelinated axons (Engelbrecht et al., 2002), structures become more complex and packed, restricting the diffusion of water molecules. Thus, differences in MD could represent differences within the intra-extra cellular spaces and reductions in the neuropil (Selemon and Goldman-Rakic, 1999)

or increases in CSF.

There are relatively few studies that have directly investigated the relationship between water diffusion parameters and tissue microstructure. Significant associations between them have been shown in clinical samples (*e.g.* multiple sclerosis, Alzheimer's disease, epilepsy). Overall, significant correlations have been found between diffusion anisotropy and MD with myelin content and several axonal characteristics, such as axon count and density (Concha et al., 2010; Gouw et al., 2008; Schmierer et al., 2008, 2007). There are multiple reasons that could be responsible for an increase/decrease in water diffusion parameters and thus, interpretation will depend on the groups studied, acquisition parameters, etc. Nonetheless, quantitative measures obtained from DTI are useful in describing white matter connectivity and alongside histological studies, they have proven to be particularly revealing about the structural properties of white matter.

2.3.3. DTI methods

There are numerous methods for measuring DTI parameters in structures of interest that can be categorised and the most optimal one will depend on the goal of the investigation. Other subdivisions are possible, but for the purpose of this thesis I will briefly describe region of interest (ROI), voxel based (VBA), and tractography analyses.

2.3.3.1. Region of interest analysis

Region of interest analysis (ROI) relies on the delineation of a predefined brain region. One of the main advantages is the high sensitivity of the method. Some ROI analyses are performed in native space and thus, post-processing errors are avoided. Because they are only carried out in specific regions of the brain defined *a priori* (hypothesis driven), rather than whole-brain analysis, ROI analyses removes the need for correcting for multiple comparisons, thus potentially improving our statistical power. This methodology can be performed in individual participants by manually selecting a brain region, although it requires a normal

distribution of the data and shows low repeatability and high variability (Hakulinen et al., 2012). On the other hand, predefining specific regions may exclude possible interesting results and thus, bias results.

2.3.3.2. Voxel-based analysis

Voxel-based analysis (VBA) is an exploratory technique that examines differences in water diffusion measures in each voxel across the whole brain and does not necessarily require *a priori* hypotheses. This technique has its own advantages and limitations when compared to ROI and tractography analyses; for instance, VBA relies on the assumption that the spatial location of each voxel is constant between subjects and thus, the registration step is an essential characteristic of this approach, avoiding spatial differences caused for example, by pathology (Ardekani et al., 2003). The spatial registration of each individual's scan must be performed in standard space, and a voxel-by-voxel unbiased whole brain statistical comparison between groups can be achieved. One disadvantage of this method is that different image quality between subjects may potentially affect the registration's step. Moreover, VBA is not appropriate for data which fails to achieve the random Gaussian assumption of water diffusion (Mukherjee et al., 2008). Thus, results using VBA are parameter dependent and will be only relevant when the registration step is successfully achieved.

2.3.3.3. Tract-based Spatial Statistics

Tract-based Spatial Statistics (TBSS) is a very popular type of VBA that investigates differences in water diffusion parameters in a white matter skeleton mask (Smith et al., 2006). TBSS is based on identifying differences in white matter parameters by registration of all individual's scans into standard space and creating a common white matter skeleton. TBSS minimises the misalignment generated by VBA by projecting all FA data into a standardised skeleton before any statistical analyses, allowing registration errors and partial volume effects

(pve) to be reduced. TBSS aims to reduce alignment and smoothing issues typically found in VBA analyses while allowing to study the whole brain and being fully automated (Smith et al., 2006). This is achieved by identifying a common registration target and aligning all participants' FA images to this target using a non-linear registration; and then creating a group mean FA skeleton that represents the centres of all white matter pathways that are common to the participants studied. Subsequently, all each participant's FA data is projected onto the mean FA skeleton to account for misalignments between participants, where each skeleton voxel takes the FA value of the local centre of the nearest relevant tract and statistics can be performed on the skeleton-space FA data. Moreover, an atlas-based segmentation analysis – or ROI analysis – can be carried in the same space using one of the available white matter atlases in FSL software package. Figure 5 shows a summary of the principal steps followed in this thesis.[1] However, as TBSS is more commonly used, certain limitations have been reported (Bach et al., 2014). Registration may be affected when using diseased individuals, resulting in large anatomical changes. Also, the skeleton of TBSS is based on peaks of FA values, which are the centre of each tract. Thus, TBSS may not be sensitive enough to discern differences that are not uniform along the tract, as Dening and Thomas (2013) pointed out, and probably less sensitive in disease. Moreover, differences in peripheral voxels may not be detected with great sensitivity by TBSS but by VBA, as voxels outside the white matter skeleton are discarded by the former (Zalesky, 2011).

[1] Chapter 4 presents the results of TBSS analysis using the John Hopkins University white matter tractography atlas.

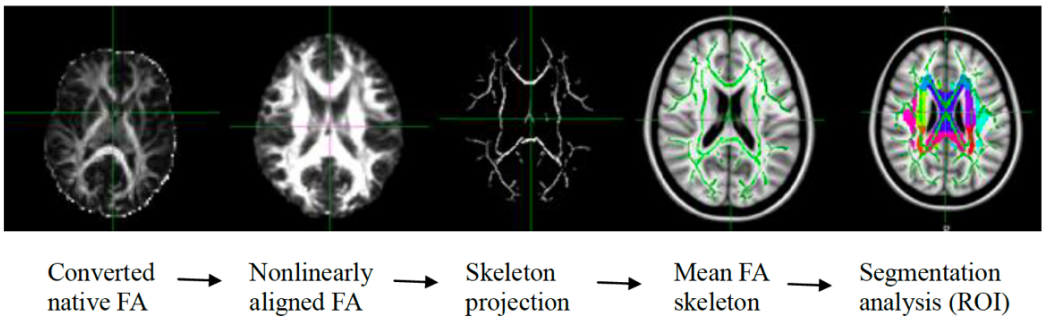

Figure 5. Summary pf the main steps used in this thesis to obtain diffusion tensor parameters.

2.3.3.4. Tractography

Tractography methods investigate white matter tract architecture at the voxel level to represent a 3D model of each tract. The majority of tractography algorithms are based on line propagation to construct white matter tracts. These methodologies are known as deterministic streamline fibre tractography. They rely on: accurate initial seed point placement, propagation of the track, and termination of the track when appropriate criteria have been met (Tournier et al., 2011). Fibre trajectories follow the primary eigenvector at each voxel and thus, deterministic tractography only provides a single estimate for each white matter tract from each seed point, is not able to track multiple fibres in each voxel (reviewed in Soares, Marques, Alves, & Sousa, 2013) and does not include estimate errors (Mukherjee et al., 2008). Thus, confidence intervals around the estimate are not represented. On the other hand, probabilistic tractography estimates the orientation distribution in each voxel (Behrens et al., 2007; Parker and Alexander, 2005), and the mean of that distribution will represent the orientation used in determinist tractography. The width of the distribution is proportional to the uncertainty in fibre direction. However, probabilistic tractography is a much more computationally demanding method compared to deterministic approaches. Probabilistic tractography was computed for all analyses presented in this thesis as implemented in the TractoR package for fibre tracking and analysis (http://www.tractor-mri.org.uk/ (Clayden et al., 2011; Muñoz Maniega et al., 2017).

2.3.4. General limitations of the model

One of the advantages of DTI is the reduction of complex neuroanatomical information into quantifiable parameters. However, this oversimplification has several implications to consider when interpreting DTI data. For instance, the lack of specificity of DTI measures, model limitations, demographics of participants, severity of clinical populations and complications during acquisition and analysis are some of the main factors that will confound the interpretation of results.

Even though it is beyond the scope of this thesis to go into detail on the limitations of the tensor model, I consider two main points to be useful when interpreting dMRI data. For instance, the tensor model assumes water diffusion as a Gaussian distribution, when in fact, intracellular diffusion is by definition hindered and therefore, does not follow a Gaussian distribution. The tensor model also assumes a unique fibre direction at each voxel, however, the mammalian neural tissue is highly complex and rarely satisfies this assumption. This complexity in tissue architecture is one of the most important confounds in DTI analysis. Crossing fibres have a significant impact on FA because in the presence of several fibres with their individual diffusion characteristics, there is no principal water diffusion direction and therefore, individual profiles average out. Abnormalities in water diffusion parameters are usually defined in relation to a comparison group because there is still a lack of established universal thresholds and standard acquisition and analysis protocols. Subject demographics such as age, sex, ethnicity, educational level, and substance abuse have been shown to be some of the confounds that should be considered when describing DTI results (Hecke et al., 2015). The interpretability and reliability of studies can then be improved by assuring proper data acquisition, reducing artefacts pre- and post-processing, and dealing accordingly with confounds in the analysis.

2.3.5. Summary

Tractography methods are an indispensable tool when studying brain connectivity.

Their main advantage is that they can be performed in the native space, avoiding some of the errors derived from projecting all dMRI data into a standardised space. Despite its own limitations, an adequate use of tractography can be a powerful tool when addressing specific questions (Jbabdi and Johansen-Berg, 2011). In addition, some studies have reported non-significant differences while comparing methods (Adluru et al., 2013). A few caveats must be considered when applying tractography to the datasets reported here. A fundamental problem is our poor knowledge of the human brain; and therefore, finding the exact termination of white matter pathways, detecting collaterals, etc., can become a difficulty (Jbabdi and Johansen-Berg, 2011). Another important limitation is the poor spatial resolution of MRI data (typically 1 to 3 mm voxels), meaning that some white matter pathways are not perfectly resolved, and mistakes can be made by jumping from one tract to another (Campbell, 2013). Nonetheless, depending on our *a priori* hypothesis we may be missing regions from our analysis that may be relevant to our study. Taken all together, the inconsistencies of DTI findings across the literature may reflect the numerous and different neuroimaging methods available, populations, heterogeneity of the disease and/or different statistical analyses.[2]

2.4. The connectome

2.4.1. Overview

Anatomical studies of the brain's architecture, cellular organization, and fibre systems have shown how highly structured the organization of the brain is. The recent advances in neuroimaging techniques have prompted the aim of trying to map the human brain's networks, which, combined with network science, studies the dynamics and structure of complex systems (Estrada, 2011; Newman, 2010). This recent affiliation has allowed the study of the brain from the perspective of a complex system. A number of studies have already begun to develop methods to measure structural brain connectivity in order to map comprehensively

[2] See Chapter 3 for a detailed summary of DTI findings across the literature.

the large-scale topological architecture of the brain through the quantification of pair-wise connections between whole-brain regions (Sporns, 2011). The term connectome was coined independently in analogy to the genome – the complete mapping of an individual genetic profile (Hagmann, 2005; Sporns et al., 2005). A quantitative approach to measure organizational properties of the structural connectome can be computed through graph theory – a mathematical framework that studies pair-wise relations between interacting elements (Bollobás, 1985). With the model proposed by Watts and Strogatz (1998) describing a small-world network (see Figure 6) with regional specialization and efficient global information transfer, the field of network science was propelled forward, especially in neuroimaging. The reductionist conceptualisation of complex systems, demonstrated for instance in the field of behaviour, highlighted the vast limitations of understanding a system exclusively through independent elements. Rather, an approach based on the interaction of those elements within the system is needed to understand the system overall. In regard to the brain, is difficult to conceive the brain as the ensemble of independent neurons or regions. However, a dynamic system of interactions between distinct brain regions may be able to explain the complexity of the brain and its emergent behaviours.

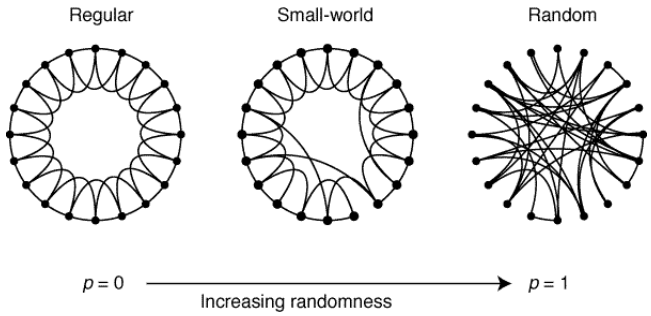

Figure 6 Small-world diagram taken from Watts and Strogatz (1998). The model started by connecting each node with its nearest neighbour, the result was the regular graph with high clustering coefficient and high average path length. With a probability *p* equal to one, edges were randomly connected, with a network with short clustering coefficient and path length.

However, with a probability *p* between zero and one, networks showed local clustering and some long-range paths. Thus, this network was a small-world, characterised by high clustering and low path length.

2.4.2. Network construction

Although currently there is not a standard method for the construction of dMRI networks, there are essential steps that are common across all studies (Fornito et al., 2012). First, parcellation of 3D T_1- weighted volumes either by (i) registration to neuroanatomical atlases or (ii) surface parcellation based on cortical sulci and gyri. The choice of the number of nodes will undoubtedly have an effect on the construction of the network and subsequent network properties. There are several approaches to parcellate the cerebral cortex that include, for instance, *a priori* anatomical parcellations and random parcellations. Second, alignment of the diffusion space and the cortical labels. Third, the construction of white matter tracts is performed by deterministic or probabilistic tractography. Connections between nodes are then computed and weighted, for instance, by a measure of white matter microstructure such as diffusion anisotropy. Finally, individual connections can be compared between groups or graph theory metrics can be derived to characterise the topological properties of the network. See Figure 7 for a simplified illustration of the main steps involved.

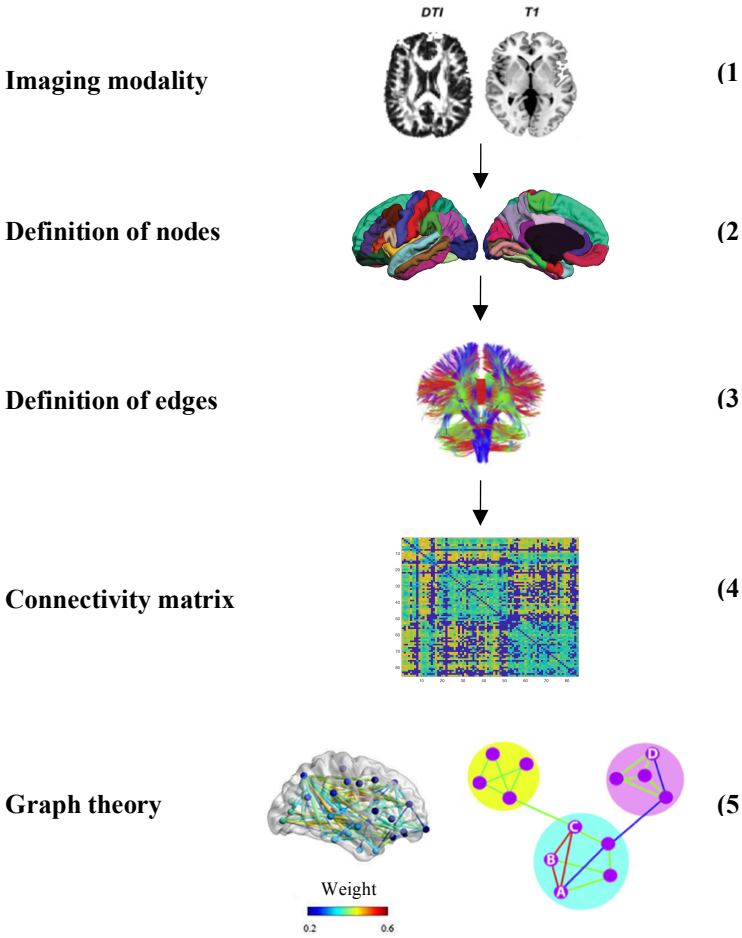

Figure 7 Illustration of the main steps involved in the construction of dMRI networks used in this thesis. The imaging modalities used here are DTI and T1-weighted imaging. The second row represents the step of anatomical parcellation into distinct nodes. The parcellation method adopted in this thesis was based on the Desikan atlas of into 85 cortical (Desikan et al., 2006) regions-of-interest (ROI) or nodes using FreeSurfer (http://surfer.nmr.mgh.harvard.edu). Once the nodes have been delineated, the edges connecting them should be defined. In this thesis whole-brain probabilistic tractography was performed using FSL's BedpostX/ProbTrackX algorithm (Behrens et al., 2007). The fourth step involved computing a weighted matrix representing inter-regional connectivity. Shown here is an example of a symmetric matrix where each voxel represents the FA value of the edge connecting two given nodes. Based on these matrices, a graph-based representation of the brain network connectivity can be computed, and several measures of network connectivity and topological properties can be derived. Adapted from Fornito et al. (2012).

2.4.3. Metrics

Before describing the individual graph theory metrics, I will first define some basic notation (Rubinov and Sporns, 2010). N represents all nodes in the network, while n is the number of nodes and b the undirected weighted graph, stored as a $n \times n$ adjacency matrix, where a_{ij} indicates the connection weight between node i and node j. The graph is defined as $G = \{V, E\}$, where V represents the nodes or vertices and E the set of edges. An edge $\{i, j\}$ is said to join the nodes i and j. Figure 8 shows a simplified network. The use of weighted measures implies that most graph theory metrics would be highly correlated with each other. For instance, as can be observed in the mathematical formulae below of the different metrics, it is quite obvious that mean edge weight and mean strength will show high collinearity. In addition, it has been highlighted what the effect density has on the computation of graph theory metrics. Ultimately, the fraction of present edges will undoubtedly alter the subsequent calculation of metrics.

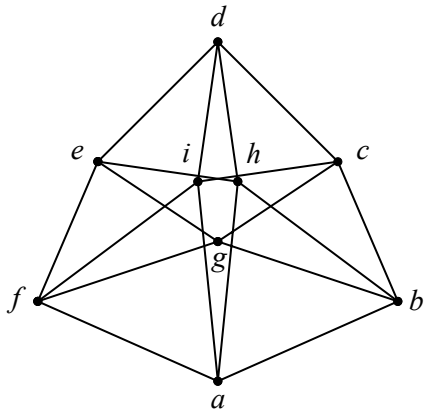

Figure 8 Example of a simple graph, with nodes a, b, …, i and edges *ab, bc, cd, de, ef, fa, ah, ai, bg, bh, cg, ci, dh, di, eh, eg, fi* and *fg*.

For a weighted graph (bounding values between 0 - 1)*, mean edge weight* is:

$$M = \frac{1}{E}\sum_{i,j\in E} a_{ij}$$

The *strength* (bounding values between zero and infinite) of a node *i*

$$w_i = \sum_{j\in N} a_{ij}$$

The *mean node strength* (network strength)

$$W = \frac{1}{n}\sum_{i\in N} w_i$$

Global efficiency (bounding values between zero and infinite; see Figure 9)

$$E = \frac{1}{n}\sum_{i\in N}\frac{\sum_{j\in N, j\neq i} d_{ij}^{-1}}{n-1}$$

Considering a node's set of directly connected neighbours, the weighted *clustering coefficient* (bounding values between zero and infinite) (Onnela et al., 2005; Watts and Strogatz, 1998) of a node *i* is calculated,

$$c_i = \frac{1}{n}\sum_{i\in N}\frac{\sum_{j,h\in N}(a_{ij}a_{ih}a_{jh})^{1/3}}{k_i(k_i-1)}$$

The *mean clustering coefficient* (bounding values between zero and infinite)is a global measure of a network's clustering (see Figure 9)

$$C = \frac{1}{n}\sum_{i\in N} c_i$$

Measures of centrality may be used to identify highly connected nodes, such as network hubs. The *betweenness centrality* (Freeman, 1978) of a node *i* is,

$$b_i = \frac{1}{(n-1)(n-2)}\sum_{h,j\in N, h\neq j, h\neq i, j\neq i}\frac{\rho_{hj}(i)}{\rho_{hj}}$$

where ρ_{hj} is the number of shortest paths between h and j and $\rho_{hj}(i)$ is the number of shortest paths between h and j that pass-through i. Essentially, betweenness centrality measures the fraction of shortest paths in the network that pass-through a given node.

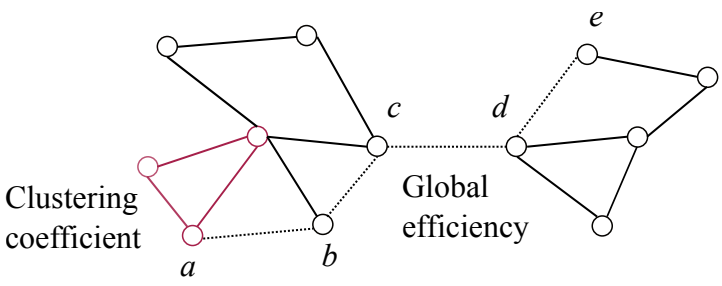

Figure 9 Graphical representation of clustering coefficient (in purple) and global efficiency (dashed lines between nodes *a* to *e* through the minimum number of steps between them: *a, b, c, d, e*).

2.4.4. Network threshold

The elevated number of possible connections that the connectome computes, raises the question of whether these pathways are biologically relevant. Each step of the process is manually checked; however, in general, the elimination of spurious connections may not be feasible, partly because of our lack of neuroanatomy knowledge. Thresholding methods aim to reduce the density of brain networks in order to eliminate those spurious connections, thus increasing specificity. Additionally, thresholding matrices allows the study of the network's topological properties that may be obscured by differences in edge weights. However, thresholding can also disregard useful information. Therefore, the approach taken will depend on the research questions.

The simplest approach is a weight-based threshold which relies on the principle that edges with a weight lower than a certain threshold will be eliminated (Sotiropoulos and Zalesky, 2017). One of the main disadvantages is the possible elimination of edges of interest combined with the lack of a principled way to choose the threshold. Therefore, when comparing networks, differences between them may ultimately be a consequence of differing network's densities. This scenario can occur in clinical studies where patients may show impaired connectivity (*i.e.* impairments in connections' weights). Thus, when differences in graph theory metrics are found, it is unclear whether this is the result of genuine differences or differing network densities.

Density-based threshold (Wijk et al., 2010) approaches aim to maintain equal density across subjects by retaining a certain percentage of the strongest edges and eliminating the rest. However, this adds a new confound as the number of spurious connections between subjects may differ. Concisely, each individual network will preserve equal density whilst not necessarily the same connections across participants. Global methods are susceptible when applied to clinical samples because they are based on the assumption that a weak connection is a spurious one. White matter impairments in schizophrenia will result in differently weighted matrices compared to healthy controls (Zalesky et al., 2011). Taken all together, both methods will fail in determining whether differences between networks are the result of inherent topological differences between them or the result of comparing networks composed of different connections.

The minimum spanning tree (MST) has been proposed to overcome the issue of network fragmentation caused by global thresholds (Alexander-Bloch et al., 2010). MST is the smallest subset of stronger edges – minimum sum of edge weights – that connects all nodes together. Additional edges can be added to the MST *a posteriori* to reach the desired density. However, this method relies on the forcing of a property onto the network.

Consensus thresholding is characterised by maintaining all edges with a weight of at least *x* in at least *y* percentage of subjects. This method ensures equal density across networks while eliminating spurious connections (de Reus and van den Heuvel, 2013). This model is based on two assumptions: first, the existence of little biological variation in the presence of connections across individuals and second, connections that are consistently identified in larger percentages of subjects are more likely to exist than those that are detected in few subjects. Therefore, in this thesis, we used consensus thresholding in most of our analyses.

Although thresholding is not a necessary step, it is often applied in order to eliminate spurious connections, facilitate the interpretation of results and control for density differences when comparing two groups, etc.; overall, maximising the specificity of brain graphs (Sotiropoulos and Zalesky, 2017; Zalesky et al., 2016).

2.4.5. Tractography and the connectome

Diffusion MRI-based tractography has offered multiple advantages to study white matter *in vivo*. However, there are still limitations regarding its anatomical accuracy, leading to challenges in the reconstruction of the connectome with both high sensitivity and high specificity. Specific limitations associated with tractography algorithms are presented in Chapter 2. Alternative approaches to DTI can be used to reconstruct white matter pathways in the brain: high-angular resolution diffusion imaging (HARDI), constrained spherical deconvolution (CSD), spherical-deconvolution informed filtering of tractograms (SIFT), Diffusion Spectrum Imaging (DSI), Q-Ball Imaging (QBI), Q-Space Imaging (QSI), etc. For instance, CSD models the diffusion profile in each voxel with multiple fibre orientations, which results in a fibre orientation distribution (FOD) that can have several peaks and allows

crossing fibres to be modelled. Another novel method, SIFT, aims to improve the quantitative nature of whole-brain tractography by applying spherical deconvolution and reconstructs fibres whose streamline densities are proportional to the cross-sectional area of the fibre.

Due to the inherent limitations of these techniques, not all white matter pathways can be computed with the same accuracy, and therefore, two main errors can be found when reconstructing the connectome, the appearance of false positive and false negative connections. False positive connections may occur when nodes are erroneously connected; while missing existing connections would give rise to false negative connections. De Reus and van den Heuvel (2013) showed that the balance between the elimination of false positives and the prevention of false negatives can be achieved by applying a group threshold. Importantly, the authors showed that the choice of threshold had substantial implications in the computation of graph theory metrics, reporting significant differences between values across the different thresholds. The tractography algorithm has a large effect on global network density, which has an effect on most graph theory metrics. Thus, research on the reconstruction of the connectome is a necessary and challenging topic. Previous work has focused on the effect of cortical parcellation, seed point placement and reproducibility of graph theory metrics. For instance, the choice of number of nodes alters significantly the computation of graph theory metrics; in a test-retest study using HARDI, Dennis et al. (2012) showed that most metrics were affected by the change in the number of nodes, specifically path length and global efficiency, as networks tend to fracture at low sparsities. Bastiani et al. (2012) supported their results by showing that the choice of tractography class, FA threshold, angle and probabilistic percentiles, influenced network measures. Zalesky et al. (2010) reported a difference of 95% between template of 100 nodes and a template of 400 nodes, while the identification of brain hubs has been shown to be affected by the placement of the tractography seed point (Li et al., 2012). Taken together, the choice of reconstruction parameters seems to have a significant impact on the resulting connectome, indicating the urgent need of more research on this topic and guidelines on quality of the reconstruction.

Chapter 3 White matter connectivity and correlates

3.1. Overview

Schizophrenia has been often described as a disorder characterised by impaired brain connectivity (Friston, 1998; Friston and Frith, 1995). Literature has frequently obviated the apparent importance of white matter – grey matter has been classically the main tissue of interest. Nonetheless, correlations between white matter, symptoms, and cognitive functions have been extensively reported, both in clinical and non-clinical samples. The high heritability and polygenicity of schizophrenia, white matter parameters, and cognitive functions provide a great opportunity to investigate the potential relationships between these factors, due to their shared genetic overlap. In this chapter, I will review the main associations between white matter connectivity and cognitive functions, genetics, and clinical symptoms in schizophrenia.

3.2. Summary of functional MRI findings in schizophrenia.

Since the introduction of MRI, fMRI has been widely used, partly due to the numerous advantages it offers regarding studies relating behavior and function. Most typically, the method applied is based on Blood Oxygenation Level-dependence (BOLD). It is based on the magnetic susceptibilities of deoxyhemoglobin; when the brain is activated under a task, there is a net increase in signal intensity, which is attributed to a greater increase in regional oxygenated blood flow that exceeds regional oxygen consumption. Although the implications derived from fMRI studies have been of great interest in the field, it is out of the scope of this thesis to comprehensibly review all fMRI literature. Therefore, I will highlight the importance of such studies only in relation to schizophrenia. There have been numerous fMRI studies in schizophrenia, with results suggesting impaired brain activity in dorsal and ventral prefrontal, anterior cingulate and posterior cortical regions (Minzenberg et al., 2009); and across several cognitive tasks: motor, working memory, attention, word fluency, emotion processing, and decision making (reviewed in Gur and Gur, 2010). However, much inconsistency is observed in the literature, with studies reporting increases in functional connectivity within the default

mode network (Whitfield-Gabrieli et al., 2009) while others finding both impairments and mixed connectivity between nodes of this network (for a review see Fornito et al., 2012). More support for the hypothesis of impaired functional connectivity in schizophrenia comes from resting state fMRI studies (Fornito and Bullmore, 2010; Jafri et al., 2008; Lynall et al., 2010; Salvador et al., 2010), defined as the statistical correlation between spatially distributed neurophysiological time-series (Friston, 1994). For instance, Damaraju et al., (2014) showed that during resting state, patients with schizophrenia showed hypoconnectivity within sensory regions (auditory, motor and visual) and hyperconnectivity between the thalamus and these sensory regions. Taken together, fMRI studies offer valuable information about the relationship between brain and behaviour; however, as with any MRI modality, much inconsistency is found in the literature, probably indicating the use of different methodological techniques and heterogeneity of the disease.

3.3. White matter abnormalities in schizophrenia

White matter impairments have been extensively reported in schizophrenia. Post-mortem studies have shown cellular and density reductions of oligodendrocytes in patients with schizophrenia, specifically in layer III and VI of the prefrontal cortex and superior frontal gyrus (Davis et al., 2003; Hof et al., 2003; Uranova et al., 2004). Thus far, a number of studies using MRI have provided evidence regarding the dysconnectivity hypothesis by reporting structural and functional connectivity abnormalities between different brain regions and across the whole spectrum of psychosis (Samartzis et al., 2014; Schmidt et al., 2015). The most common finding in terms of localisation, is the frontal lobe, and to a lesser extent, fronto-temporal, corpus callosum and dysconnectivity from the anterior cingulate cortex to other cortical and subcortical areas (Pettersson-Yeo et al., 2011). It has been suggested that abnormalities in white matter microstructure may produce the anatomical substrate for the dysconnectivity hypothesis (Alvarado-Alanis et al., 2015a; Weinberger, 1987).

White matter parameters are highly heritable, though the extent is a function of the white matter tract under study (Kochunov et al., 2015; Skudlarski et al., 2013). Such heritability seems to be relatively consistent across lifespan, with peaks during the neonatal and childhood periods (Kochunov et al., 2012, 2011; Voineskos, 2015). White matter impairments have been also reported in first-degree relatives, suggesting that white matter may be a potential phenotype to study in schizophrenia. Thus, imaging, post-mortem, and genetic studies have suggested the essential functional and structural role of white matter in schizophrenia, potentially identifying it as a target for pharmacological interventions (Rapoport et al., 2005).

The study of the early phases of psychosis has led to the development of a novel research approach that overcomes the difficulties associated with illness chronicity, such as the effects of medication, age, etc. Thus, the study of those at clinical high risk (CHR) and first episode of psychosis (FEP) has improved our understanding of the disorder and the early changes found in these patients. For instance, during the prodromal phase, cognitive impairments can be observed along with deficits in social functioning and quality of life (see Figure 1). These impairments are associated with an underlying affected neurobiological structural and functional connectivity. In a recent review, Samartzis et al. (2014) reported that the most common impairment found in white matter in the early stages of the disorder was localized in fronto, fronto-temporal, and fronto-limbic connections, with reductions in FA.

3.3.1. Clinical High Risk (CHR)

Samartzis et al. (2014) also reported consistent impairments in the cingulum bundle in CHR subjects, and deficits mainly in frontal, temporal, and to a lesser extent, occipital and parietal regions. However, increased FA in specific areas has also been reported in the CHR group (Hoptman et al., 2008), highlighting the need for increased sample sizes and

standardisation of imaging protocols. In a longitudinal study, Saito et al. (2017) reported reduced FA in the corpus callosum in CHR compared to healthy controls. Moreover, this reduction in FA was significantly correlated with a deterioration in negative symptoms in the CHR group. Increased MD in the CHR sample in the superior longitudinal fasciculus, posterior corona radiata, and corpus callosum has been reported (von Hohenberg et al., 2014). Muñoz Maniega et al. (2008) reported reduced FA in the limbs of the internal capsule of relatives of patients with schizophrenia compared to healthy participants. Interestingly, a progressive deterioration of FA has been identified in a study that analysed three groups: CHR, FEP, and healthy controls. The authors showed that CHR presented FA impairments compared to healthy participants, but less severely than FEP. Particularly, frontal regions were more affected in those CHR that later transitioned to schizophrenia than those who did not (Carletti et al., 2012).

3.3.2. First Episode of Psychosis (FEP)

Specific reductions in FA in FEP compared to healthy controls have been reported in the inferior longitudinal fasciculus (Cheung et al., 2008; Liu et al., 2013), superior longitudinal fasciculus (Guo et al., 2012), cingulum (Wang et al., 2013), fornix (Fitzsimmons et al., 2014; Guo et al., 2012), internal and external capsule (Cheung et al., 2008; Filippi et al., 2014; Guo et al., 2012), uncinate fasciculus (Mandl et al., 2013), anterior corona radiata (Wang et al., 2013), arcuate (Mandl et al., 2013), genu and splenium (Cheung et al., 2008; Gasparotti et al., 2009), and occipital-frontal fasciculus (Cheung et al., 2008; Liu et al., 2013). A recent study by Alvarado-Alanis et al. (2015a) also reported reductions in FA in projection, association, commissural, and brain stem tracts compared to healthy participants. Taken all together, it has been consistently reported that even in first-episode drug-naïve patients, white matter impairments are already present, discarding the hypothesis that long-term use of medication is the only factor that alters white matter microstructure.

3.3.3. Chronic patients

Several publications have investigated the effects of white matter coherence on chronic patients diagnosed with schizophrenia and found significant reductions in FA in several white matter tracts (Ellison-Wright and Bullmore, 2009); however, due to the heterogeneity of the results, it remains unclear which specific white matter tracts are consistently impaired. The most replicated finding is a reduction in FA in the cingulate, a structure involved in error checking, attention, and is a link between limbic and higher cortical functions (White et al., 2008). Impairments in white matter have also been observed in the corpus callosum and in the frontal lobe. The corpus callosum integrates both hemispheres and is implicated in the adequate transfer of neural signals. Several studies have reported decreased FA in the corpus callosum, with global decreases, only on the genu or the splenium (Bora et al., 2011; Buchsbaum et al., 2006; Holleran et al., 2014). Other reductions in FA have been reported in the parietal, temporal, and occipital lobes (White et al., 2008).

In particular, white matter tracts responsible for intralobal and interlobal signal communication have also been reported to have lower FA. Examples include the superior, inferior, and longitudinal fasciculus (Asami et al., 2013; Bora et al., 2011; Liu et al., 2013), fronto-occipital longitudinal fasciculi (Liu et al., 2013), uncinate (Burns et al., 2003; Mori et al., 2007), frontal longitudinal fasciculus (Buchsbaum et al., 2006), and arcuate (Burns et al., 2003). In addition, several other white matter tracts have been shown to have reduced FA. These include the fornix (Bora et al., 2011), cerebellar peduncles, cingulum (Mitelman et al., 2007; Mori et al., 2007), internal and external capsules (Bora et al., 2011; Holleran et al., 2014), and the thalamic and optic radiations (Bora et al., 2011; Mitelman et al., 2007). Reduced FA was also found in the anterior limb of the internal capsule, the posterior thalamic radiation, as well as the genu and body of the corpus callosum (Oestreich et al., 2017; White

et al., 2013). The ENIGMA consortium has recently published one of the largest meta-analytic DTI studies, consisting of 2359 healthy controls and 1963 schizophrenia patients, and reported widespread significant reductions in FA. Notably, the greatest effect sizes were found for the anterior corona radiata (d = 0.40) and corpus callosum (d = 0.39). Figure 10 shows the most commonly reported white matter tracts in schizophrenia.

Thus, the literature on white matter abnormalities in schizophrenia is extensive, however, the heterogeneity of these results is outstanding. The varied imaging methods, statistical approaches, and the diversity of the disorder itself contribute altogether to such distinct results. Moreover, the neurological marks that characterise schizophrenia usually lack diagnostic specificity, as sometimes they are shared across different disorders, such as bipolar disorder and other major affective disorders (Ahmed et al., 2013). Thus, the significance of neuroimaging to the phenomenology of schizophrenia has to be established through studies that investigate neuroanatomy in relation with symptomatology, cognition, and genetics.

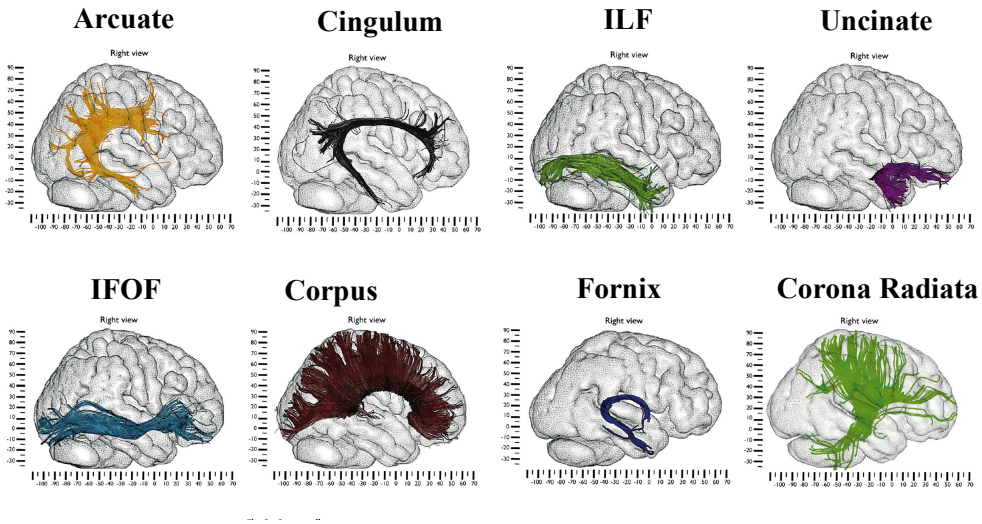

Figure 10 Right sagittal views of some of the most commonly reported white matter tracts impaired in schizophrenia. Figure adapted from Catani and Thiebaut de Schotten (2008). ILF: Inferior longitudinal fasciculus; IFOF: inferior fronto-occipital fasciculus.

3.4. Connectome alterations in schizophrenia

Volume, tract-based, and network analyses suggest an overall reduced white matter volume and altered microstructure of large-scale projections, indicating that white matter plays an essential role in the pathology of schizophrenia. White matter abnormalities have relatively pronounced effects on the organization of the connectome in schizophrenia, which suggests a more segregated pattern of network organization. Alterations in structural brain connectivity and network topology have been reported in schizophrenia (Wheeler and Voineskos, 2014). Impairments in structural connectivity have been reported within subnetworks in chronic patients (Collin et al., 2013; Skudlarski et al., 2010; Zalesky et al., 2011), first episode medication naïve patients (Zhang et al., 2015), and unaffected relatives (Collin et al., 2014) who are at higher genetic risk for developing the disorder, suggesting that altered connectome organization may be reflective of an inherited neurodevelopmental vulnerability to schizophrenia.

Graph theoretical studies of the whole network have reported small-world organization and reductions in integration and efficiency in chronic patients (Bassett et al., 2008; Ottet et al., 2013; van den Heuvel et al., 2013, 2010; Wang et al., 2012; Zalesky et al., 2011; Zhang et al., 2012), first episode medication naïve (Zhang et al., 2015), and unaffected relatives (Collin et al., 2014). Reductions in overall structural connectivity, specifically projections linking frontal, temporal, and parietal regions in chronic patients and their unaffected siblings have been reported (Collin et al., 2014; van den Heuvel et al., 2013). Structural studies have generally found evidence of increased segregation (i.e., clustering and modularity), reduced integration (higher path length and lower global efficiency and rich-club organization), and a loss of frontal hubs (van den Heuvel et al., 2010; van den Heuvel and Fornito, 2014). These studies have also found evidence of longer path lengths and reductions

in global communication efficiency, suggesting a reduced communication between more distal brain regions (van den Heuvel and Fornito, 2014).

Frontal and temporal brain regions showed altered clustering and longer communication paths, as well as reduced global efficiency. Numerous investigations focusing on different morphometric parameters have revealed altered network topology and a reduced hierarchical structure, indicating an impaired organization, particularly in cortical regions. Some regions such as the superior frontal cortex and lateral precuneus have shown reduced levels of closeness and betweeness centrality, suggesting that these structures may have a less central role in the network (van den Heuvel and Fornito, 2014).

In contrast, abnormalities in functional connectivity are less consistent, usually reporting reductions in connectivity; however, several investigations reported increases in specific neural systems (review in Fornito and Bullmore, 2015), likely as a result of neurodevelopmental or compensatory features (O'Donoghue et al., 2015). Nevertheless, much inconsistency is present in brain connectivity studies, and network comparability issues represent one of the major challenges in the field (Sotiropoulos and Zalesky, 2017; Wijk et al., 2010). These discrepancies are likely due to differences in methodological approaches for connectome construction and posterior analyses, as currently there is no consensus on a preferred approach to analyse the connectome. Another source of variability is the high complexity of schizophrenia, with pathological manifestations and symptoms' profiles extremely variant between patients.

3.5. Symptoms

There is a growing body of literature that recognises the importance of white matter in the clinical presentations observed in the disorder. Impaired connectivity may be the

neuroanatomical substrate for positive psychotic symptoms, showing short and long-range frontal connectivity deficits in schizophrenia (O'Donoghue et al., 2015). Although white matter impairments are likely to be clinically relevant, much uncertainty remains regarding its role in symptom severity. Most studies have approached this issue using exploratory analyses resulting in bivariate correlations between DTI measures and different scales: SANS (Scale for the Assessment of Negative Symptoms (Andreasen, 1983)) and PANSS negative (Positive and Negative Syndrome Scale). The majority of studies report positive associations between FA and positive symptoms and negative associations between FA and negative symptoms (Samartzis et al., 2014). In this chapter, I will highlight some of the most recent studies that have addressed this issue.

3.5.1. Positive symptoms

Reduced FA in the corpus callosum of schizophrenia patients is a well-documented finding and has been reported to be positively associated with psychotic symptom severity (Hubl et al., 2004; Knöchel et al., 2012; Rotarska-Jagiela et al., 2008; Whitford et al., 2010). Several other tracts (measured using FA) have been positively associated with psychotic symptoms; for instance, the cingulum bundle (Hubl et al., 2004), arcuate fasciculus (Hubl et al., 2004), superior longitudinal fasciculus (Seok et al., 2007), and inferior fronto-occipital fasciculus (Szeszko et al., 2008). On the other hand, reduced FA of the right inferior longitudinal fasciculus, arcuate fasciculus, medial temporal lobe, and medial-frontal regions have been reported to be associated with increasing severity in positive symptoms (Ahmed et al., 2013; Ohtani et al., 2015; Seitz et al., 2016). Specific domains have also been investigated; Bopp et al. (2016) reported significant associations between FA and core symptom dimensions in schizophrenia using TBSS and factor-analysis of symptoms. For instance, hallucinations were positively associated with FA of the left uncinate fasciculus and left corticospinal tract. Ego-disturbances was positively correlated with the FA of the right anterior thalamic radiation

and positive formal thought disorders negatively with the right cingulum bundle. In contrast, Viher et al. (2016) reported significant associations between the FA of motor tracts and the psychomotor domain, reporting non-significant associations between FA and delusions, hallucinations, and disorganised speech.

Similarly, correlations between the structural connectome and positive symptoms have been documented. For instance, positive symptoms have been negatively associated with network efficiency (Wang et al., 2012). Drakesmith et al. (2015) found topological differences in the structural connectome in individuals with subclinical psychotic experiences, particularly, reductions in global efficiency and density. Patients with 22q11.2 deletion syndrome (22q11DS) are exposed to a higher risk of developing schizophrenia, and it has been suggested that altered structural connectivity is predictive of psychotic symptoms in the disorder (Padula et al., 2017). Hence, the authors proposed structural network properties as a possible biomarker for an increased risk of psychosis.

3.5.2. Negative symptoms

Thus far, negative symptoms have been greatly studied, mainly indicating significant negative associations between white matter and severity of negative symptoms. For instance, reductions in FA of the inferior frontal white matter have been significantly associated with increased negative symptoms (Szeszko et al., 2008; Wolkin et al., 2003). Szeszko et al. (2008) examined correlations between FA and negative symptoms in recent-onset schizophrenia and reported that lower FA in the bilateral uncinate fasciculus was correlated with greater severity of negative symptoms – in particular, alogia and affective flattening– and worse verbal learning/memory function. Several other white matter tracts have been linked to the presence of negative symptoms: the left internal capsule, left superior fronto-occipital fasciculus, anterior parts of the corpus callosum (Asami et al., 2014), connections of the medial orbito-

frontal cortex and the rostral anterior cingulate cortex (Ohtani et al., 2014a), right ventral cingulum bundle (Bopp et al., 2016), reductions in FA of the medial-frontal regions (Ohtani et al., 2015), white matter microstructure of the prefrontal, right and medial temporal lobes (Ahmed et al., 2013; Viher et al., 2016). Decreased FA in frontal areas has also been associated with impaired social functioning in schizophrenia (Ahmed et al., 2013). However, findings are inconclusive, including positive associations between FA and negative symptoms in certain white matter tracts such as the right anterior thalamic radiation (Bopp et al., 2016) and the right inferior fronto-occipital fasciculus (Lee et al., 2013).

3.6. Cognition and white matter

As summarised previously, patients with schizophrenia show a broad spectrum of cognitive deficits. These impairments have been suggested to precipitate psychotic symptoms, to be relatively stable over time, persist after the remission of positive symptoms, and to be associated to negative symptoms (reviewed in Antonova, 2004). Notably, brain structure and intelligence have been shown to be positively correlated, and this correlation is strongly influenced by genetic factors. However, very little is known about how variation in brain structure and intelligence interacts with schizophrenia.

There is an emerging consensus that intelligence cannot be circumscribed to the function of a unique region, but rather it is best described as the result of the interaction between multiple areas or networks. This conceptualization implies that for the correct transmission of cognitive information, the system must be undisrupted. The study of intelligence has established that individual differences exist in three different levels: general intelligence, domains of distinctive cognitive functioning, and test-specific variations (Deary, 2012). So far, several studies have reported significant associations between FA and intelligence in healthy participants (Chiang et al., 2009; Deary et al., 2006; Penke et al., 2010;

Yu et al., 2008). However, the relationship between white matter connectivity and cognition in schizophrenia is still an active area of research.

Nevertheless, some associations have been reported in the disorder. Wexler et al. (2009) reported that those schizophrenia patients with no cognitive impairment (within 0.5 SD of healthy participants) did not show white matter differences when compared to healthy participants. On the other hand, patients with cognitive deficits had significant white matter reductions in various brain regions. The authors suggested that white matter may have an essential role in cognitive functions and the differences found between the two groups may relate to differences in the disease process. Specific white matter tracts have been associated with cognitive performance; Seitz et al. (2016) reviewed significant correlations between the FA and RD of the cingulum bundle with memory performance and processing speed in schizophrenia. Nestor et al. (2013) found similar results, showing that patients with the greatest impairments in intelligence showed correlations with the FA of the cingulum bundle, which was consistent with previous work from the same group (Nestor et al., 2010). Roalf et al. (2015) found significant FA reductions in patients diagnosed with schizophrenia compared to healthy controls, and from these FA values, the authors were able to predict cognitive performance after correcting for sex, age, and education.

To date, several studies have investigated the associations between the structural connectome and intelligence. In a sample of 79 healthy young adults, Li et al. (2009) reported significant associations between the summary metrics of the Chinese Revised Weschler Adult Intelligence Scale and clustering coefficient, path length, and global efficiency. Significant associations between the structural connectome and cognition in schizophrenia have also been studied. Zalesky et al. (2011) reported correlations between clustering coefficient, path length, and efficiency with scores of the Wechsler Test of Adult Reading – premorbid cognitive function – in controls and patients. In a longitudinal study, Collin et al. (2016) found that

altered organization of the connectome – measured using clustering coefficient – was significantly associated with a decrease in IQ (r = 0.54) over a period of three years in a group of patients diagnosed with schizophrenia. Notably, this effect was not found for their relatives or the control group. Yeo et al. (2016) found that longer characteristic path length and reduced overall connectivity were able to predict general cognitive ability across both patients with schizophrenia and healthy controls.

3.7. Genetic associations

3.7.1. Heritability of white matter connectivity

As previously mentioned, several studies have found white matter connectivity impairments not only in patients diagnosed with schizophrenia but also in their relatives, identifying overlapping areas between them. This suggests that familial and genetic factors may possibly contribute to this effect. Among white matter heritability studies, the most used neuroimaging phenotype are volumetric, white matter hyperintensities, diffusion-weighted measures or quantitative T1 or T2-weighted imaging. For the purpose of this thesis, I will focus on the findings derived from the main diffusion-weighted parameters FA and MD and the structural connectome. It is important to bear in mind that the different approaches available will affect the heritability estimate; for instance, the choice of voxel-wise analysis, ROI, or tractography analysis, and also the timepoint of the lifespan used will all undoubtedly have an impact on the results (Voineskos, 2015).

The first study on DTI heritability of the corpus callosum comprised 15 monozygotic and 18 dizygotic twins (Pfefferbaum et al., 2001). The authors found that the variance explained by genetic factors was 67% and 49% for the FA of the genu and splenium, respectively. However, Chiang et al. (2009) reported that the variance explained by genetic factors was between 75-90% in almost every white matter region, particularly the genu,

splenium, the right cerebral peduncle, right inferior longitudinal fasciculus, right inferior fronto-occipital fasciculus, and the anterior limbs of the internal capsule bilaterally. The authors showed that FA was under strong genetic control and was highly heritable in bilateral parietal, bilateral frontal, and left occipital lobes. This study also examined the association between FA and intellectual performance, reporting to be highly correlated in the corpus callosum, cingulum, optic radiations, superior fronto-occipital fasciculus, internal capsule, isthmus, and the corona radiata. They concluded that common genetic factors mediated the association between intelligence and FA, suggesting a common underlying physiological and genetic mechanism for both. The same group examined the heritability of FA in a younger sample, controlling for IQ, age, sex, and socioeconomic status, finding that the heritability of FA was related to the level of IQ: above average IQ showed a higher heritability of FA up to 80% in certain tracts while for the lower IQ group, heritability dropped to 40% (Chiang et al., 2011).

Meta and mega-analyses have supported even further white matter heritability. One meta-analysis study reported that FA of the genu and splenium of the corpus callosum and longitudinal fasciculus showed moderate heritability values (Blokland et al., 2012). A mega-analysis conducted with the ENIGMA consortium using a sample size of 2248 individuals found that practically every white matter tract's FA showed high rates of heritability, ranging from 0.4 to 0.7 (Kochunov et al., 2014). The B-SNIP (Bipolar Schizophrenia Network on Intermediate Phenotypes) consortium group published a multi-site study that involved patients with schizophrenia and psychotic bipolar disorder, their unaffected first-degree relatives, and a group of healthy controls. Their results showed a significant decrease in FA in multiple white matter tracts in patients compared to healthy controls. The authors reported no significant differences in FA between psychotic disorders nevertheless relatives showed decreases in FA compared to healthy controls, representing a continuum of decreased FA from healthy participants to relatives to psychotic patients.

In a recent study, Bohlken et al. (2016) reported that reductions in white matter coherence had a genetic overlap with schizophrenia liability. The authors reported that 83.4% of the association between global white matter and schizophrenia liability was explained by common genes, with 8.1% of genetic variation in global FA being shared with genetic variance in liability for schizophrenia. However, due to its novelty, much uncertainty still exists about the heritability of the topological properties of the structural connectome, and only a handful of studies have addressed this issue. In a previous study, Bohlken et al. (2014) investigated the heritability of these topological measures, namely path length and clustering coefficient. The authors established the heritability to be 68% and 57%, respectively. These genetic influences were found to overlap with microstructural and volumetric properties of white matter; however, the largest component of genetic variance was unique to the network metrics, indicating that network metrics are able to provide distinctive information on the genetic influences on brain structure. Other studies support this hypothesis by reporting network impairments in unaffected relatives (Collin et al., 2014).

3.7.2. Polygenic risk score for schizophrenia

The largest GWAS performed to date identified 179 schizophrenia-associated genetic loci that were enriched among genes expressed in the brain and tissues involved in the immune system (Pardiñas et al., 2018; Schizophrenia Working Group of the Psychiatric Genomics Consortium, 2014). Thus, schizophrenia is established as a highly polygenic disorder, with thousands of alleles of very small effect. Consequently, the study of szPGRS may more precisely capture the nature of the disorder, rather than single mutations.

To date, very few investigations have studied the effects of szPGRS on the white matter phenotype. A recent study investigating the association between white matter FA and szPGRS reported that after multiple comparison correction, no significant correlations were

found between szPGRS and the neuroimaging phenotype (Voineskos et al., 2016a). However, Oertel-Knöchel et al. (2015) found in a smaller sample that higher szPGRS was significantly correlated with reductions in white matter volume. Ritchie et al. (2017) reported a significant longitudinal association between szPGRS and a general factor of tract-averaged MD (β = -0.120, SE = 0.059, p = 0.041, where a negative association indicates a link with unhealthy ageing), using a threshold of p = 1.00 (Schizophrenia Working Group of the Psychiatric Genomics Consortium, 2014) and 3-year change in a dataset comprised of relatively healthy elderly (LBC1936). This nominal association did not, however, survive correction for multiple comparisons ($p_{FDR} > 0.05$). A recent study using UKBiobank data did not find any significant associations between white matter microstructure – measured using FA and MD – and PGRS for major psychiatric disorders, including schizophrenia (Reus et al., 2017).

Given the common overlap between schizophrenia and cognitive functions, there is an increasing interest in determining whether this relationship may be mediated by shared genetic mechanisms. Despite being an emerging field of research, some significant associations have already been found between szPGRS and cognitive functions. Shafee et al. (2018) reported that higher szPGRS was significantly associated with lower scores on the Brief Assessment of Cognition in Schizophrenia (BACS; r = - 0.17, $p = 6.6 \times 10^{-4}$ at $P_T = 1 \times 10^{-4}$), but not with premorbid intelligence or educational attainment, and even among healthy older adults, szPGRS has been reported to be negatively associated with cognitive functions (Liebers et al., 2016). Two other studies have addressed this issue: McIntosh et al. (2013a) found a negative association between szPGRS and cognitive decline between the ages of 11 to 70 in the LBC36, and Lencz et al. (2014) who also found a negative association between szPGRS and cognitive functioning in a meta-analysis of 4302 healthy participants. Interestingly, creativity has been found to be positively correlated with szPGRS, suggesting that both traits share common genetic variants (Power et al., 2015).

These findings contribute to the understanding of the genetic overlap between schizophrenia, white matter, and cognition; however, its striking variability highlights the need of increasing sample size in order to improve risk prediction. Research on polygenic risk scores is mainly focused on functional connectivity, and scores are often derived from major depressive disorder and other major disorders. Therefore, further research is required to assess and validate these results with an explicit focus on schizophrenia. Moreover, the high polygenicity of intelligence (Davies et al., 2011) and schizophrenia (Pardiñas et al., 2018; Schizophrenia Working Group of the Psychiatric Genomics Consortium, 2014) together with the high the heritability of white matter provides a great opportunity to investigate their potential relationships due to the genetic overlap shared among these factors.

3.7.3. Genetic and environmental factors

The onset of schizophrenia has been associated with several environmental factors; migration, childhood trauma, urbanicity, substance abuse and gender are among the most commonly reported, suggesting that exposure to these factors may have an impact on the developing brain in more vulnerable life-periods. For instance, in siblings of patients diagnosed with schizophrenia, who are at higher genetic risk for developing the disorder, the psychotomimetic effects of cannabis and growing up in a urban environment are higher compared to controls (reviewed in van Os et al., 2010). Another possibility is that environment may moderate the levels of expression in a gene that is in the causal pathway to schizophrenia (van Os et al., 2008). Thus, the conceptualization that genetic or environmental influences may independently and on their own be determinants in the development of schizophrenia seems somehow reductionist. Genetic factors without an interaction with environment may be limited in their ability to comprehensibly describe schizophrenia.

3.8. Schizophrenia and accelerated white matter ageing

It has been previously suggested that schizophrenia and other disorders are characterised by accelerated ageing with an elevated rate of aging-related clinical, functional, and biological decline. In particular, schizophrenia has been postulated to increase the risk for accelerated ageing and interestingly, the literature suggests that white matter connectivity may be affected by this process.

The transition from adolescence to adulthood entails profound changes in the brain's architecture, involving synaptic elimination, dendritic pruning, and myelination. Interestingly, this period is not only characterised by these processes that constitute normal maturation, but it is also associated with the highest incidence rates of psychoses. In addition, ageing is characterised by regional changes in tissue properties and a general brain shrinkage. Thus, dynamic changes in brain structure occur in development, maturation, and aging.

Several recent studies have shown that changes in grey and white matter volumes associated with ageing are not characterised by neuronal loss but by microstructural changes in brain connectivity (reviewed in Collin and van den Heuvel, 2013). These changes include loss in myelinated fibres, alterations in fibre diameter, degeneration of myelin sheath, and morphological changes in dendritic the arbor, spines and synapses (Morrison and Hof, 1997; Paus, 2010; Peters, 2002; Salat, 2011). Consistent with this are the findings of diffusion MRI parameters across lifespan, characterised by a slow decline in FA and an increase in MD in the fourth decade until midlife and an abrupt decline in the last decade of life. White matter diffusion MRI parameters are highly heritable and describe a quadratic change for most white matter tracts, showing a rapid development in childhood followed by a slower maturation in adolescence and young adulthood, and a stabilization and/or reversal of developmental

processes during adulthood and older age (Cox et al., 2016; Hasan et al., 2010; Kochunov et al., 2015, 2012, 2011; Lebel et al., 2012; Westlye et al., 2010). These microstructural changes are thought to have an effect in information transfer and efficacy and therefore, it is possible that these age-related impairments may impact the overall functioning and organization of the brain. In particular, long cortico-cortical connections have been shown to be more susceptible to ageing (Peters and Rosene, 2003), which may underlie the reported reduced connectivity strength with advancing age. Moreover, this decline in white matter has been associated with cognitive impairments. Together, these findings suggest a link between the decline of the structural connectome and decreasing cognitive functions.

This pattern in white matter ageing seems to share certain characteristics with schizophrenia and, as noted previously, Kirkpatrick et al. (2008) suggested the conceptualization of schizophrenia as a syndrome of accelerated ageing. Significant declines in white matter coherence more than twice that of age-matched controls have been reported (Kochunov et al., 2013), with this reduction being linear from early adulthood and steeper as a function of increasing age (Cropley et al., 2017). Machine learning approaches have been used to predict the age of an individual based on MRI parameters, and when applied to patients diagnosed with schizophrenia, the authors found that the average brain-age of the patients was more than three years greater than their chronological age (Koutsouleris et al., 2014; Schnack et al., 2016). This accelerated decline in white matter may reflect the neuropathology associated with the loss of microstructural properties (e.g. loss of axonal myelin, oligodendrocytes, etc.) characteristic of the disorder.

Chapter 4 Information processing speed mediates the relationship between white matter and general intelligence in schizophrenia

4.1. Overview

This chapter investigates the relationship between a general factor for intelligence and two general factors derived from white matter diffusion parameters (FA and MD) in a sample of patients diagnosed with schizophrenia. Due to the apparent overlap between brain structure and intelligence, we hypothesised that decline in white matter structure would be linked to worse cognitive performance. In addition, information processing speed –which measures the individual's ability to perform a cognitive task– may act as a key cognitive resource facilitating higher order cognition by allowing multiple cognitive processes to be simultaneously available and therefore we hypothesised that processing speed would mediate the relationship between white matter and intelligence. These associations have not yet been studied in schizophrenia. This chapter has been published in Psychiatry Research: Neuroimaging.

This study was conceived by CA, SRC, MEB, HCW and SML. CA processed and analysed the data and wrote the manuscript. SRC, MEB, HCW and SML were the main supervisors of this project. BD and SIS collected the cognitive and imaging data. All authors reviewed the manuscript for publication.

Citation: Alloza, C., Cox, S.R., Duff, B., Semple, S.I., Bastin, M.E., Whalley, H.C., Lawrie, S.M., 2016. Information processing speed mediates the relationship between white matter and general intelligence in schizophrenia. Psychiatry Res. 254, 26–33. https://doi.org/10.1016/j.pscychresns.2016.05.008

4.2. Abstract

Several authors have proposed that schizophrenia is the result of impaired connectivity between specific brain regions rather than differences in local brain activity. White matter abnormalities have been suggested as the anatomical substrate for this

dysconnectivity hypothesis. Information processing speed may act as a key cognitive resource facilitating higher order cognition by allowing multiple cognitive processes to be simultaneously available. However, there is a lack of established associations between these variables in schizophrenia. We hypothesised that the relationship between white matter and general intelligence would be mediated by processing speed. White matter water diffusion parameters were studied using Tract-based Spatial Statistics and computed within 46 regions-of-interest (ROI). Principal component analysis was conducted on these white matter ROI for fractional anisotropy (FA) and mean diffusivity, and on neurocognitive subtests to extract general factors of white mater structure (g_{FA}, g_{MD}), general intelligence (g) and processing speed (g_{speed}). There was a positive correlation between g and g_{FA} ($r = 0.67$, $p = 0.001$) that was partially and significantly mediated by g_{speed} (56.22% CI: 0.10 to 0.62). These findings suggest a plausible model of structure-function relations in schizophrenia, whereby white matter structure may provide a neuroanatomical substrate for general intelligence, which is partly supported by speed of information processing.

4.3. Introduction

Several authors have proposed that schizophrenia is the result of impaired connectivity between specific brain regions rather than differences in local brain activity (Wernicke, 1906; Friston, 1998; Friston and Frith, 1995). This dysconnection hypothesis suggests that schizophrenia may be understood in terms of cognition and pathophysiology as aberrant brain integration (Friston, 1998). It has been suggested that abnormalities in white matter microstructure may produce the anatomical substrate for the dysconnectivity hypothesis (Alvarado-Alanis et al., 2015b; Weinberger, 1987). White matter deficits are the most consistent neuroimaging findings in this disorder and it has been shown that white matter integrity may be predictive of conversion to schizophrenia and functional outcome (reviewed in Karlsgodt et al., 2012). Furthermore, Kochunov and Hong (2014) reviewed the overlap between the developmental trajectory of cerebral white matter and the onset of schizophrenia

linking the neurodevelopmental and neurodegenerative theories with white matter as the strategic component.

Thus far, a number of studies using functional and diffusion tensor MRI (DT-MRI) have provided evidence regarding the dysconnectivity hypothesis by reporting structural and functional connectivity abnormalities between specific brain regions (Samartzis et al., 2014; Schmidt et al., 2015). The most replicated findings are fronto-temporal, corpus callosum and anterior cingulate cortex dysconnectivity to other cortical and subcortical areas (Pettersson-Yeo et al., 2011). As the symptomatology of schizophrenia is so varied, it is unlikely to be attributable to a circumscribed brain deficit, while the dysconnectivity hypothesis may be able to explain its heterogeneous and complex manifestations (Fornito et al., 2012).

Cognitive impairments are a core characteristic of schizophrenia (Elvevåg and Goldberg, 2000). For example, patients diagnosed with schizophrenia often show cognitive deficits in numerous domains, such as attention, learning, memory and executive functions (Elvevåg and Goldberg, 2000). Recent evidence suggests that differences in white matter may account for this variance in cognitive performance (Wexler et al., 2009). Complex cognitive functioning depends on synchronised activity between distributed brain networks. Thus, proper speed and efficiency of information transfer between distal brain regions relies on white matter microstructure (Turken et al., 2008). Indeed, information processing speed has been proposed as a key cognitive resource facilitating higher order cognition by allowing multiple cognitive processes to be simultaneously available (Kail and Salthouse, 1994). Individual differences in processing speed are likely to be dependent on structural variations in white matter, which facilitates and constrains communication among nodes of brain pathways (Turken et al., 2008).

Slowed information processing speed has been proposed as a potential endophenotype for schizophrenia (Antila et al., 2011). These deficits have been repeatedly reported in patients

and high risk individuals (Badcock et al., 2015; Bora et al., 2009; Dickinson D et al., 2007; Mesholam-Gately et al., 2009; Morgan et al., 2014; Muñoz Maniega et al., 2008; Rodríguez-Sánchez et al., 2007; Sprooten et al., 2011). Rodriguez-Sanchez et al. (2007) reported that when processing speed was removed from a multivariate model, the cognitive deficits observed in patients with schizophrenia were no longer significant compared with healthy controls. Furthermore, schizophrenia patients show an accelerated ageing decline in cerebral white matter linked to an accelerated decay in processing speed when compared to healthy participants in cross-sectional and longitudinal studies (Karbasforoushan et al., 2015; Kochunov et al., 2013; Liu et al., 2013; Ritchie et al., 2015). Thus, deficits in speed of information processing represent an important cognitive marker of risk (Gur et al., 2014; Seidman et al., 2010).

Two previous studies of cognitive ageing have reported that nearly half the variance in water diffusion parameters across major white matter tracts can be accounted for by a single general factor in a large cohort of healthy subjects in their seventies (Penke et al., 2012, 2010). Moreover, this general factor of white matter fractional anisotropy (FA) was positively correlated with general intelligence, and this was completely mediated by processing speed. However, whether an association between FA and general intelligence holds in schizophrenia – and is mediated by processing speed - has not yet been studied (Penke et al., 2012, 2010; Turken et al., 2008).

The aim of this paper is therefore to examine the relationship between white matter structure and general intelligence in schizophrenia and the possible attenuation effect caused by processing speed. We hypothesise that a general factor of white matter integrity can be extracted from water diffusion parameters measured in patients diagnosed with schizophrenia, and this general factor accounts for a substantial amount of variance in general intelligence, with a statistically significant portion of this variance mediated by processing speed.

4.4. Methods

Participants

Information about participants has been reported in detail previously (Whalley et al., 2015a). Participants were recruited across Scotland as part of the Scottish Family Mental Health Study. DT-MRI data were acquired from a total of 28 individuals diagnosed with schizophrenia aged between 23 and 57 years old, with the diagnosis confirmed using the structured clinical interview for DSM IV (SCID) administered by one of two trained psychiatrists (First et al., 2002). No control cohort was included in the current analysis. Exclusion criteria included any major medical or neurological conditions, or any personal history of substance misuse in the last year. Additionally, subjects were excluded if there were MRI safety considerations. A detailed description of the study and written informed consent were given to all recruited individuals. The study was approved by the Multicentre Research Ethics Committee for Scotland (09/MRE00/81).

Scan acquisition

MRI data were collected on a Siemens Magnetom Verio 3T scanner running the syngo MR B17 software (Siemens Healthcare, Erlangen, Germany). Whole brain diffusion-weighted MRI scans were acquired using a single-shot spin-echo echo-planar (EP) imaging sequence with diffusion-encoding gradients applied in 56 directions (b=1000 s/mm^2); six T_2-weighted (b=0 s/mm^2) baseline scans were collected at the beginning of the acquisition scheme. Fifty-five 2.5 mm thick axial slices were acquired with a field-of-view of 240 mm and matrix 96 × 96 giving 2.5 mm isotropic voxels. The repetition and echo times for the EP sequence were 10200 and 74 ms respectively. The examination took approximately 12 minutes.

Imaging analysis

DT-MRI data pre-processing

DT-MRI datasets were pre-processed using FSL tools (http://www.fmrib.ox.ac.uk/fsl). All volumes were aligned to the first T_2-weighted EP volume using eddy_correct. This alignment corrects for eddy current induced distortions produced by different diffusion gradient directions and head movement (Horsfield, 1999). Images were visually assessed at every stage of pre-processing. Next, brain extraction was performed using FSL's Brain Extraction Tool (BET) (Smith, 2002), which removes non-brain tissue. FMRIB's Diffusion Toolbox (FDT/FSL) (Behrens et al., 2003) was then used to fit a diffusion tensor model to the data to obtain parametric maps of FA and mean diffusivity (MD).

Tract-based Spatial Statistics (TBSS)

Whole brain statistical analysis of each subject's FA and MD data was performed using Tract-based Spatial Statistics (TBSS; Smith et al., 2007, 2006) as part of the FSL software package. First, the FA data were non-linearly registered into standard space (FMRIB58_FA) to make local comparison possible while controlling for overall white matter structure. Next, a mean of all FA volumes was obtained, and an FA skeleton created. The mean FA skeleton was thresholded at 0.2 in order to exclude voxels that were grey matter or CSF (Smith et al., 2006). Then each subject's aligned FA and MD data were projected onto the mean FA skeleton to account for misalignments between participants.

Following the protocol described by the ENIGMA consortium (http://enigma.ini.usc.edu; Jahanshad et al., 2013), an atlas-based segmentation was performed on the FA skeletons using binary masks derived from the John Hopkins University (JHU) white matter atlas available in FSL (see Figure 11). We extracted 46 white matter structures as indicated by this atlas (see Table 3). Mean FA and MD values were calculated from voxels in each subject's white matter skeleton within these regions-of-interest (ROI),

thereby minimising individual anatomical differences, registration errors and partial volume effects.

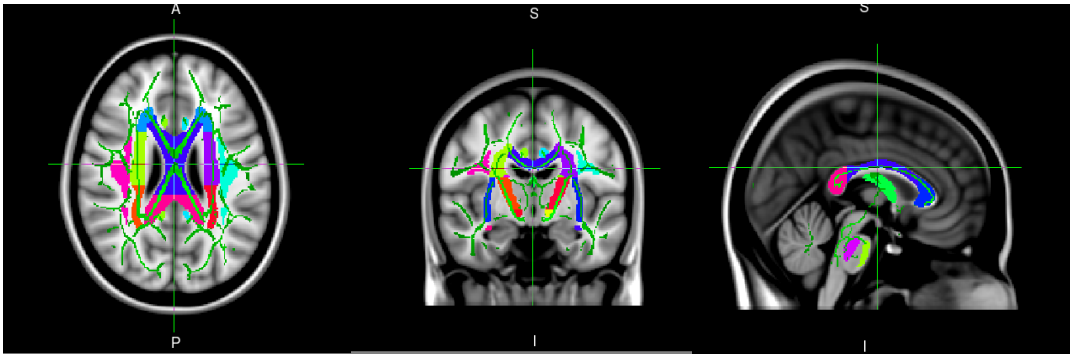

Figure 11. Axial (left), coronal (centre) and sagittal (right) views from an individual subject's white matter skeleton with ROIs provided by the JHU white matter atlas. Average white matter water diffusion parameters were obtained from these labelled regions (see Table 3).

Table 3. White matter regions analysed in this study obtained from the JHU white matter atlas.

Abbreviations	White matter tract
GCC	Genu of corpus callosum
BCC	Body of corpus callosum
SCC	Splenium of corpus callosum
FX	Fornix (column and body of fornix)
CST-R,L	Corticospinal tract
ML-R,L	Medial lemniscus
ICP-R,L	Inferior cerebellar peduncle
SCP-R,L	Superior cerebellar peduncle
CP-R,L	Cerebral peduncle
ALIC-R,L	Anterior limb of internal capsule
PLIC-R,L	Posterior limb of internal capsule
RLIC-R,L	Retrolenticular part of internal capsule
ACR-R,L	Anterior corona radiata
SCR-R,L	Superior corona radiata
PCR-R,L	Posterior corona radiata
PTR-R,L	Posterior thalamic radiation (include optic radiation)

(*Cont.*)

SS-R,L	Sagittal stratum (include inferior longitudinal fasciculus and inferior fronto-occipital fasciculus)
EC-R,L	External capsule
CGC-R,L	Cingulum (cingulate gyrus)
CGH-R,L	Cingulum (hippocampus)
FX/ST-R,L	Fornix / Stria terminalis (cannot be resolved with current resolution)
SLF-R,L	Superior longitudinal fasciculus
SFO-R,L	Superior fronto-occipital fasciculus
IFO-R,L	Inferior fronto-occipital fasciculus
UNC-R,L	Uncinate fasciculus

Note: R: right, L: left.

Cognitive testing

Patients underwent cognitive assessment using tests from the Brief Assessment of Cognition in Schizophrenia (BACS; Keefe et al., 2004), Cambridge Neuropsychological Test Automated Battery (CANTAB; Robbins et al., 1994), Wechsler Adult Intelligence Scale (WASI; Wechsler, 1955) and the National Adult Reading Test (NART; Nelson and Willison, 1991) using standard administration and scoring procedures. Participants also provided information on antipsychotic medication which was transformed into chlorpromazine equivalents (CPZ) (Woods, 2003).

To calculate a general intelligence factor, we used the raw scores of Symbol Coding and Digit Sequencing from the BACS, Spatial Working Memory from the CANTAB, Block Design and Matrix Reasoning from the WASI and Vocabulary from the NART. These tests were selected because they represent different cognitive domains and for their high reliability; though the general intelligence factor appears to remain constant, irrespective of the specific tests used (Johnson et al., 2004). The tests used for the calculation of the processing speed factor are shown in Table 4.

Table 4. Individual cognitive tests used for the calculation of general intelligence (*g*) and information processing speed (g_{speed}). The table describes the cognitive domain each test represents and the outcome measure of each test.

	Outcome measure
General intelligence factor	
Digit Sequencing [a]	Number of correct responses and longest sequence recalled
Spatial Working Memory [b]	Number of correct responses
Block Design [c]	Number of correct responses in increasing complexity and limit of time
Matrix Reasoning [c]	Number of correct responses
Vocabulary [d]	Total number of errors
Processing speed factor	
Symbol Coding [a]	Number of correct responses in 90 s
Reaction Time 5-Choice [b]	Response latency and movement time
Reaction Time task [b]	Response latency and movement time

[a]Tests from the BACS; [b]from the CANTAB; [c]from the WASI; [d]from the NART.

Statistical analysis

Principal component analysis (PCA) was performed on all FA and MD ROI data and cognitive task raw scores. Specifically, we ran a separate PCA for each of FA, MD, general intelligence and processing speed. All PCA was performed with no rotation and age was partialed from all the general factors. For the calculation of the PCA for white matter diffusion parameters we took a highly conservative approach by entering left and right tracts separately (rather than averaging the tracts in both hemispheres), which results in a greater degree of potentially residual left-right variance which may not necessarily be explained by a first component. Using this form of data reduction allows the relatively robust quantification of an

underlying construct which is theoretically being measured to a large degree by all entered terms. Thus, test-specific error variance (and also some other test-specific variance) present in the scores of each individual cognitive test are theoretically excluded from the resultant component score. For instance, diffusion measures of white tracts across the brain tend to be highly collinear. A latent score of FA therefore captures this tendency, quantifying the general level of FA for each participant which is shared across all tracts (such that those with a higher gFA tend to have generally higher FA across all tracts). In order to conserve data points, we imputed those values where missingness was ≤ 40% using multiple imputation in SPSS version 20.0 (www.ibm.com/software/analytics/spss). Missing data was random for participants with ≤ 40% of missing data (Little's MCAR test $p>0.05$). For participants who were not able to complete cognitive testing (missingness > 40%) imputation was not performed.

The tests used in this study were partly determined by the distribution of the data and outliers and partly by the type of data obtained from TBSS. Partial correlational analyses were used to study possible relationships between the white matter (FA and MD) and cognitive factors (general intelligence and processing speed) controlling for age. Mediation analysis was then used to examine the hypothesis that impaired white matter integrity is related to poorer general intelligence via processing speed. We employed the MEDIATE macro in SPSS 20.0 (Hayes and Preacher, 2014) to formally quantify mediation effects using 5000 bootstrapped samples. Due to our clear directional hypothesis, one tailed test of mediation was conducted (http://www.afhayes.com). Mediation effects were considered significant if the confidence interval did not include zero (Preacher and Hayes, 2008). Results were considered significant at $P < 0.05$ for bivariate analyses. All statistical analyses were performed with SPSS version 20.0, with age as a covariate in all analyses.

4.5. Results

Demographics

Characteristics and cognitive scores of the sample are presented in Table 5.

Table 5. Demographic and cognitive scores for each subtest used in the calculation of principal factors.

	Mean (SD)
Age in years	39.0 (10.1)
Antipsychotic medication [a]	434.9 (371.9)
Gender (%) F:M	57.1 : 42.9
5-Choice Reaction Time (ms)	401.7 (91.7)
Block Design	43.3 (15.8)
Digit Sequencing	21.7 (4.6)
Matrix Reasoning	26.3 (4.8)
Reaction Time task Simple (ms)	560.2 (155.9)
Spatial Working Memory	30.0 (18.8)
Symbol Coding	49.1 (12.1)

[a] Measured using CPZ equivalents (Woods, 2003)

Principal component analyses

General white matter factors

The results for FA showed a clear principal component; the first unrotated component explained 46.4% of the variance among all white matter regions. The left uncinate showed the lowest loading (r = 0.408), while the right superior corona radiata showed the highest (r = 0.863). The principal component for MD explained 53.8% of the variance. The left superior fronto-occipital fasciculus showed the lowest loading (r = 0.351), while the right superior corona radiata showed the highest (r = 0.918). The pattern of tract loadings did not exhibit any

clear pattern (strongest-weakest) based on tract functionality or hemisphere. While we found no influence of the number of voxels on mean levels of FA or MD measured for each tract, smaller tracts exhibited a significantly greater variability in their estimates across participants for FA (r = 0.729, p < 0.001) and MD (r = -0.636, p < 0.01). All loadings are presented in Appendix I Supplementary Tables 1 and 2. Scree plots of the PCAs for FA and MD are presented in Appendix I Supplementary Figures 1 and 2.

General cognitive factors

There was a clear principal component for general intelligence which explained 63.83% of the variance, with all loadings > 0.7. The general processing speed factor showed a clear first component which explained 57.51% of the variance, with all loadings > 0.6. Higher values on this factor indicate slower information processing speed. The loadings are presented in Appendix I Supplementary Tables 3 and 4. Scree plots of the general factor for general intelligence and processing speed are presented in Appendix I Supplementary Figures 3 and 4.

Correlational analyses

Partial correlations are presented in Figure 12. Accounting for age, we found that the general intelligence factor was significantly positively correlated with the general FA factor, sharing over half the variance (r = 0.667; p =0.001; R^2 = 0.445). There was no significant association between the general MD factor and general intelligence (r = -0.212; p > 0.05; R^2 = 0.045). General factors of FA and processing speed showed a significant correlation (r = -0.626, p < 0.001) but not between the general factors of MD and processing speed (r = 0.197, p > 0.05). The negative correlation between FA and processing speed indicates that generally less coherent water diffusion (lower FA) across all measured tracts is associated with slower processing speed. Even though the correlations with MD were non-significant they were in the expected direction. Antipsychotic medication (CPZ equivalents) and gender were not

significantly associated with any of the variables studied.

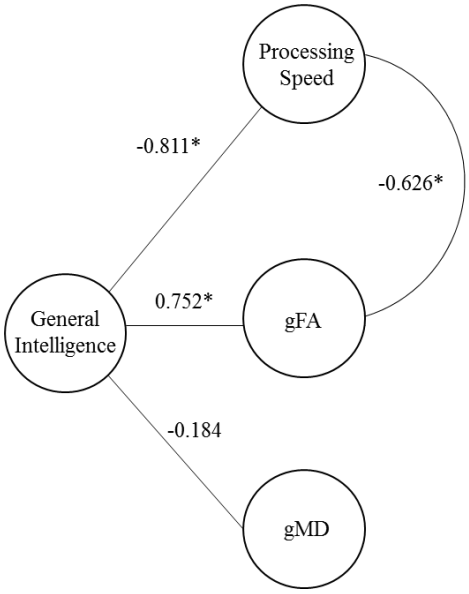

Figure 12 Partial correlations between the main variables analysed, controlled for age. The numbers indicate the correlation coefficient between each pair of variables. Note that higher values of g_{speed} indicate slower processing speed (less favourable). *$p < 0.05$. g_{FA} and g_{MD} are the general FA and MD factors.

Mediation analysis

The results of these bivariate associations indicate that FA-processing speed-intelligence is a viable candidate for mediation analysis. As illustrated in Figure 13A, we tested whether the direct effect of white matter FA and intelligence was significantly mediated by processing speed (i.e. magnitude of change from path c to path c'). The results are shown in Figure 13B. A bias-corrected bootstrap confidence interval for the indirect effect (c' = 0.142, $p = 0.292$) based on 5000 bootstrap samples served as a formal statistical test of the degree to which processing speed mediated the relationship between FA and intelligence. The change in magnitude (0.667 to 0.292; 56.22%) was significant (confidence intervals entirely above zero; 0.1025 to 0.6165). There was no significant mediation effect for MD-processing speed-intelligence (90% CI (-0.4030 to 0.2003)).

We further analysed the possible mediation effect of age in the associations between FA, general intelligence and processing speed. There was a significant mediation effect of age in the association between the FA and processing speed 90% CI (-0.2733 to -0.0011) but not between FA and general intelligence (90% CI (-0.0293 to 0.0013)). Thus, results from mediation analysis shown above are controlled for age due to its significant effect on white matter parameters and cognitive performance.

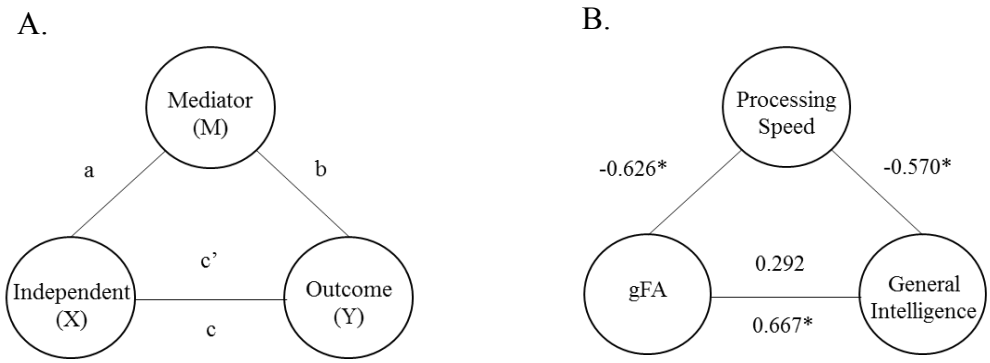

Figure 13. A) Schematic representation of relationships where an independent variable (*X*) and an outcome (*Y*) are hypothesised to be explained by a mediator (*M*). The direct effect of *X* on *M* is *a*, the effect of *M* on *Y* is *b*, and *c* the effect of *X* on *Y*. *c'* denotes the effect of *X* on *Y* when *M* is taking into account in the model. B) Representation of the variables analysed in this study, where X= the general FA factor (g_{FA}), Y= General intelligence and M= Processing speed. Asterisks represent statistically significant partial correlations.

4.6. Discussion

Our aim was to investigate possible associations between general intelligence, processing speed and structural brain parameters in a clinical cohort diagnosed with schizophrenia. We did this by adopting a recently established approach taken in non-pathological ageing research described by Penke et al. (2010). Their results suggest that individual differences in white matter water diffusion measures are, to some extent, common

across tracts in older age, and that this common variance is cognitively meaningful. In the current study, we have shown that the same phenomenon seems to occur in schizophrenia, with white matter FA correlating with general intelligence through speed of information processing. For instance, the fact that the general FA factor accounts for a large proportion of the shared variance between tracts indicates that when one has high FA in one tract, there is a strong tendency to also exhibit high FA in all other tracts included in the PCA. Similarly, for general intelligence, the high degree of shared variance between tests reflects the fact that individuals who perform well on one test tend to perform well on others. Thus, associations between general FA and general intelligence indicate that having a generally higher level of cognitive performance, relative to the other participants included in the cognitive PCA, is associated with having generally higher FA across the tracts included in the PCA. In the context of the dysconnectivity hypothesis, these findings suggest a plausible model of structure-function relations in schizophrenia, where white matter structure may provide a neuroanatomical substrate for general intelligence, which is partly supported by speed of information processing within brain networks.

Results showed that the right superior corona radiata has the highest communality for FA and MD, suggesting that this tract shares the highest amount of variance with all other white matter tracts. On the other hand, the left uncinate and left superior fronto-occipital fasciculus for FA and MD, respectively, shared the lowest amount of variance with all other tracts. These results indicate that, while there was clearly a strong tendency for all tracts measured to share variance in diffusion characteristics, not all white matter tracts exhibited this general tendency to the same degree.

In the current study, we found that correlations of white matter DT-MRI biomarkers and cognitive variables were stronger for FA than MD, though both were in the expected directions. These two parameters provide distinct, but complementary information about the

diffusion of water molecules *in vivo*. Thus, our findings indicate that cognitive abilities in our schizophrenia participants were more strongly related to the directional coherence of water diffusion than to its general magnitude. It has been suggested that FA is highly sensitive to a variety of subtle microstructural changes, whereas MD more specifically represents an inverse measure of membrane density and fluid viscosity (Alexander et al., 2011), though diffusion data in isolation precludes a direct inference on specific microstructural tissue properties which underlie the associations reported herein.

We found that the correlation between general intelligence and FA was higher (R^2 = 0.445) than that reported by Penke et al. (2012, 2010) who found that approximately 10% of the variance in general intelligence was accounted for by a general white matter factor in a study of generally healthy older subjects in their seventies. Consistent with functional and structural data, our findings suggest that patients with schizophrenia present a broader distribution of white matter networks associated with cognitive performance (Tan et al., 2006; Voineskos et al., 2013). Therefore, subtle perturbations in vulnerable networks may more dramatically affect cognitive performance in this disorder, potentially due to decreased cognitive reserve. This hypothesis is supported by several authors (reviewed in Tucker-Drob, 2009) who propose a model of ability differentiation in which intercorrelations between cognitive tests are higher in those subjects with lower IQ. Detterman and Daniel (1989) postulate that subjects with cognitive deficits experience impairments in central processes by limiting the efficiency of all other processes in the system. Thus, these participants will perform more uniformly on cognitive tests, whereas, subjects without deficits will show more variable performance as their central processes remain intact. Nevertheless, the sample size of the current study hampers our ability to make an accurate and definitive estimate of the precise magnitude of association between intelligence and white matter microstructure in schizophrenia, and it is likely that larger samples would provide a more readily-generalizable estimate.

There is an increasing interest in correlating measures of higher cognitive functions with structural and functional features of individual brain regions (Jung and Haier, 2007). Some neural correlates have been described, suggesting that the interaction between parietal and frontal brain regions sustained by efficacious white matter tracts supports individual intelligence differences (Jung and Haier, 2007; Ritchie et al., 2015). Processing speed has been proposed as a key cognitive resource, an intermediate between brain structure and cognition. Prior studies have noted the importance of white matter coherence for synchronised brain activity. Impairments in white matter structure may be the result of neurodevelopmental or degenerative processes which ultimately affect brain connectivity (Davis et al., 2003; Wright et al., 2015). Thus, appropriate performance in processing speed relies on white matter coherence. Lower cerebral FA and lower speed of information processing are highly replicable findings in schizophrenia that are likely interlinked (Wright et al., 2015), yet this is the first study to examine whether such relationships might partly underpin intellectual ability in schizophrenia.

The dysconnectivity hypothesis proposed for schizophrenia is often characterised by impairments in white matter coherence. General disturbances in neural networks caused by white matter disruptions could account for the key global characteristics of the illness, including cognitive deficits (Knowles et al., 2010; White et al., 2011). Moreover, this dysconnectivity leads to an impaired speed of information processing which may also influence other cognitive functions (de Weijer et al., 2011; McCarthy-Jones et al., 2015). Thus, the dysconnectivity hypothesis may be in keeping with the diverse spectrum of deficits and symptoms observed in schizophrenia.

Processing speed and white matter coherence decline during normal ageing. It has been suggested that this decline in processing speed is caused by a reduction in the propagation of action potentials across cortical networks (Wright et al., 2015). In recent years, several

authors (Friedman et al., 2008; Mori et al., 2007; Phillips et al., 2012; Wright et al., 2015, 2014) have reported that schizophrenia patients show a more pronounced ageing of white matter compared with controls. This might be a rational line of enquiry for future studies using the approach described here. Furthermore, increased cognitive decline has been described in subjects with high genetic risk for schizophrenia (McIntosh et al., 2013). Another potential hypothesis is that relationships between white matter microstructure and processing speed are driven by share genetic factors which influence variations in FA and processing speed. For example, Kochunov et al. (2016) suggest that common genetic variations that contribute to white matter integrity may also sustain their associated cognitive performance. These two phenotypes may be uncovering the genetic risk factors for schizophrenia where reduced FA and decreased speed of information processing are consistently reported and thought to be interlinked (Ellison-Wright and Bullmore, 2009; Penke et al., 2010; Rodríguez-Sánchez et al., 2007).

Previous studies have examined the association between intelligence and white matter structure in healthy controls, albeit usually with respect to individual cognitive tests and/or individual white matter tracts (Nestor et al., 2010, 2008; Ohtani et al., 2014b; Pérez-Iglesias et al., 2010; Ritchie et al., 2015; Royle et al., 2013; Yamawaki et al., 2015). This is the first time, to our knowledge, where principal components of white matter water diffusion parameters and a broad variety of cognitive domains have been analysed in a clinical cohort diagnosed with schizophrenia. We report results which suggest that a common white matter integrity factor provides the neuroanatomical substrate for a general intelligence factor, partly mediated by speed of information processing within brain networks.

4.7. Limitations

This study was limited by being unable to assess whether the relationship between white matter water diffusion parameters and general intelligence also exists in a fully-matched control cohort of similar size; therefore, it is unknown if the effects found in patients are analogous or dissimilar to healthy participants, beyond the older non-pathological samples analysed elsewhere. Moreover, this is a cross-sectional study; thus, it is difficult to make any causal inference based on these results. Also, the patients sample size is relatively small by contemporary standards raising the possibility of Type II error. Given the relatively small sample size we choose to control for age rather than examine its effects.

One potential criticism is the use of PCA in such a small sample with large number of variables, especially for several white matter tracts. However, it has been suggested that considering the variables-to-observations ratio is not an optimal way to determine the suitability of applying such data reduction techniques to small sample sizes, particularly in instances where the variables in question exhibit a high degree of collinearity (de Winter et al., 2009; Preacher and MacCallum, 2002). Both the cognitive and DT-MRI data exhibit a clear first component with high loadings and explained variance comparable to prior studies using similar data in larger samples (Penke et al., 2012, 2010). PCA allows the quantification of important tendencies in the data, and the resulting latent measures (principal components, in this case) have the advantage of excluding error variance specific to each individual measure, mitigating for instance the higher variability found in smaller tracts. However, this method also necessarily excludes variance specific to individual white matter tracts or cognitive tests which may also be of interest. For instance, we did only analyse the first component of each PCA, excluding other components that may be of interest in the future.

However, we chose to study the first component since it explains by far the largest amount variance compared to the rest. We also acknowledge the limitation inherent to TBSS in that it only includes the centre of the white matter tracts common to all participants, and that the estimates of the smaller ROIs may be less reliable (though they did not exhibit systematically different diffusion estimates, they did exhibit greater SD). Nevertheless, when this point is considered with the lack of power and possibility of redundant hypothesis testing (and the increased multiple comparisons and necessary correction that this entails), we believe this statistical approach is the most suitable, but clearly precludes direct comment on the nature of tract- and test- specific effects.

4.8. Acknowledgements

We would like to thank all the participants who took part in this study and the radiographers who acquired the MRI data at the Clinical Research Imaging Centre, University of Edinburgh (http://www.cric.ed.ac.uk). We are also grateful to Professor Edwin van Beek for assistance with overall co-ordination of the study and for radiological reporting of the structural MRI scans. The investigators also acknowledge the financial support of National Health Service (NHS) Research Scotland, through the Scottish Mental Health Research Network (http://www.smhrn.org.uk) who provided assistance with subject recruitment and cognitive assessments. This work was supported by an award from the Translational Medicine Research Collaboration – a consortium made up of the Universities of Aberdeen, Dundee, Edinburgh and Glasgow, the four associated NHS Health Boards (Grampian, Tayside, Lothian, and Greater Glasgow and Clyde), Scottish Enterprise and Pfizer, who have reviewed and approved the manuscript. Imaging aspects also received financial support from the Dr Mortimer and Theresa Sackler Foundation. The authors would also like to thank Dr. Thorsten Feiweier from Siemens Healthcare for providing the prototype diffusion sequence used in this study.

4.9. Chapter discussion

This chapter offers valuable data on the relationship between general intelligence and brain structure in schizophrenia. These results suggest that patients with schizophrenia present a broader distribution of white matter networks associated with cognitive performance whereby subtle perturbations in vulnerable networks may more dramatically affect cognitive performance, potentially due to decreased cognitive reserve. Taken all together, our results suggest that in schizophrenia, white matter structure may provide a neuroanatomical substrate for general intelligence, which is partly mediated by speed of information processing within brain networks.

Chapter 5 Central and non-central networks, cognition, clinical symptoms and polygenic risk scores in schizophrenia

5.1. Overview

This chapter focuses on the study of two subnetworks derived from the connectome and their associations with the pathophysiology of schizophrenia in a sample comprised by patients and healthy controls. Using graph theory metrics obtained from the average network, this chapter also investigates the topological characteristics of the brain and their relationships with intelligence, symptoms and genetics. The paper is published in the journal Human Brain Mapping.

This study was conceived by CA, SRC, MEB, HCW and SML. CA analysed the data and wrote the manuscript. SRC, MEB, HCW and SML were the main supervisors of this project. MEB processed the imaging data and calculated the graph theory metrics. JG created the polygenic risk scores. BD and SIS collected the cognitive and imaging data. All authors reviewed the manuscript for publication.

Citation: Alloza, C., Bastin, M.E., Cox, S.R., Gibson, J., Duff, B., Semple, S.I., Whalley, H.C., Lawrie, S.M., 2017. Central and non-central networks, cognition, clinical symptoms, and polygenic risk scores in schizophrenia. Hum. Brain Mapp. https://doi.org/10.1002/hbm.23798

5.2. Abstract

Schizophrenia is a complex disorder that may be the result of aberrant connections between specific brain regions rather than focal brain abnormalities. Here, we investigate relationships between brain structural connectivity as described by network analysis, intelligence, symptoms and polygenic risk scores (PGRS) for schizophrenia in a group of patients with schizophrenia and a group of healthy controls. Recently, researchers have shown

an interest in the role of high centrality networks in the disorder. However, the importance of non-central networks still remains unclear. Thus, we specifically examined network-averaged fractional anisotropy (mean edge weight) in central and non-central subnetworks. Connections with the highest betweenness centrality within the average network (>75% of centrality values) were selected to represent the central subnetwork. The remaining connections were assigned to the non-central subnetwork. Additionally, we calculated graph theory measures from the average network (connections that occur in at least 2/3 of participants). Density, strength, global efficiency and clustering coefficient were significantly lower in patients compared with healthy controls for the average network ($p_{FDR} < 0.05$). All metrics across networks were significantly associated with intelligence ($p_{FDR} < 0.05$). There was a tendency towards significance for a correlation between intelligence and PGRS for schizophrenia ($r = -0.508$, $p = 0.052$) that was significantly mediated by central and non-central mean edge weight and most graph metrics from the average network. These results are consistent with the hypothesis that intelligence deficits are associated with a genetic risk for schizophrenia which is mediated via the disruption of distributed brain networks.

5.3. Introduction

Schizophrenia is a neuropsychiatric disorder characterised by delusions, hallucinations, absence of function and cognitive impairments. It is increasingly seen as the result of aberrant connections between specific brain regions rather than focal brain abnormalities (Friston, 1998; Friston and Frith, 1995; Stephan et al., 2009, 2006). The dysconnectivity hypothesis of schizophrenia suggests that abnormal brain integration may underlie the cognitive profile and symptoms found in the disorder. There is consistent evidence supporting reduced levels of overall structural connectivity in schizophrenia using diffusion tensor MRI (DT-MRI) with frontal, parietal and temporal projections being the most consistently impaired in the disorder (Skudlarski et al., 2010; van den Heuvel et al., 2010; van

den Heuvel and Fornito, 2014; Zalesky et al., 2011). Additionally, more specific white matter alterations in the uncinate fasciculus, corpus callosum, cingulum and arcuate fasciculus are consistently described (reviewed in Burns et al., 2003; Ellison-Wright and Bullmore, 2009; McIntosh et al., 2005). Even though a number of studies have discussed the importance of white matter impairments in schizophrenia, there is still no consensus on how to measure structural dysconnectivity in the disorder. One approach is to characterise how impairments in white matter microstructure affect the organization of the structural connectome using graph theory, which conceives the brain as a network composed of nodes and the connections (edges) between them (Bullmore and Sporns, 2009).

Graph theory segregation measures, such as clustering coefficient and modularity, are reportedly altered in schizophrenia (Alexander-Bloch et al., 2010; van den Heuvel et al., 2013; van den Heuvel and Fornito, 2014; Zalesky et al., 2011) suggesting a more segregated pattern of network organization. In line with this hypothesis, numerous authors have found longer path lengths and reductions in communication efficiency, proposing reduced communication between more segregated areas of the brain (reviewed in van den Heuvel and Fornito, 2014).

Nodes and edges can be associated with peripheral or more central tasks, depending on their degree of connectivity and their position within or between modules (Sporns, 2011). Nodes characterised by high degree and high centrality are termed ‘hubs’. Several lines of investigation have suggested that topological organization of hub nodes appear to be altered in schizophrenia. Both structural covariance and structural connectivity studies in schizophrenia suggest a less hierarchical organization, a less prominent role of high degree hub regions such as the prefrontal and parietal cortex, while non-frontal hubs emerge more prominently (Bassett et al., 2008; Collin et al., 2013; Zhang et al., 2012). Rubinov et al.

(2009a) suggested that a characteristic of the disorder is a randomization of connections, an alteration of community structure which results in impaired integration and segregation, and reduced centrality of cortical hubs. Most brain imaging studies in schizophrenia focus on these effects in networks with high centrality while the remaining connections are overlooked (Collin et al., 2014; Schmidt et al., 2016). Due to the apparent hierarchical disorganization of the brain in schizophrenia the role of these central nodes may be displaced to other brain regions or networks. Thus, in this study we address specifically networks based on centrality to investigate this hypothesis. Even though the cognitive and symptomatic implications of various network metrics have been addressed, there has been little discussion about the role of non-central networks in the disorder.

Schizophrenia is associated with cognitive deficits; some correlations between intelligence and the brain's function and structure have been described in healthy participants. Although there are a small number of established associations between intelligence and brain basic structural parameters, such as fractional anisotropy (FA), the relationship between the observed white matter alterations in schizophrenia and intelligence remains unclear. However, graph theory metrics may be able to provide greater explanatory power for these cognitive deficits in schizophrenia than more traditional structural connectivity measures, such as FA (Alloza et al., 2016). There is some evidence that structural network metrics are related to intelligence and that there is a degree of shared genetic overlap between schizophrenia and these measures. For instance, Li et al. (2009) found significant correlations between intelligence and network properties in a healthy cohort of subjects. Specifically, higher intelligence scores were associated with shorter path lengths and higher global efficiency. Yeo et al. (2016) showed that global measures of increased characteristic path length and reduced overall connectivity predicted lower general intelligence in a group of patients with schizophrenia, while van den Heuvel et al. (2009b) also found a strong negative correlation

between characteristic path length and IQ suggesting that more efficiently connected brains tend to show higher levels of intelligence. Hence, graph theory metrics may provide an insight into the underlying brain structural substrate for intelligence.

Differences in structural connectivity are useful for establishing brain topology abnormalities in schizophrenia compared with healthy participants. However, as our aim is to shed light on the clinical manifestation of schizophrenia we therefore examine the extent to which clinical symptoms are associated with brain extracted measures. What we know about brain connectivity and clinical symptoms is largely based upon empirical studies that investigate the relationship between white matter and different symptom's scales. For instance, FA of specific white matter tracts has been significantly associated with positive symptoms in the disorder. These tracts include the internal capsule, fronto-occipital fasciculus, superior longitudinal fasciculus, cingulum and corpus callosum (Mitelman et al., 2007; Rotarska-Jagiela et al., 2008; Seok et al., 2007). To date, several authors have examined the effects of graph theory metrics of connectivity on symptomatology in schizophrenia. Positive symptom severity has been associated with reduced overall connectivity, increases and decreases in structural and functional coupling, strength of temporal and frontal regions, reduced network efficiency and reduced clustering (reviewed van den Heuvel and Fornito, 2014). Wang et al. (2012b) found significant associations between global efficiency and positive, negative and total symptoms. However, most studies focus on functional connectivity determined using fMRI and thus, uncertainty remains regarding the relationship between structural connectivity measured in central, non-central and average networks and genetic risk factors.

Graph theory analysis has shown that impairments present in patients with schizophrenia are also found in their relatives suggesting a genetic basis (Clemm von Hohenberg et al., 2014; Collin et al., 2014; Skudlarski et al., 2013). Moreover, topological

network properties have been found to be heritable (see Thompson et al., 2013). For instance, in white matter FA, the variance explained by genetic factors has been reported to be between 75-90% in almost every white matter tract (Chiang et al., 2011). Moreover, in the same study, heritability of FA was associated with the level of IQ. Genome-wide association studies (GWAS) have indicated a polygenic component of schizophrenia with hundreds of common alleles of small effect at the population level having been reported (International Schizophrenia Consortium et al., 2009; Schizophrenia Working Group of the Psychiatric Genomics Consortium, 2014). Thus far, only a small number of studies have analysed the relationship between polygenic risk scores (PGRS), neuroimaging biomarkers and/or cognition (Birnbaum and Weinberger, 2013; McIntosh et al., 2013; Whalley et al., 2015b). Connectomic measures are, potentially, possible intermediate phenotypes between genetic liability and cognitive deficits in schizophrenia.

In the current study we investigate relationships between brain structural connectivity described by network-averaged FA (mean edge weight) measured in central and non-central networks and by graph theory metrics calculated from the average network (defined as networks in which connections that occur in at least 2/3 of participants are retained) in relation to intelligence, clinical symptoms and PGRS for schizophrenia in patients with schizophrenia and healthy controls. We will focus on graph theory metrics that have been consistently reported to be impaired in schizophrenia, namely mean edge weight, density, strength, clustering coefficient and global efficiency in the average network. Due to the severely affected hierarchical disorganization of the brain found in schizophrenia, our aim is to investigate the roles central and non-central network mean edge weight play in this disorder. Thus, this is the first study where intelligence, symptoms and PGRS have been studied together in relation to networks based on their centrality. Specifically, we hypothesized that impaired structural organization of the networks (decreased mean edge weight, density, strength, clustering coefficient and global efficiency) will be associated with lower intelligence, higher genetic risk factor for schizophrenia and higher symptom score.

5.4. Methods

Participants

Information about participants has been reported in detail previously (Whalley et al., 2015). Participants were recruited across Scotland as part of the Scottish Family Mental Health Study. DT-MRI data were acquired from a total of 28 individuals diagnosed with schizophrenia and 36 healthy controls. Diagnosis of schizophrenia was confirmed using the structured clinical interview for DSM IV (SCID) administered by one of two trained psychiatrists (First et al., 2002). Exclusion criteria included any major medical or neurological conditions, or any personal history of substance misuse in the last year. Additionally, subjects were excluded if there were MRI safety considerations. A detailed description of the study and written informed consent were given to all recruited individuals. The study was approved by the Multicentre Research Ethics Committee for Scotland (09/MRE00/81).

Scan acquisition

All imaging data were collected on a MAGNETOM Verio 3T MRI scanner running Syngo MR B17 software (Siemens Healthcare, Erlangen, Germany). For each subject, whole brain DT-MRI data were acquired using a prototype single-shot spin-echo echo-planar (EP) imaging sequence with diffusion-encoding gradients applied in 56 directions (b=1000 s/mm^2) and six T2-weighted (b=0 s/mm^2) baseline scans. Fifty-five 2.5 mm thick axial slices were acquired with a field-of-view of 240 × 240 mm and matrix 96 × 96 giving 2.5 mm isotropic voxels. In the same session, a 3D T1-magnetization-prepared rapidly acquired gradient-echo (MPRAGE) volume was acquired in the coronal plane with 160 contiguous slices and 1 mm isotropic voxel resolution.

Image analysis

Image processing

Each 3D T1-weighted MPRAGE volume was parcellated into 85 (Desikan-Killiany atlas; Desikan et al., 2006) and 165 (Destrieux atlas) regions-of-interest (ROI) using FreeSurfer (http://surfer.nmr.mgh.harvard.edu). The results of the segmentation procedure were then used to construct grey and white matter masks for use in network construction and to constrain the tractography output as described below. Using tools provided by the FDT package in FSL (http://fsl.fmrib.ox.ac.uk/fsl), the DT-MRI data were pre-processed to reduce systematic imaging distortions and bulk subject motion artifacts by affine registration of all subsequent EP volumes to the first T2-weighted EP volume (Jenkinson and Smith, 2001). Skull stripping and brain extraction were performed on the registered T2-weighted EP volumes and applied to the FA volume calculated by DTIFIT in each subject (Basser and Pierpaoli, 1996; Smith, 2002). The neuroanatomical ROIs determined by Freesurfer were then aligned from 3D T1-weighted volume to diffusion space using a cross-modal nonlinear registration method. As a first step, linear registration was used to initialize the alignment of each brain-extracted FA volume to the corresponding FreeSurfer extracted 3D T1-weighted brain volume using a mutual information cost function and an affine transform with 12 degrees of freedom (Jenkinson and Smith, 2001). Following this initialization, a nonlinear deformation field based method (FNIRT) was used to refine local alignment (Andersson et al., 2007). FreeSurfer segmentations and anatomical labels were then aligned to diffusion space using nearest neighbour interpolation.

Tractography

Whole-brain probabilistic tractography was performed using FSL's BedpostX/ProbTrackX algorithm (Behrens et al., 2007). Probability density functions, which describe the uncertainty in the principal directions of diffusion, were computed with a two-fibre model per voxel (Behrens et al., 2007). Streamlines were then constructed by sampling

from these distributions during tracking using 100 Markov Chain Monte Carlo iterations with a fixed step size of 0.5 mm between successive points. Tracking was initiated from all white matter voxels (Buchanan et al., 2014) and streamlines were constructed in two collinear directions until terminated by the following stopping criteria designed to minimize the amount of anatomically implausible streamlines: (i) exceeding a curvature threshold of 70 degrees; (ii) entering a voxel with FA below 0.1 (Verstraete et al., 2011); (iii) entering an extra-cerebral voxel; (iv) exceeding 200 mm in length; and (v) exceeding a distance ratio metric of 10. The distance ratio metric (Bullitt et al., 2003), excludes implausibly tortuous streamlines. For instance, a streamline with a total path length 10 times longer than the distance between end points was considered to be invalid. The values of the curvature, anisotropy and distance ratio metric constraints were set empirically and informed by visual assessment of the resulting streamlines.

Network construction

FA-weighted networks were constructed by recording the mean FA value along streamlines connecting all ROI (network node) pairs. The endpoint of a streamline was considered to be the first grey matter ROI encountered when tracking from the seed location.

In this study we assume the existence of a central subnetwork that is shared across participants (Reijmer et al., 2016). To identify this central subnetwork, the average brain network across both patients and controls was determined by including those connections which occurred in more than 2/3 of the participants (de Reus and van den Heuvel, 2013). Connections with the highest centrality (the fraction of all shortest paths in the network that contain a given connection, also referred as "edge betweenness centrality") within this average network (> threshold value of 75 %) were selected and used to create a mask representing the central subnetwork. The remaining connections were assigned to the non-central subnetwork

mask. Therefore, connections with high values of centrality are involved in a large number of shortest paths and as a consequence contribute to the global efficiency of the network. These masks were then used as templates and applied to each participant's connectivity matrix to select central and non-central subnetworks. Since the threshold value of 75% is arbitrary, analyses were repeated for thresholds of 25 and 50 % of connections with highest centrality.

Organizational properties of the different networks were then obtained using the brain connectivity toolbox (www.brain-connectivity-toolbox.net). For each FA-weighted connectivity matrix for the average network, five global network measures were computed, namely: mean edge weight (mean value of FA across the network), density (the fraction of present connections to possible connections), strength (the average sum of weights per node), clustering coefficient (fraction of triangles around a node) and global efficiency (the average of the inverse shortest path length). As a result of possible alterations in topology when extracting central and non-central networks, only mean edge weight was computed for these subnetworks (Reijmer et al., 2016).

Polygenic risk score calculation

PGRS is a method to aggregate the small effects that contribute to the liability of schizophrenia on predicting the disorder. The capacity to predict onset of schizophrenia has been established and has been reported to explain up to 7% of additive genetic liability for the disorder (Schizophrenia Working Group of the Psychiatric Genomics Consortium, 2014). PGRS for schizophrenia were created for all individuals with suitable genotype data; only genotypes passing stringent quality control were used in analyses. PGRS for schizophrenia were estimated using summary data from an independent GWAS of schizophrenia in 150064 individuals (36989 cases and 113075 controls), conducted by the Psychiatry Genomics Consortium (Schizophrenia Working Group of the Psychiatric Genomics Consortium, 2014).

PGRS were estimated using the PRSice software package according to previously described protocols (Euesden et al., 2015), with linkage disequilibrium and distance thresholds for clumping of $r^2 = 0.2$ and within a 300kb window. Five scores were created for each individual using single-nucleotide polymorphisms (SNPs) selected according to the significance of their association with the phenotype at nominal p-value thresholds of 0.01, 0.05, 0.1, 0.5 and 1.0 (all SNPs). For the analysis we used the threshold of 0.5 which explained the most variance in our data and has been reported to maximally capture schizophrenia liability (International Schizophrenia Consortium et al., 2009). The four multidimensional scaling factors were entered as additional 'nuisance' covariates to control for population stratification, along with age.

Cognitive testing and medication

Participants underwent cognitive assessment using tests from the Wechsler Adult Intelligence Scale (WASI; Wechsler, 1955) using standard administration and scoring procedures. Symptom severity was assessed using the Positive and Negative Symptoms Scale (PANSS; Kay et al., 1987). Full-scale IQ was derived from four subtests of the WASI: Vocabulary, Block Design, Similarities and Matrix Reasoning. Participants also provided information on antipsychotic medication which was transformed into chlorpromazine equivalents (CPZ) (Woods, 2003).

Statistical analysis

Group differences were analysed using a multivariate general linear model (GLM). Dependent variables were mean edge weight for central, non-central and connectivity metrics for the average networks separately. Age, sex, diagnosis and the interaction between diagnosis and sex were entered as predictors. FA was added as additional predictor in the average network analysis. Due to small sample size, effect sizes were then calculated using Hedges' g

and based on the p-value of the individual analysis of covariance (ANCOVAS). Using the whole sample, regression analyses were then performed separately for central, non-central and average metrics and IQ. Due to the distribution of data, PANSS positive, negative and total symptom scores were only analysed in the patient sample. For both models, age, gender and CPZ were used as covariates. P-values (alpha = 0.05) were corrected for multiple comparisons using False Discovery Rate (FDR; p_{FDR}) (Benjamini and Hochberg, 1995). Analyses were repeated for varying threshold values to define the number of central connections (25, 50 and 75 %). Analyses were also repeated for different Freesurfer brain atlases (Desikan and Destrieux). Regression models were then applied to investigate the association between risk score and case-control status in the whole sample. Connectivity metrics were dependent variables and principal components for population stratification, PGRS, age, gender and diagnosis as predictors. All statistical analyses were performed with R version 3.2.3 (https://www.r-project.org).

Mediation analysis was subsequently used to examine the hypothesis that higher PGRS is related to poorer intelligence via reduced structural connectivity. We employed the PROCESS macro in SPSS 22.0 (Hayes and Rockwood, 2016) to formally quantify mediation effects using 5000 bootstrapped samples. Due to our clear directional hypothesis, a one tailed test of mediation was conducted (http://www.afhayes.com). Mediation effects were considered significant if the confidence interval did not include zero (Preacher and Hayes, 2008).

5.5. Results

Table 6 shows demographic data for both healthy controls and schizophrenia patients.

	HC	SZ	*p-value*
Age in years (SD)	37.22 (14.99)	38.04 (10.34)	0.807
Sex, M/F (%)	53/47	57/43	0.733
IQ (SD)	**116.11 (10.75)**	**105.09 (15.89)**	**0.003**
PANSS positive (SD) [Range]		12.30 (5.19) [7, 28]	
PANSS negative (SD) [Range]		13 (7.05) [7,35]	
PANSS total (SD) [Range]		51.64 (17.33) [34, 91]	
Age of onset in years		25.25 (9.89)	
Duration of illness in years		13.58 (10.30)	
CPZ (SD)		434.97 (371.90)	

Note. HC = healthy controls, SZ = schizophrenia. CPZ= chlorpromazine equivalents. SD= Standard deviation. Bold typeface indicates significant group difference ($p < 0.05$*)*.

Average network

Diagnosis (F (5, 54) = 703.1, $p < 0.001$, partial eta squared = 0.080), age (F (5, 54) = 137.64, $p < 0.001$, partial eta squared = 0.030), sex (F (5, 54) = 19.80, $p < 0.001$, partial eta squared = 0.032), mean edge weight (FA) (F (5, 54) = 15263.7, $p < 0.001$, partial eta squared = 0.001) effects were significant for the average network graph theory metrics.

As indicated in Table 7, there were significant differences in network density (Hedges' g = 0.54 (0.03, 1.05), $p_{FDR} = 0.04$), strength (Hedges' g = 1.08 (0.54, 1.62), $p_{FDR} < 0.001$), global efficiency (Hedges' g = 1.95 (1.34, 2.56), $p_{FDR} < 0.001$) and clustering coefficient (Hedges' g = 1.94 (1.33, 2.55), $p_{FDR} < 0.001$) between groups. Mean edge weight showed a tendency towards significance (Hedges' g = 0.43 (-0.07, 0.93), $p_{FDR} = 0.08$). All

metrics were reduced in patients compared to healthy controls. Boxplots for group differences can be found in Appendix II Supplementary Material Figure 1.

Table 7. Mean ± standard deviation (SD) values of connectivity metrics the average network for healthy controls and patients with schizophrenia.

	Average		
Metric	HC	SZ	p_{FDR}
Mean edge weight	0.44 ± 0.02	0.43 ± 0.02	0.08
Density	**33.15 ± 0.92**	**32.56 ± 1.25**	**0.04**
Strength	**12.31 ± 0.57**	**11.88 ± 0.73**	**< 0.001**
Global efficiency	**0.30 ± 0.01**	**0.30 ± 0.01**	**< 0.001**[a]
Clustering coefficient	**0.30 ± 0.01**	**0.30 ± 0.01**	**< 0.001**[a]

Note: HC = healthy controls, SZ = schizophrenia; bold typeface indicates significant group difference ($p_{FDR} < 0.05$).

[a] These results are a consequence of the fact that in this covariance analysis we decided to add mean edge weight as a nuisance variable due to the computation of the graph theory metrics in this study. Because we chose to compute FA-weighted matrices, and our aim was to study topological properties, we considered necessary to remove the effect of FA in each participant, making the group differences significant.

Central subnetwork

Figure 14 shows network maps for the central (> 75 % of centrality values) and non-central subnetworks across all participants. There was no significant difference in central subnetwork mean edge weight between patients with schizophrenia and healthy controls (mean $_{HC}$ = 0.45, SD = ± 0.02; mean $_{SZ}$ = 0.44, SD = ± 0.02) (Hedges' g = 0.36 95% CI (-0.14,

0.86), p > 0.05). Central mean edge weight was reduced in patients compared with healthy controls.

Figure 14. Medial view of (A) central (> 75 % of centrality values) and (B) non-central subnetworks for all participants indicating node location and edge (FA) strength. The nodes which are connected by edges with the highest weights (FA > 0.5) in the central subnetwork are brainstem, left hemisphere precuneus cortex, thalamus, caudate, ventral diencephalon and superior frontal gyrus, and bilateral caudal anterior division of the cingulate cortex and isthmus division of the cingulate gyrus. Nodes are colour-coded to indicate in which lobe they are situated.

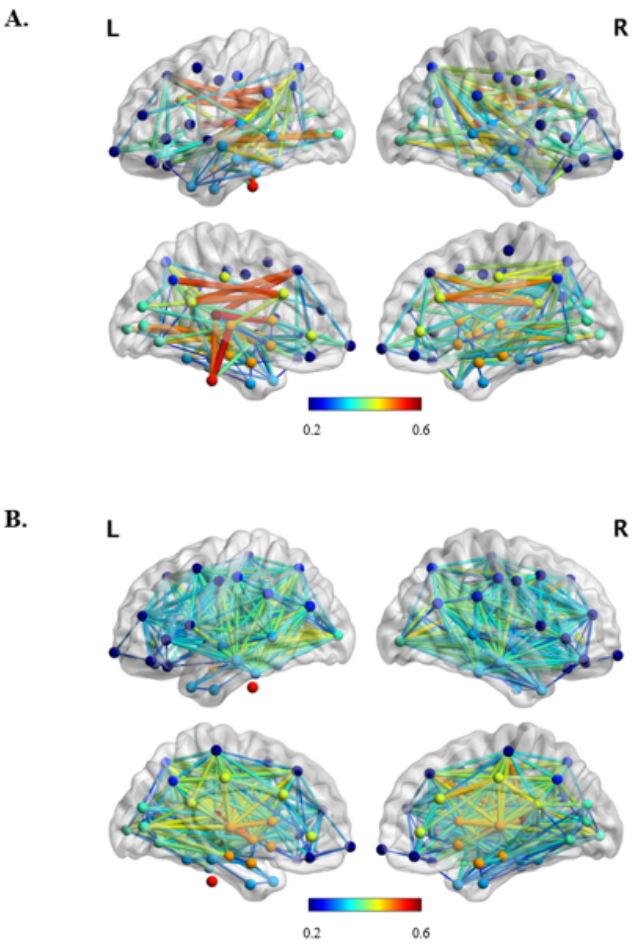

Non-central subnetwork

There was a tendency towards significance for a difference in mean edge weight between patients with schizophrenia and healthy controls (mean $_{HC}$ = 0.44, SD = ± 0.02; mean

$_{SZ}$ = 0.43, SD = ± 0.02) (Hedges' g = 0.45 95% CI (-0.06, 0.95), p = 0.07). Non-central mean edge weight was reduced in patients compared with healthy controls.

Age, antipsychotic medication and illness duration

There were positive significant associations between age, mean edge weight (r = -0.290, p = 0.02) and clustering coefficient (r = -0.269, p = 0.03) for the average network. However, these associations did not survive multiple comparison correction (p_{FDR} > 0.05). Antipsychotic medication shows a significant effect on mean edge weight (r = -0.262, p_{FDR} = 0.048), strength (r = -0.287, p_{FDR} = 0.048), global efficiency (r = -0.263, p_{FDR} = 0.048) and clustering coefficient (r = -0.270, p_{FDR} = 0.048) for the average network. Neither antipsychotic medication nor age had a significant effect on central mean edge weight. However, age (r = -0.313, p = 0.012) and CPZ (r = -0.271, p = 0.033) showed a significant effect on non-central mean edge weight. There were no significant associations between network metrics and illness duration for any of the metrics (p_{FDR} > 0.05).

IQ

Regression coefficients between IQ and the average network graph theory metrics are shown in Table 8. All metrics were significantly associated with IQ (r range 0.284 to 0.471). For central network, mean edge weight was significantly associated with IQ (r = 0.344, p = 0.010). For non-central network, mean edge weight was also significantly associated with IQ (r = 0.338, p = 0.014). Medication, as CPZ equivalents, did not show any significant effect in central, non-central and average networks. Scatterplots with the associations between metrics and IQ can be found in Appendix II Supplementary material Figures 2 and 3.

Table 8. Correlation matrix for IQ and connectivity metrics for the average network.

Metric	r	p_{FDR}
Mean edge weight	**0.343**	**0.016**
Density	**0.284**	**0.045**
Strength	**0.471**	**0.004**
Global efficiency	**0.394**	**0.007**
Clustering coefficient	**0.434**	**0.004**

Note: Bold type indicates significant associations ($p_{FDR} < 0.05$).

Clinical symptoms

Table 9 shows the regression coefficients for positive, negative and total symptom scores and central, non-central mean edge weight and average network connectivity metrics. Central network mean edge weight showed a tendency towards significance in relation to total symptoms ($r = -0.348$, $p = 0.073$). The addition of medication as a covariate in the model made the associations weaker and non-significant ($p > 0.05$). However, medication did not have any significant effect in the regression model.

Table 9. Correlation matrix for PANSS and connectivity metrics for central (> 75% of centrality values), non-central and average networks.

	Metric	Positive	Negative	Total
	Central mean edge weight	-0.282	-0.184	-0.348
	Non-central mean edge weight	-0.206	-0.163	-0.268
Average	Mean edge weight	-0.101	-0.118	-0.178
	Density	-0.195	-0.041	-0.092
	Strength	-0.201	-0.114	-0.193
	Global efficiency	-0.132	-0.133	-0.195
	Clustering coefficient	-0.114	-0.119	-0.178

Note: This table shows the associations between symptoms and metrics using CPZ as a covariate.

Polygenic risk score

The association between genetic risk score at a threshold of $p \leq 0.5$ and case-control status in the total sample was significant ($p < 0.05$). The regression estimate of the genetic risk score at the threshold $p \leq 0.5$ was 0.44 (Adjusted R-square = 0.057; $p = 0.029$).

Next, we studied the association between central and non-central mean edge weight and average network graph theory measures and PGRS. None of the connectivity metrics were significantly associated with PGRS across networks ($p_{FDR} > 0.05$). Regression analysis between IQ and PGRS at a threshold of $p \leq 0.5$ showed a tendency towards significance (r = -0.742, $p = 0.052$). There were no significant correlations between PGRS and symptoms ($p_{FDR} > 0.05$).

Mediation analysis

We aimed to identify mediation candidates that were consistent with the hypothesis that a greater genetic predisposition for schizophrenia is partly related to lower intelligence through the disruption of brain connectivity. As indicated by the bivariate association, the correlation between IQ and PGRS (r = -0.742, p = 0.052) showed a tendency towards significance. The negative correlation between PGRS and IQ suggests a genetic liability to intelligence; mediation analysis allows us to quantify the role of topological network measures in this relationship. Given the substantial effect sizes, and the need to consider mediation in terms of zero and non-zero rather than using p-values in isolation (Hayes, 2009), we tested whether the direct effect of PGRS and IQ was significantly mediated by mean edge weight and average network metrics (i.e. magnitude of change from path c to path c′; see Figure 15A). The results are shown in Figures 15B and 15C. A bias-corrected bootstrap confidence interval for the indirect effect based on 5000 bootstrap samples served as a formal statistical test of the degree to which mean edge weight mediated the relationship between PGRS and IQ. The 30.52 % reduction in magnitude (β = -0.154 to β = -0.107) identified central mean edge weight as a significant partial mediator (confidence interval not containing zero; -0.363 to -0.055). For non-central mean edge weight (Figure 13C), the reduction in magnitude was 46.62% (β = -0.474 to β = -0.253) identifying also non-central mean edge weight as a significant partial mediator (confidence interval -0.673 to -0.050). The model was corrected for age and population stratification components. Additionally, Table 10 shows mediation results for the metrics of the average network.

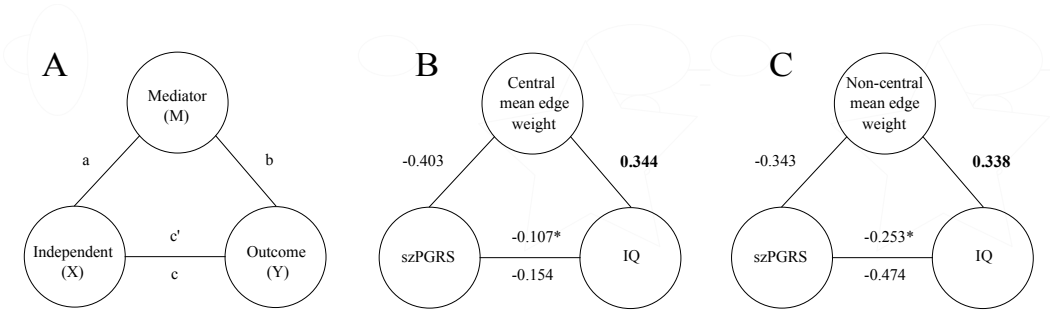

Figure. 15. A) Schematic representation of relationships where an independent variable (X) and an outcome (Y) are hypothesised to be explained by a mediator (M). The direct effect of X on M is a, the effect of M on Y is b, and c the effect of X on Y. c′ denotes the effect of X on Y when M is taking into account in the model. B) Representation of the variables analysed in this study, where X= Polygenic risk score for schizophrenia (PGRS at $p \leq 0.5$), Y= IQ and M= mean edge weight (central). C) X= Polygenic risk score for schizophrenia (PGRS at $p \leq 0.5$), Y= IQ and M= mean edge weight (non-central). Asterisks represent statistically significant mediations and bold indicates significant associations.

Table 10. Mediation analysis for the average network.

			β		%	Mediation model		
X	Y	M	c	c'	Attenuation	F(df)	Lower CI	Upper CI
PGRS	IQ	Mean edge weight	-0.456	-0.269	**41.01**	**8.32 (2, 43)**	**-0.671**	**-0.057**
PGRS	IQ	Density	-0.514	-0.179	65.17	4.87 (2, 43)	-0.483	0.006
PGRS	IQ	Strength	-0.267	-0.454	**-70.03**	**14.15 (2, 43)**	**-0.911**	**-0.121**
PGRS	IQ	Global efficiency	-0.383	-0.342	**10.7**	**10.82 (2,43)**	**-0.776**	**-0.091**
PGRS	IQ	Clustering coefficient	-0.403	-0.325	**19.36**	**12.04 (2, 43)**	**-0.776**	**-0.076**

X: independent variable, Y: outcome variable, M: mediator, c: path from X to Y, c': path from X to Y accounting for M. Bold type face indicates significant mediation effect (confidence intervals do not include 0; Preacher and Hayes, 2008). All tests of mediation are one-tailed and bias-corrected. Bold type face indicates significant mediation effect after FDR-correction ($p_{FDR} < 0.05$).

Additional analyses: Network density

Using network density as a covariate did not significantly affect the results of any of the regression models described above.

Additional analyses: Thresholds

Results for the different thresholds of centrality (25 and 50 %) showed that associations between intelligence, symptoms and mean edge weight were comparable across thresholds (data not shown).

Additional analyses: Destrieux atlas

Group differences using the Destrieux atlas (165 regions) as a parcellation scheme showed no significant differences between patients and controls for mean edge weight for both central and non-central mean edge weight ($p > 0.05$). Graph theory metric results from the average network showed larger differences between groups and stronger associations with intelligence. Results were in the expected direction. Nevertheless, analyses showed comparable results across both atlases for central and non-central mean edge weight and metrics from the average network (data not shown).

5.6. Discussion

This study was set out to assess the ability of graph theory metrics in schizophrenia to build a coherent model from brain structure, cognition and genetics. This is, to our knowledge, the first study reporting results for both high and low centrality networks in schizophrenia and provides much-needed structural MRI perspective on links between brain connectivity and intelligence in this population. We sought to investigate the evolving

hypothesis that schizophrenia is a hub disease in which central connections are more severely affected in contrast to non-central connections. Our data indicate that this may not be the case. Instead, schizophrenia may be a disorder characterised by the disruption of distributed brain regions affecting the whole brain, rather than exclusively affecting hubs. Our study supports the conceptualization of schizophrenia as a disorder characterised by impaired integration between brain regions rather than local brain abnormalities.

The network analysis reported here shows that structural connectivity abnormalities are present in the schizophrenia patient group. Specifically, most graph theory metrics from the average network were significantly reduced in the patient sample compared with healthy controls. These results are consistent with previous findings (van den Heuvel and Fornito, 2014), in particular, density, strength, global efficiency and clustering coefficient were significantly reduced in the patient group compared with controls. The central subnetwork was principally composed of subcortical areas and regions located in the frontal and parietal lobes. Mean edge weight (FA) for central and non-central subnetworks, was not significantly different between patients and healthy controls. Taken together, these results suggest that in schizophrenia the structural connectome is characterised by weaker connections being less segregated and less integrated compared with healthy controls. Thus, here we have shown that differences between patients and controls can be found in the average network, suggesting the presence of more extensive impairments that are seemingly not limited to central connections.

We also found that every graph theory metric across the different networks was significantly associated with IQ. These results are likely to reflect the integrative nature of intelligence, involving distributed brain networks that comprise a wide variety of cognitive functions (Colom et al., 2010). The absence of an interaction between graph theory metrics and group indicates that the same effect occurs in healthy participants and schizophrenia patients. These results are consistent with those of Li et al. (2009) who reported that IQ was

positively correlated with global efficiency and negatively with path length. Central and non-central mean edge weight (FA) were positively associated with IQ, this is in accordance with numerous investigations assessing for instance, relationships between intelligence and general factors of FA (Alloza et al., 2016; Chiang et al., 2009; Deary et al., 2006; Penke et al., 2010; Yu et al., 2008). Thus, in this study we have been able to establish robust associations between intelligence and the structural connectome in schizophrenia.

The dysconnection hypothesis proposes that altered topological connectivity and abnormal integration between distinct brain regions may underlie the symptomatology found in the disorder (Stephan et al., 2009, 2006). In this study, none of the graph metrics were significantly associated with positive, negative or total symptoms. These results suggest that symptoms may be specifically based on deficiencies in distinctive networks. For instance, positive symptoms include hallucinations, delusions and thought disorders, while negative symptoms comprise blunted affect, alogia, anhedonia, asociality and avolition. These processes are likely to comprise distant and unique regions (i.e. visual hallucinations could be associated with visual processing) and therefore, may not be captured by an average network or by networks based on centrality. Thus far, a number of functional studies have investigated the effects of graph theory metrics on symptomatology (Bassett et al., 2012; Skudlarski et al., 2010). One study reported that higher levels of positive and negative symptoms were associated with reduced clustering coefficient and increased path lengths (Shim et al., 2014). A further study found that local connectome organization relates to longitudinal increases in overall PANSS, in particular, these associations were driven by clustering coefficient (Collin et al., 2016). Previous studies have found negative correlations between FA (using DTI) and positive, negative and total PANSS score (Michael et al., 2008; Skelly et al., 2008). For instance, negative correlations between FA and negative symptoms in specific white matter tracts, such as the corpus callosum, have been reported (Nakamura et al., 2012). However, the inconsistency of the findings may be the result of different methodological techniques, use of

medication and heterogeneity of the disease.

In the central and non-central subnetworks, comparable associations were found between intelligence and mean edge weights across all thresholds. Stronger associations were found for symptoms with non-central mean edge weight when considering the top 75% of network connections based on their centrality. A lower centrality threshold (25-50% central connections) showed weaker correlations; probably because of a reduced specificity of the subnetwork and exclusion of some important connections.

There is an overlap between the genetic risk factor for schizophrenia and intelligence (Glahn et al., 2007; McIntosh et al., 2013; Toulopoulou et al., 2007) and thus, brain structure may be an intermediate phenotype between genetics and intelligence. In this study we have shown that central and non-central mean edge weight significantly mediated the relationship between genetics and intelligence between 30 and 47%, respectively. Moreover, most graph theory metrics from the average network significantly mediated this relationship. Thus, we propose that structural brain topology measures are potential intermediate phenotypes in this model. Although metrics were not significantly associated with polygenic risk scores, statistical significance of all paths is not a pre-requisite to determining a mediation model (Hayes and Rockwood, 2016). The approach taken here detected moderate effect sizes and had the ability to formally quantify the degree and significance of the mediation. However, better-powered studies are needed to confirm this.

These findings suggest that prominent associations and disruptions occur also in average and non-central networks which are not driven by medication effects and are present across different brain parcellation schemes. We hypothesise that the construction of subnetworks in schizophrenia may be affected by its inherent reduced centrality and thus, central networks may include less central connections. This is in line with a recent publication

where the authors propose that schizophrenia may not be entirely, nor specifically, a hub disease (Griffa et al., 2015). Based on previous literature and the limitation of our own study, we propose that schizophrenia is a disorder characterised by the disruption of distributed brain regions affecting the whole brain rather than hubs exclusively. Our study therefore supports the conceptualization of schizophrenia as a disorder characterised by impaired integration between brain regions rather than local brain abnormalities.

5.7. Limitations

Our findings are limited by the intrinsic nature of the methodology implemented. For example, limitations associated with DT-MRI, a technique that relies on water diffusion as an indirect marker for white matter microstructure which has not yet been able to resolve complex fibre architecture (Jones et al., 2013), need to be acknowledged. Other limitations include the fact that most of the patients in this study used antipsychotic medication, which may affect structural brain connectivity (Szeszko et al., 2014). Nonetheless, it should be noted that impaired white matter connectivity has also been shown in never-medicated patients (Cheung et al., 2008; Mandl et al., 2013). Additionally, the patients were recruited from outpatient clinics, thus generalisability of the results may be less applicable to more severely affected populations. Moreover, the sample size used is small by contemporary standards raising the possibility of Type II errors. Thus, interpretations of our novel but preliminary results should be taken cautiously. To further validate the results presented here, replication of this study using larger datasets is needed.

5.8. Acknowledgements

We would like to thank all the participants who took part in this study and the radiographers who acquired the MRI data at the Clinical Research Imaging Centre, University of Edinburgh (http://www.cric.ed.ac.uk). We are also grateful to Professor Edwin van Beek

for assistance with overall co-ordination of the study and for radiological reporting of the structural MRI scans. The investigators also acknowledge the financial support of National Health Service (NHS) Research Scotland, through the Scottish Mental Health Research Network (http://www.smhrn.org.uk) who provided assistance with subject recruitment and cognitive assessments. This work was supported by an award from the Translational Medicine Research Collaboration – a consortium made up of the Universities of Aberdeen, Dundee, Edinburgh and Glasgow, the four associated NHS Health Boards (Grampian, Tayside, Lothian, and Greater Glasgow and Clyde), Scottish Enterprise and Pfizer, who have reviewed and approved the manuscript. Imaging aspects also received financial support from the Dr Mortimer and Theresa Sackler Foundation. Dr Simon Cox gratefully acknowledges support from an MRC grant (MR/M013111/1). The authors would also like to thank Dr. Thorsten Feiweier from Siemens Healthcare for providing the prototype diffusion sequence used in this study.

5.9. Chapter conclusion

This chapter supports the conceptualization of schizophrenia as a dysconnection syndrome characterised by impaired integration between brain regions rather than local brain abnormalities. Moreover, this study has shown significant associations between topological properties of the networks and general intelligence, reflecting the integrative nature of intelligence, which involves distributed brain networks comprising a wide variety of cognitive functions. Therefore, even though we were not able to conclude that schizophrenia is a hub disease, our results suggest that schizophrenia may be characterised by more widespread impairments involving the whole brain and that topological brain properties may be an intermediate phenotype in the association between genetic risk for schizophrenia and intelligence.

Chapter 6 Polygenic risk score for schizophrenia and structural brain connectivity in older age: a longitudinal connectome and tractography study

6.1. Overview

This chapter is dedicated to the study of the longitudinal change in white matter connectivity and its associations with genetic risk for schizophrenia in relatively healthy, community-dwelling older adults. White matter connectivity was measured using two methods: graph theory measures derived from the connectome and probabilistic tractography of twelve major white matter tracts. We hypothesised that there would be a decline in brain connectivity (water diffusion MRI parameters and connectome network properties) over time, and that lower initial levels and steeper declines in these brain parameters would be found in those subjects with higher genetic liability for schizophrenia. The paper is published in the journal NeuroImage.

This study was conceived by CA, SRC and MEB. CA analysed the data and wrote the manuscript. SRC and MEB were the main supervisors of this project with co-supervision provided by HCW and SML. MEB, SMM and MDC processed the imaging data, diffusion parameters and graph theory metrics. SJR created the polygenic risk scores. PR provided all the data. MBC and EMT-D aided with the interpretation of the results. JMW and IJD are the Principal Investigators of this cohort. All authors reviewed the manuscript for publication.

Citation: Alloza, C., Cox, S.R., Blesa Cábez, M., Redmond, P., Whalley, H.C., Ritchie, S.J., Muñoz Maniega, S., Del C Valdés Hernández, M., Tucker-Drob, E.M., Lawrie, S.M., Wardlaw, J.M., Deary, I.J., Bastin, M.E., 2018. Polygenic risk score for schizophrenia and structural brain connectivity in older age: A longitudinal connectome and tractography study. NeuroImage. https://doi.org/10.1016/j.neuroimage.2018.08.075

6.2. Abstract

Higher polygenic risk score for schizophrenia (szPGRS) has been associated with lower cognitive function and might be a predictor of decline in brain structure in apparently healthy populations. Age-related declines in structural brain connectivity—measured using white matter diffusion MRI —are evident from cross-sectional data. Yet, it remains unclear how graph theoretical metrics of the structural connectome change over time, and whether szPGRS is associated with differences in ageing-related changes in human brain connectivity. Here, we studied a large, relatively healthy, same-year-of-birth, older age cohort over a period of 3 years (age ~ 73 years, N = 731; age ~76 years, N = 488). From their brain scans we derived tract-averaged fractional anisotropy (FA) and mean diffusivity (MD), and network topology properties. We investigated the cross-sectional and longitudinal associations between these structural brain variables and szPGRS. Higher szPGRS showed significant associations with longitudinal increases in MD in the splenium (β = 0.132, p_{FDR} = 0.040), arcuate (β = 0.291, p_{FDR} = 0.040), anterior thalamic radiations (β = 0.215, p_{FDR} = 0.040) and cingulum (β = 0.165, p_{FDR} = 0.040). Significant declines over time were observed in graph theory metrics for FA-weighted networks, such as mean edge weight (β = -0.039, p_{FDR} = 0.048) and strength (β = -0.027, p_{FDR} = 0.048). No significant associations were found between szPGRS and graph theory metrics. These results are consistent with the hypothesis that szPGRS confers risk for ageing-related degradation of some aspects of structural connectivity.

6.3. Introduction

Patients with schizophrenia show white matter impairments in post-mortem examinations and in *in vivo* studies using diffusion MRI (Harrison, 1999; Kubicki and Shenton, 2014). Less healthy brain white matter microstructure and the structural connectome have been associated with cognitive impairments in schizophrenia (Alloza et al., 2017, 2016; Kochunov et al., 2017; Yeo et al., 2016). Reports of less healthy water diffusion MRI

parameters in schizophrenia are well documented; specifically, impairments are observed in the uncinate fasciculus, corpus callosum, cingulum and arcuate fasciculus (Burns et al., 2003; Ellison-Wright and Bullmore, 2009; Kelly et al., 2017; McIntosh et al., 2005). Likewise, healthy relatives who are at high risk of developing schizophrenia for genetic reasons also show white matter abnormalities in several tracts (Muñoz Maniega et al., 2008).

Graph theory segregation measures, such as clustering coefficient and modularity, have been reported to be altered in schizophrenia (Alexander-Bloch et al., 2010; Collin et al., 2013; van den Heuvel and Fornito, 2014; Zalesky et al., 2011), suggesting a more segregated pattern of network organization. Longer path lengths and reductions in communication efficiency between regions have also been found in patients diagnosed with schizophrenia, suggesting that schizophrenia may be characterized by reduced communication between distal brain regions (reviewed in van den Heuvel and Fornito, 2014). Graph theoretical studies have also reported small-world organization and reductions in integration and efficiency in unaffected relatives (Collin et al., 2014), indicating a genetic basis for schizophrenia. Despite the difficulties of coupling graph theory metrics and the underlying neurobiology, graph theory metrics have consistently shown associations with cognitive functions (Alloza et al., 2017; Collin et al., 2016; Li et al., 2009), symptoms (Collin et al., 2016; van den Heuvel and Fornito, 2014; Wang et al., 2012), heritability (Bohlken et al., 2014) and sensitivity to disease (Lynall et al., 2010; Rubinov et al., 2009b), indicating that they do compute relevant properties of the brain's structure in this disorder.

Schizophrenia is both highly heritable and polygenic, with many common alleles of small effect, and increasing numbers of genome-wide significant loci being identified as sample sizes increase (Hilker et al., 2018; International Schizophrenia Consortium et al., 2009;

Schizophrenia Working Group of the Psychiatric Genomics Consortium, 2014). The largest twin study in schizophrenia to date estimated its heritability to be 79%, and the proband-wise concordance rate in monozygotic twins to be 33%, suggesting that illness vulnerability is partly, but not exclusively, due to indicated by genetic factors (Hilker et al., 2018). The latest schizophrenia genome wide association study (GWAS) included a meta-analysis with 40675 cases and 64643 controls; it identified 179 independent genome-wide significant single nucleotide polymorphisms (SNPs) ($P < 5 \times 10^{-8}$) associated with a diagnosis of schizophrenia (Pardiñas et al., 2018; Schizophrenia Working Group of the Psychiatric Genomics Consortium, 2014). Summary statistics from large-scale GWAS allow the degree of genetic liability for a heritable trait (in this case, schizophrenia) to be estimated in healthy subjects outside the population in which the original GWAS was conducted (Van der Auwera et al., 2017, 2015).

In addition to schizophrenia, advancing age is associated with an increased risk for neurodegeneration, including white matter microstructure (Aboitiz et al., 1992; Cox et al., 2016; Hasan et al., 2010; Kochunov et al., 2015, 2012, 2011; Lebel et al., 2012; Marner et al., 2003; Meier-Ruge et al., 1992; Peters, 2002; Westlye et al., 2010) and cognitive decline (Deary et al., 2009; Verhaeghen and Salthouse, 1997). Therefore, identifying the determinants of the degree to which an individual experiences these cognitive and brain declines with age is a high priority (Corley et al., 2018). In ageing populations, a higher genetic risk for schizophrenia has been associated with both poorer cognitive function and with less healthy white matter (McIntosh et al., 2013; Muñoz Maniega et al., 2008). However, the neurobiological underpinnings of these apparent differences in cognitive ageing have not yet been fully explored.

Thus far, only a small number of studies have analysed the relationship between polygenic risk score for schizophrenia (szPGRS) and neuroimaging biomarkers in healthy and patient samples (Alloza et al., 2017; Birnbaum and Weinberger, 2013; McIntosh et al., 2013; Ritchie et al., 2017; Van der Auwera et al., 2015; Whalley et al., 2015b). Emerging evidence suggests that higher szPGRS might be a predictor of accelerated decline in brain microstructure in older age. Ritchie et al. (2017) reported a significant longitudinal association between szPGRS and a general factor of tract-averaged mean diffusivity (MD; $\beta = -0.120$, SE = 0.059, $p = 0.041$, where a negative association indicates a link with unhealthy ageing), using a threshold of $p = 1.00$ derived from a previous GWAS (Schizophrenia Working Group of the Psychiatric Genomics Consortium, 2014) and 3-year change in the same dataset presented here (the Lothian Birth Cohort 1936, LBC1936). This nominal association did not, however, survive correction for multiple comparisons. Nevertheless, the largest published schizophrenia GWAS to date has improved considerably its predictive power (Pardiñas et al., 2018) and fibre tracking and analysis have been updated significantly to improve tract segmentation in this sample (Muñoz Maniega et al., 2017). These developments allow a more thorough investigation of the relationships between genetic risk for schizophrenia and structural brain connectivity in this ageing population than has hitherto been possible.

In this paper, we therefore investigated the hypothesis that szPGRS relates to white matter microstructure in older age by first mapping the trajectories of water diffusion MRI parameters (using fractional anisotropy (FA) and mean diffusivity (MD)) measured in twelve major tracts and the topological properties of FA-weighted networks in the LBC1936 across a three-year period. Secondly, we investigated the effect of szPGRS on these longitudinal tractography and connectome microstructural properties. We hypothesised that there would be a decline in brain connectivity (water diffusion MRI parameters and connectome network properties) over time, and that lower initial levels and steeper declines in these brain

parameters would be found in those subjects with higher genetic liability for schizophrenia. As an additional analysis, we also investigated the hypothesis that higher szPGRS is associated with a steeper decline in cognition via change in white matter structure in older age.

6.4. Methods

Participants

The LBC1936 study (Deary et al., 2012, 2007; Taylor et al., 2018) provides longitudinal data on cognitive and brain ageing. The cohort comprises participants of the Scottish Mental Survey of 1947 (*SMS1947, n* = 70,805) in which most Scottish schoolchildren born in 1936 sat the Moray House Test Number 12 at ~11 years of age (Scottish Council for Research in Education, 1949). Most participants resided in the Edinburgh and Lothian regions of Scotland at recruitment age ~70 years. The sample has been repeatedly tested in later life with participants undergoing detailed medical, physical, and psycho-social assessments, including a brain MRI examination (Wardlaw et al., 2011). The first testing wave took place at a mean age of 69.53 years (SD, 0.83 years) in 2004–2007 (n = 1,091, 543 females); the second testing wave took place at a mean age of 72.49 years (SD, 0.71 years) in 2007–2010 (n = 866, 418 females); and the third testing wave took place at a mean age of 76.25 years (SD, 0.68 years) in 2011–2014 (n = 697, 337 females). The data in the present report come from the second and third waves of the study at which points structural brain imaging was performed. A total of 731 participants (343 females) agreed to undergo brain imaging at a mean age of 72.68 years (SD, 0.72 years), and 488 (228 females) at a mean age of 76.38 years (SD, 0.65 years), none of whom were known to have schizophrenia. Only one participant was diagnosed with bipolar disorder. However, the data indicated that this participant was not an outlier (+/- 2.5 SD for all brain imaging measures) and therefore, this subject was not excluded from the analysis. The study was approved by the Multi-Centre Research Ethics Committee

for Scotland (MREC/01/0/56), the Lothian Research Ethics Committee (LREC/2003/2/29) and the Scotland A Research Ethics Committee (07/MRE00/58). All participants completed written informed consent forms before any cognitive, MRI, or other measurements were taken.

Scan Acquisition

All structural and diffusion MRI data were acquired using a GE Signa Horizon HDx 1.5 T clinical scanner (General Electric, Milwaukee, WI, USA) using a self-shielding gradient set with maximum gradient strength of 33 mT · m^{-1}, and eight-channel head array coil. Diffusion-weighted echo-planar volumes (b = 1000 s · mm^{-2}) were acquired in 64 non-collinear directions, along with seven T_2-weighted volumes (b = 0 s · mm^{-2}). Each volume comprised seventy-two contiguous axial 2-mm-thick slices acquired with 2 × 2 mm in-plane resolution. Repetition and echo times were 16.5 s and 95.5 ms respectively. A 3D T_1-weighted inversion recovery-prepared fast spoiled gradient-echo (FSPGR) volume was also acquired in the coronal plane with 160 contiguous slices and 1.3 mm^3 voxel dimensions. Full details of the imaging protocol are available (Wardlaw et al., 2011). The scanner underwent a major upgrade just prior to the first wave of imaging and was regulated continuously within a tight quality control environment across the duration of the study; all scans were acquired with the same imaging protocol and scanner software platform (Wardlaw et al., 2011) throughout.

Image processing

Each 3D T_1-weighted FSPGR volume was parcellated into 85 cortical (Desikan et al., 2006) regions-of-interest (ROI) using FreeSurfer (http://surfer.nmr.mgh.harvard.edu), which comprised 34 cortical ROIs and eight sub-cortical ROIs per hemisphere, plus the brainstem. Segmentations were visually checked, then used to construct grey and white matter masks for use in network construction and to constrain the tractography output as described below. Using tools provided by the FDT package in FSL (http://fsl.fmrib.ox.ac.uk/fsl), the diffusion MRI data were pre-processed to reduce systematic imaging distortions and bulk subject motion

artefacts by affine registration of all subsequent EP volumes to the first T_2-weighted EP volume (Jenkinson and Smith, 2001). Skull stripping and brain extraction were performed on the registered T_2-weighted EP volumes and applied to the mean diffusivity/fractional anisotropy (MD/FA) volumes calculated by DTIFIT in each subject (Basser and Pierpaoli, 1996; Smith, 2002). The neuroanatomical ROIs determined by FreeSurfer were then aligned from 3D T_1-weighted volume to diffusion space using a cross-modal nonlinear registration method. As a first step, linear registration was used to initialize the alignment of each brain-extracted FA volume to the corresponding FreeSurfer extracted 3D T_1-weighted brain volume using a mutual information cost function and an affine transform with 12 degrees of freedom (Jenkinson and Smith, 2001). Following this initialization, a nonlinear deformation field based method (FNIRT) was used to refine local alignment (Andersson et al., 2007). FreeSurfer segmentations and anatomical labels were then aligned to diffusion space using nearest neighbour interpolation.

Tractography

Whole-brain probabilistic tractography was performed using FSL's BedpostX/ProbTrackX algorithm (Behrens et al., 2007). Probability density functions, which describe the uncertainty in the principal directions of water diffusion, were computed using a two-fibre model per voxel (Behrens et al., 2007). Twelve major tracts were identified in each participant using probabilistic neighbourhood tractography (PNT), as implemented in the TractoR package for fibre tracking and analysis (http://www.tractor-mri.org.uk/ (Clayden et al., 2011; Muñoz Maniega et al., 2017); PNT is an automatic tract segmentation method that has shown good reproducibility (Clayden et al., 2009b). This technique optimizes the choice of seed point placement for tractography by estimating the best matching tract from a series of candidate tracts generated from a neighbourhood of voxels (typically $7 \times 7 \times 7$) placed around a central voxel transferred from standard to native space against a reference tract that was derived from a group of healthy volunteers aged 25 to 64 years (Muñoz Maniega et al.,

2017). The topological tract model was also used to reject any false positive connections, thereby significantly improving tract segmentation (Clayden et al., 2009a). The seed point best matching each tract to the reference was determined in this manner and probabilistic white matter tracts masks were reconstructed by sampling 5000 streamlines. All segmented white matter tracts were visually assessed to ensure they were an anatomically accurate representation of the fasciculi-of-interest. The resulting tractography masks were applied to the MD/FA volumes of each participant; this permitted tract-specific mean values of FA and MD, weighted by the connection probability, to be obtained for each tract in each subject. The twelve tracts segmented were the genu and splenium of corpus callosum, and bilateral cingulum, anterior thalamic radiations (ATR), arcuate, uncinate and inferior longitudinal fasciculi.

Structural connectome

Using the probability density functions generated from BedpostX/ProbTractX, streamlines were then constructed by sampling from these distributions during a tracking process that involved all white matter voxels using 100 Markov Chain Monte Carlo iterations with a fixed step size of 0.5 mm between successive points. Tracking was initiated from all white matter voxels (Buchanan et al., 2014) in two collinear directions until terminated by the following stopping criteria designed to minimize the amount of anatomically implausible streamlines: (i) exceeding a curvature threshold of 70 degrees; (ii) entering a voxel with FA below 0.1 (Verstraete et al., 2011); (iii) entering an extra-cerebral voxel; (iv) exceeding 200 mm in length; and (v) exceeding a distance ratio metric of 10. The distance ratio metric (Bullitt et al., 2003), excludes implausibly tortuous streamlines. For instance, a streamline with a total path length 10 times longer than the distance between end points was considered to be invalid. The values of the curvature, anisotropy and distance ratio metric constraints were set empirically and informed by visual assessment of the resulting streamlines.

Network construction

FA-weighted networks were constructed by recording the mean FA value along streamlines connecting all 85 ROI (network node) pairs from the default FreeSurfer cortical (Desikan et al., 2006) and subcortical regions. The endpoint of a streamline was considered to be the first grey matter ROI encountered when tracking from the seed location. The average brain network across the cohort was determined by including those connections which occurred in more than 2/3 of the participants at baseline (de Reus and van den Heuvel, 2013). This baseline network mask was then propagated to the second wave of connectivity matrices. Organizational properties of the different networks were then obtained using the brain connectivity toolbox (www.brain-connectivity-toolbox.net). For each FA-weighted connectivity matrix for the average network, five global network measures were computed, namely mean edge weight (mean value of FA across the network), density (the fraction of present connections to possible connections), strength (the average sum of weights per node), clustering coefficient (fraction of triangles around a node) and global efficiency (the average of the inverse shortest path length).

Polygenic risk score calculation

The majority of participants provided blood samples at the first testing wave (age 70 years) that were used to extract DNA for the genetic analyses. To measure single-nucleotide polymorphisms (SNPs) we used the Illumina 610-Quadv1 whole-genome SNP array; measurements were completed at the Wellcome Trust Clinical Research Facility Genetics Core, Western General Hospital, Edinburgh (https://www.wtcrf.ed.ac.uk). Stringent quality control analyses were applied to the genotype data which resulted in 549692 of the 599011 SNPs on the Illumina 610 chip being retained in 3511 individuals (2115 females). The sample collection, quality control and genotyping process is described in greater detail elsewhere and non-European individuals were carefully excluded from the current analysis (Davies et al., 2011). PGRS summarise the small effects across all SNPs that contribute to the genetic

liability of a phenotype (in this case, schizophrenia). The out-of-sample validation of the capacity of szPGRS to predict onset of schizophrenia has been reported to explain 24.43% (the estimate assumes a population risk of 1%) of the variance in liability (Pardiñas et al., 2018). szPGRS were created for all individuals with suitable genotype data; only genotypes passing stringent quality control were used in analyses. szPGRS were estimated using the recent summary data from a GWAS of schizophrenia comprising a meta-analysis of two studies (Pardiñas et al., 2018; Schizophrenia Working Group of the Psychiatric Genomics Consortium, 2014), which included 40675 cases and 64643 controls. szPGRS were estimated using the PRSice software package according to previously described protocols (Euesden et al., 2015), with linkage disequilibrium and distance thresholds for clumping of $r^2 = 0.2$ and within a 250kb window. Five scores were created for each individual using SNPs selected according to the significance of their association with the phenotype at nominal p-value thresholds of 0.01, 0.05, 0.1, 0.5 and 1.0 (all SNPs). Our primary analyses used scores generated from a list of SNPs with a GWAS training set of $p \leq 1.0$ threshold as recommended previously in order to allow replication by other studies and to maximise the potential predictive capacity (Ware et al., 2017). However, results at $p \leq 0.1$ and $p \leq 0.5$ thresholds are presented in Appendix III Supplementary Material Tables 3 and 4. Four multidimensional scaling factors (estimated from SNP data) were entered into the models as additional 'nuisance' covariates to control for population stratification, along with age. These multidimensional scaling factors have been previously identified to be adequate for accounting for population structure in this sample (Davies et al., 2011).

Statistical analyses

First, age-related changes for white matter tract MD/FA values and global graph theory measures were calculated using linear mixed models for those participants who completed both assessments. The package used for the linear mixed models was 'nlme' (Pinheiro et al., 2018) in R and standardised betas were reported. Age in days at the time of

MRI acquisition and sex were entered as fixed effects and participant as a random effect. Moreover, for each connectivity metric, residuals were calculated from a linear regression predicting each metric from density (fraction of present connections to possible connections), and these were used in all analyses. This is because several global graph theory metrics depend on density and comparisons at constant density allow differences related to the topological reorganization of links to be assessed longitudinally. The use of graph theory to study network topology is a valuable framework while also being a challenging task. For instance, the number of nodes (N) or network's degree (k) will influence the computation of global theory metrics (see Brain Connectivity Toolbox for a detailed description of metrics: https://sites.google.com/site/bctnet). Therefore, comparing networks with different N or k can yield spurious results (Wijk et al., 2010). Instead of restraining all networks to a fixed k parameter, we chose to control each subject's graph theory measure for edge density. Therefore, models presented below compute density as a fixed effect for each graph metric. This allowed us to compare metrics longitudinally independently of their differences in density.

We then estimated a structural equation model (SEM) for each white matter tract MD/FA values and global graph theory measures. We estimated a separate model for each MRI metric (density-corrected network metric or white matter tract MD/FA value), which were set as the dependent variable in each model. Latent change score models (McArdle, 2009) were used to assess associations of szPGRS with the cross-sectional (baseline level, age ~73 years) and longitudinal change (73-76 years) in diffusion MRI parameters. Latent scores were derived from bilateral white matter tracts. We constrained the loadings for left and right tracts across waves to be equal (i.e. the left loadings were equal across waves and independent of right loadings) (Persson et al., 2014). For interhemispheric white matter tracts (genu and splenium) and graph theory metrics, we used a single indicator model (Gollwitzer et al., 2014). Figure 16 shows a simplified diagram of the SEM framework. Within the model, each brain

imaging measure was adjusted for its respective age in days at the time of scanning and sex at the manifest level, while szPGRS was adjusted for sex and population stratification components. Due to the apparent association between schizophrenia and cardiovascular disease (Curkendall et al., 2004), we adjusted the linear mixed models and latent change score models for high blood pressure at each time point in order to reject the hypothesis that higher cardiovascular risk may contribute to a steeper decline in diffusion MRI parameters over time. For each model, we tested the association at the brain baseline level and change with szPGRS. SEM was performed using the package 'lavaan' (Rosseel, 2012) in R with full-information maximum likelihood estimation to use all data available.

As an additional analysis, we examined the hypothesis that higher szPGRS was associated with a steeper decline in cognition via change in white matter structure. We used SEM in the 'lavaan' package (Rosseel, 2012) with full-information maximum likelihood estimation to derived a latent score of general fluid intelligence (g_f) for each wave from six non-verbal tests of cognitive function from the Weschler Adult Intelligence Scale III^{UK} (Wechsler, 1955): matrix reasoning (non-verbal reasoning), block design (constructional ability), symbol search and digit symbol (processing speed), letter number sequencing and digit span backwards (working memory). Within the model, each cognitive test was adjusted for age in days at the time of assessment and sex at the manifest level. We constrained the loadings for each individual raw score across waves (i.e. equal loadings for matrix reasoning at baseline and follow-up). Beyond the analyses of szPGRS to the mediator (A path), to test whether the mediation (change from path C to C') was statistically significant ($p_{FDR} < 0.05$), we tested whether the direct path of szPGRS to g_f (path C) and the indirect path from the mediator to g_f (path B) were significant. Figure 17 shows a simplified diagram of the model that was used to examine this hypothesis. All significance (p) values ($\alpha = 0.05$) were corrected for multiple comparisons using false discovery rate (FDR, p_{FDR}) (Benjamini and Hochberg, 1995).

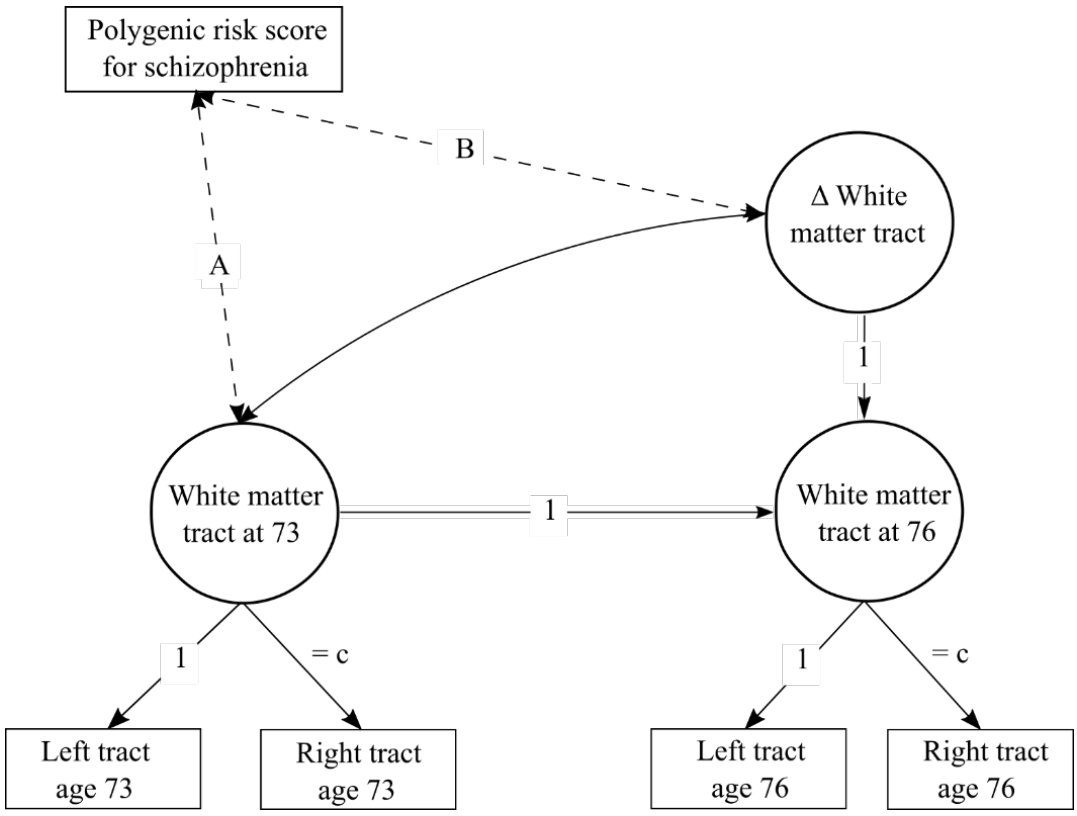

Figure 16. Diagram of the structural equation model (SEM) for white matter connectivity. A separate model was applied to each white matter tract (FA and MD) and each graph theory measure. Water diffusion and graph theory metrics were measured at baseline (age 73) and follow-up (age 76). From each individual bilateral white matter tract, a latent score was calculated for FA and MD. For callosal tracts and graph theory metrics a latent score was derived after the manifest variable was corrected for scaled age at scanning and sex. From these models, a latent change score variable was calculated for each model (Δ Connectivity). Relation between baseline FA/MD/graph theory measures and polygenic risk score for schizophrenia (szPGRS) is indicated by path A; path B represents the association between change in white matter FA/MD/graph theory measures and szPGRS. For all bilateral tracts, we further constrained equality of the factor loading of the left hemisphere (c). szPGRS was

corrected for sex and population stratification while water diffusion MRI and graph theory measures at the manifest level were corrected for scaled age at scanning and sex at each time point within the model (paths not shown). Note that graph theory metrics were corrected for density outside the SEM model.

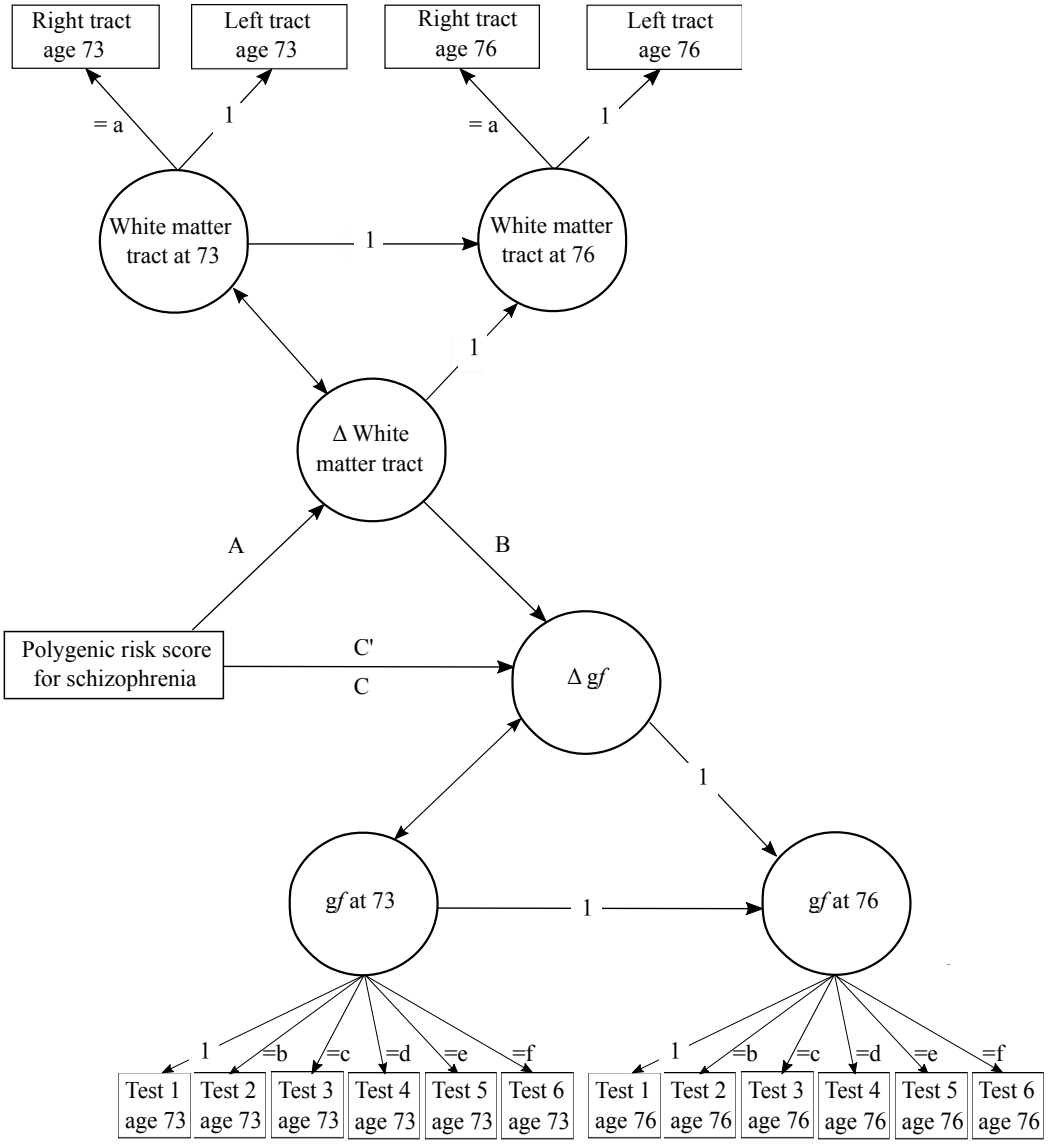

Figure 17. Diagram of the mediation model. The SEM model for white matter connectivity has been already described in Figure 16. From each individual cognitive test, a latent score was calculated for general fluid intelligence (g_f). From this model, a latent change score variable was calculated (Δ g_f). Relation between polygenic risk score for schizophrenia (szPGRS) and change in white matter is indicated by path A; path B represents the association

between change in white matter and change in g_f. Path C represents the association between szPGRS and change in g_f. C' denotes the effect of szPGRS on change in g_f when change in white matter is taken into account in the model.

6.5. Results

Descriptive statistics, valid sample sizes after quality controls and longitudinal change for each brain imaging measure are provided in Tables 11 and 12. At baseline, seven hundred and thirty-one subjects met the inclusion criteria with a mean age at MRI scanning of 72.73 (SD 0.72) years. At follow-up, four hundred eighty-eight subjects with a mean age at MRI of 76.43 (SD 0.65) years were scanned. Baseline data (age 73) on the structural connectome have already been published elsewhere (Wiseman et al., 2018). Descriptive statistics of cognitive tests and health conditions are presented in Appendix III Supplementary Material Tables 1 and 2.

Table 11. Demographic information across both waves (age 73 and 76 years).

	n	Age 73	*n*	Age 76
Age in years (SD)	731	72.73 (0.72)	488	76.43 (0.65)
Females (%)	731	46.92	488	46.72
szPGRS (SD)	640	-6.4 (0.2)		
Diabetes		10.71%		12.03%
Hypertension		48.81%		54.22%
High cholesterol		41.52%		47.68%
History of cardiovascular disease		27.23%		33.34%
Cognition				
Matrix reasoning (SD)	690	13.37 (4.90)	574	13.16 (5.00)
letter-number sequencing (SD)	690	10.98 (3.02)	573	10.49 (2.98)
Block Design (SD)	690	34.07 (10.07)	577	32.43 (10.15)
Symbol search (SD)	689	24.63 (6.19)	573	24.53 (6.58)
Digit symbol (SD)	689	56.24 (12.27)	570	53.73 (12.78)
Digit span backwards (SD)	692	7.84 (2.33)	581	7.76 (2.36)

Note: SD: Standard deviation.

Table 12. Descriptive statistics for bilaterally averaged white matter water diffusion MRI parameters and graph theory metrics across both waves (age 73 and 76 years).

	n	Age 73	*n*	Age 76	*Overlapping sample*	*r*	*SE*	p_{FDR}
White matter tracts								
FA								
Genu (SD)	633	0.376 (0.047)	457	0.375 (0.044)	415	-0.027	0.024	0.392
Splenium (SD)	652	0.508 (0.067)	458	0.504 (0.071)	427	-0.056	0.021	0.019*
Arcuate (SD)	616	0.425 (0.035)	439	0.422 (0.036)	397	-0.062	0.016	< 0.001*
ATR (SD)	641	0.329 (0.030)	444	0.333 (0.030)	410	0.056	0.022	0.019*
Cingulum (SD)	631	0.424 (0.044)	457	0.425 (0.043)	413	-0.014	0.023	0.541
Uncinate (SD)	606	0.322 (0.028)	420	0.331 (0.028)	383	0.117	0.024	< 0.001*
Inferior longitudinal fasciculus (SD)	662	0.379 (0.042)	463	0.380 (0.045)	437	-0.018	0.016	0.489
MD								
Genu (SD)	633	798.55 (79.17)	457	854.05 (87.01)	415	0.333	0.023	< 0.001*
Splenium (SD)	652	816.76 (130.66)	458	864.22 (174.86)	427	0.171	0.023	< 0.001*
Arcuate (SD)	616	653.02 (48.44)	439	691.62 (54.86)	397	0.377	0.014	< 0.001*
ATR (SD)	641	747.45 (58.28)	444	792.59 (67.58)	410	0.361	0.021	< 0.001*
Cingulum (SD)	631	630.39 (39.06)	457	668.07 (39.95)	413	0.452	0.020	< 0.001*
Uncinate (SD)	606	763.01 (46.80)	420	795.68 (52.19)	383	0.345	0.019	< 0.001*
Inferior longitudinal fasciculus (SD)	662	767.84 (80.42)	463	816.80 (111.64)	437	0.279	0.023	< 0.001*
Network connectivity measures								
Mean edge weight (SD)	534	0.379 (0.020)	416	0.380 (0.019)	335	-0.039	0.017	0.048*
Strength (SD)	534	8.554 (0.719)	416	8.704 (0.628)	335	-0.027	0.011	0.048*
Global efficiency (SD)	534	0.242 (0.015	416	0.244 (0.013)	335	-0.027	0.016	0.120
Clustering coefficient (SD)	534	0.249 (0.015)	416	0.252 (0.014)	335	-0.001	0.016	0.935

Note: SD: Standard deviation, FA: fractional anisotropy, MD: mean diffusivity, beta: standardised estimates from the linear mixed models, SE: standard error. ILF: inferior longitudinal fasciculus. Asterisks represent significance from the linear mixed models (p_{FDR} < 0.05).

Longitudinal Changes in Brain Structural Connectivity

White matter FA

Results of the linear mixed models for FA are presented in Table 12 and Figure 18.A. Significant longitudinal reductions in FA were found for the splenium (β = -0.056, SE = 0.021, p_{FDR} = 0.019) and arcuate fasciculus (β = -0.062, SE = 0.016, p_{FDR} < 0.001). The genu (β = -0.027, SE = 0.024, p = 0.280), cingulum (β = -0.014, SE = 0.023, p = 0.541) and inferior longitudinal fasciculus (β = -0.018, SE = 0.016, p = 0.420) showed a non-significant decline over time (p_{FDR} > 0.05). Two white matter tracts showed significant longitudinal increases in FA, specifically the anterior thalamic radiations (ATR; β = 0.056, SE = 0.022, p_{FDR} = 0.019) and uncinate fasciculus (β = 0.117, SE = 0.024, p_{FDR} < 0.001). Sex had a significant effect on the FA of the splenium (β_{sex} = 0.111, SE = 0.036, p_{FDR} = 0.007), cingulum (β_{sex} = -0.093, SE = 0.035, p_{FDR} = 0.019) and inferior longitudinal fasciculus (β_{sex} = 0.142, SE = 0.035, p_{FDR} < 0.001). Positive effects (β_{sex}) represent higher FA values in females compared to males, whereas negative effects represent higher FA values in males compared to females. As an additional analysis we tested for blood pressure effects; however, we did not find any significant effect of higher blood pressure on the longitudinal change of FA for any white matter tract (p_{FDR} > 0.05).

White matter MD

Results of the linear mixed models for MD are presented in Table 12 and Figure 18.B. Significant longitudinal increases in MD were found for genu (β = 0.333, SE=0.023, p_{FDR} < 0.001), splenium (β = 0.171, SE=0.023, p_{FDR} < 0.001), arcuate (β = 0.377, SE=0.014, p_{FDR} < 0.001), ATR (β = 0.361, SE = 0.021, p_{FDR} < 0.001), cingulum (β = 0.452, SE = 0.020, p_{FDR} < 0.001), uncinate (β = 0.345, SE = 0.019, p_{FDR} < 0.001) and inferior longitudinal fasciculus (β = 0.279, SE = 0.023, p_{FDR} < 0.001). Sex had a significant effect on the MD of the genu (β_{sex} = -0.117, SE = 0.033, p_{FDR} = 0.001), arcuate (β_{sex} = 0.116, SE = 0.036, p_{FDR} = 0.003), cingulum (β_{sex} = 0.127, SE = 0.032, p_{FDR} < 0.001) and inferior longitudinal fasciculus (β_{sex} = -0.079, SE

= 0.033, p_{FDR} = 0.027). Positive effects (β_{sex}) represent higher MD values in females compared to males, whereas negative effects represent higher MD values in males compared to females. Higher blood pressure was not significantly associated with longitudinal change in MD for any white matter tract ($p_{FDR} > 0.05$).

Figure 18. A. Trajectories of water diffusion MRI parameters over time. Each colour represents a different fibre for FA (plot A) and MD (plot B). The *x*-axis represents age in days at MRI scanning. The black line denotes linear regression. ATR = Anterior thalamic radiations; ILF = Inferior longitudinal fasciculus. Beta: standardised estimates from the linear mixed models. Asterisks represent significance from the linear mixed models ($p_{FDR} < 0.05$).

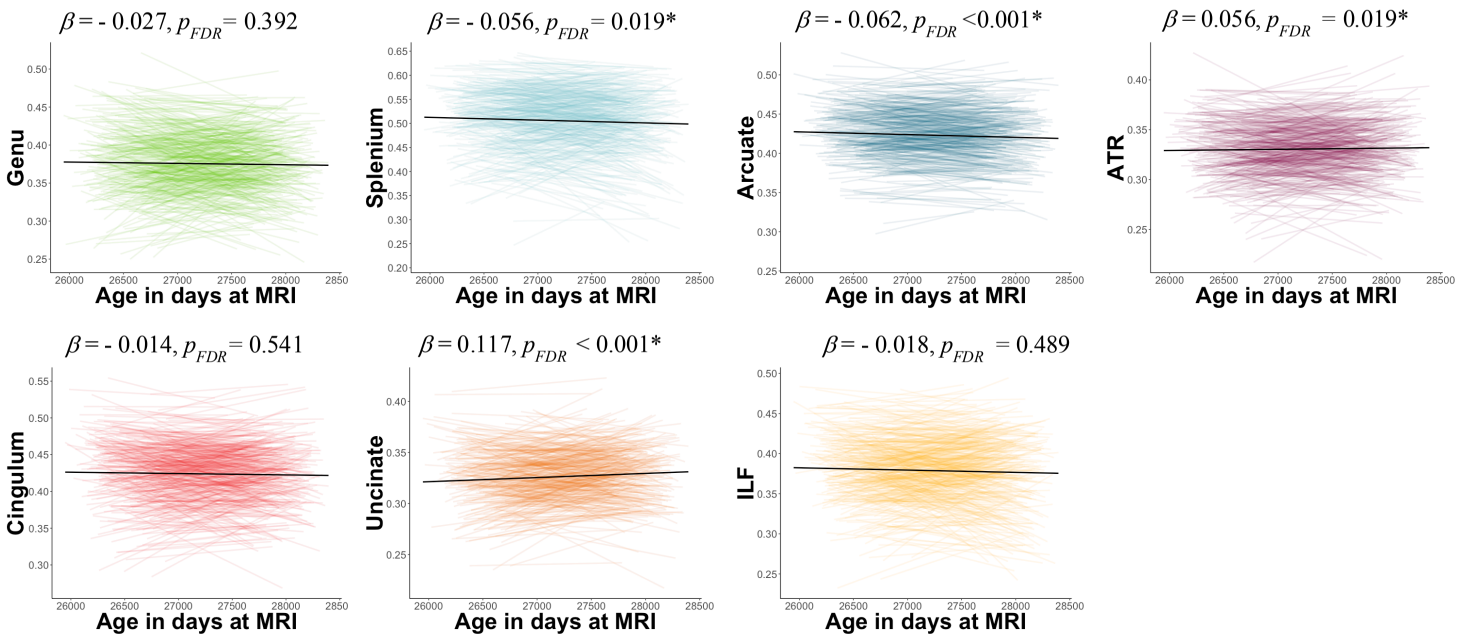

Figure 18. B. Trajectories of water diffusion MRI parameters over time. Each colour represents a different fibre for FA (plot A) and MD (plot B). The *x*-axis represents age in days at MRI scanning. The black line denotes linear regression. ATR = Anterior thalamic radiations; ILF = Inferior longitudinal fasciculus. Beta: standardised estimates from the linear mixed models. Asterisks represent significance from the linear mixed models ($p_{FDR} < 0.05$).

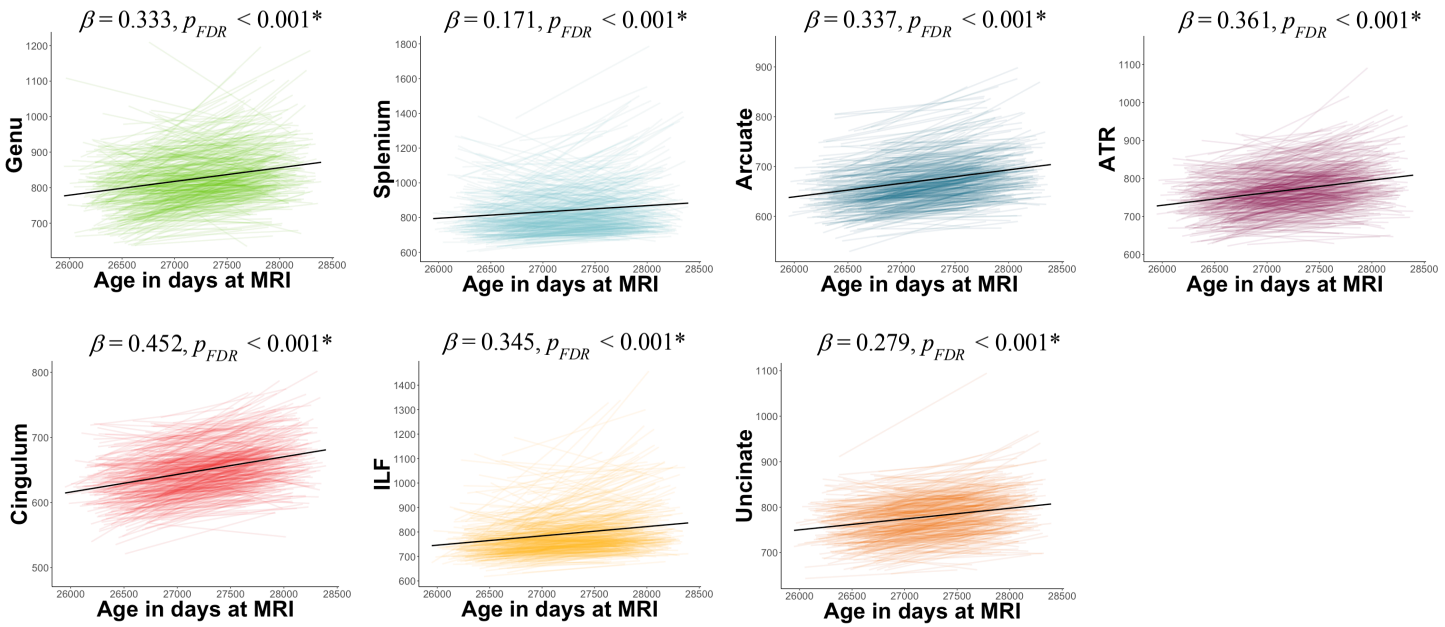

Graph theory metrics

Results of the linear mixed models for graph theory are presented in Figure 19 and Table 12. There were longitudinal decreases in most graph theory metrics across all subjects. For instance, mean edge weight (β = -0.039, SE = 0.017, p_{FDR} = 0.048) and strength (β = -0.027, SE = 0.011, p_{FDR} = 0.048) declined significantly between waves. Global efficiency (β = -0.027, SE=0.016, p_{FDR} = 0.120) and clustering coefficient showed no significant changes over time (β = -0.001, SE=0.016, p_{FDR} = 0.935). Sex did not have any significant effect on graph theory metrics (p_{FDR} > 0.05).

Figure 19 Trajectories of graph theory metrics between age 73 and 76 years. Plotted are residuals for each participant from the regression of the graph metric as the dependent variable and density and sex as the predictor variables. The *x*-axis represents age in days at MRI scanning. The black line represents linear regression. Beta: standardised estimates from the linear mixed models. Asterisks represent significance from the linear mixed models (p_{FDR} < 0.05).

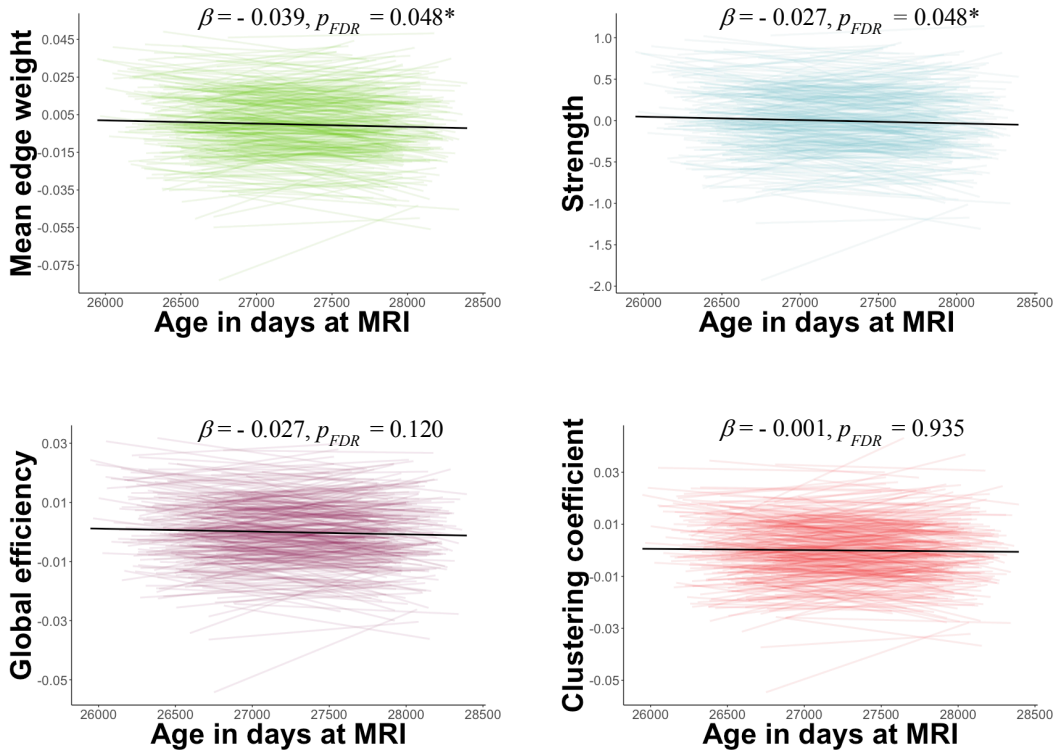

Latent Change Score Modelling

Results of the SEM analyses are shown in Table 13. The models examining associations of szPGRS with white matter water diffusion MRI parameters fit the data well (white matter tract FA: RMSEA < 0.058, CFI > 0.940, SRMR < 0.030 and white matter tract MD: RMSEA < 0.075, CFI > 0.923, SRMR < 0.039). Associations between FA and szPGRS were non-significant for level or change in any tract (p_{FDR} > 0.05). Associations between MD and szPGRS were non-significant for level (p_{FDR} > 0.05). However, change in MD showed significant associations with szPGRS for the splenium (r = 0.132, p_{FDR} = 0.040), arcuate (r = 0.291, p_{FDR} = 0.040), ATR (r = 0.215, p_{FDR} = 0.040) and cingulum (r = 0.165, p_{FDR} = 0.040). Scatterplots of the relationship between the percentage of change in MD from significant associations in the SEM models (from 73 years to 76 years) and szPGRS at p ≤ 1.0 are presented in Appendix III Supplementary Material Figure 1. Results of the SEM analyses for FA and MD using szPGRS at P ≤ 0.1 and 0.5 thresholds are presented in Appendix III Supplementary Material Tables 3 and 4.

Models examining associations between the level and change of szPGRS and graph theory metrics showed excellent fit to the data (RMSEA < 0.029, CFI > 0.985, SRMR < 0.021). There were no significant associations between szPGRS and the baseline level of graph theoretical metrics (r < 0.042, p_{FDR} > 0.05) or with their 3-year change (r < -0.039, p_{FDR} > 0.05; Table 13). The addition of blood pressure as a covariate did not have any significant effect on the results of any of the SEM models described above (p_{FDR} > 0.05). Results of the SEM analyses for graph theory measures using szPGRS at P ≤ 0.1 and 0.5 thresholds are presented in Appendix III Supplementary Material Tables 3 and 4.

Table 13. Structural equation modelling results. Standardised estimates from the associations between polygenic risk score for schizophrenia (szPGRS) at a threshold of P ≤ 1.0 and level and change in connectivity.

	Level (age 73)			Change (age 73 to 76)		
	r	*SE*	p_{FDR}	*r*	*SE*	p_{FDR}
FA						
Genu	0.039	0.040	0.674	-0.042	0.049	0.477
Splenium	-0.009	0.058	0.930	-0.082	0.063	0.266
Arcuate	0.021	0.003	0.930	-0.073	0.002	0.477
ATR	0.019	< 0.001	0.930	-0.135	0.001	0.266
Cingulum	0.125	0.004	0.147	-0.268	0.004	0.266
Uncinate	0.061	0.002	0.674	-0.074	0.003	0.477
ILF	-0.005	0.003	0.930	-0.156	0.004	0.477
MD						
Genu	0.003	0.069	0.946	0.007	0.093	0.875
Splenium	-0.037	0.112	0.821	0.132	0.158	0.040*
Arcuate	0.007	< 0.001	0.946	0.291	< 0.001	0.040*
ATR	-0.035	< 0.001	0.830	0.215	0.001	0.040*
Cingulum	-0.118	< 0.001	0.098	0.165	< 0.001	0.040*
Uncinate	-0.052	< 0.001	0.821	0.024	0.001	0.704
ILF	-0.032	0.007	0.830	0.304	0.011	0.434
Connectome						
Mean edge weight	0.042	0.002	0.369	-0.039	0.001	0.551
Strength	0.037	0.038	0.369	-0.035	0.033	0.551
Global efficiency	0.039	0.001	0.369	-0.035	0.001	0.551
Clustering coefficient	0.040	0.001	0.369	-0.034	0.001	0.551

Note: SE: Standard error, FA: fractional anisotropy, MD: mean diffusivity, ATR: anterior thalamic radiations, ILF: inferior longitudinal fasciculus, *p*-values are corrected for multiple comparison using FDR. Asterisks represent significance ($p_{FDR} < 0.05$).

Associations between extracted slopes from the SEM models and baseline levels for FA, MD and graph theory metrics are presented in Figure 20. These results illustrate that changes are highly coupled within diffusion MRI parameters and graph theory measures for level (age 73) and longitudinal change (age 73 to age 76) for structural brain connectivity in older age. Diagonal coefficients show the associations between level and change for structural connectivity and indicates that participants with lower ('healthier') MD values show greater increases in MD, and those with higher ('healthier') FA values show steeper decreases in FA. Similarly, those with higher graph theoretical metrics at baseline showed steeper declines over time.

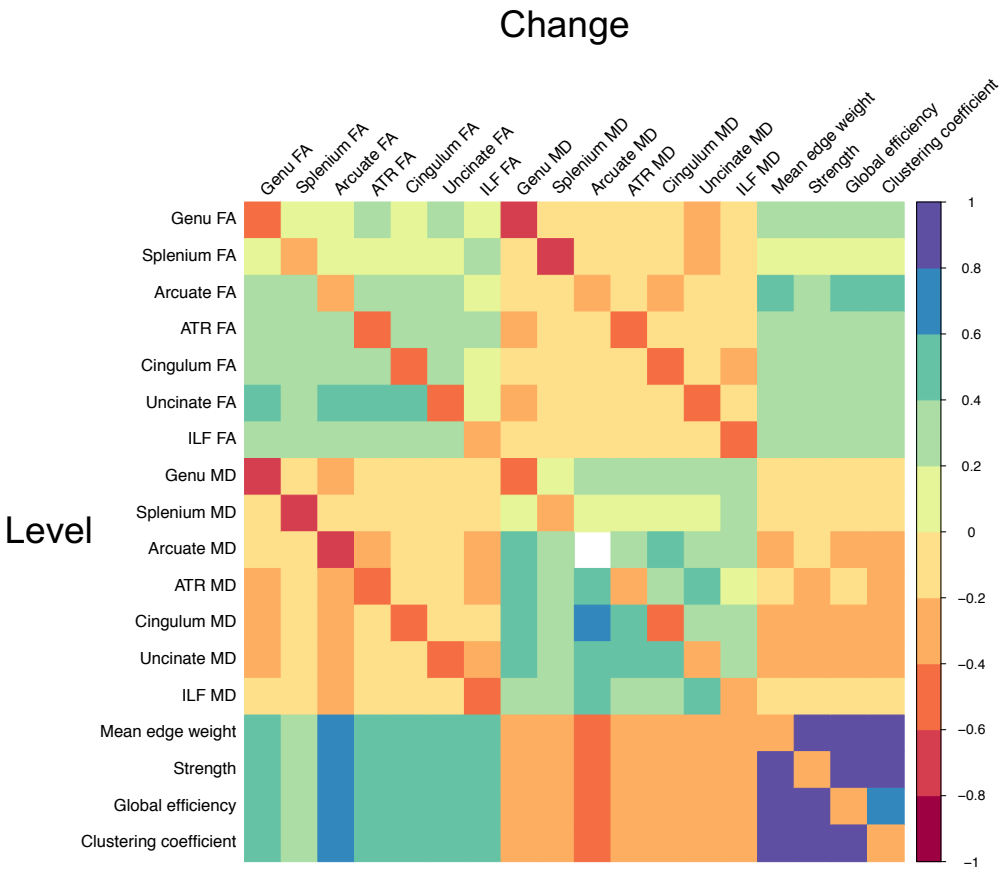

Figure 20. Heatmap illustrating Spearman's correlation coefficients for baseline level (age 73 years old, lower diagonal) and change (73 to 76 years old, upper diagonal) in white matter diffusion parameters and graph theory metrics. Diagonal coefficients represent the association between baseline and change for each metric derived from the SEM models described in Figure 16. Individual slopes for change were derived from the SEM models. Blank cells

denote those associations that did not survive multiple comparisons correction ($p_{FDR} < 0.05$). ATR = Anterior thalamic radiations; ILF = Inferior longitudinal fasciculus.

Mediation analysis

We aimed to identify mediation candidates that were consistent with the hypothesis that a higher genetic predisposition to schizophrenia is related to lower cognitive functions through the disruption of structural brain connectivity (for a detailed description of the model see Figure 17). First of all, a model examining associations between szPGRS and g_f was computed which showed good fit to the data (RMSEA = 0.059, CFI = 0.935, SRMR = 0.049). There was a significant association between szPGRS and the baseline level of g_f (r = -0.145, p = 0.001) but not with 3-year change in g_f (r = 0.003, p = 0.962). Full results of associations between szPGRS and in baseline levels and changes g_f and MD are presented in Appendix III Supplementary Material Tables 5. Given we did not find any significant associations between szPGRS and level/change in g_f and MD, there were no plausible candidates for a mediation model.

6.6. Discussion

The present study found significant associations between a greater genetic risk for schizophrenia and longitudinal increases in MD in the splenium, arcuate, ATR and cingulum fasciculi over 3 years using the largest schizophrenia GWAS to date (Pardiñas et al., 2018) and an improved reference tract segmentation analysis (Muñoz Maniega et al., 2017). We did not find any significant associations between szPGRS and change in FA or graph theoretical metrics. The results of this investigation show that there were significant differences in the microstructure of most white matter tracts studied here and network topology over a short period of time in this older age cohort. Over a three-year-old period we found significant differences in white matter microstructure for a range of major white matter tracts; for some

of these tracts we reported significant age-related decreases in FA and increases in all white matter tract's MD as well as reductions in all graph theory measures.

Numerous studies have shown consistent structural brain alterations in patients with schizophrenia. These include reductions in both grey and white matter compared to healthy controls. However, cross-sectional studies analysing the effect of szPGRS on brain structure in non-clinical samples have not been conclusive (Van der Auwera et al., 2017, 2015). Ritchie et al. (2017) showed a significant positive longitudinal association between szPGRS - derived from a previous GWAS- and 3-year change in a general factor of tract-averaged MD in the sample used in the present study. However, a limitation of generating a general factor from water diffusion MRI parameters measured in multiple tracts is that it describes commonalities among white matter tracts while excluding tract-specific individualities. Our findings indicate that the association of szPGRS with white matter MD is strongly driven by the splenium, arcuate, ATR and cingulum, all tracts previously implicated in schizophrenia. Structural abnormalities in the corpus callosum in schizophrenia have been well documented affecting interhemispheric communication in patients (Foong et al., 2000; Woodruff et al., 1995). The arcuate fasciculus as an associative fibre connects the frontal cortex with the temporal and parietal cortices and may underlie language processing anomalies in the disorder (Abdul-Rahman et al., 2012). The ATR serves as a link between the thalamic nuclei and the prefrontal cortex, and dysfunction of the thalamus has been associated with the pathophysiology of schizophrenia, particularly with cognitive deficits and negative symptoms (Mamah et al., 2010). The cingulum is the most prominent white matter tract in the limbic system and has been previously reported to be impaired in schizophrenia (Fujiwara et al., 2007).

To our knowledge, there are no studies that have investigated the association between the structural connectome and genetic risk for schizophrenia; the fact that we did not find a significant effect of szPGRS on either the baseline level or change in structural brain connectivity (as measured by graph theoretical metrics) suggests that common genetic variants

for schizophrenia and topological brain characteristics may not share a direct genetic mechanism. Nevertheless, szPGRS evinced non-significant detrimental relations with all brain structural metrics. The fact that the LBC1936 comprises relatively healthy, community-dwelling older adults, none of whom have schizophrenia, coupled with the relatively brief (3 year) period of follow-up may have limited our ability to detect slighter effects. Interestingly, a previous study on targeted genetic analysis showed that differentially expressed genes in a well-characterised rat model of vascular white matter disease were associated with white matter hyperintensities (which exhibit elevated MD and reduced FA) in the LBC1936 and these included genes associated with schizophrenia and neurodevelopmental intellectual disabilities (Lopez et al., 2015). These results suggest that genetic risk for schizophrenia may have a role in age-related changes in brain structural connectivity, even among individuals who are not diagnosed with schizophrenia. Previous studies have suggested the conceptualization of schizophrenia as a syndrome of accelerated ageing (Kirkpatrick et al., 2008) indicating, for instance, significant declines in white matter coherence more than twice that of age-matched controls (Kochunov et al., 2013), with this reduction being linear from early adulthood and steeper as a function of increasing age (Cropley et al., 2017). Therefore, it may be possible that higher szPGRS confers certain risks for accelerated white matter ageing in healthy older participants. It is also likely that other factors such as gene-gene interactions, rare variants, and gene-environment interplay may help to explain the association between risk variants for schizophrenia and brain structural impairments (Van der Auwera et al., 2017).

Some white matter tracts showed significant reductions and increases in FA (standardised *r* from 0.056 to -0.062) and all showed increases in MD (standardised *r* from 0.171 to 0.452) as a function of increasing age. These results are in line with those of previous studies where white matter microstructure declines with age (reviewed in Bennett & Madden, 2014). For instance, we found that MD of more frontal white matter tracts was more affected

while more occipital tracts were more resilient to the effects of age (see Table 12). This is consistent with the hypothesis that ageing has region-specific effects, in particular the existence of an anterior-posterior gradient of age-related decline whereby tracts that are the last to develop are the most vulnerable to the ageing process (Bennett and Madden, 2014; Cox et al., 2016; Qiu et al., 2015). This pattern could be a consequence of the finding that later developed tracts are more thinly myelinated and therefore more susceptible to decline (Bartzokis et al., 2004). ATR and uncinate fasciculi, conversely, showed an increase in FA with age in this study. White matter fibres within these tracts are known to have a complex architecture due to the presence of a large number of crossing fibres (Niida et al., 2013; Olson et al., 2015). Since FA is highly dependent on white matter architecture (Pierpaoli et al., 1996), it is possible that a loss of white matter fibres might lead to an increase in FA if the remaining fibres are more uniformly orientated than they were previously (Jones et al., 2006). Therefore, the observed increase of FA in the ATR and uncinate fasciculi may reflect the overall effect of loss of crossing fibres resulting from age-related neurodegeneration. This combination of observations provides some support for the conceptual premise that diffusion MRI parameters are significantly associated with cognitive decline in ageing cohorts (Madden et al., 2012) as well as in patients diagnosed with schizophrenia (Alloza et al., 2016; Kochunov et al., 2017).

This study found that those participants with 'healthier' white matter at baseline showed a steeper decline over time (see Figure 20). This same pattern for other brain imaging parameters has previously been reported in this sample and has been suggested to represent the Law of Initial Value and regression to the mean (Ritchie et al., 2015; Wilder, 1957), indicating that there may be more neurobiological processes that can affect those with 'healthier' white matter at baseline than those with a less healthy white matter. Given that there were no significant associations between szPGRS and baseline white matter measures in this study, it is perfectly reasonable for the associations between szPGRS and change in

MD, and between baseline level of MD and change in MD to be non-coincidental phenomena – that is, for the common variance between szPGRS and change, and between baseline and change, to be mutually exclusive.

As an additional analysis we tested whether change in MD would mediate the association between szPGRS and change in fluid intelligence. We found significant negative associations between baseline levels of MD in the splenium, arcuate and ATR and baseline levels of g_f as well as a significant negative association between szPGRS and baseline g_f. These results indicate that higher baseline g_f is associated with a 'healthier' baseline white matter microstructure in this cohort. However, we did not find an association between szPGRS and change in g_f and thus, the data did not support the hypothesis that these candidates were plausible for a mediation model. It is likely that the relatively brief (3 year) period of follow-up may have limited our ability to detect modest effects, indicating that longer follow-ups and potentially the study of other factors that contribute to cognitive decline in older age, may be required. Ritchie et al. (2015) reported significant associations between change in FA and change in fluid intelligence, indicating that MD of the white matter tracts studied here may be more pertinent to other cognitive functions. Further work is required to investigate this hypothesis. Therefore, these data show that szPGRS is related to some selective MD changes over time, but not to cognitive decline over this same period.

This study is one of the first to examine the ageing of the human structural connectome longitudinally from healthy older participants. By taking a longitudinal approach, our results shed light on age-related brain structural decline by minimizing problems inherent to cross-sectional mediation methods (Hofer and Sliwinski, 2001; Lindenberger et al., 2011) while allowing age-related changes and associations with genetic risk factors to be

investigated independently of age. The current study found subtle decreases in all graph theory metrics over a period of three years. Mean edge weight and strength decreased significantly over time while decreases in global efficiency and clustering coefficient did not reach significance. Reductions in graph theory measures, which describe topological aspects of the brain's networks were found to co-exist with microstructural declines in white matter tracts over time as shown in Figure 20. These results are consistent with the modest pre-existent literature on structural connectivity in ageing populations (Damoiseaux, 2017). In a cross-sectional study, Gong et al. (2009) reported lower overall connectivity and local efficiency as a function of age, but no differences in global efficiency. Zhao et al. (2015) using streamline density as a weighted measure, found an inverted U-shape for strength and global efficiency and a U-shape trajectory for clustering coefficient across the lifespan. This latter finding may be able to explain the nominal change in clustering coefficient in our study. Moreover, functional and structural connectivity studies seem to show closely related differences associated with age (Betzel et al., 2014; Fjell et al., 2016; Zimmermann et al., 2016).

6.7. Limitations

The generalisability of these results is subject to certain limitations. For instance, this study only covered a period of three years, which may not be sufficient to capture the effect of more subtle age-related changes. Measurement across only two occasions precludes consideration on non-linear trends or accelerating changes as a function of genetic liability to schizophrenia. Likewise, as sample sizes increases for GWAS better predictive power will be achieved by szPGRS. The choice of the most liberal SNP inclusion threshold (all SNPs, p = 1.00) may have affected the results presented here; however, this threshold has been recommended previously in order to allow replication by other studies and to maximise the potential predictive capacity (Ware et al., 2017). Furthermore, we present results for the SEM

analysis at $p \leq 0.1$ and $p \leq 0.5$ szPGRS thresholds in Appendix III Supplementary Material Tables 3 and 4.

For tractography, we extracted water diffusivity MRI parameters from twelve major white matter tracts, overlooking the rest of the connections. However, these tracts were well-characterised and reliably measured as previously reported (Bastin et al., 2010; Muñoz Maniega et al., 2017); moreover, we took account of all these connections by calculating whole-brain mean edge weight to include mean FA of all connections identified in the structural connectome. We also acknowledge the possibility that tract measures of FA and MD could potentially be affected by partial volume effects (pve) of cerebrospinal fluid (CSF). However, in the current analysis we segmented the tracts of interest using probabilistic neighbourhood tractography, which uses single seed point tractography, followed up by a streamline rejection criterion where individual streamlines are retained or rejected based on their probabilities under the topology model (Clayden et al., 2009a). This results in a tract made up from a 'core' of the streamlines that follow the expected tract topology, which is potentially less sensitive to pve than other tractography methods which segment larger white matter regions. In addition, we calculated tract-averaged MD and FA values weighted by the connection probability, which is usually lower at the edges of the tract, with the result that white matter voxels closer to CSF structures would have lower contribution to the mean.

The global metrics calculated across the entire structural connectome cannot address the possibility that specific networks (i.e. subsets of nodes or edges) show age-related changes that are more sensitive to szPGRS. In addition, network comparability issues may arise as a result of differing density between networks since the number of nodes or network's degree influences the computation of global theory metrics (see Brain Connectivity Toolbox for a detailed description of metrics: https://sites.google.com/site/bctnet). Therefore, we chose to control each subject's graph theory measure for edge density. The validity of the correction

of density remains an issue in need of further exploration. For instance, correcting for density may affect regression coefficients due to the apparent multicollinearity between graph theory metrics. Further limitations inherent to longitudinal studies include attrition and loss of follow-up. However, we implemented maximum likelihood estimation methods that reduce missing data bias derived from longitudinal attrition. Finally, we implemented latent change score models across all parameters, including those in which we only had a single indicator (graph theoretical and callosal metrics). We did so to maintain comparability of analytic approach and results across all analyses, but the single indicator change score models should essentially be considered difference scores because they are unable to parse out error variance (Gollwitzer et al., 2014).

Finally, further research is required to examine whether any of the associations between water diffusion metrics and szPGRS are sex-specific, or alternatively show similar patterns in males and females. Recently, a growing number of studies have suggested a reduced leftward structural asymmetry in schizophrenia compared to healthy controls (Ribolsi et al., 2014), hence in this study we did not constrain the loadings to be equal for the left and right white matter tracts in the SEM analysis. However, further research is needed to address in greater detail this hypothesis.

Conclusion

The present longitudinal study was designed to determine the association of genetic risk for schizophrenia with brain structure. We found a significant association between higher szPGRS and increasing MD for the splenium, arcuate, ATR and cingulum, consistent with the hypothesis that higher genetic liability for schizophrenia is related to accelerated brain ageing among relatively healthy older adults. We also present some valuable data on the nature of brain connectivity changes in older age. Over a three-year-old period we found significant

differences in white matter microstructure for a range of major white matter tracts; for some of these tracts we reported significant age-related decreases in FA and increases in all white matter tract's MD. This decline in white matter microstructure was accompanied by disruptions at the topological level. All graph theory metrics showed subtle decreases over this narrow timeframe. However, only mean edge weight and strength reached our specified significance level. In this study we also examined the hypothesis that higher szPGRS is associated with a steeper decline in cognition via change in white matter structure in older age. Significant negative associations between baseline levels of general fluid intelligence and szPGRS and baseline levels of MD in the splenium, arcuate and ATR were found. Taken together, these findings suggest subtle age-related declines in white matter connectivity which take place over a relatively short period of time in older age with szPGRS conferring some risk for these changes in brain structure.

6.8. Acknowledgements

This work was funded by Age UK (Disconnected Mind project http://www.disconnectedmind.ed.ac.uk) and the UK Medical Research Council (MR/M01311/1 and G1001245/96077). This study was conducted in the Centre of Cognitive Ageing and Cognitive Epidemiology (CCACE; http://www.ccace.ed.ac.uk), part of the cross-council Lifelong Health and Wellbeing Initiative (MR/K026992/1). The work was also supported by the US National Institutes of Health (National Institute on Aging; 1R01AG054628-01A1), the Scottish Funding Council through the Scottish Imaging Network, a Platform for Scientific Excellence (SINAPSE; http://www.sinapse.ac.uk) and the Row Fogo Charitable Trust. Brain imaging was performed in the Brain Research Imaging Centre (BRIC; http://www.bric.ed.ac.uk). We thank the Lothian Birth Cohort 1936 participants who took part in this study, the radiographers at BRIC, and LBC1936 team research associates who assisted

with data collection. The authors report no real or potential conflicts of interest concerning this work.

6.9. Chapter discussion

This study found significant associations between higher genetic risk for schizophrenia and greater decline in white matter microstructure in a sample of healthy elderly participants; consistent with the hypothesis that higher genetic liability for schizophrenia is related to accelerated brain ageing among relatively healthy older adults. Moreover, this chapter offers valuable data in regard to longitudinal trajectories of white matter connectivity and is one of the first studies investigating the longitudinal change in graph theory metrics in older age.

Chapter 7 Neurostructural properties of the salience network and polygenic risk scores for schizophrenia in UK Biobank

7.1. Overview

This chapter focuses on the investigation of the neurostructural properties of the salience network in a large sample of healthy participants. Functional and structural MRI studies of the salience network have consistently reported impairments in schizophrenia. From a connectome perspective, a mask containing all nodes implicated in the salience network was derived and the FA of the connecting pathways between nodes was computed. Therefore, the aim of this chapter was to analyse the potential associations between genetic risk for schizophrenia and white matter FA and grey matter volume and thickness of the nodes within this network. We hypothesised that higher genetic risk for schizophrenia would be associated with less 'healthy' brain structure (lower FA in connecting pathways and lower grey matter volume/thickness). Moreover, we sought to investigate whether the grey or white matter components of this network would mediate the relationship between genetic risk for schizophrenia and psychotic symptoms.

This study was conceived by CA, SRC and MEB. CA derived the networks, analysed the data and wrote the manuscript. SRC and MEB were the main supervisors of this project with co-supervision provided by HCW and SML. SRC and MEB derived the connectivity matrices from structural MRI data provided by UKBiobank group. MBC aided with the imaging analysis. JG created the polygenic risk scores.

Citation: Alloza, C., Blesa Cábez, M., Bastin, M.E., Buchanan, C., Gibson, J., Whalley, H.C., Cox, S.R, Lawrie, S.M. Psychotic-like experiences, polygenic risk scores for schizophrenia and structural properties of the salience, default mode and central-executive networks in healthy participants from UK Biobank (*in preparation*).

7.2. Introduction

Schizophrenia is a highly heritable neuropsychiatric disorder with a lifetime prevalence around 1%, being placed as one of the leading causes of disability worldwide (Gurung and Prata, 2015). Schizophrenia has a multiple and varied phenotypic expression which hinders an adequate definition and thus, the lack of appropriate clinical descriptions that relates to the underlying pathophysiology impedes an improved treatment or prognosis for the patients; and thus, increasing effort is being directed to define an adequate biologically construct of the disorder. Patients usually present with a range of positive and negative symptoms that may be accompanied by cognitive impairments. Positive symptoms include delusions, hallucinations, and disorganised thinking and while not in a consistent manner, its severity has been linked to impaired brain structure. From the early descriptions by Bleuler (1911-1950) and subsequently by Friston and Frith (1995), the study of schizophrenia has been directed towards its conceptualization as a "dysconnection syndrome", suggesting that the disorder may be understood in terms of cognition and pathophysiology as a brain integration failure (Friston, 1998). Neuroimaging studies have supported this hypothesis by reporting multiple structural connectivity impairments with specific brain networks being implicated in schizophrenia.

The human brain consists of several distinct, interactive networks. In this context, the salience network is a system involved in the identification of biological and behaviourally relevant stimuli and the subsequent coordination of neural resources to guide flexible behaviour (Menon, 2015; Uddin, 2015). This network has been identified through resting state fMRI studies (Seeley et al., 2007; Sridharan et al., 2008), involving mainly the cortical regions of the insula and the anterior cingulate cortex and limbic areas of the amygdala, thalamus, ventral striatum, and substantia nigra. Further evidence comes from DTI studies which have

identified white matter tracts connecting the insula and the anterior cingulate cortex by performing deterministic tractography between these two nodes (Uddin et al., 2011; van den Heuvel et al., 2009a). However, the precise pathways connecting cortical and subcortical regions within the salience network have so far only been described in non-human primates (Mesulam and Mufson, 1982; Nieuwenhuys, 2012; Schmahmann and Pandya, 2009). Recent structural and functional studies have suggested that impairments within the salience network are a key feature of many neuropsychiatric diseases; with aberrant intrinsic functional connectivity of the salience network in schizophrenia (Manoliu et al., 2014; Orliac et al., 2013) and in individuals at risk for psychosis (Wotruba et al., 2014). In addition, cortical thickness and white matter have been proposed as possible endophenotypes of schizophrenia due to their high heritability (Gogtay et al., 2007; Goldman et al., 2009; Jahanshad et al., 2013; Kochunov et al., 2010; Winkler et al., 2010).

Schizophrenia is both highly heritable and polygenic, with many common alleles of small effect, and increasing numbers of genome-wide significant loci have been identified as sample sizes increase (Hilker et al., 2018; International Schizophrenia Consortium et al., 2009; Schizophrenia Working Group of the Psychiatric Genomics Consortium, 2014). One of the largest schizophrenia genome-wide association studies (GWAS) performed to date included 36989 cases and 113075 controls; it identified 108 independent genome-wide significant single nucleotide polymorphisms (SNPs) ($P < 5 \times 10^{-8}$) associated with a diagnosis of schizophrenia (Schizophrenia Working Group of the Psychiatric Genomics Consortium, 2014). It is further noteworthy that summary statistics from large-scale GWAS allow the degree of genetic liability for a heritable trait (in this case, schizophrenia) to be estimated in healthy subjects outside the population in which the original GWAS was conducted (Van der Auwera et al., 2017, 2015).

Nevertheless, thus far, only a small number of studies have analysed the relationship between polygenic risk score for schizophrenia (szPGRS) and neuroimaging biomarkers in healthy and patient samples (Alloza et al., 2018, 2017; Birnbaum and Weinberger, 2013; McIntosh et al., 2013; Ritchie et al., 2017; Van der Auwera et al., 2015; Whalley et al., 2015b). All these studies used a previous GWAS (Schizophrenia Working Group of the Psychiatric Genomics Consortium, 2014), while a previous study from our centre (Alloza et al., 2018),[3] the largest GWAS currently available (Pardiñas et al., 2018). Even though the PGRS predictive power is principally driven by the number of participants in the originating GWAS, it is also true that sufficiently large samples in the 'test' sample are also required in order to more reliably detect the likely modest effect sizes.

Thus, in this paper, we investigated the hypothesis that szPGRS relates to the neuroanatomy of the salience network by mapping the trajectories of water diffusion MRI parameters (using fractional anisotropy (FA)), grey matter thickness and volume of the regions involved in this network in a large sample of healthy participants from UK Biobank (N = 1789). We used a novel approach based on ROI-ROI analysis (derived from connectome processing) which allows a much finer-grained network approach than using other approaches to quantifying white matter connectivity without specific linkage to cortical or subcortical regions.

7.3. Methods

Participants

UK Biobank (http://www.ukbiobank.ac.uk/) comprises around 500,000 community-dwelling participants recruited from across Great Britain between 2006 and 2014 (Allen et al. 2012; Collins 2012; Miller et al., 2016). A subset of the participants who were part of the initial recruitment began attending for head MRI scanning. MRI and genetic data from 1789

[3] See Chapter 6 for full results of this analysis.

participants were available for the present study (mean age = 62.59 years, SD = 7.59, range = 45.42 – 78), collected at an average of around 4 years after the initial visit, and completed on an MRI scanner in Manchester, UK (all data presented in this analysis were collected on the same scanner). There were 789 females (mean age = 62.21, years, SD = 7.45, range = 45.58 to 78) and 1000 males (mean age = 62.90 years, SD = 7.68, range = 45.42 to 77.83). UK Biobank received ethical approval from the Research Ethics Committee (reference 11/NW/0382). The present analyses were conducted as part of UK Biobank application 16124. All participants provided informed consent to participate. Further information on the consent procedure can be found here: http://biobank.ctsu.ox.ac.uk/crystal/field.cgi?id = 200.

Scan Acquisition

Full details of the image acquisition and processing can be found on the UK Biobank website (http://biobank.ctsu.ox.ac.uk/crystal/refer.cgi?id=2367), Brain Imaging Documentation (http://biobank.ctsu.ox.ac.uk/crystal/refer.cgi?id=1977) and in Miller et al. (2016). MRI data for all participants were acquired on a single Siemens Skyra 3 T scanner. Briefly, the acquired 3D MPRAGE T1-weighted volumes were preprocessed and analyzed using FSL tools (http://www.fmrib.ox.ac.uk/fsl) by the UK Biobank brain imaging team. This included a raw, de-faced T1-weighted volume, a reduced field-of-view (FoV) T1-weighted volume, and further processing, which included skull stripping, bias field correction and gross tissue segmentation using FNIRT (Andersson et al., 2007) and FAST (Zhang et al., 2001), yielding cerebrospinal fluid (CSF), grey and white matter volumes. Where large, common artefacts, such as head movement, were identified during scanning, image acquisition was re-started. However, visual quality control was not systematically undertaken by the UK Biobank team; this would be unfeasible due to the very large sample size (Alfaro-Almagro et al., 2018). No significant changes were made to scanner hardware or software during the period of MRI data acquisition; full details on protocol phases and relevant upgrades are available at the following URL: http://biobank.ctsu.ox.ac.uk/crystal/docs/brain_mri.pdf.

Image processing

Each 3D T_1-weighted FSPGR volume was parcellated into 85 (Desikan et al., 2006) regions-of-interest (ROI) using FreeSurfer (http://surfer.nmr.mgh.harvard.edu), which comprised 34 cortical ROIs and eight sub-cortical ROIs per hemisphere, plus the brainstem. Segmentations were visually checked, then used to construct grey and white matter masks for use in network construction and to constrain the tractography output as described below. Using tools provided by the FDT package in FSL (http://fsl.fmrib.ox.ac.uk/fsl), the diffusion MRI data were pre-processed to reduce systematic imaging distortions and bulk subject motion artefacts by affine registration of all subsequent EP volumes to the first T_2-weighted EP volume (Jenkinson and Smith, 2001). Skull stripping and brain extraction were performed on the registered T_2-weighted EP volumes and applied to the mean diffusivity/fractional anisotropy (MD/FA) volumes calculated by DTIFIT in each subject (Basser and Pierpaoli, 1996; Smith, 2002). The neuroanatomical ROIs determined by FreeSurfer were then aligned from 3D T_1-weighted volume to diffusion space using a cross-modal nonlinear registration method. As a first step, linear registration was used to initialize the alignment of each brain-extracted FA volume to the corresponding FreeSurfer extracted 3D T_1-weighted brain volume using a mutual information cost function and an affine transform with 12 degrees of freedom (Jenkinson and Smith, 2001). Following this initialization, a nonlinear deformation field based method (FNIRT) was used to refine local alignment (Andersson et al., 2007). FreeSurfer segmentations and anatomical labels were then aligned to diffusion space using nearest neighbour interpolation.

Structural connectome

Whole-brain probabilistic tractography was performed using FSL's BedpostX/ProbTrackX algorithm (Behrens et al., 2007). Probability density functions, which describe the uncertainty in the principal directions of water diffusion, were computed using a

two-fibre model per voxel (Behrens et al., 2007). Streamlines were then constructed by sampling from these distributions during a tracking process that involved all white matter voxels using 100 Markov Chain Monte Carlo iterations with a fixed step size of 0.5 mm between successive points. Tracking was initiated from all white matter voxels (Buchanan et al., 2014) in two collinear directions until terminated by the following stopping criteria designed to minimize the amount of anatomically implausible streamlines: (i) exceeding a curvature threshold of 70 degrees; (ii) entering a voxel with FA below 0.1 (Verstraete et al., 2011); (iii) entering an extra-cerebral voxel; (iv) exceeding 200 mm in length; and (v) exceeding a distance ratio metric of 10. The distance ratio metric (Bullitt et al., 2003), excludes implausibly tortuous streamlines. For instance, a streamline with a total path length 10 times longer than the distance between end points was considered to be invalid. The values of the curvature, anisotropy and distance ratio metric constraints were set empirically and informed by visual assessment of the resulting streamlines.

Network construction

For each subject, two networks were constructed, the number of streamline (NOS) network, that was created using the number of streamlines connecting each pair of the 85 ROI (network node) pairs from the default FreeSurfer cortical (Desikan et al., 2006) and subcortical regions; and the FA-weighted networks, that were constructed by recording the mean FA value along streamlines. The endpoint of a streamline was considered to be the first grey matter ROI encountered when tracking from the seed location. In order to reduce the number of spurious connections derived from probabilistic tractography, we applied to the NOS matrices, using the numbers of streamlines connecting all 85 ROI and preserving exclusively the top 30% white matter tracts that were more consistent across subjects (Roberts et al., 2017). This mask was then applied to the FA-weighted connectivity matrices. For each FA-weighted connectivity matrix for the thresholded network, the salience network mask was applied based on our bilateral nodes of interest: insula, caudal anterior cingulate (CAC), thalamus, amygdala

and ventral diencephalon (VDC).

Polygenic risk score calculation

The details of the array design, genotyping, quality control and imputation have been described previously (Hagenaars et al., 2016). Quality control included removal of participants based on missingness, relatedness, gender mismatch and non-British ancestry. Polygenic profiles were created for schizophrenia in all the genotyped participants using PRSice (Euesden et al., 2015). PRSice calculates the sum of alleles associated with the phenotype of interest across many genetic loci, weighted by their effect sizes estimated from a genome-wide association study of that phenotype in an independent sample. Before creating the scores, the SNPs with a minor allele frequency <1% were removed and clumping was used to obtain SNPs in linkage equilibrium with an $r^2 < 0.25$ within a 200 bp window. Five scores were created for each individual using SNPs selected according to the significance of their association with the phenotype at nominal p-value thresholds of 0.01, 0.05, 0.1, 0.5 and 1.0 (all SNPs). Our primary analyses used scores generated from a list of SNPs with a GWAS training set of $p \leq 0.1$, 0.5 and 1.0 thresholds. Fifteen multidimensional scaling factors (estimated from SNP data) were entered into the models as additional 'nuisance' covariates to control for population stratification, along with age and genotyping array. For the present study, data was available for 1789 participants who were unrelated, survived the quality control process and had full imaging data available.

Statistical analyses

First, associations between szPGRS and white matter tract FA values, cortical thickness and volume were calculated using linear regression models. Previous studies have suggested that schizophrenia is a syndrome of accelerated ageing (Kirkpatrick et al., 2008) indicating, for instance, significant declines in white matter coherence more than twice that of age-matched controls (Kochunov et al., 2013). Therefore, we included an interaction between

age at MRI and szPGRS in all analyses. Age at the time of MRI acquisition and sex were entered as covariates and the interaction between were entered as a predictor. For each node's cortical thickness, average total brain cortical thickness and for each node's volume, intracranial volume (ICV) were entered as additional covariates. Analyses were performed in R (https://www.r-project.org) and standardised betas were reported.

We then estimated a structural equation model (SEM) for FA values, cortical thickness and volume. We estimated a separate model for each MRI metric, which were set as the dependent variable in each model. Latent score models were used to assess associations of szPGRS with MRI parameters. Specifically, three latent scores were derived: a cortical thickness factor was derived from the bilateral cortical nodes, a volume factor including all bilateral cortical and subcortical nodes, and an FA factor derived from all pathways connecting bilateral nodes. Figure 21 shows a simplified diagram of the SEM framework. Within the model, each brain imaging measure was adjusted for its respective sex and ICV (for volume) at the manifest level, while szPGRS was adjusted for sex, population stratification components and genotyping array. Due to the apparent association between schizophrenia and accelerated ageing (Kirkpatrick et al., 2008), we added the interaction between szPGRS and age in the SEM analysis in order to test the hypothesis that higher risk for schizophrenia is associated with a steeper decline in brain structure as a function of increasing age. SEM was performed using the package 'lavaan' (Rosseel, 2012) in R with full-information maximum likelihood estimation to use all data available. All significance (p) values ($\alpha = 0.05$) were corrected for multiple comparisons using false discovery rate within each szPGRS threshold (FDR, p_{FDR}) (Benjamini and Hochberg, 1995).

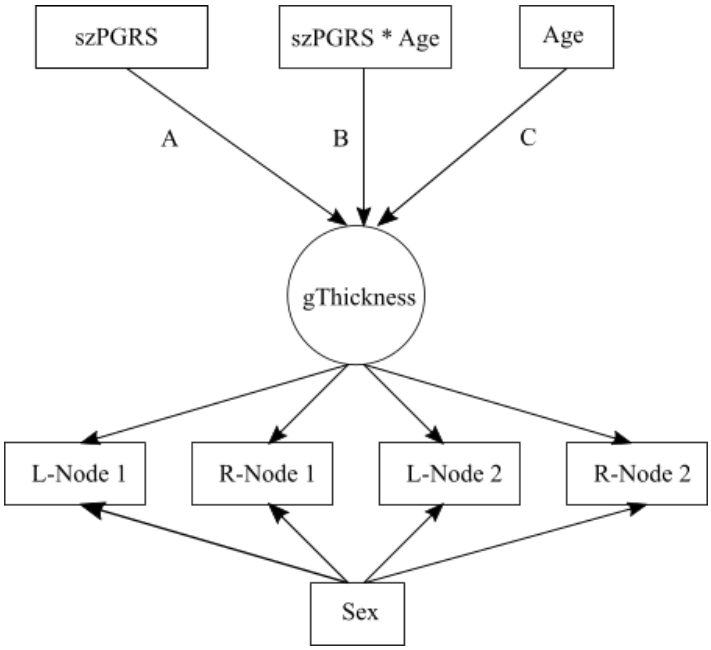

Figure 21. Diagram of the structural equation model (SEM) for neurostructural properties of the salience network. A separate model was applied to FA, grey matter thickness and grey matter volume. From each individual bilateral node (L: left; R: right) or pathway, a latent score was calculated for FA, grey matter thickness and grey matter volume. Relation between FA/thickness/volume and polygenic risk score for schizophrenia (szPGRS) is indicated by path A; path B represents the association between the interaction of age and szPGRS and FA/thickness/volume factors; path C represents the association between age and the latent factor. szPGRS was corrected for sex and population stratification (paths not shown).

7.4. Results

Demographic, pairwise complete data for genetic and imaging sample sizes after quality control and each brain imaging measure are provided in Tables 14 and 15.

Table 14. Demographic data and descriptives for nodes within the salience network for white matter water diffusion MRI.

	Valid N	Mean	SD	Min	Max
Age (years)	1789	62.59	7.59	45.42	78
Sex (% females)	1789	44.10%			
szPGRS 0.1	1789	-0.00143	$6.74x10^{-05}$	-0.00165	-0.00121
szPGRS 0.5	1789	-0.00079	$2.71\ x10^{-05}$	-0.00087	-0.00070
szPGRS 1	1789	-0.00051	$1.73\ x10^{-05}$	-0.00057	-0.00045
Grey Matter Thickness (mm)					
L - CAC	1789	2.754	0.278	1.484	3.847
R - CAC	1789	2.587	0.257	1.712	3.631
L - Insula	1789	2.954	0.156	1.822	3.460
R - Insula	1789	2.942	0.163	2.392	3.588
Grey Matter Volume (mm^3)					
L - CAC	1789	1878.42	474.41	673	4258
R - CAC	1789	2130.84	484.55	808	4006
L - Insula	1789	6539.52	733.76	2957	9010
R - Insula	1789	6827.79	811.02	4488	9519
L - Thalamus	1789	7853.40	775.23	4209	11051
R - Thalamus	1789	7664.37	749.24	4988	10668
L - Amygdala	1789	1282.87	250.26	552	2240
R - Amygdala	1789	1243.20	281.93	418	2437
ICV (mm^3)	1789	1215648.46	116203.83	866567.8	1665260.9

Note: SD: Standard deviation, Min: minimum value, Max: maximum value, szPGRS: polygenic risk score for schizophrenia, L: left, R: right, CAC: caudal anterior cingulate, ICV: intracranial volume.

Table 15. Descriptives for pathways identified connecting nodes within the salience network for white matter water diffusion MRI.

White matter tract	Valid N	Mean FA	SD	Min	Max
L-Thalamus : L-VDC	1789	0.653	0.034	0.446	0.777
L-Thalamus : R-Thalamus	1789	0.570	0.028	0.322	0.667
L-Thalamus : R-VDC	1789	0.580	0.026	0.402	0.674
L-Thalamus : L-CAC	1788	0.497	0.028	0.413	0.614
L-Thalamus : L-Insula	1789	0.502	0.032	0.307	0.641
L-Thalamus : R-Insula	1789	0.554	0.025	0.465	0.638
L-Amygdala : L-VDC	1789	0.282	0.034	0.180	0.429
L-Amygdala : L-Insula	1789	0.311	0.042	0.182	0.510
R-Thalamus : R-VDC	1789	0.538	0.057	0.359	0.719
R-Thalamus : R-CAC	1788	0.508	0.029	0.382	0.614
R-Thalamus : R-Insula	1789	0.477	0.029	0.318	0.588
R-Amygdala : R-VDC	1789	0.300	0.040	0.177	0.456
R-Amygdala : R-Insula	1789	0.296	0.042	0.163	0.459
R-VDC : R-Insula	1789	0.445	0.063	0.255	0.618

Note: SD: Standard deviation, Min: minimum value, Max: maximum value, FA: fractional anisotropy, L: left, R: right, CAC: caudal anterior cingulate, VDC: ventral diencephalon.

SEM analyses

Latent factor for grey matter volume within the Salience Network

The models examining associations of szPGRS at $p \leq 0.1$, 0.5 and 1.0 thresholds and grey matter thickness fit the data well (RMSEA < 0.037, CFI = 0.991, SRMR < 0.022). The association between the latent factor for grey matter volume and szPGRS at a threshold of $p \leq 0.1$ was significant (r = -0.050, SE = 0.014, $p = 0.036$), however this association did not survive FDR-correction ($p_{FDR} = 0.108$). Associations between the latent factor for volume and szPGRS at $p \leq 0.5$ and 1.0 were not significant (r = -0.030, SE = 0.015, $p_{FDR} = 0.314$; r = -0.022, SE = 0.015, $p_{FDR} = 0.366$, respectively). Age showed a significant negative effect on

the latent factor (r = -0.204, SE = 0.015, $p < 0.001$). However, the interaction between age and szPGRS was not significant at any threshold ($p_{FDR} > 0.05$). Figure 22 shows the standardised coefficients for all latent factors across all szPGRS thresholds.

Latent factor for grey matter thickness within the Salience Network

The models examining associations of szPGRS at $p \leq 0.1$, 0.5 and 1.0 thresholds and grey matter thickness fit the data well (RMSEA < 0.044, CFI > 0.982, SRMR < 0.019). Associations between the latent factor for grey matter thickness and szPGRS were significant at a threshold of $p \leq 0.1$ (r = -0.071, SE = 0.018, $p_{FDR} = 0.048$). At the thresholds of $p \leq 0.5$ (r = -0.058, SE = 0.019, $p_{FDR} = 0.061$) and $p \leq 1.0$ (r = -0.050, SE = 0.019, $p_{FDR} = 0.061$), the associations showed a tendency towards significance. Age showed a significant positive effect on the latent factor (r = 0.120, SE = 0.021, $p < 0.001$). The interaction between age and szPGRS was not significant at any threshold ($p_{FDR} > 0.05$).

Latent factor for white matter FA within the Salience Network

The models examining associations of szPGRS at $p \leq 0.1$, 0.5 and 1.0 thresholds and white matter FA fit the data well (RMSEA = 0.048, CFI = 0.933, SRMR = 0.036). There were no significant associations between the latent factor for FA and szPGRS at any threshold ($p_{FDR} > 0.05$). Age showed a significant effect on the latent factor (r = 0.058, SE = 0.021, $p = 0.022$). The interaction between age and szPGRS was not significant at any threshold.

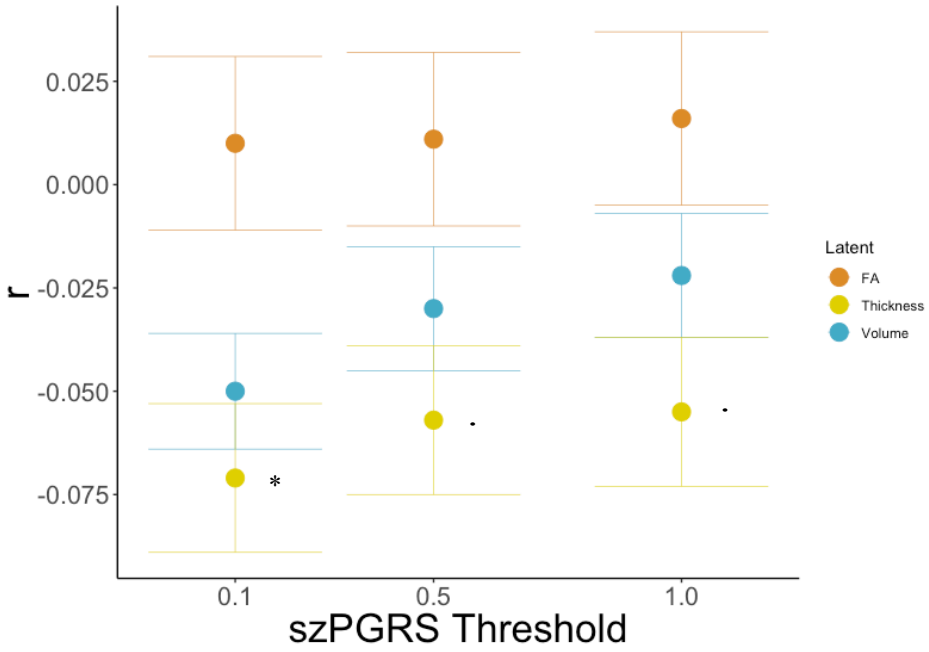

Figure 22. Magnitude of standardised r coefficients (represented in circles) and standard errors (in bars) from the SEM analysis across all szPGRS thresholds for grey matter volume, cortical thickness and fractional anisotropy (FA). Asterisks indicate significance from the SEM models ($p_{FDR} < 0.05$) and black dots tendency towards significance ($p_{FDR} = 0.06$).

Linear regressions between szPGRS and individual Salience Network components

Cortical and subcortical volumes

The volume of the right thalamus showed a negative significant association with szPGRS at a threshold of 0.1 (β = -0.037, SE = 0.014, $p = 0.011$). However, this association did not survive multiple comparison correction ($p_{FDR} = 0.087$). The volumes of the right thalamus and left CAC showed a tendency towards significance at a threshold of 0.5 (β = -0.027, SE = 0.014 , $p = 0.067$ and β = -0.042, SE = 0.022, $p = 0.059$), but none survived multiple comparison correction ($p_{FDR} = 0.244$ for both). Age and sex showed some significant associations with grey matter volumes ($p_{FDR} < 0.05$; see Appendix IV Supplementary Material Table 1 for more detailed information). There were no significant age × sex interaction effects ($p_{FDR} > 0.05$).

Cortical thickness

Significant negative associations were found between the right insula and szPGRS at a threshold of 0.1 (β = -0.046, SE = 0.021, p = 0.024), 0.5 (β = -0.049, SE = 0.021, p = 0.016) and 1 (β = -0.049, SE = 0.021, p =0.018). However, none of these associations survived multiple comparison correction (p_{FDR} = 0.070, p_{FDR} = 0.067, p_{FDR} = 0.071, respectively). The left insula showed a significant association with szPGRS at a threshold of 0.1 (β = -0.042, SE = 0.021, p = 0.034) but did not survive multiple comparison correction (p_{FDR} = 0.070). There were no significant associations between the thickness of the CAC and szPGRS at any threshold (p_{FDR} > 0.05). Age and sex showed significant associations with cortical thickness (p_{FDR} > 0.05; see Appendix IV Supplementary Material Table 1 for more detailed information). We found a significant age × sex interaction for the right CAC at a threshold of 0.1 (β = -0.064, SE = 0.023, p_{FDR} = 0.025). Figure 23 shows the beta coefficients of the associations between cortical thickness and szPGRS across all thresholds.

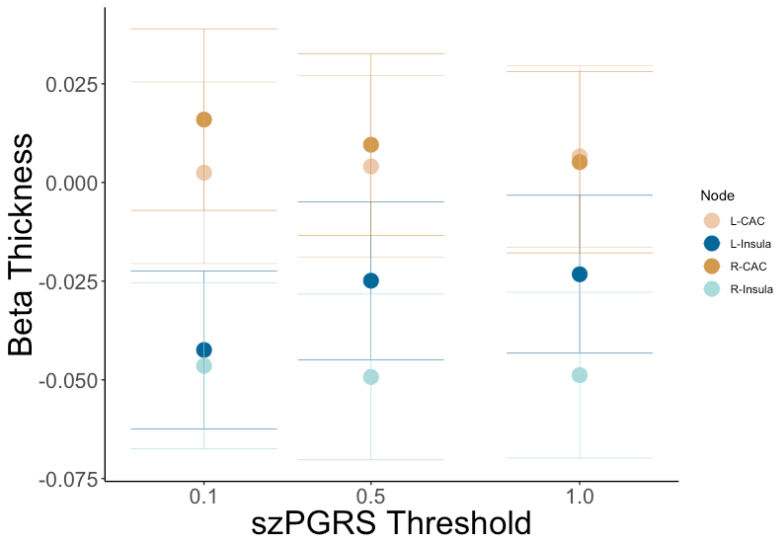

Figure 23. Magnitude of standardised beta values (represented in circles) and standard errors (in bars) from the linear regression analysis across all szPGRS thresholds for cortical thickness. CAC: caudal anterior cingulate, L: left, R: right.

White matter FA

There were no significant associations between white matter FA and szPGRS at any threshold ($p_{FDR} > 0.05$). Age and sex showed significant associations with several white matter tracts ($p_{FDR} > 0.05$; see Appendix IV Supplementary Material Table 2 for more detailed information). In addition, there were no significant age × sex interaction effects ($p_{FDR} > 0.05$).

Additional analysis: Specificity of the salience network

In order to test whether the significant effect of szPGRS on cortical thickness of the salience network was specific to this network, as an additional analysis we computed the average cortical thickness of all non-salience nodes and performed linear regression analysis between this factor and szPGRS. We found that the non-salience network was not significantly associated with szPGRS at any thresholds ($p \leq 0.1$: $\beta = -0.0024$, SE = 0.0054, $p = 0.654$; $p \leq 0.5$: $\beta = -0.0047$, SE = 0.0054, $p = 0.930$; $p \leq 1$: $\beta = -0.0016$, SE = 0.0054, $p = 0.977$). Moreover, we were able to reject the null hypothesis that standardised coefficients from the association between cortical thickness and szPGRS were equal for the salience and non-salience networks (szPGRS threshold $p \leq 0.1$: 95%CI [-0.0986, -0.0385], $p \leq 0.5$: 95% CI [-0.0856, -0.0255] and $p \leq 1$: 95%CI [-0.0776, -0.0175]). Differences between correlations were considered significant if the confidence interval did not include zero (Zou, 2007).

7.5. Discussion

The present study found significant associations between genetic risk for schizophrenia and certain neurostructural properties of the salience network in a large sample of healthy participants. In particular, greater genetic risk for schizophrenia was associated with a lower latent measure of cortical thickness across the salience network which was specific to this network, which was strongest in the insular cortex. However, we did not find any

significant association between the FA of the pathways involved in the salience network and szPGRS. This is, to our knowledge, the first study to investigate the structural properties of the salience network from a connectome perspective.

Due to its relevance in the identification of biological and cognitive events and its role in facilitating the flexibility of subsequent responses, abnormalities in the salience network have been previously linked to several neuropsychiatric disorders. Impairments in the salience network have been observed in schizophrenia, proposing that a misattribution of salience to external and internal stimuli may be able to explain the characteristic psychotic symptoms. While functional studies report deficiencies in functional connectivity (Palaniyappan et al., 2012; Uddin, 2015), reductions in the volume and cortical thickness of the insula and reductions in the volume of the anterior cingulate have been consistently reported in schizophrenia (White et al., 2010); with these impairments being linked to severity of reality distortion (Palaniyappan et al., 2011). White matter impairments are also frequently reported in schizophrenia, in particular in commissural and associative fibres (Burns et al., 2003; Ellison-Wright and Bullmore, 2009; Kelly et al., 2017; McIntosh et al., 2005; Rotarska-Jagiela et al., 2008). However, the relationship between white matter architecture of the salience network in schizophrenia has not yet been fully explored.

In this study, we found that a latent factor for cortical thickness was significantly associated with genetic risk for schizophrenia that was specific to the salience network. However, we did not find any significant association between the latent factors for grey matter volume and FA and szPGRS. As previously discussed, brain structure and schizophrenia are highly heritable, with evidence indicating impaired brain structure in patients diagnosed with schizophrenia and their relatives (Carletti et al., 2012; Lawrie et al., 2008; Muñoz Maniega et

al., 2008).[4] Thus, the null findings observed here may partly be due to the aggregation of genetic and environmental risk factors in affected individuals and their relatives compared to healthy individuals. Figure 22 shows the pattern of distribution of standardised coefficients from SEM for all latent factors across all szPGRS thresholds, suggesting that more restrictive thresholds showed numerically larger associations with cortical thickness and grey matter volumes while the opposite is observed for FA.

Studies in humans using DWI analysis have shown connections from the anterior insula to the anterior cingulate, frontal and orbitofrontal and anterior temporal regions, while the posterior section of the insula showed connections to the posterior temporal, parietal and sensorimotor areas (Cerliani et al., 2012; Cloutman et al., 2012; Ghaziri et al., 2017; Uddin et al., 2017, 2011). The insula has been repeatedly implicated in schizophrenia with consistent reductions in cortical thickness and volume. In one of the largest meta-analysis to date which comprised 4474 schizophrenia patients and 5098 healthy controls, the ENIGMA consortium reported that the thickness of the bilateral insula showed one of the largest negative effect sizes compared with healthy controls (van Erp et al., 2018). In addition, the authors found that earlier age of onset and longer duration of illness were associated with a thinner insula. In this study, we have found significant associations between the right insula and szPGRS albeit none of these associations survived multiple comparison corrections. However, these associations did not survive our correction for multiple comparisons due to our design based on correcting within szPGRS threshold instead of per node of interest. Figure 23 shows the pattern of distribution of beta coefficients for cortical thickness and szPGRS; indicating that szPGRS may indeed have a negative effect on the cortical thickness of the right insula. Although abnormalities in grey matter thickness, volume, cellular structure, and protein's expression

[4] See Chapter 3 for a detailed summary of white matter impairments in patients diagnosed with schizophrenia and their relatives.

have been observed in the insula of patients diagnosed with schizophrenia, the contribution of the insula to disease pathology remains unknown (reviewed in Wylie and Tregellas, 2010). The insula plays a significant role in processing emotional and sensory stimuli and is involved in interoception. This awareness of the body's internal state comprises emotional responses, complex cognitive states, and the sense of self (Critchley et al., 2004; Damasio, 2003); this loss of self-awareness is a common characteristic of schizophrenia where there is a difficulty in discriminating self-generated from externally-generated stimuli. An example of this duality is represented by psychotic symptoms where those patients who present hallucinations make more errors in external attributions that those without hallucinations (Costafreda et al., 2008; Johns et al., 2001).

Results of the present study showed negative associations between the volume of the right thalamus and genetic risk for schizophrenia. However, this association did not remain significant after accounting for multiple comparisons. The thalamus acts as a relay for information passing between sensory pathways, brain stem, cerebellar and subcortical areas to distributed cortical regions. For instance, Csernansky et al. (2004) reported a significant reduction in thalamic volume in schizophrenia compared with healthy controls. However, this reduction became non-significant once total brain volume was taken into account. In a meta-analysis comprising 485 cases and 500 controls, Konick and Friedman (2001) reported also a significant reduction in the volume of the thalamus, although the effect size was statistically significant, it was modest compared to other brain regions involved in schizophrenia.

Impairments in white matter microstructure are commonly reported in schizophrenia mostly being localised in commissural and associative tracts. Similarly, healthy relatives who are genetically at higher risk of developing schizophrenia also exhibit impairments in FA in several tracts (Muñoz Maniega et al., 2008). Albeit given these numerous findings, there is still much inconsistency in the results. In this study, we did not find any significant association

between the FA of the pathways involved in the salience network and szPGRS. These results are in accordance to those reported by Reus et al. (2017), who also found non-significant associations between a general factor of FA (including 27 major white matter tracts across the brain) and szPGRS in a previous release of this data (n = 816). Despite the apparent impairments in white matter structure in schizophrenia, only a small number of studies have reported significant associations between genetic risk factor and white matter in healthy and clinical samples (Alloza et al., 2018, 2017; Ritchie et al., 2017; Terwisscha van Scheltinga et al., 2013). Interestingly, Hulshoff Pol et al. (2004) reported significant reductions in global white matter volume in dizygotic twins discordant for schizophrenia while reductions in global grey matter were exclusively observed in patients diagnosed with schizophrenia. A more recent study supported their results by concluding that white matter has a stronger genetic component (explaining 63% of the variance) while grey matter volumes are more likely to be associated with environmental factors (43%) (van Haren et al., 2012). Therefore, it is possible that other factors such as gene-gene interactions, rare variants, and gene-environment interplay may help to explain the association between risk variants for schizophrenia and brain structural impairments (Van der Auwera et al., 2017).

7.6. Limitations

The generalisability of these results is subject to certain limitations. Due to our *a priori* hypothesis, this study only looked at a specific brain network overlooking with the same fidelity the rest of the brain, suggesting that the salience network may not be sufficient to capture the effect of szPGRS across different structural parameters in a healthy sample. However, in order to determine whether the effect of szPGRS on cortical thickness was specific to the salience network, we computed an average cortical thickness factor including all non-salience nodes. We found that szPGRS was not significantly associated with the non-salience cortical thickness at any threshold. However, due to our approach, it is possible that

we were not able to detect more subtle variation within the non-salience network. Future studies should investigate the implication of szPGRS in other brain networks such as the default-mode network and the central-executive network and additional structural properties such as surface area. Moreover, as sample sizes increase for GWAS, better predictive power will be achieved by szPGRS (Visscher et al., 2017). In regard to tractography, in order to remove spurious connections, we applied a consistency-based threshold preserving exclusively the top 30% white matter tracts that were more consistent across subjects. However, principles of white matter connectivity in humans are not sufficiently comprehensive (when compared to the mouse, for example; Goulas et al., 2017) to allow the confident implementation of anatomical priors; therefore, it is possible that pathways identified as part of the salience network may not be anatomically plausible. Nonetheless, constraining tractography using a priori anatomical information in order to reduce false-positives may hinder the ability of the technique to describe pathways that are currently unknown. Finally, we aimed to investigate whether the neurostructural properties of the salience network would mediate the association between szPGRS and psychotic experiences. However, only a minority of participants responded affirmatively to the questions regarding psychotic experiences (see Appendix IV Supplementary Material Table 3). Therefore, due to the low frequencies found in this sample, we could not proceed with the computation of the mediation models. Therefore, further research is needed to address the hypothesis that the salience network may mediate the association between polygenic risk scores and psychotic symptoms.

The present study was designed to determine the association of genetic risk for schizophrenia with several neurostructural properties of the salience network. We found significant associations between higher szPGRS and decreases in cortical thickness, in particular, in a latent factor for cortical thickness including both the insula and CAC. This study also found a significant negative association between thalamic volume and szPGRS and

cortical thickness of the insula and szPGRS, albeit none these associations survived multiple comparison correction. We also present valuable descriptive information on cortical thickness, volumes and white matter microstructure of the salience network, alongside their associations with age, sex and the interaction between age and genetic risk factor for schizophrenia. Taken together, these results are consistent with the hypothesis that higher genetic liability for schizophrenia is related to subtle neurostructural impairments among healthy participants.

7.7. Chapter discussion

This chapter was dedicated to the study of the neurostructural properties of the salience network and their relationships with genetic risk for schizophrenia in a large sample of healthy participants. Significant associations were found between szPGRS and a latent factor of cortical thickness. The computation of pathways from the connectome tends to result in numerous possible connections and without appropriate neuroanatomical priors, it is likely that spurious connections were included. These results suggest that improved tractography algorithms with previous anatomical knowledge and strict rejection criteria may better describe white matter microstructure.

Chapter 8 Discussion and conclusions

8.1. Overview

The work presented in this thesis focused on the study of white matter connectivity in schizophrenia. The main goal of this work was to investigate white matter (using DTI and brain network topology) in relation to cognition and symptoms among both patients diagnosed with schizophrenia, and in healthy individuals along a continuum of genetic risk for schizophrenia. Three different populations were studied here: the Scottish Family Mental Health (SFMH) study, which comprises patients with schizophrenia and a group of healthy controls, the Lothian Birth Cohort 1936 (LBC36), a longitudinal sample of healthy elderly community-dwelling participants and UK Biobank, a large healthy UK-based cohort.[5]

As described in Chapter 1, schizophrenia is a chronic and heterogenous neuropsychiatric disease, characterised by a complex underlying neurobiology and genetic profile; it results in the expression of positive and negative symptoms that may be accompanied by cognitive impairments. Research has proposed that schizophrenia is the result of a failure in brain's integration caused by neuroanatomical abnormalities in distributed brain regions and the networks to which they conform. Indeed, several neuroimaging studies have supported this hypothesis by showing significant white matter impairments and aberrant network properties in the disorder; with these alterations in brain connectivity being linked to cognitive impairments and severity of symptoms.[6] However, these results are highly inconsistent across the literature, possibly reflecting the inherent limitations of the field, such as the use of small sample sizes and varied methodological approaches. In particular, network analysis is yet a novel approach in neuroimaging and very few studies have investigated its application in schizophrenia and its corresponding psychopathology.

[5] Chapters 4 and 5 report the results from the analysis of the SFMH study; Chapter 6 is dedicated to the longitudinal analysis of the LBC36 and Chapter 7 presents the results from UKB.

[6] For a detailed review on white matter connectivity, cognitive impairments and symptoms see Chapter 3.

Chapter 3 describes the high heritability of schizophrenia, white matter, and cognitive functions has prompted several scientific studies, establishing a genetic overlap between them. Interestingly, this genetic overlap allows the study of healthy individuals based on their genetic profile and genetic risk for developing schizophrenia. Although distinct associations between white matter, cognition and symptoms have been reported in the disorder, the role of genetic risk for schizophrenia it is yet unclear.

There is an emerging consensus that intelligence cannot be circumscribed to the function of a single region, but rather it is best described as the result of the interaction between multiple areas or networks. This conceptualization implies that for the correct transmission of cognitive information, the system must be undisrupted and dependent on synchronised activity between distributed networks. Recent evidence suggests that differences in white matter may account for variance in cognitive performance (Wexler et al., 2009); with proper speed and efficiency of information transfer between distal brain regions relying on white matter microstructure. One of the main characteristics of schizophrenia is the presence of cognitive impairments, which have been previously linked to white matter deficiencies;[7] supporting the idea that cognitive functions depend upon white matter coherence. Albeit the apparent link between them, most of the studies to date have been performed in healthy populations (Chiang et al., 2009; Deary et al., 2006; Penke et al., 2010; Yu et al., 2008); and therefore, it is necessary to further investigate whether cognitive impairments in schizophrenia have a neurostructural basis.

Although pharmacological treatments can alleviate psychotic symptoms, there is still no effective treatment for negative symptoms, cognitive and social functioning. Given the

[7] For a detailed summary of published articles on associations between white matter and cognitive functions see Chapter 3.

complexity of the disorder and the need for an improved diagnosis; a thorough study and comprehension of the pathology of schizophrenia is needed in order to develop individualised treatments and reduce diagnostic error.

This thesis therefore aimed:

1. To investigate the cross-sectional pattern of white matter connectivity in patients diagnosed with schizophrenia and based on previous findings in healthy older adults (Penke et al., 2010), to determine if a general factor of processing speed – a key cognitive resource that allows multiple cognitive processes to be simultaneously available–, would mediate the association between white matter and general intelligence.
2. To determine whether schizophrenia is characterised by impairments in high centrality networks – or hubs – and whether graph theory metrics derived from distinct brain networks would be associated with genetic risk for schizophrenia, cognitive functions and symptoms in a sample that included both patients and healthy controls.
3. To test the hypothesis of accelerated ageing in schizophrenia by examining longitudinally whether a higher genetic risk factor for schizophrenia would confer an increased risk of decline in white matter diffusion parameters and graph theory metrics in a group of relatively healthy community-dwelling older adults.
4. To assess whether a higher genetic risk factor for schizophrenia would affect the neurostructural properties of the salience network, a network that has been previously identified to be linked to schizophrenia.

To achieve this, data from patients diagnosed with schizophrenia was analysed and contrasted with healthy participants (to address aims 1 & 2), and healthy samples were examined based on their genetic profile and risk for developing schizophrenia (with respect

to aims 3 & 4). The aim of this thesis was to investigate the associations among latent constructs in the first instances and then examine secondary exploratory analyses of the individual white matter tracts, given the degree of ambiguity in the extant literature. The use of latent approaches allows the study of latent constructs that would be unrealistic to expect from single indicators (*i.e* a single test on cognitive performance will not be a reliable measure of higher-order cognitive functions); instead, the use of multiple indicators or manifest variables will capture better the underlying structure of the data while simultaneously accounting for measurement error. The work presented here used advanced statistical methods –including longitudinal designs–, leveraging genetic data to investigate schizophrenia hypotheses in healthy samples, to allow more stringent testing of a causal hypothesis using observational data. Moreover, the use of the connectome and graph theory measures alongside more standard microstructural indices of white matter, allowed us to examine the hypothesis that microstructural changes would have an effect on the organizational properties of the brain networks.

Since each of the result chapters contains its own discussion, here I will briefly summarise the main results and offer a general discussion. I will also aim to discuss the strengths and limitations of the work described here and offer some ideas for further work and general implications of the findings. For a detailed summary of the parameters used in this thesis, please refer to Appendix V.

8.2. Main results

Overall, this work found that white matter connectivity impairments are present not only in schizophrenia but also in those healthy participants with a higher genetic risk for developing the disorder. Associations between structural connectivity, cognition, symptoms, and genetics were identified, supporting the hypothesis that schizophrenia is the result of the

disruption in brain's connectivity. Interestingly, already in the early descriptions of schizophrenia by the psychiatrist Bleuler (1911-1950), who described the core characteristic of the disorder to be the presence of thought fragmentation – referred to as "loosening of associations"–, termed the disorder derived from the Greek verb *schizein* to the split ("schizo") of the mind ("phrene"). Followed by Friston and Frith, who described schizophrenia as a "dysconnectivity syndrome"; suggesting that schizophrenia may be understood in terms of cognition and pathophysiology as a brain integration failure (Friston, 1998). Neuroimaging studies have supported this conceptualization of schizophrenia by reporting structural connectivity deficits in patients. This thesis provides even further evidence of this phenomenon, finding not only significant connectivity impairments in schizophrenia, but also associations between brain structure and schizophrenia's psychopathology. In particular, the work presented here have shown that white matter connectivity –using microstructural indices of white matter and organizational properties of the brain networks– provides the neuroanatomical substrate for higher-order cognitive functions in schizophrenia.[8] The novel approach of using genetic data to investigate schizophrenia hypotheses in healthy participants indicated that higher genetic risk factor for schizophrenia is associated with less healthy brain structure. Chapter 6 showed that this genetic risk factor was also linked to a worse decline in white matter connectivity in healthy older participants; supporting the hypothesis of accelerated ageing in schizophrenia. Interestingly, we were able to show that longitudinal change in microstructural indices of white matter was coupled with changes in the organization of the brain networks which suggests that white matter microstructure has an apparent effect on the topological organization of the brain. Taken all together, the difficulty of understanding schizophrenia as a circumscribed brain deficit indicates that an integrative

[8] In particular, Chapters 4 and 5 address this issue by reporting significant associations between white matter connectivity and cognitive functions in schizophrenia.

perspective may be able to better encapsulate the heterogeneous and complex presentation of the disorder.

Previous studies have emphasised the importance of white matter coherence for synchronised brain activity that results in optimal cognitive performance; suggesting that impairments in brain connectivity may result in individual differences in cognitive functions. The work presented in this thesis investigating cognitive functions and their relationships with brain structure in schizophrenia suggested that white matter connectivity may (at least partly) underlie the deficits in higher cognitive functions exhibited in schizophrenia. By using TBSS, probabilistic tractography and graph theory analysis, we were able to report significant associations between brain structure and intelligence both in schizophrenia and healthy participants (see Chapters 4 and 5). In addition, this thesis provides further evidence for the overlap between the genetic risk factor for schizophrenia and intelligence (Glahn et al., 2007; McIntosh et al., 2013; Toulopoulou et al., 2007), suggesting that brain structure may be an intermediate phenotype between genetics and intelligence.

It has been previously suggested that schizophrenia is characterised by accelerated ageing with an elevated rate of aging-related clinical, functional, and biological decline (Kirkpatrick et al., 2008); suggesting that white matter connectivity may be affected by this process. However, this would ideally require longitudinal data to asses (problems associated with cross-sectional data such as the inability to study causal relationships or model time). Thus, the difficulty of testing this hypothesis partly relies on the study design; in Chapter 6, by taking a longitudinal approach, advanced statistical methods and follow-up of a large same-year-old cohort of healthy elderly participants, we were able to adequately test the hypothesis of accelerated white matter ageing in schizophrenia. In this thesis, we found longitudinal associations between change in white matter and polygenic risk for schizophrenia. In particular, participants with higher genetic risk for schizophrenia showed a higher decline in

brain structure over time. This evidence supports the conceptualization of schizophrenia as an accelerated white matter ageing disorder, with microstructural changes in white matter being coupled with changes in the organizational properties of the brains network. This accelerated decline in white matter may reflect the neuropathology associated with the loss of microstructural properties (*e.g.* loss of axonal myelin, oligodendrocytes, etc.) which are a feature of the disorder.

In an attempt to address one of the main disadvantages of diffusion tensor imaging and try to model complex fibre architecture, such as crossing fibres, we aimed to apply spherical deconvolution to the SFMH study. Briefly, spherical deconvolution estimates a white matter fibre Orientation Distribution Function (fODF) by assuming that the diffusion signal measured from any white matter tract is properly described by a single response function (Tournier et al., 2007). In particular, we applied spherical deconvolution to two clinical groups, including patients diagnosed with schizophrenia and carriers of the genetic translocation DISC1, and an additional healthy control group. However, the quality of the resulting images was suboptimal. This may have been a consequence of the acquisition parameters used in this study. For instance, Dell'Acqua and Tournier (2018), offer some considerations in order to properly apply methods such as spherical deconvolution or multi-shell approaches, for instance consisting of 60-90 diffusion weighted directions at b = 2000/3000 s/mm^2, which were not available for the SFMH study (b =1000 s/mm^2 , 56 diffusion weighted directions and 2.5 mm isotropic voxels).

8.3. Challenges and future work

Brain imaging, in particular magnetic resonance imaging, has undoubtedly contributed to our understanding of schizophrenia and other neuropsychiatric disorders. However, its practicality within the clinical psychiatric practice is very limited; MRI is mostly used for diagnosing organic diseases whose imaging hallmarks are well-known, but not for

diagnosing and designing a therapeutic plan for the patient. This is especially true for schizophrenia, where the specific cerebral features are not well established. A thorough study of the possibilities and challenges in translating neuroimaging findings in the clinical practice is needed in order to improve the diagnosis, develop individualised treatments, predict the effects of the intervention and potentially implement those before the onset.

As previously described, DTI is currently the only available technique to study white matter structure *in vivo* which is characterised by an easy implementation and has provided some plausible results. However, even though DTI provides invaluable information, several caveats need to be addressed.[9] For instance, diffusion MRI measures, such as FA and MD, have limitations when describing complex tissue architecture. FA and MD can be conceived as sensitive and reliable metrics albeit being non-specific; thus, post-morten studies are necessary in order to describe adequately the source of variation in these metrics (*e.g* myelination, axonal damage, etc.) and their biological causes. The use of new imaging maps (*e.g* neurite orientation dispersion and density imaging (NODDI)) in conjunction with already existing maps may improve the interpretability of results; however, the majority of these maps require multi-shell acquisitions (Zhang et al., 2012), which were not applied in the work presented here. Moreover, the use of low b-values (< 1000 s mm^{-2}) leads to almost no signal attenuation due to the displacement of intra-axonal water perpendicular to the axon (Jones et al., 2013). Higher b-values compared to the ones used in this thesis (1000 s mm^{-2}), obtained from strong gradients and long diffusion times, will lead to complete dephasing and total loss of signal for the extra-axonal water molecules and to anisotropic signal loss for the intra-axonal water; therefore, higher b-values are more sensitive to fibre orientation and profile description.

[9] See Chapter 2 for a full description of limitations associated with DTI.

The reconstruction of the connectome involves several distinct steps, and currently there are multiple available methods that can be applied at each level. I have previously mentioned other available techniques at the level of tractography, such as DSI, CSD, etc. [10] At the level of the connectome, it has been shown that the brain is economically but not minimally wired; meaning that the sum of all distances between nodes is less than if the same nodes were randomly connected. This observation implies that evolution may have promoted large-scale brain networks (Bullmore and Bassett, 2011). However, most brain networks derived from MRI have short wiring length, with a probability distribution heavily tailed and minimal presence of long edges; in addition, strength has shown an exponential decay with connection length (Sotiropoulos and Zalesky, 2017). To minimize this issue, distance between nodes can be used as a weighting measure, in which the edge's weights are used in the computation of graph theory measures. Other approaches to preserve long-distance white matter tracts can be achieved through thresholding methods; one available technique is to apply a consistency-based threshold (Roberts et al., 2017), which preserves connections strong for their length. A recent development has taken into account the fact that these consistency-based thresholds still favor short-range connections because consistency across subjects is in itself distance-dependent, with short connections appearing more consistently. Thus, Betzel et al. (2018) propose a new method that overcomes this issue by allowing the threshold to vary as a function of distance. Advances in fibre reconstruction software, connectome reconstruction and translational approaches using for instance post-mortem data – which allows the study of cytoarchitectural properties of brain tissue, validation of neuroanatomy, comparative neuroanatomy, etc.–, will help future studies to develop and validate these issues.

Functional connectivity from resting state fMRI is generally inferred from the correlations in BOLD signals between grey matter regions; providing complementary

[10] Please see Chapter 2 "Tractography and the connectome".

information to that of structural connectivity. Currently, the challenge remains in developing effective methods to merge these techniques and interpret results adequately. A variety of approaches have already been implemented, such as studies investigating the structural connectivity of functional networks or the functional connectivity between two structurally connected nodes. The extensive evidence of the brain's resting state provides a unique opportunity to link the pattern of functional connectivity with the underlying structural networks. Several studies have indicated that structural connectivity is highly predictive of functional connections, suggesting that topological properties are generally conserved between modalities (reviewed in Bullmore and Sporns, 2009). However, as Uddin (2013) points out, functional connectivity shows high plasticity and flexibility with observable changes due to development, injury and possibly, disease; this indicates that the interpretation of the relationship between structure-function may not be as straightforward as believed. Mišić et al. (2016) found robust statistically patterns between functional and structural subnetworks. However, the authors reported a non-one-to-one correspondence between edges and concluded that the brain network's organization promotes the occurrence of several functional networks that sometimes differ from the underlying structural connectivity. This is supported by recent evidence highlighting the difficulties of conflating two matrices with different sparsities; suggesting that brain structure is not best described by fully connected matrix, whereas under functional connectivity, given its flexibility (state-dependent) and the fluctuations in BOLD signal, this scenario is plausible (Park and Friston, 2013).

In regard to the connectome, one of the most concerning issues is the lack of apparent reliability and repeatability between studies. Nowadays, there is a great variety of methodologies available to generate the connectome. Each of the steps involved in deriving the networks contributes to errors in the pipeline; and unfortunately, there is yet no consensus on the preferred approach, which contributes to the lack of consistency in the field. Thus, further research is required to develop a standardised protocol that will reliably measure brain

connectivity and allow for comparability across studies. However, the approach taken here has been explicitly tested for test-retest and has features which have offered improvements over more standard methods (*e.g.* seeding in the white matter) (Buchanan et al., 2014). In addition, specific issues that arise when comparing networks across groups is the fact that the number of nodes (N) or network's degree (*k*) will influence the computation of global theory metrics. Therefore, the choice of N will determine the topology of the network and hinder the comparison between networks with different N or *k*. Instead of restraining all networks to a fixed *k* parameter, in this thesis I chose to fix N and to control each subject's graph theory measure for edge density. Therefore, the results presented in this thesis have computed density as a fixed effect for each graph theory metric.

Another important issue is the validation of the connectome from a neuroanatomical perspective. The elevated number of possible connections that the connectome computes, raises the question of whether these pathways are biologically relevant. Each step of the process must be manually checked and rejected if necessary in order to avoid false positives; however, in general, the elimination of spurious connections may not be feasible, partly because of our lack of neuroanatomy knowledge. In addition to this, currently there is a lack of a standardised parcellation protocol and the different choice of parcellation granularity may have great implications for the resultant connectome. However, in this thesis we have consistently used the Desikan atlas (85 parcellations, Desikan et al., 2006) in order to aid comparability with other studies and its reasonable correspondence to major cytoarchitectural fields. Moreover, in Chapter 5, we applied the Destrieux atlas (165 parcellations) in order to validate our graph theory results. Therefore, a better characterisation of the brain's neuroanatomy may lead to a development in tractography methods and constraints; ultimately improving the computation of networks and interpretability of results.

Despite all the evidence suggesting the crucial role of white matter in psychosis and particularly in schizophrenia, scientific research has mainly focused on the structural properties of grey matter, as can be observed in the literature. In spite of the rapid implementation, progress and increasing evidence for the involvement of white matter in neuropsychiatry, diffusion MRI parameters obtained from DTI are not sufficient to describe adequately white matter microstructure; and thus, a translational approach including histological, cellular and molecular studies is necessary in order to fully understand white matter pathology. Therefore, even though we have reported, for instance, associations between decreasing MD and higher szPGRS, we cannot interpret this confidently as being related to a specific neurobiological process. Even though it is now clear that white matter plays a significant role in brain integration and information processing, due to its complexity, a great deal remains to be discovered before we can make inferences about its pathology in schizophrenia.

Schizophrenia is both highly heritable and polygenic, with many common alleles of small effect, and increasing numbers of genome-wide significant loci being identified as sample sizes increase (Davies et al., 2011). However, so far very few studies have investigated the association between polygenic risk scores and brain structure, with most studies reporting null associations (Oertel-Knöchel et al., 2015; Reus et al., 2017; Voineskos et al., 2016b). This may be due to the fact that current studies have a lack of power to detect modest effects; and therefore, as sample sizes increase for GWAS, better predictive power will be achieved by PGRS. In addition, a limitation that may have obscured significant results is the use of healthy (rather than patients diagnosed with schizophrenia) participants. In this thesis, three datasets were studied with only the SFMH study including patients diagnosed with schizophrenia. As stated before, observed white matter impairments in schizophrenia tend to have modest effect sizes and therefore, associations between white matter connectivity and genetic risk for schizophrenia in healthy samples may be too subtle to be detected in smaller sample sizes.

One of the most comprehensive studies, UK Biobank, has aimed to follow up the health and wellbeing of 500 000 participants and provides a wide range of medical and psychological measurements. This tendency of increasing sample sizes will undoubtedly increase not only the predictive power of PGRS but of other neuroimaging phenotypes; for instance, improving the diagnostic accuracy by using the genetic profile and neuroimaging and cognitive biomarkers of the patient.

In this work, we found significant negative associations between szPGRS and longitudinal change in MD.[11] However, in Chapter 7 we reported non-significant associations between the FA of the salience network and the interaction of szPGRS and age. Further work would therefore constitute computing MD-weighted matrices in the LBC1936 and UKBiobank datasets to examine: i) whether pathways derived from the salience network would be significantly associated with the interaction between szPGRS and age, and ii) whether the longitudinal MD findings are stronger in the salience network connections. Unfortunately, it is out of the scope of this thesis to address these issues due to the large amount of re-processing required to generate the MD-weighted matrices.

Although schizophrenia is highly heritable, recent work in environmental risk factors highlights its importance in the development of the disorder; indicating that the aetiology of schizophrenia is the result of the interaction between genes and environment. The following are a brief mention of potentially important risk factors for schizophrenia diagnosis, depending on the phase they may act during the life course: neurodevelopmental, childhood and adulthood. Aspects such as obstetric complications, infections or maternal stress are categorised as risk factors involved in the neurodevelopmental phase. Child abuse would constitute the most determinant risk factor in childhood; while migration, ethnicity, social

[11] Chapter 6 presents results from this analysis.

status and urbanization some of the most prominent during adulthood (reviewed in Dean and Murray, 2005). In particular, the relationship between socio-economic status (SES) and mental illness has been the object of intense study and debate over decades. Unfortunately, it is out of the scope of this thesis to fully address this fundamental issue; nevertheless, due to the extensive evidence of a negative association between SES and psychotic disorders along with cognitive functions, I consider pertinent to mention the main studies carried out (Adler et al., 1994; Goldberg et al., 2011; Holzer et al., 1986). SES is amongst the strongest predictors of health and yet, paradoxically, its measurement represents still a highly challenging task. Therefore, based on the considerable evidence and in the context of increasingly aggressive neoliberal policies, further refinement and more robust methods for assessing associations between lower SES and poorer mental health offer a vital opportunity to improve global health and prevent psychiatric (and other SES-related) diseases.

The differential diagnosis of schizophrenia from other psychotic disorders such as bipolar disorder and mood disorders currently represents a major clinical challenge. For instance, both schizophrenia and bipolar disorder share genetic risk factors and tend to present overlapping features. Traditionally, these two disorders have been described as separate entities with differing underlying etiologies. However, some authors have proposed a continuum approach to psychosis (Crow, 1990); suggesting that there may not be a neat biological distinction between schizophrenia and bipolar disorder. For instance, a recent study found that szPGRS is a better predictor of bipolar disorder (BD) with manic psychosis than other subgroups of BD, suggesting that bipolar patients with manic psychosis are genetically more similar to schizophrenia than to other BD patients (Markota et al., 2018). Therefore, the results presented in this thesis investigating the role of a genetic risk factor for schizophrenia in brain structure and cognitive functions may not be entirely unique to schizophrenia but common to closely related disorders. Future studies should address this issue using larger sample sizes and integrating several imaging modalities in order to establish the

neuroanatomical and neurophysiological correlates that are unique to schizophrenia and distinct from other neuropsychiatric disorders.

8.4. Concluding remarks

This thesis investigated the role of white matter connectivity in schizophrenia using diffusion MRI and network approaches. We sought to study the associations within the pathophysiology of the disorder, including white matter, cognitive functions, symptoms and a genetic risk factor for schizophrenia. Through cross-sectional and longitudinal approaches, our findings suggest that white matter impairments are present in patients diagnosed with schizophrenia at the microstructural level, measured using tractography and at the organizational level, measured using graph theory. Network analyses showed topological impairments within the average, central and non-central networks in patients compared to healthy controls. Interestingly, graph theory metrics were associated with cognitive functioning and served as mediators for the association between genetic risk for schizophrenia and intelligence. These results are consistent with the hypothesis that intelligence deficits are associated with a genetic risk for schizophrenia, which is mediated via the disruption of distributed brain networks.

Several studies have suggested that schizophrenia is characterised by accelerated aging. Through a longitudinal design, we were able to report that in healthy elderly participants, those with higher genetic risk for developing schizophrenia showed more prominent connectivity impairments over time; supporting the hypothesis that schizophrenia is characterised by accelerated white matter aging. This was the first study to investigate the longitudinal trajectories of graph theory measures and their associations with szPGRS in older age, and comprehensibly described white matter connectivity changes over a period of three years in the same-year-old cohort.

This work also found significant associations between genetic risk for schizophrenia and certain neurostructural properties of the salience network in a large sample of healthy participants. The novel approach taken here was based on the computation of a subnetwork derived from the structural connectome. Built on previous literature on the salience network, certain nodes were selected, and their connecting pathways computed. In particular, using this method, we found that increased genetic liability was significantly associated with reduced cortical thickness.

Results from this thesis are consistent with the hypothesis that higher genetic liability for schizophrenia is related to subtle neurostructural impairments even among healthy participants. The diverse age ranges, clinical status and design (*e.g* cross-sectional versus longitudinal) of our studies may well have hindered our ability to describe and comprehensively elucidate the phenomena, but the work in this thesis has shed some light on the pathophysiology of schizophrenia and supported its conceptualization as a "dysconnection" syndrome.

References

Abdul-Rahman, M.F., Qiu, A., Woon, P.S., Kuswanto, C., Collinson, S.L., Sim, K., 2012. Arcuate Fasciculus Abnormalities and Their Relationship with Psychotic Symptoms in Schizophrenia. PLoS ONE 7. https://doi.org/10.1371/journal.pone.0029315

Aboitiz, F., Scheibel, A.B., Zaidel, E., 1992. Morphometry of the Sylvian fissure and the corpus callosum, with emphasis on sex differences. Brain J. Neurol. 115 (Pt 5), 1521–1541.

Adler, N.E., Boyce, T., Chesney, M.A., Cohen, S., Folkman, S., Kahn, R.L., Syme, S.L., 1994. Socioeconomic status and health. The challenge of the gradient. Am. Psychol. 49, 15–24.

Adluru, N., Zhang, H., Tromp, D.P.M., Alexander, A.L., 2013. Effects of DTI spatial normalization on white matter tract reconstructions. Proc. SPIE 8669. https://doi.org/10.1117/12.2007130

Ahmed, A.O., Bhat, I.A., 2014. Psychopharmacological treatment of neurocognitive deficits in people with schizophrenia: a review of old and new targets. CNS Drugs 28, 301–318. https://doi.org/10.1007/s40263-014-0146-6

Ahmed, A.O., Buckley, P.F., Hanna, M., 2013. Neuroimaging schizophrenia: a picture is worth a thousand words, but is it saying anything important? Curr. Psychiatry Rep. 15, 345. https://doi.org/10.1007/s11920-012-0345-0

Alberts, B., Johnson, A., Lewis, J., Raff, M., Roberts, K., Walter, P., 2002. Molecular Biology of the Cell, 4th ed. Garland Science.

Alexander, A.L., Hurley, S.A., Samsonov, A.A., Adluru, N., Hosseinbor, A.P., Mossahebi, P., Tromp, D.P.M., Zakszewski, E., Field, A.S., 2011. Characterization of cerebral white matter properties using quantitative magnetic resonance imaging stains. Brain Connect. 1, 423–446. https://doi.org/10.1089/brain.2011.0071

Alexander-Bloch, A.F., Gogtay, N., Meunier, D., Birn, R., Clasen, L., Lalonde, F., Lenroot, R., Giedd, J., Bullmore, E.T., 2010. Disrupted modularity and local connectivity of brain functional networks in childhood-onset schizophrenia. Front. Syst. Neurosci. 4, 147. https://doi.org/10.3389/fnsys.2010.00147

Alfaro-Almagro, F., Jenkinson, M., Bangerter, N.K., Andersson, J.L.R., Griffanti, L., Douaud, G., Sotiropoulos, S.N., Jbabdi, S., Hernandez-Fernandez, M., Vallee, E., Vidaurre, D., Webster, M., McCarthy, P., Rorden, C., Daducci, A., Alexander, D.C., Zhang, H., Dragonu, I., Matthews, P.M., Miller, K.L., Smith, S.M., 2018. Image processing and

Quality Control for the first 10,000 brain imaging datasets from UK Biobank. NeuroImage 166, 400–424. https://doi.org/10.1016/j.neuroimage.2017.10.034

Alloza, C., Bastin, M.E., Cox, S.R., Gibson, J., Duff, B., Semple, S.I., Whalley, H.C., Lawrie, S.M., 2017. Central and non-central networks, cognition, clinical symptoms, and polygenic risk scores in schizophrenia. Hum. Brain Mapp. https://doi.org/10.1002/hbm.23798

Alloza, C., Cox, S.R., Blesa Cábez, M., Redmond, P., Whalley, H.C., Ritchie, S.J., Muñoz Maniega, S., Del C Valdés Hernández, M., Tucker-Drob, E.M., Lawrie, S.M., Wardlaw, J.M., Deary, I.J., Bastin, M.E., 2018. Polygenic risk score for schizophrenia and structural brain connectivity in older age: A longitudinal connectome and tractography study. NeuroImage. https://doi.org/10.1016/j.neuroimage.2018.08.075

Alloza, C., Cox, S.R., Duff, B., Semple, S.I., Bastin, M.E., Whalley, H.C., Lawrie, S.M., 2016. Information processing speed mediates the relationship between white matter and general intelligence in schizophrenia. Psychiatry Res. 254, 26–33. https://doi.org/10.1016/j.pscychresns.2016.05.008

Alvarado-Alanis, P., León-Ortiz, P., Reyes-Madrigal, F., Favila, R., Rodríguez-Mayoral, O., Nicolini, H., Azcárraga, M., Graff-Guerrero, A., Rowland, L.M., de la Fuente-Sandoval, C., 2015a. Abnormal white matter integrity in antipsychotic-naïve first-episode psychosis patients assessed by a DTI principal component analysis. Schizophr. Res. 162, 14–21. https://doi.org/10.1016/j.schres.2015.01.019

Andersson, J.L., Jenkinson, M., Smith, S., 2007. Non-linear registration, aka Spatial normalisation FMRIB technical report TR07JA2. FMRIB Anal. Group Univ. Oxf. 2.

Antila, M., Kieseppä, T., Partonen, T., Lönnqvist, J., Tuulio-Henriksson, A., 2011. The effect of processing speed on cognitive functioning in patients with familial bipolar I disorder and their unaffected relatives. Psychopathology 44, 40–45. https://doi.org/10.1159/000317577

Antonova, E., 2004. The relationship between brain structure and neurocognition in schizophrenia: a selective review. Schizophr. Res. 70, 117–145. https://doi.org/10.1016/j.schres.2003.12.002

Ardekani, B.A., Nierenberg, J., Hoptman, M.J., Javitt, D.C., Lim, K.O., 2003. MRI study of white matter diffusion anisotropy in schizophrenia. Neuroreport 14, 2025–2029. https://doi.org/10.1097/01.wnr.0000093290.85057.0d

Asami, T., Hyuk Lee, S., Bouix, S., Rathi, Y., Whitford, T.J., Niznikiewicz, M., Nestor, P., McCarley, R.W., Shenton, M.E., Kubicki, M., 2014. Cerebral white matter abnormalities and their associations with negative but not positive symptoms of

schizophrenia. Psychiatry Res. 222, 52–59. https://doi.org/10.1016/j.pscychresns.2014.02.007

Asami, T., Saito, Y., Whitford, T.J., Makris, N., Niznikiewicz, M., McCarley, R.W., Shenton, M.E., Kubicki, M., 2013. Abnormalities of middle longitudinal fascicle and disorganization in patients with schizophrenia. Schizophr. Res. 143, 253–259. https://doi.org/10.1016/j.schres.2012.11.030

Bach, M., Laun, F.B., Leemans, A., Tax, C.M.W., Biessels, G.J., Stieltjes, B., Maier-Hein, K.H., 2014. Methodological considerations on tract-based spatial statistics (TBSS). NeuroImage 100, 358–369. https://doi.org/10.1016/j.neuroimage.2014.06.021

Badcock, J.C., Clark, M.L., Pedruzzi, R.A., Morgan, V.A., Jablensky, A., 2015. Intact speed of processing in a community-based sample of adults with high schizotypy: A marker of reduced psychosis risk? Psychiatry Res. 228, 531–537. https://doi.org/10.1016/j.psychres.2015.06.003

Bartzokis, G., Sultzer, D., Lu, P.H., Nuechterlein, K.H., Mintz, J., Cummings, J.L., 2004. Heterogeneous age-related breakdown of white matter structural integrity: implications for cortical "disconnection" in aging and Alzheimer's disease. Neurobiol. Aging 25, 843–851. https://doi.org/10.1016/j.neurobiolaging.2003.09.005

Basser, P.J., Mattiello, J., LeBihan, D., 1994a. MR diffusion tensor spectroscopy and imaging. Biophys. J. 66, 259–267. https://doi.org/10.1016/S0006-3495(94)80775-1

Basser, P.J., Mattiello, J., LeBihan, D., 1994b. Estimation of the effective self-diffusion tensor from the NMR spin echo. J. Magn. Reson. B 103, 247–254.

Basser, P.J., Pierpaoli, C., 1996. Microstructural and physiological features of tissues elucidated by quantitative-diffusion-tensor MRI. J. Magn. Reson. B 111, 209–219.

Bassett, D.S., Bullmore, E., Verchinski, B.A., Mattay, V.S., Weinberger, D.R., Meyer-Lindenberg, A., 2008. Hierarchical organization of human cortical networks in health and schizophrenia. J. Neurosci. Off. J. Soc. Neurosci. 28, 9239–9248. https://doi.org/10.1523/JNEUROSCI.1929-08.2008

Bassett, D.S., Nelson, B.G., Mueller, B.A., Camchong, J., Lim, K.O., 2012. Altered resting state complexity in schizophrenia. NeuroImage 59, 2196–2207. https://doi.org/10.1016/j.neuroimage.2011.10.002

Bastiani, M., Shah, N.J., Goebel, R., Roebroeck, A., 2012. Human cortical connectome reconstruction from diffusion weighted MRI: The effect of tractography algorithm. NeuroImage 62, 1732–1749. https://doi.org/10.1016/j.neuroimage.2012.06.002

Bastin, M.E., Muñoz Maniega, S., Ferguson, K.J., Brown, L.J., Wardlaw, J.M., MacLullich, A.M.J., Clayden, J.D., 2010. Quantifying the effects of normal ageing on white matter

structure using unsupervised tract shape modelling. NeuroImage 51, 1–10. https://doi.org/10.1016/j.neuroimage.2010.02.036

Bauer, S.M., Schanda, H., Karakula, H., Olajossy-Hilkesberger, L., Rudaleviciene, P., Okribelashvili, N., Chaudhry, H.R., Idemudia, S.E., Gscheider, S., Ritter, K., Stompe, T., 2011. Culture and the prevalence of hallucinations in schizophrenia. Compr. Psychiatry 52, 319–325. https://doi.org/10.1016/j.comppsych.2010.06.008

Beaulieu, C., 2011. What Makes Diffusion Anisotropic in the Nervous System? Oxford University Press.

Beaulieu, C., 2002. The basis of anisotropic water diffusion in the nervous system - a technical review. NMR Biomed. 15, 435–455. https://doi.org/10.1002/nbm.782

Behrens, T.E.J., Berg, H.J., Jbabdi, S., Rushworth, M.F.S., Woolrich, M.W., 2007. Probabilistic diffusion tractography with multiple fibre orientations: What can we gain? NeuroImage 34, 144–155. https://doi.org/10.1016/j.neuroimage.2006.09.018

Behrens, T.E.J., Woolrich, M.W., Jenkinson, M., Johansen-Berg, H., Nunes, R.G., Clare, S., Matthews, P.M., Brady, J.M., Smith, S.M., 2003. Characterization and propagation of uncertainty in diffusion-weighted MR imaging. Magn. Reson. Med. 50, 1077–1088. https://doi.org/10.1002/mrm.10609

Benjamini, Y., Hochberg, Y., 1995. Controlling the False Discovery Rate: A Practical and Powerful Approach to Multiple Testing. J. R. Stat. Soc. Ser. B Methodol. 57, 289–300. https://doi.org/10.2307/2346101

Bennett, I.J., Madden, D.J., 2014. Disconnected aging: cerebral white matter integrity and age-related differences in cognition. Neuroscience 276, 187–205. https://doi.org/10.1016/j.neuroscience.2013.11.026

Betzel, R.F., Byrge, L., He, Y., Goñi, J., Zuo, X.-N., Sporns, O., 2014. Changes in structural and functional connectivity among resting-state networks across the human lifespan. NeuroImage 102, 345–357. https://doi.org/10.1016/j.neuroimage.2014.07.067

Betzel, R.F., Griffa, A., Hagmann, P., Misic, B., 2018. Distance-dependent consistency thresholds for generating group-representative structural brain networks. bioRxiv 412346. https://doi.org/10.1101/412346

Biedermann, F., Fleischhacker, W.W., 2016. Psychotic disorders in DSM-5 and ICD-11. CNS Spectr. 21, 349–354. https://doi.org/10.1017/S1092852916000316

Birnbaum, R., Weinberger, D.R., 2013. Functional neuroimaging and schizophrenia: a view towards effective connectivity modeling and polygenic risk. Dialogues Clin. Neurosci. 15, 279–289.

Bleuler, E., 1950. Dementia praecox or the group of schizophrenias, Dementia praecox or the group of schizophrenias. International Universities Press, Oxford, England.

Blokland, G.A.M., de Zubicaray, G.I., McMahon, K.L., Wright, M.J., 2012. Genetic and environmental influences on neuroimaging phenotypes: a meta-analytical perspective on twin imaging studies. Twin Res. Hum. Genet. Off. J. Int. Soc. Twin Stud. 15, 351–371. https://doi.org/10.1017/thg.2012.11

Bob, P., Mashour, G.A., 2011. Schizophrenia, dissociation, and consciousness. Conscious. Cogn., From Dreams to Psychosis: A European Science Foundation Exploratory Workshop 20, 1042–1049. https://doi.org/10.1016/j.concog.2011.04.013

Bohlken, M.M., Brouwer, R.M., Mandl, R.C.W., Heuvel, M.P.V. den, Hedman, A.M., Hert, M.D., Cahn, W., Kahn, R.S., Pol, H.E.H., 2016. Structural Brain Connectivity as a Genetic Marker for Schizophrenia. JAMA Psychiatry 73, 11–19. https://doi.org/10.1001/jamapsychiatry.2015.1925

Bohlken, M.M., Mandl, R.C.W., Brouwer, R.M., van den Heuvel, M.P., Hedman, A.M., Kahn, R.S., Hulshoff Pol, H.E., 2014. Heritability of structural brain network topology: a DTI study of 156 twins. Hum. Brain Mapp. 35, 5295–5305. https://doi.org/10.1002/hbm.22550

Bollobás, B., 1985. Random Graphs. Cambridge University Press, Cambridge, UK.

Bopp, M.H.A., Zöllner, R., Jansen, A., Dietsche, B., Krug, A., Kircher, T.T.J., 2016. White matter integrity and symptom dimensions of schizophrenia: A diffusion tensor imaging study. Schizophr. Res. https://doi.org/10.1016/j.schres.2016.11.045

Bora, E., Fornito, A., Radua, J., Walterfang, M., Seal, M., Wood, S.J., Yücel, M., Velakoulis, D., Pantelis, C., 2011. Neuroanatomical abnormalities in schizophrenia: a multimodal voxelwise meta-analysis and meta-regression analysis. Schizophr. Res. 127, 46–57. https://doi.org/10.1016/j.schres.2010.12.020

Bora, E., Lin, A., Wood, S.J., Yung, A.R., McGorry, P.D., Pantelis, C., 2014. Cognitive deficits in youth with familial and clinical high risk to psychosis: a systematic review and meta-analysis. Acta Psychiatr. Scand. 130, 1–15. https://doi.org/10.1111/acps.12261

Bora, E., Murray, R.M., 2014. Meta-analysis of Cognitive Deficits in Ultra-high Risk to Psychosis and First-Episode Psychosis: Do the Cognitive Deficits Progress Over, or After, the Onset of Psychosis? Schizophr. Bull. 40, 744–755. https://doi.org/10.1093/schbul/sbt085

Bora, E., Yucel, M., Pantelis, C., 2009. Cognitive endophenotypes of bipolar disorder: a meta-analysis of neuropsychological deficits in euthymic patients and their first-degree relatives. J. Affect. Disord. 113, 1–20. https://doi.org/10.1016/j.jad.2008.06.009

Buchanan, C.R., Pernet, C.R., Gorgolewski, K.J., Storkey, A.J., Bastin, M.E., 2014. Test-retest reliability of structural brain networks from diffusion MRI. NeuroImage 86, 231–243. https://doi.org/10.1016/j.neuroimage.2013.09.054

Buchsbaum, M.S., Friedman, J., Buchsbaum, B.R., Chu, K.-W., Hazlett, E.A., Newmark, R., Schneiderman, J.S., Torosjan, Y., Tang, C., Hof, P.R., Stewart, D., Davis, K.L., Gorman, J., 2006. Diffusion tensor imaging in schizophrenia. Biol. Psychiatry 60, 1181–1187. https://doi.org/10.1016/j.biopsych.2005.11.028

Bullitt, E., Gerig, G., Pizer, S.M., Lin, W., Aylward, S.R., 2003. Measuring tortuosity of the intracerebral vasculature from MRA images. IEEE Trans. Med. Imaging 22, 1163–1171. https://doi.org/10.1109/TMI.2003.816964

Bullmore, E., Sporns, O., 2009. Complex brain networks: graph theoretical analysis of structural and functional systems. Nat. Rev. Neurosci. 10, 186–198. https://doi.org/10.1038/nrn2575

Bullmore, E.T., Bassett, D.S., 2011. Brain graphs: graphical models of the human brain connectome. Annu. Rev. Clin. Psychol. 7, 113–140. https://doi.org/10.1146/annurev-clinpsy-040510-143934

Burdick, K.E., Gunawardane, N., Woodberry, K., Malhotra, A.K., 2009. The role of general intelligence as an intermediate phenotype for neuropsychiatric disorders. Cognit. Neuropsychiatry 14, 299–311. https://doi.org/10.1080/13546800902805347

Burns, J., Job, D., Bastin, M.E., Whalley, H., Macgillivray, T., Johnstone, E.C., Lawrie, S.M., 2003. Structural disconnectivity in schizophrenia: a diffusion tensor magnetic resonance imaging study. Br. J. Psychiatry J. Ment. Sci. 182, 439–443.

Campbell, J., Pike, B., 2013. Potential and limitations of diffusion MRI tractography for the study of language. Brain Lang. https://doi.org/10.1016/j.bandl.2013.06.007

Cannon, T.D., Kaprio, J., Lönnqvist, J., Huttunen, M., Koskenvuo, M., 1998. The genetic epidemiology of schizophrenia in a Finnish twin cohort. A population-based modeling study. Arch. Gen. Psychiatry 55, 67–74.

Cardno, A.G., Marshall, E.J., Coid, B., Macdonald, A.M., Ribchester, T.R., Davies, N.J., Venturi, P., Jones, L.A., Lewis, S.W., Sham, P.C., Gottesman, I.I., Farmer, A.E., McGuffin, P., Reveley, A.M., Murray, R.M., 1999. Heritability estimates for psychotic disorders: the Maudsley twin psychosis series. Arch. Gen. Psychiatry 56, 162–168.

Carletti, F., Woolley, J.B., Bhattacharyya, S., Perez-Iglesias, R., Fusar Poli, P., Valmaggia, L., Broome, M.R., Bramon, E., Johns, L., Giampietro, V., Williams, S.C.R., Barker, G.J., McGuire, P.K., 2012. Alterations in white matter evident before the onset of psychosis. Schizophr. Bull. 38, 1170–1179. https://doi.org/10.1093/schbul/sbs053

Catani, M., Thiebaut de Schotten, M., 2008. A diffusion tensor imaging tractography atlas for virtual in vivo dissections. Cortex J. Devoted Study Nerv. Syst. Behav. 44, 1105–1132. https://doi.org/10.1016/j.cortex.2008.05.004

Cerliani, L., Thomas, R.M., Jbabdi, S., Siero, J.C.W., Nanetti, L., Crippa, A., Gazzola, V., D'Arceuil, H., Keysers, C., 2012. Probabilistic tractography recovers a rostrocaudal trajectory of connectivity variability in the human insular cortex. Hum. Brain Mapp. 33, 2005–2034. https://doi.org/10.1002/hbm.21338

Chen, E.Y.-H., Hui, C.L.-M., Dunn, E.L.-W., Miao, M.Y.-K., Yeung, W.-S., Wong, C.-K., Chan, W.-F., Tang, W.-N., 2005. A prospective 3-year longitudinal study of cognitive predictors of relapse in first-episode schizophrenic patients. Schizophr. Res. 77, 99–104. https://doi.org/10.1016/j.schres.2005.02.020

Cheung, V., Cheung, C., McAlonan, G.M., Deng, Y., Wong, J.G., Yip, L., Tai, K.S., Khong, P.L., Sham, P., Chua, S.E., 2008. A diffusion tensor imaging study of structural dysconnectivity in never-medicated, first-episode schizophrenia. Psychol. Med. 38, 877–885. https://doi.org/10.1017/S0033291707001808

Chiang, M.-C., Barysheva, M., Shattuck, D.W., Lee, A.D., Madsen, S.K., Avedissian, C., Klunder, A.D., Toga, A.W., McMahon, K.L., Zubicaray, G.I. de, Wright, M.J., Srivastava, A., Balov, N., Thompson, P.M., 2009. Genetics of Brain Fiber Architecture and Intellectual Performance. J. Neurosci. 29, 2212–2224. https://doi.org/10.1523/JNEUROSCI.4184-08.2009

Chiang, M.-C., McMahon, K.L., de Zubicaray, G.I., Martin, N.G., Hickie, I., Toga, A.W., Wright, M.J., Thompson, P.M., 2011. Genetics of white matter development: a DTI study of 705 twins and their siblings aged 12 to 29. NeuroImage 54, 2308–2317. https://doi.org/10.1016/j.neuroimage.2010.10.015

Clayden, J.D., King, M.D., Clark, C.A., 2009a. Shape Modelling for Tract Selection, in: Medical Image Computing and Computer-Assisted Intervention – MICCAI 2009, Lecture Notes in Computer Science. Presented at the International Conference on Medical Image Computing and Computer-Assisted Intervention, Springer, Berlin, Heidelberg, pp. 150–157. https://doi.org/10.1007/978-3-642-04271-3_19

Clayden, J.D., Maniega, S.M., Storkey, A.J., King, M.D., Bastin, M.E., Clark, C.A., 2011. TractoR: Magnetic Resonance Imaging and Tractography with R. J. Stat. Softw. 44, 18.

Clayden, J.D., Storkey, A.J., Muñoz Maniega, S., Bastin, M.E., 2009b. Reproducibility of tract segmentation between sessions using an unsupervised modelling-based approach. NeuroImage 45, 377–385. https://doi.org/10.1016/j.neuroimage.2008.12.010

Clemm von Hohenberg, C., Pasternak, O., Kubicki, M., Ballinger, T., Vu, M.-A., Swisher, T., Green, K., Giwerc, M., Dahlben, B., Goldstein, J.M., Woo, T.-U.W., Petryshen, T.L., Mesholam-Gately, R.I., Woodberry, K.A., Thermenos, H.W., Mulert, C., McCarley, R.W., Seidman, L.J., Shenton, M.E., 2014. White Matter Microstructure in Individuals at Clinical High Risk of Psychosis: A Whole-Brain Diffusion Tensor Imaging Study. Schizophr. Bull. 40, 895–903. https://doi.org/10.1093/schbul/sbt079

Cloutman, L.L., Binney, R.J., Drakesmith, M., Parker, G.J.M., Lambon Ralph, M.A., 2012. The variation of function across the human insula mirrors its patterns of structural connectivity: evidence from in vivo probabilistic tractography. NeuroImage 59, 3514–3521. https://doi.org/10.1016/j.neuroimage.2011.11.016

Collin, G., de Nijs, J., Hulshoff Pol, H.E., Cahn, W., van den Heuvel, M.P., 2016. Connectome organization is related to longitudinal changes in general functioning, symptoms and IQ in chronic schizophrenia. Schizophr. Res. 173, 166–173. https://doi.org/10.1016/j.schres.2015.03.012

Collin, G., de Reus, M.A., Cahn, W., Hulshoff Pol, H.E., Kahn, R.S., van den Heuvel, M.P., 2013. Disturbed grey matter coupling in schizophrenia. Eur. Neuropsychopharmacol. J. Eur. Coll. Neuropsychopharmacol. 23, 46–54. https://doi.org/10.1016/j.euroneuro.2012.09.001

Collin, G., Kahn, R.S., Reus, D., A, M., Cahn, W., Heuvel, V.D., P, M., 2014. Impaired Rich Club Connectivity in Unaffected Siblings of Schizophrenia Patients. Schizophr. Bull. 40, 438–448. https://doi.org/10.1093/schbul/sbt162

Collin, G., van den Heuvel, M.P., 2013. The Ontogeny of the Human Connectome: Development and Dynamic Changes of Brain Connectivity Across the Life Span. The Neuroscientist 19, 616–628. https://doi.org/10.1177/1073858413503712

Colom, R., Karama, S., Jung, R.E., Haier, R.J., 2010. Human intelligence and brain networks. Dialogues Clin. Neurosci. 12, 489–501.

Concha, L., Livy, D.J., Beaulieu, C., Wheatley, B.M., Gross, D.W., 2010. In Vivo Diffusion Tensor Imaging and Histopathology of the Fimbria-Fornix in Temporal Lobe

Epilepsy. J. Neurosci. 30, 996–1002. https://doi.org/10.1523/JNEUROSCI.1619-09.2010

Corley, J., Cox, S.R., Deary, I.J., 2018. Healthy cognitive ageing in the Lothian Birth Cohort studies: marginal gains not magic bullet. Psychol. Med. 48, 187–207. https://doi.org/10.1017/S0033291717001489

Costafreda, S.G., Brébion, G., Allen, P., McGuire, P.K., Fu, C.H.Y., 2008. Affective modulation of external misattribution bias in source monitoring in schizophrenia. Psychol. Med. 38, 821–824. https://doi.org/10.1017/S0033291708003243

Cox, S.R., Ritchie, S.J., Tucker-Drob, E.M., Liewald, D.C., Hagenaars, S.P., Davies, G., Wardlaw, J.M., Gale, C.R., Bastin, M.E., Deary, I.J., 2016. Ageing and brain white matter structure in 3,513 UK Biobank participants. Nat. Commun. 7, ncomms13629. https://doi.org/10.1038/ncomms13629

Critchley, H.D., Wiens, S., Rotshtein, P., Ohman, A., Dolan, R.J., 2004. Neural systems supporting interoceptive awareness. Nat. Neurosci. 7, 189–195. https://doi.org/10.1038/nn1176

Cropley, V.L., Klauser, P., Lenroot, R.K., Bruggemann, J., Sundram, S., Bousman, C., Pereira, A., Di Biase, M.A., Weickert, T.W., Weickert, C.S., Pantelis, C., Zalesky, A., 2017. Accelerated Gray and White Matter Deterioration With Age in Schizophrenia. Am. J. Psychiatry 174, 286–295. https://doi.org/10.1176/appi.ajp.2016.16050610

Crow, T.J., 1990. The continuum of psychosis and its genetic origins. The sixty-fifth Maudsley lecture. Br. J. Psychiatry J. Ment. Sci. 156, 788–797.

Csernansky, J.G., Schindler, M.K., Splinter, N.R., Wang, L., Gado, M., Selemon, L.D., Rastogi-Cruz, D., Posener, J.A., Thompson, P.A., Miller, M.I., 2004. Abnormalities of thalamic volume and shape in schizophrenia. Am. J. Psychiatry 161, 896–902. https://doi.org/10.1176/appi.ajp.161.5.896

Curkendall, S.M., Mo, J., Glasser, D.B., Stang, M.R., Jones, J.K., 2004. Cardiovascular Disease in Patients With Schizophrenia in Saskatchewan, Canada. J. Clin. Psychiatry 65, 715–720. https://doi.org/10.4088/JCP.v65n0519

Curran, K.M., Emsell, L., Leemans, A., 2016. Quantitative DTI Measures, in: Diffusion Tensor Imaging. Springer, New York, NY, pp. 65–87. https://doi.org/10.1007/978-1-4939-3118-7_5

Damaraju, E., Allen, E.A., Belger, A., Ford, J.M., McEwen, S., Mathalon, D.H., Mueller, B.A., Pearlson, G.D., Potkin, S.G., Preda, A., Turner, J.A., Vaidya, J.G., van Erp, T.G., Calhoun, V.D., 2014. Dynamic functional connectivity analysis reveals

transient states of dysconnectivity in schizophrenia. NeuroImage Clin. 5, 298–308. https://doi.org/10.1016/j.nicl.2014.07.003

Damasio, A., 2003. Mental self: The person within. Nature 423, 227. https://doi.org/10.1038/423227a

Damoiseaux, J.S., 2017. Effects of aging on functional and structural brain connectivity. NeuroImage, Functional Architecture of the Brain 160, 32–40. https://doi.org/10.1016/j.neuroimage.2017.01.077

Davies, G., Tenesa, A., Payton, A., Yang, J., Harris, S.E., Liewald, D., Ke, X., Le Hellard, S., Christoforou, A., Luciano, M., McGhee, K., Lopez, L., Gow, A.J., Corley, J., Redmond, P., Fox, H.C., Haggarty, P., Whalley, L.J., McNeill, G., Goddard, M.E., Espeseth, T., Lundervold, A.J., Reinvang, I., Pickles, A., Steen, V.M., Ollier, W., Porteous, D.J., Horan, M., Starr, J.M., Pendleton, N., Visscher, P.M., Deary, I.J., 2011. Genome-wide association studies establish that human intelligence is highly heritable and polygenic. Mol. Psychiatry 16, 996–1005. https://doi.org/10.1038/mp.2011.85

Davis, K.L., Stewart, D.G., Friedman, J.I., Buchsbaum, M., Harvey, P.D., Hof, P.R., Buxbaum, J., Haroutunian, V., 2003. White matter changes in schizophrenia: evidence for myelin-related dysfunction. Arch. Gen. Psychiatry 60, 443–456. https://doi.org/10.1001/archpsyc.60.5.443

de Reus, M.A., van den Heuvel, M.P., 2013. Estimating false positives and negatives in brain networks. NeuroImage 70, 402–409. https://doi.org/10.1016/j.neuroimage.2012.12.066

de Weijer, A.D., Mandl, R.C.W., Diederen, K.M.J., Neggers, S.F.W., Kahn, R.S., Hulshoff Pol, H.E., Sommer, I.E.C., 2011. Microstructural alterations of the arcuate fasciculus in schizophrenia patients with frequent auditory verbal hallucinations. Schizophr. Res. 130, 68–77. https://doi.org/10.1016/j.schres.2011.05.010

de Winter, J.C.F., Dodou, D., Wieringa, P.A., 2009. Exploratory Factor Analysis With Small Sample Sizes. Multivar. Behav. Res. 44, 147–181. https://doi.org/10.1080/00273170902794206

Dean, K., Murray, R.M., 2005. Environmental risk factors for psychosis. Dialogues Clin. Neurosci. 7, 69–80.

Deary, I.J., 2012. Intelligence. Annu. Rev. Psychol. 63, 453–482. https://doi.org/10.1146/annurev-psych-120710-100353

Deary, I.J., Bastin, M.E., Pattie, A., Clayden, J.D., Whalley, L.J., Starr, J.M., Wardlaw, J.M., 2006. White matter integrity and cognition in childhood and old age. Neurology 66, 505–512. https://doi.org/10.1212/01.wnl.0000199954.81900.e2

. https://doi.org/10.1212/01.wnl.0000199954.81900.e2

Deary, I.J., Corley, J., Gow, A.J., Harris, S.E., Houlihan, L.M., Marioni, R.E., Penke, L., Rafnsson, S.B., Starr, J.M., 2009. Age-associated cognitive decline. Br. Med. Bull. 92, 135–152. https://doi.org/10.1093/bmb/ldp033

Deary, I.J., Gow, A.J., Pattie, A., Starr, J.M., 2012. Cohort profile: the Lothian Birth Cohorts of 1921 and 1936. Int. J. Epidemiol. 41, 1576–1584. https://doi.org/10.1093/ije/dyr197

Deary, I.J., Gow, A.J., Taylor, M.D., Corley, J., Brett, C., Wilson, V., Campbell, H., Whalley, L.J., Visscher, P.M., Porteous, D.J., Starr, J.M., 2007. The Lothian Birth Cohort 1936: a study to examine influences on cognitive ageing from age 11 to age 70 and beyond. BMC Geriatr. 7, 28. https://doi.org/10.1186/1471-2318-7-28

Dell'Acqua, F., Tournier, J.-D., 2018. Modelling white matter with spherical deconvolution: How and why? NMR Biomed. e3945. https://doi.org/10.1002/nbm.3945

Dening, T., Thomas, A. (Eds.), 2013. Oxford Textbook of Old Age Psychiatry, Second Edition. ed. Oxford Textbooks in Psychiatry.

Dennis, E.L., Jahanshad, N., Toga, A.W., McMahon, K.L., de Zubicaray, G.I., Martin, N.G., Wright, M.J., Thompson, P.M., 2012. Test-Retest Reliability of Graph Theory Measures of Structural Brain Connectivity. Med. Image Comput. Comput.-Assist. Interv. MICCAI Int. Conf. Med. Image Comput. Comput.-Assist. Interv. 15, 305–312.

Desikan, R.S., Ségonne, F., Fischl, B., Quinn, B.T., Dickerson, B.C., Blacker, D., Buckner, R.L., Dale, A.M., Maguire, R.P., Hyman, B.T., Albert, M.S., Killiany, R.J., 2006. An automated labeling system for subdividing the human cerebral cortex on MRI scans into gyral based regions of interest. NeuroImage 31, 968–980. https://doi.org/10.1016/j.neuroimage.2006.01.021

Detterman, D.K., Daniel, M.H., 1989. Correlations of mental tests with each other and with cognitive variables are highest for low IQ groups. Intelligence 13, 349–359. https://doi.org/10.1016/S0160-2896(89)80007-8

Dickinson D, Ramsey ME, Gold JM, 2007. Overlooking the obvious: A meta-analytic comparison of digit symbol coding tasks and other cognitive measures in schizophrenia. Arch. Gen. Psychiatry 64, 532–542. https://doi.org/10.1001/archpsyc.64.5.532

Drakesmith, M., Caeyenberghs, K., Dutt, A., Lewis, G., David, A.S., Jones, D.K., 2015. Overcoming the effects of false positives and threshold bias in graph theoretical analyses of neuroimaging data. Neuroimage 118, 313–333. https://doi.org/10.1016/j.neuroimage.2015.05.011

Ellison-Wright, I., Bullmore, E., 2009. Meta-analysis of diffusion tensor imaging studies in schizophrenia. Schizophr. Res. 108, 3–10. https://doi.org/10.1016/j.schres.2008.11.021

Elvevåg, B., Goldberg, T.E., 2000. Cognitive impairment in schizophrenia is the core of the disorder. Crit. Rev. Neurobiol. 14, 1–21.

Engelbrecht, V., Scherer, A., Rassek, M., Witsack, H.J., Mödder, U., 2002. Diffusion-weighted MR imaging in the brain in children: findings in the normal brain and in the brain with white matter diseases. Radiology 222, 410–418. https://doi.org/10.1148/radiol.2222010492

Engwer, C., Hillen, T., Knappitsch, M., Surulescu, C., 2015. Glioma follow white matter tracts: a multiscale DTI-based model. J. Math. Biol. 71, 551–582. https://doi.org/10.1007/s00285-014-0822-7

Erlenmeyer-Kimling, L., Rock, D., Roberts, S.A., Janal, M., Kestenbaum, C., Cornblatt, B., Adamo, U.H., Gottesman, I.I., 2000. Attention, memory, and motor skills as childhood predictors of schizophrenia-related psychoses: the New York High-Risk Project. Am. J. Psychiatry 157, 1416–1422.

Estrada, E., 2011. The Structure of Complex Networks: Theory and Applications. Oxford University Press, Oxford, New York.

Euesden, J., Lewis, C.M., O'Reilly, P.F., 2015. PRSice: Polygenic Risk Score software. Bioinforma. Oxf. Engl. 31, 1466–1468. https://doi.org/10.1093/bioinformatics/btu848

Falkai, P., Rossner, M.J., Schulze, T.G., Hasan, A., Brzózka, M.M., Malchow, B., Honer, W.G., Schmitt, A., 2015. Kraepelin revisited: schizophrenia from degeneration to failed regeneration. Mol. Psychiatry 20, 671–676. https://doi.org/10.1038/mp.2015.35

Fields, R.D., 2008. White matter in learning, cognition and psychiatric disorders. Trends Neurosci. 31, 361–370. https://doi.org/10.1016/j.tins.2008.04.001

Filippi, M., Canu, E., Gasparotti, R., Agosta, F., Valsecchi, P., Lodoli, G., Galluzzo, A., Comi, G., Sacchetti, E., 2014. Patterns of brain structural changes in first-contact, antipsychotic drug-naive patients with schizophrenia. AJNR Am. J. Neuroradiol. 35, 30–37. https://doi.org/10.3174/ajnr.A3583

Fitzsimmons, J., Hamoda, H.M., Swisher, T., Terry, D., Rosenberger, G., Seidman, L.J., Goldstein, J., Mesholam-Gately, R., Petryshen, T., Wojcik, J., Kikinis, R., Kubicki, M., 2014. Diffusion tensor imaging study of the fornix in first episode schizophrenia and in healthy controls. Schizophr. Res. 156, 157–160. https://doi.org/10.1016/j.schres.2014.04.022

Fjell, A.M., Sneve, M.H., Storsve, A.B., Grydeland, H., Yendiki, A., Walhovd, K.B., 2016. Brain Events Underlying Episodic Memory Changes in Aging: A Longitudinal Investigation of Structural and Functional Connectivity. Cereb. Cortex 26, 1272–1286. https://doi.org/10.1093/cercor/bhv102

Foong, J., Maier, M., Clark, C., Barker, G., Miller, D., Ron, M., 2000. Neuropathological abnormalities of the corpus callosum in schizophrenia: a diffusion tensor imaging study. J. Neurol. Neurosurg. Psychiatry 68, 242–244. https://doi.org/10.1136/jnnp.68.2.242

Fornito, A., Bullmore, E.T., 2015. Reconciling abnormalities of brain network structure and function in schizophrenia. Curr. Opin. Neurobiol. 30, 44–50. https://doi.org/10.1016/j.conb.2014.08.006

Fornito, A., Bullmore, E.T., 2010. What can spontaneous fluctuations of the blood oxygenation-level-dependent signal tell us about psychiatric disorders? Curr. Opin. Psychiatry 23, 239–249. https://doi.org/10.1097/YCO.0b013e328337d78d

Fornito, A., Zalesky, A., Pantelis, C., Bullmore, E.T., 2012. Schizophrenia, neuroimaging and connectomics. NeuroImage 62, 2296–2314. https://doi.org/10.1016/j.neuroimage.2011.12.090

Freeman, L.C., 1978. Centrality in social networks conceptual clarification. Soc. Netw. 1, 215–239. https://doi.org/10.1016/0378-8733(78)90021-7

Friedman, J.I., Harvey, P.D., Coleman, T., Moriarty, P.J., Bowie, C., Parrella, M., White, L., Adler, D., Davis, K.L., 2001. Six-year follow-up study of cognitive and functional status across the lifespan in schizophrenia: a comparison with Alzheimer's disease and normal aging. Am. J. Psychiatry 158, 1441–1448. https://doi.org/10.1176/appi.ajp.158.9.1441

Friedman, J.I., Tang, C., Carpenter, D., Buchsbaum, M., Schmeidler, J., Flanagan, L., Golembo, S., Kanellopoulou, I., Ng, J., Hof, P.R., Harvey, P.D., Tsopelas, N.D., Stewart, D., Davis, K.L., 2008. Diffusion tensor imaging findings in first-episode and chronic schizophrenia patients. Am. J. Psychiatry 165, 1024–1032. https://doi.org/10.1176/appi.ajp.2008.07101640

Friston, K.J., 1998. The disconnection hypothesis. Schizophr. Res. 30, 115–125.

Friston, K.J., 1994. Functional and effective connectivity in neuroimaging: A synthesis. Hum. Brain Mapp. 2, 56–78. https://doi.org/10.1002/hbm.460020107

Friston, K.J., Frith, C.D., 1995. Schizophrenia: a disconnection syndrome? Clin. Neurosci. N. Y. N 3, 89–97.

Fujiwara, H., Namiki, C., Hirao, K., Miyata, J., Shimizu, M., Fukuyama, H., Sawamoto, N., Hayashi, T., Murai, T., 2007. Anterior and posterior cingulum abnormalities and their association with psychopathology in schizophrenia: a diffusion tensor imaging study. Schizophr. Res. 95, 215–222. https://doi.org/10.1016/j.schres.2007.05.044

Gasparotti, R., Valsecchi, P., Carletti, F., Galluzzo, A., Liserre, R., Cesana, B., Sacchetti, E., 2009. Reduced fractional anisotropy of corpus callosum in first-contact, antipsychotic drug-naive patients with schizophrenia. Schizophr. Res. 108, 41–48. https://doi.org/10.1016/j.schres.2008.11.015

Gauvain, K.M., McKinstry, R.C., Mukherjee, P., Perry, A., Neil, J.J., Kaufman, B.A., Hayashi, R.J., 2001. Evaluating Pediatric Brain Tumor Cellularity with Diffusion-Tensor Imaging. Am. J. Roentgenol. 177, 449–454. https://doi.org/10.2214/ajr.177.2.1770449

Ghaziri, J., Tucholka, A., Girard, G., Houde, J.-C., Boucher, O., Gilbert, G., Descoteaux, M., Lippé, S., Rainville, P., Nguyen, D.K., 2017. The Corticocortical Structural Connectivity of the Human Insula. Cereb. Cortex N. Y. N 1991 27, 1216–1228. https://doi.org/10.1093/cercor/bhv308

Glahn, D.C., Almasy, L., Blangero, J., Burk, G.M., Estrada, J., Peralta, J.M., Meyenberg, N., Castro, M.P., Barrett, J., Nicolini, H., Raventós, H., Escamilla, M.A., 2007. Adjudicating neurocognitive endophenotypes for schizophrenia. Am. J. Med. Genet. B Neuropsychiatr. Genet. 144B, 242–249. https://doi.org/10.1002/ajmg.b.30446

Gogtay, N., Greenstein, D., Lenane, M., Clasen, L., Sharp, W., Gochman, P., Butler, P., Evans, A., Rapoport, J., 2007. Cortical brain development in nonpsychotic siblings of patients with childhood-onset schizophrenia. Arch. Gen. Psychiatry 64, 772–780. https://doi.org/10.1001/archpsyc.64.7.772

Goldberg, S., Fruchter, E., Davidson, M., Reichenberg, A., Yoffe, R., Weiser, M., 2011. The Relationship Between Risk of Hospitalization for Schizophrenia, SES, and Cognitive Functioning. Schizophr. Bull. 37, 664–670. https://doi.org/10.1093/schbul/sbr047

Goldberg, T.E., Greenberg, R.D., Griffin, S.J., Gold, J.M., Kleinman, J.E., Pickar, D., Schulz, S.C., Weinberger, D.R., 1993. The effect of clozapine on cognition and psychiatric symptoms in patients with schizophrenia. Br. J. Psychiatry J. Ment. Sci. 162, 43–48.

Goldman, A.L., Pezawas, L., Mattay, V.S., Fischl, B., Verchinski, B.A., Chen, Q., Weinberger, D.R., Meyer-Lindenberg, A., 2009. Widespread reductions of cortical thickness in schizophrenia and spectrum disorders and evidence of heritability. Arch. Gen. Psychiatry 66, 467–477. https://doi.org/10.1001/archgenpsychiatry.2009.24

Gollwitzer, M., Christ, O., Lemmer, G., 2014. Individual differences make a difference: On the use and the psychometric properties of difference scores in social psychology. Eur. J. Soc. Psychol. 44, 673–682. https://doi.org/10.1002/ejsp.2042

Gong, G., Rosa-Neto, P., Carbonell, F., Chen, Z.J., He, Y., Evans, A.C., 2009. Age- and Gender-Related Differences in the Cortical Anatomical Network. J. Neurosci. 29, 15684–15693. https://doi.org/10.1523/JNEUROSCI.2308-09.2009

Gottesman, I.I., 1991. Schizophrenia genesis: The origins of madness, Schizophrenia genesis: The origins of madness. W H Freeman/Times Books/ Henry Holt & Co, New York, NY, US.

Gottesman, I.I., Erlenmeyer-Kimling, L., 2001. Family and twin strategies as a head start in defining prodromes and endophenotypes for hypothetical early-interventions in schizophrenia. Schizophr. Res. 51, 93–102.

Gottesman, I.I., Shields, J., 1976. A critical review of recent adoption, twin, and family studies of schizophrenia: behavioral genetics perspectives. Schizophr. Bull. 2, 360–401.

Goulas, A., Uylings, H.B.M., Hilgetag, C.C., 2017. Principles of ipsilateral and contralateral cortico-cortical connectivity in the mouse. Brain Struct. Funct. 222, 1281–1295. https://doi.org/10.1007/s00429-016-1277-y

Gouw, A.A., Seewann, A., Vrenken, H., Flier, V.D., M, W., Rozemuller, J.M., Barkhof, F., Scheltens, P., Geurts, J.J.G., 2008. Heterogeneity of white matter hyperintensities in Alzheimer's disease: post-mortem quantitative MRI and neuropathology. Brain 131, 3286–3298. https://doi.org/10.1093/brain/awn265

Grice, J.W., 2001. Computing and evaluating factor scores. Psychol. Methods 6, 430–450.

Griffa, A., Baumann, P.S., Ferrari, C., Do, K.Q., Conus, P., Thiran, J.-P., Hagmann, P., 2015. Characterizing the connectome in schizophrenia with diffusion spectrum imaging. Hum. Brain Mapp. 36, 354–366. https://doi.org/10.1002/hbm.22633

Guo, W., Liu, F., Liu, Z., Gao, K., Xiao, C., Chen, H., Zhao, J., 2012. Right lateralized white matter abnormalities in first-episode, drug-naive paranoid schizophrenia. Neurosci. Lett. 531, 5–9. https://doi.org/10.1016/j.neulet.2012.09.033

Gur RC, Calkins ME, Satterthwaite TD, et al, 2014. NEurocognitive growth charting in psychosis spectrum youths. JAMA Psychiatry 71, 366–374. https://doi.org/10.1001/jamapsychiatry.2013.4190

Gur, R.E., Gur, R.C., 2010. Functional magnetic resonance imaging in schizophrenia. Dialogues Clin. Neurosci. 12, 333–343.

Gurung, R., Prata, D.P., 2015. What is the impact of genome-wide supported risk variants for schizophrenia and bipolar disorder on brain structure and function? A systematic review. Psychol. Med. 45, 2461–2480. https://doi.org/10.1017/S0033291715000537

Hagenaars, S.P., Harris, S.E., Davies, G., Hill, W.D., Liewald, D.C.M., Ritchie, S.J., Marioni, R.E., Fawns-Ritchie, C., Cullen, B., Malik, R., Consortium, M., Gwas, I.C. for B.P., Consortium, S., Group, C.C.P., Group, C.C.A. and L., Worrall, B.B., Sudlow, C.L.M., Wardlaw, J.M., Gallacher, J., Pell, J., McIntosh, A.M., Smith, D.J., Gale, C.R., Deary, I.J., 2016. Shared genetic aetiology between cognitive functions and physical and mental health in UK Biobank (*N*=112 151) and 24 GWAS consortia. Mol. Psychiatry 21, 1624–1632. https://doi.org/10.1038/mp.2015.225

Hagmann, P., 2005. From diffusion MRI to brain connectomics. https://doi.org/10.5075/epfl-thesis-3230

Hakulinen, U., Brander, A., Ryymin, P., Öhman, J., Soimakallio, S., Helminen, M., Dastidar, P., Eskola, H., 2012. Repeatability and variation of region-of-interest methods using quantitative diffusion tensor MR imaging of the brain. BMC Med. Imaging 12, 30. https://doi.org/10.1186/1471-2342-12-30

Harrison, P.J., 1999. The neuropathology of schizophrenia. A critical review of the data and their interpretation. Brain J. Neurol. 122 (Pt 4), 593–624.

Hasan, K.M., Kamali, A., Abid, H., Kramer, L.A., Fletcher, J.M., Ewing-Cobbs, L., 2010. Quantification of the spatiotemporal microstructural organization of the human brain association, projection and commissural pathways across the lifespan using diffusion tensor tractography. Brain Struct. Funct. 214, 361–373. https://doi.org/10.1007/s00429-009-0238-0

Hashemi, R.H., Bradley, W.G., Lisanti, C.J., Ovid Technologies, I., 2004. MRI : the basics, 2nd ed. ed. Philadelphia : Lippincott Williams & Wilkins.

Hayes, A.F., 2009. Beyond Baron and Kenny: Statistical Mediation Analysis in the New Millennium. Commun. Monogr. 76, 408–420. https://doi.org/10.1080/03637750903310360

Hayes, A.F., Preacher, K.J., 2014. Statistical mediation analysis with a multicategorical independent variable. Br. J. Math. Stat. Psychol. 67, 451–470. https://doi.org/10.1111/bmsp.12028

Hayes, A.F., Rockwood, N.J., 2016. Regression-based statistical mediation and moderation analysis in clinical research: Observations, recommendations, and implementation. Behav. Res. Ther. https://doi.org/10.1016/j.brat.2016.11.001

Hecke, W.V., Emsell, L., Sunaert, S., 2015. Diffusion Tensor Imaging: A Practical Handbook. Springer.

Heinrichs, R.W., Zakzanis, K.K., 1998. Neurocognitive deficit in schizophrenia: a quantitative review of the evidence. Neuropsychology 12, 426–445.

Heston, L.L., 1966. Psychiatric disorders in foster home reared children of schizophrenic mothers. Br. J. Psychiatry J. Ment. Sci. 112, 819–825.

Hilker, R., Helenius, D., Fagerlund, B., Skytthe, A., Christensen, K., Werge, T.M., Nordentoft, M., Glenthøj, B., 2018. Heritability of Schizophrenia and Schizophrenia Spectrum Based on the Nationwide Danish Twin Register. Biol. Psychiatry 83, 492–498. https://doi.org/10.1016/j.biopsych.2017.08.017

Hof, P.R., Haroutunian, V., Friedrich, V.L., Byne, W., Buitron, C., Perl, D.P., Davis, K.L., 2003. Loss and altered spatial distribution of oligodendrocytes in the superior frontal gyrus in schizophrenia. Biol. Psychiatry 53, 1075–1085.

Hofer, S.M., Sliwinski, M.J., 2001. Understanding Ageing. An evaluation of research designs for assessing the interdependence of ageing-related changes. Gerontology 47, 341–352.

Holleran, L., Ahmed, M., Anderson-Schmidt, H., McFarland, J., Emsell, L., Leemans, A., Scanlon, C., Dockery, P., McCarthy, P., Barker, G.J., McDonald, C., Cannon, D.M., 2014. Altered interhemispheric and temporal lobe white matter microstructural organization in severe chronic schizophrenia. Neuropsychopharmacol. Off. Publ. Am. Coll. Neuropsychopharmacol. 39, 944–954. https://doi.org/10.1038/npp.2013.294

Holzer, C.E., Shea, B.M., Swanson, J.W., Leaf, P.J., et al, 1986. The increased risk for specific psychiatric disorders among persons of low socioeconomic status. Am. J. Soc. Psychiatry 6, 259–271.

Hoptman, M.J., Nierenberg, J., Bertisch, H.C., Catalano, D., Ardekani, B.A., Branch, C.A., Delisi, L.E., 2008. A DTI study of white matter microstructure in individuals at high genetic risk for schizophrenia. Schizophr. Res. 106, 115–124. https://doi.org/10.1016/j.schres.2008.07.023

Horsfield, M.A., 1999. Mapping eddy current induced fields for the correction of diffusion-weighted echo planar images. Magn. Reson. Imaging 17, 1335–1345.

Hubl, D., Koenig, T., Strik, W., Federspiel, A., Kreis, R., Boesch, C., Maier, S.E., Schroth, G., Lovblad, K., Dierks, T., 2004. Pathways that make voices: white matter changes

in auditory hallucinations. Arch. Gen. Psychiatry 61, 658–668. https://doi.org/10.1001/archpsyc.61.7.658

Hulshoff Pol, H.E., Brans, R.G.H., van Haren, N.E.M., Schnack, H.G., Langen, M., Baaré, W.F.C., van Oel, C.J., Kahn, R.S., 2004. Gray and white matter volume abnormalities in monozygotic and same-gender dizygotic twins discordant for schizophrenia. Biol. Psychiatry 55, 126–130.

International Schizophrenia Consortium, Purcell, S.M., Wray, N.R., Stone, J.L., Visscher, P.M., O'Donovan, M.C., Sullivan, P.F., Sklar, P., 2009. Common polygenic variation contributes to risk of schizophrenia and bipolar disorder. Nature 460, 748–752. https://doi.org/10.1038/nature08185

Jafri, M.J., Pearlson, G.D., Stevens, M., Calhoun, V.D., 2008. A method for functional network connectivity among spatially independent resting-state components in schizophrenia. NeuroImage 39, 1666–1681. https://doi.org/10.1016/j.neuroimage.2007.11.001

Jahanshad, N., Kochunov, P., Sprooten, E., Mandl, R.C., Nichols, T.E., Almassy, L., Blangero, J., Brouwer, R.M., Curran, J.E., de Zubicaray, G.I., Duggirala, R., Fox, P.T., Hong, L.E., Landman, B.A., Martin, N.G., McMahon, K.L., Medland, S.E., Mitchell, B.D., Olvera, R.L., Peterson, C.P., Starr, J.M., Sussmann, J.E., Toga, A.W., Wardlaw, J.M., Wright, M.J., Hulshoff Pol, H.E., Bastin, M.E., McIntosh, A.M., Deary, I.J., Thompson, P.M., Glahn, D.C., 2013. Multi-site genetic analysis of diffusion images and voxelwise heritability analysis: A pilot project of the ENIGMA–DTI working group. NeuroImage 81, 455–469. https://doi.org/10.1016/j.neuroimage.2013.04.061

Jbabdi, S., Johansen-Berg, H., 2011. Tractography - where do we go from here? Brain Connect. 1, 169–183. https://doi.org/10.1089/brain.2011.0033

Jenkinson, M., Smith, S., 2001. A global optimisation method for robust affine registration of brain images. Med. Image Anal. 5, 143–156.

Johansen-Berg, H., Behrens, T.E.J., 2009. Diffusion MRI: From Quantitative Measurement to In-vivo Neuroanatomy. Elsevier/Academic Press.

Johns, L.C., Rossell, S., Frith, C., Ahmad, F., Hemsley, D., Kuipers, E., McGuire, P.K., 2001. Verbal self-monitoring and auditory verbal hallucinations in patients with schizophrenia. Psychol. Med. 31, 705–715.

Johnson, W., Bouchard Jr., T.J., Krueger, R.F., McGue, M., Gottesman, I.I., 2004. Just one g: consistent results from three test batteries. Intelligence 32, 95–107. https://doi.org/10.1016/S0160-2896(03)00062-X

Jones, D.K., 2011. Diffusion MRI: theory, methods and applications. Oxford University Press, Oxford.

Jones, D.K., Catani, M., Pierpaoli, C., Reeves, S.J.C., Shergill, S.S., O'Sullivan, M., Golesworthy, P., McGuire, P., Horsfield, M.A., Simmons, A., Williams, S.C.R., Howard, R.J., 2006. Age effects on diffusion tensor magnetic resonance imaging tractography measures of frontal cortex connections in schizophrenia. Hum. Brain Mapp. 27, 230–238. https://doi.org/10.1002/hbm.20179

Jones, D.K., Knösche, T.R., Turner, R., 2013. White matter integrity, fiber count, and other fallacies: the do's and don'ts of diffusion MRI. NeuroImage 73, 239–254. https://doi.org/10.1016/j.neuroimage.2012.06.081

Jung, R.E., Haier, R.J., 2007. The Parieto-Frontal Integration Theory (P-FIT) of intelligence: converging neuroimaging evidence. Behav. Brain Sci. 30, 135–154; discussion 154-187. https://doi.org/10.1017/S0140525X07001185

Kail, R., Salthouse, T.A., 1994. Processing speed as a mental capacity. Acta Psychol. (Amst.) 86, 199–225. https://doi.org/10.1016/0001-6918(94)90003-5

Karbasforoushan, H., Duffy, B., Blackford, J.U., Woodward, N.D., 2015. Processing speed impairment in schizophrenia is mediated by white matter integrity. Psychol. Med. 45, 109–120. https://doi.org/10.1017/S0033291714001111

Karlsgodt, K.H., Jacobson, S.C., Seal, M., Fusar-Poli, P., 2012. The relationship of developmental changes in white matter to the onset of psychosis. Curr. Pharm. Des. 18, 422–433.

Kay, S.R., Fiszbein, A., Opler, L.A., 1987. The positive and negative syndrome scale (PANSS) for schizophrenia. Schizophr. Bull. 13, 261–276.

Keefe, R.S.E., Eesley, C.E., Poe, M.P., 2005. Defining a cognitive function decrement in schizophrenia. Biol. Psychiatry 57, 688–691. https://doi.org/10.1016/j.biopsych.2005.01.003

Keefe, R.S.E., Goldberg, T.E., Harvey, P.D., Gold, J.M., Poe, M.P., Coughenour, L., 2004. The Brief Assessment of Cognition in Schizophrenia: reliability, sensitivity, and comparison with a standard neurocognitive battery. Schizophr. Res. 68, 283–297. https://doi.org/10.1016/j.schres.2003.09.011

Kelly, S., Jahanshad, N., Zalesky, A., Kochunov, P., Agartz, I., Alloza, C., Andreassen, O.A., Arango, C., Banaj, N., Bouix, S., Bousman, C.A., Brouwer, R.M., Bruggemann, J., Bustillo, J., Cahn, W., Calhoun, V., Cannon, D., Carr, V., Catts, S., Chen, J., Chen, J.-X., Chen, X., Chiapponi, C., Cho, K.K., Ciullo, V., Corvin, A.S., Crespo-Facorro, B., Cropley, V., De Rossi, P., Diaz-Caneja, C.M., Dickie, E.W., Ehrlich, S., Fan, F.-

M., Faskowitz, J., Fatouros-Bergman, H., Flyckt, L., Ford, J.M., Fouche, J.-P., Fukunaga, M., Gill, M., Glahn, D.C., Gollub, R., Goudzwaard, E.D., Guo, H., Gur, R.E., Gur, R.C., Gurholt, T.P., Hashimoto, R., Hatton, S.N., Henskens, F.A., Hibar, D.P., Hickie, I.B., Hong, L.E., Horacek, J., Howells, F.M., Hulshoff Pol, H.E., Hyde, C.L., Isaev, D., Jablensky, A., Jansen, P.R., Janssen, J., Jönsson, E.G., Jung, L.A., Kahn, R.S., Kikinis, Z., Liu, K., Klauser, P., Knöchel, C., Kubicki, M., Lagopoulos, J., Langen, C., Lawrie, S., Lenroot, R.K., Lim, K.O., Lopez-Jaramillo, C., Lyall, A., Magnotta, V., Mandl, R.C.W., Mathalon, D.H., McCarley, R.W., McCarthy-Jones, S., McDonald, C., McEwen, S., McIntosh, A., Melicher, T., Mesholam-Gately, R.I., Michie, P.T., Mowry, B., Mueller, B.A., Newell, D.T., O'Donnell, P., Oertel-Knöchel, V., Oestreich, L., Paciga, S.A., Pantelis, C., Pasternak, O., Pearlson, G., Pellicano, G.R., Pereira, A., Pineda Zapata, J., Piras, F., Potkin, S.G., Preda, A., Rasser, P.E., Roalf, D.R., Roiz, R., Roos, A., Rotenberg, D., Satterthwaite, T.D., Savadjiev, P., Schall, U., Scott, R.J., Seal, M.L., Seidman, L.J., Shannon Weickert, C., Whelan, C.D., Shenton, M.E., Kwon, J.S., Spalletta, G., Spaniel, F., Sprooten, E., Stäblein, M., Stein, D.J., Sundram, S., Tan, Y., Tan, S., Tang, S., Temmingh, H.S., Westlye, L.T., Tønnesen, S., Tordesillas-Gutierrez, D., Doan, N.T., Vaidya, J., van Haren, N.E.M., Vargas, C.D., Vecchio, D., Velakoulis, D., Voineskos, A., Voyvodic, J.Q., Wang, Z., Wan, P., Wei, D., Weickert, T.W., Whalley, H., White, T., Whitford, T.J., Wojcik, J.D., Xiang, H., Xie, Z., Yamamori, H., Yang, F., Yao, N., Zhang, G., Zhao, J., van Erp, T.G.M., Turner, J., Thompson, P.M., Donohoe, G., 2017. Widespread white matter microstructural differences in schizophrenia across 4322 individuals: results from the ENIGMA Schizophrenia DTI Working Group. Mol. Psychiatry. https://doi.org/10.1038/mp.2017.170

Kety, S.S., Rosenthal, D., Wender, P.H., Schulsinger, F., Jacobsen, B., 1976. Mental illness in the biological and adoptive families of adopted individuals who have become schizophrenic. Behav. Genet. 6, 219–225.

Kirkpatrick, B., Messias, E., Harvey, P.D., Fernandez-Egea, E., Bowie, C.R., 2008. Is Schizophrenia a Syndrome of Accelerated Aging? Schizophr. Bull. 34, 1024–1032. https://doi.org/10.1093/schbul/sbm140

Knöchel, C., Oertel-Knöchel, V., O'Dwyer, L., Prvulovic, D., Alves, G., Kollmann, B., Hampel, H., 2012. Cognitive and behavioural effects of physical exercise in psychiatric patients. Prog. Neurobiol. 96, 46–68. https://doi.org/10.1016/j.pneurobio.2011.11.007

Knowles, E.E.M., David, A.S., Reichenberg, A., 2010. Processing Speed Deficits in Schizophrenia: Reexamining the Evidence. Am. J. Psychiatry 167, 828–835. https://doi.org/10.1176/appi.ajp.2010.09070937

Kochunov, P., Coyle, T.R., Rowland, L.M., Jahanshad, N., Thompson, P.M., Kelly, S., Du, X., Sampath, H., Bruce, H., Chiappelli, J., Ryan, M., Fisseha, F., Savransky, A., Adhikari, B., Chen, S., Paciga, S.A., Whelan, C.D., Xie, Z., Hyde, C.L., Chen, X., Schubert, C.R., O'Donnell, P., Hong, L.E., 2017. Association of White Matter With Core Cognitive Deficits in Patients With Schizophrenia. JAMA Psychiatry 74, 958–966. https://doi.org/10.1001/jamapsychiatry.2017.2228

Kochunov, P., Glahn, D.C., Lancaster, J., Thompson, P.M., Kochunov, V., Rogers, B., Fox, P., Blangero, J., Williamson, D.E., 2011. Fractional anisotropy of cerebral white matter and thickness of cortical gray matter across the lifespan. NeuroImage 58, 41–49. https://doi.org/10.1016/j.neuroimage.2011.05.050

Kochunov, P., Glahn, D.C., Lancaster, J.L., Winkler, A.M., Smith, S., Thompson, P.M., Almasy, L., Duggirala, R., Fox, P.T., Blangero, J., 2010. Genetics of microstructure of cerebral white matter using diffusion tensor imaging. NeuroImage 53, 1109–1116. https://doi.org/10.1016/j.neuroimage.2010.01.078

Kochunov, P., Glahn, D.C., Rowland, L.M., Olvera, R.L., Winkler, A., Yang, Y.-H., Sampath, H., Carpenter, W.T., Duggirala, R., Curran, J., Blangero, J., Hong, L.E., 2013. Testing the hypothesis of accelerated cerebral white matter aging in schizophrenia and major depression. Biol. Psychiatry 73, 482–491. https://doi.org/10.1016/j.biopsych.2012.10.002

Kochunov, P., Hong, L.E., 2014. Neurodevelopmental and neurodegenerative models of schizophrenia: white matter at the center stage. Schizophr. Bull. 40, 721–728. https://doi.org/10.1093/schbul/sbu070

Kochunov, P., Jahanshad, N., Marcus, D., Winkler, A., Sprooten, E., Nichols, T.E., Wright, S.N., Hong, L.E., Patel, B., Behrens, T., Jbabdi, S., Andersson, J., Lenglet, C., Yacoub, E., Moeller, S., Auerbach, E., Ugurbil, K., Sotiropoulos, S.N., Brouwer, R.M., Landman, B., Lemaitre, H., den Braber, A., Zwiers, M.P., Ritchie, S., van Hulzen, K., Almasy, L., Curran, J., deZubicaray, G.I., Duggirala, R., Fox, P., Martin, N.G., McMahon, K.L., Mitchell, B., Olvera, R.L., Peterson, C., Starr, J., Sussmann, J., Wardlaw, J., Wright, M., Boomsma, D.I., Kahn, R., de Geus, E.J.C., Williamson, D.E., Hariri, A., van 't Ent, D., Bastin, M.E., McIntosh, A., Deary, I.J., Hulshoff Pol, H.E., Blangero, J., Thompson, P.M., Glahn, D.C., Van Essen, D.C., 2015. Heritability of fractional anisotropy in human white matter: a comparison of Human Connectome

Project and ENIGMA-DTI data. NeuroImage 111, 300–311. https://doi.org/10.1016/j.neuroimage.2015.02.050

Kochunov, P., Jahanshad, N., Sprooten, E., Nichols, T.E., Mandl, R.C., Almasy, L., Booth, T., Brouwer, R.M., Curran, J.E., de Zubicaray, G.I., Dimitrova, R., Duggirala, R., Fox, P.T., Hong, L.E., Landman, B.A., Lemaitre, H., Lopez, L.M., Martin, N.G., McMahon, K.L., Mitchell, B.D., Olvera, R.L., Peterson, C.P., Starr, J.M., Sussmann, J.E., Toga, A.W., Wardlaw, J.M., Wright, M.J., Wright, S.N., Bastin, M.E., McIntosh, A.M., Boomsma, D.I., Kahn, R.S., den Braber, A., de Geus, E.J.C., Deary, I.J., Hulshoff Pol, H.E., Williamson, D.E., Blangero, J., van 't Ent, D., Thompson, P.M., Glahn, D.C., 2014. Multi-site study of additive genetic effects on fractional anisotropy of cerebral white matter: Comparing meta and megaanalytical approaches for data pooling. NeuroImage 95, 136–150. https://doi.org/10.1016/j.neuroimage.2014.03.033

Kochunov, P., Thompson, P.M., Winkler, A., Morrissey, M., Fu, M., Coyle, T.R., Du, X., Muellerklein, F., Savransky, A., Gaudiot, C., Sampath, H., Eskandar, G., Jahanshad, N., Patel, B., Rowland, L., Nichols, T.E., O'Connell, J.R., Shuldiner, A.R., Mitchell, B.D., Hong, L.E., 2016. The common genetic influence over processing speed and white matter microstructure: Evidence from the Old Order Amish and Human Connectome Projects. NeuroImage 125, 189–197. https://doi.org/10.1016/j.neuroimage.2015.10.050

Kochunov, P., Williamson, D.E., Lancaster, J., Fox, P., Cornell, J., Blangero, J., Glahn, D.C., 2012. Fractional anisotropy of water diffusion in cerebral white matter across the lifespan. Neurobiol. Aging 33, 9–20. https://doi.org/10.1016/j.neurobiolaging.2010.01.014

Konick, L.C., Friedman, L., 2001. Meta-analysis of thalamic size in schizophrenia. Biol. Psychiatry 49, 28–38.

Koutsouleris, N., Davatzikos, C., Borgwardt, S., Gaser, C., Bottlender, R., Frodl, T., Falkai, P., Riecher-Rössler, A., Möller, H.-J., Reiser, M., Pantelis, C., Meisenzahl, E., 2014. Accelerated brain aging in schizophrenia and beyond: a neuroanatomical marker of psychiatric disorders. Schizophr. Bull. 40, 1140–1153. https://doi.org/10.1093/schbul/sbt142

Kraepelin, E., 1971. Dementia praecox and paraphrenia. R. E. Krieger Pub. Co.

Kraepelin, E., Robertson, G.M., 1919. Dementia praecox and paraphrenia. Edinburgh: Livingstone.

Kubicki, M., Shenton, M.E., 2014. Diffusion Tensor Imaging findings and their implications in schizophrenia. Curr. Opin. Psychiatry 27, 179–184. https://doi.org/10.1097/YCO.0000000000000053

Lawrie, S.M., McIntosh, A.M., Hall, J., Owens, D.G.C., Johnstone, E.C., 2008. Brain structure and function changes during the development of schizophrenia: the evidence from studies of subjects at increased genetic risk. Schizophr. Bull. 34, 330–340. https://doi.org/10.1093/schbul/sbm158

Le Bihan, D., Breton, E., Lallemand, D., Grenier, P., Cabanis, E., Laval-Jeantet, M., 1986. MR imaging of intravoxel incoherent motions: application to diffusion and perfusion in neurologic disorders. Radiology 161, 401–407. https://doi.org/10.1148/radiology.161.2.3763909

Le Bihan, D., Poupon, C., Amadon, A., Lethimonnier, F., 2006. Artifacts and pitfalls in diffusion MRI. J. Magn. Reson. Imaging JMRI 24, 478–488. https://doi.org/10.1002/jmri.20683

Lebel, C., Gee, M., Camicioli, R., Wieler, M., Martin, W., Beaulieu, C., 2012. Diffusion tensor imaging of white matter tract evolution over the lifespan. NeuroImage 60, 340–352. https://doi.org/10.1016/j.neuroimage.2011.11.094

Lee, S.-H., Kubicki, M., Asami, T., Seidman, L.J., Goldstein, J.M., Mesholam-Gately, R.I., McCarley, R.W., Shenton, M.E., 2013. Extensive white matter abnormalities in patients with first-episode schizophrenia: A diffusion tensor imaging (DTI) study. Schizophr. Res. 143, 231–238. https://doi.org/10.1016/j.schres.2012.11.029

Lencz, T., Knowles, E., Davies, G., Guha, S., Liewald, D.C., Starr, J.M., Djurovic, S., Melle, I., Sundet, K., Christoforou, A., Reinvang, I., Mukherjee, S., DeRosse, P., Lundervold, A., Steen, V.M., John, M., Espeseth, T., Räikkönen, K., Widen, E., Palotie, A., Eriksson, J.G., Giegling, I., Konte, B., Ikeda, M., Roussos, P., Giakoumaki, S., Burdick, K.E., Payton, A., Ollier, W., Horan, M., Donohoe, G., Morris, D., Corvin, A., Gill, M., Pendleton, N., Iwata, N., Darvasi, A., Bitsios, P., Rujescu, D., Lahti, J., Hellard, S.L., Keller, M.C., Andreassen, O.A., Deary, I.J., Glahn, D.C., Malhotra, A.K., 2014. Molecular genetic evidence for overlap between general cognitive ability and risk for schizophrenia: a report from the Cognitive Genomics consorTium (COGENT). Mol. Psychiatry 19, 168–174. https://doi.org/10.1038/mp.2013.166

Li, L., Rilling, J.K., Preuss, T.M., Glasser, M.F., Hu, X., 2012. The effects of connection reconstruction method on the interregional connectivity of brain networks via

diffusion tractography. Hum. Brain Mapp. 33, 1894–1913. https://doi.org/10.1002/hbm.21332

Li, Y., Liu, Y., Li, J., Qin, W., Li, K., Yu, C., Jiang, T., 2009. Brain anatomical network and intelligence. PLoS Comput. Biol. 5, e1000395. https://doi.org/10.1371/journal.pcbi.1000395

Lieberman, J.A., Perkins, D., Belger, A., Chakos, M., Jarskog, F., Boteva, K., Gilmore, J., 2001. The early stages of schizophrenia: speculations on pathogenesis, pathophysiology, and therapeutic approaches. Biol. Psychiatry 50, 884–897.

Liebers, D.T., Pirooznia, M., Seiffudin, F., Musliner, K.L., Zandi, P.P., Goes, F.S., 2016. Polygenic Risk of Schizophrenia and Cognition in a Population-Based Survey of Older Adults. Schizophr. Bull. 42, 984–991. https://doi.org/10.1093/schbul/sbw001

Lindenberger, U., von Oertzen, T., Ghisletta, P., Hertzog, C., 2011. Cross-sectional age variance extraction: what's change got to do with it? Psychol. Aging 26, 34–47. https://doi.org/10.1037/a0020525

Lipkovich, I.A., Deberdt, W., Csernansky, J.G., Sabbe, B., Keefe, R.S., Kollack-Walker, S., 2009. Relationships among neurocognition, symptoms and functioning in patients with schizophrenia: a path-analytic approach for associations at baseline and following 24 weeks of antipsychotic drug therapy. BMC Psychiatry 9, 44. https://doi.org/10.1186/1471-244X-9-44

Liu, X., Lai, Y., Wang, X., Hao, C., Chen, L., Zhou, Z., Yu, X., Hong, N., 2013. Reduced white matter integrity and cognitive deficit in never-medicated chronic schizophrenia: a diffusion tensor study using TBSS. Behav. Brain Res. 252, 157–163. https://doi.org/10.1016/j.bbr.2013.05.061

Lopez, L.M., Hill, W.D., Harris, S.E., Valdes Hernandez, M., Munoz Maniega, S., Bastin, M.E., Bailey, E., Smith, C., McBride, M., McClure, J., Graham, D., Dominiczak, A., Yang, Q., Fornage, M., Ikram, M.A., Debette, S., Launer, L., Bis, J.C., Schmidt, R., Seshadri, S., Porteous, D.J., Starr, J., Deary, I.J., Wardlaw, J.M., 2015. Genes from a translational analysis support a multifactorial nature of white matter hyperintensities. Stroke 46, 341–347. https://doi.org/10.1161/STROKEAHA.114.007649

Lynall, M.-E., Bassett, D.S., Kerwin, R., McKenna, P.J., Kitzbichler, M., Muller, U., Bullmore, E., 2010. Functional connectivity and brain networks in schizophrenia. J. Neurosci. Off. J. Soc. Neurosci. 30, 9477–9487. https://doi.org/10.1523/JNEUROSCI.0333-10.2010

Madden, D.J., Bennett, I.J., Burzynska, A., Potter, G.G., Chen, N., Song, A.W., 2012. Diffusion Tensor Imaging of Cerebral White Matter Integrity in Cognitive Aging. Biochim. Biophys. Acta 1822, 386–400. https://doi.org/10.1016/j.bbadis.2011.08.003

Mamah, D., Conturo, T.E., Harms, M.P., Akbudak, E., Wang, L., McMichael, A.R., Gado, M.H., Barch, D.M., Csernansky, J.G., 2010. Anterior Thalamic Radiation Integrity in Schizophrenia: A Diffusion-Tensor Imaging Study. Psychiatry Res. 183. https://doi.org/10.1016/j.pscychresns.2010.04.013

Mandl, R.C.W., Rais, M., van Baal, G.C.M., van Haren, N.E.M., Cahn, W., Kahn, R.S., Pol, H.E.H., 2013. Altered white matter connectivity in never-medicated patients with schizophrenia. Hum. Brain Mapp. 34, 2353–2365. https://doi.org/10.1002/hbm.22075

Manoliu, A., Riedl, V., Zherdin, A., Mühlau, M., Schwerthöffer, D., Scherr, M., Peters, H., Zimmer, C., Förstl, H., Bäuml, J., Wohlschläger, A.M., Sorg, C., 2014. Aberrant dependence of default mode/central executive network interactions on anterior insular salience network activity in schizophrenia. Schizophr. Bull. 40, 428–437. https://doi.org/10.1093/schbul/sbt037

Markota, M., Coombes, B.J., Larrabee, B.R., McElroy, S.L., Bond, D.J., Veldic, M., Colby, C.L., Chauhan, M., Cuellar-Barboza, A.B., Fuentes, M., Kung, S., Prieto, M.L., Rummans, T.A., Bobo, W.V., Frye, M.A., Biernacka, J.M., 2018. Association of schizophrenia polygenic risk score with manic and depressive psychosis in bipolar disorder. Transl. Psychiatry 8, 188. https://doi.org/10.1038/s41398-018-0242-3

Marner, L., Nyengaard, J.R., Tang, Y., Pakkenberg, B., 2003. Marked loss of myelinated nerve fibers in the human brain with age. J. Comp. Neurol. 462, 144–152. https://doi.org/10.1002/cne.10714

McArdle, J.J., 2009. Latent variable modeling of differences and changes with longitudinal data. Annu. Rev. Psychol. 60, 577–605. https://doi.org/10.1146/annurev.psych.60.110707.163612

McCarthy-Jones, S., Oestreich, L.K.L., Australian Schizophrenia Research Bank, Whitford, T.J., 2015. Reduced integrity of the left arcuate fasciculus is specifically associated with auditory verbal hallucinations in schizophrenia. Schizophr. Res. 162, 1–6. https://doi.org/10.1016/j.schres.2014.12.041

McIntosh, A.M., Gow, A., Luciano, M., Davies, G., Liewald, D.C., Harris, S.E., Corley, J., Hall, J., Starr, J.M., Porteous, D.J., Tenesa, A., Visscher, P.M., Deary, I.J., 2013. Polygenic risk for schizophrenia is associated with cognitive change between childhood and old age. Biol. Psychiatry 73, 938–943. https://doi.org/10.1016/j.biopsych.2013.01.011

McIntosh, A.M., Job, D.E., Moorhead, T.W.J., Harrison, L.K., Lawrie, S.M., Johnstone, E.C., 2005. White matter density in patients with schizophrenia, bipolar disorder and their unaffected relatives. Biol. Psychiatry 58, 254–257. https://doi.org/10.1016/j.biopsych.2005.03.044

Meier-Ruge, W., Bruder, A., Theodore, D., 1992. Histochemical and morphometric investigation of the pathogenesis of acute brain infarction in primates. Acta Histochem. Suppl. 42, 59–70.

Menon, V., 2015. Salience Network, in: Brain Mapping. Elsevier, pp. 597–611. https://doi.org/10.1016/B978-0-12-397025-1.00052-X

Mesholam-Gately, R.I., Giuliano, A.J., Goff, K.P., Faraone, S.V., Seidman, L.J., 2009. Neurocognition in first-episode schizophrenia: a meta-analytic review. Neuropsychology 23, 315–336. https://doi.org/10.1037/a0014708

Mesulam, M.M., Mufson, E.J., 1982. Insula of the old world monkey. I. Architectonics in the insulo-orbito-temporal component of the paralimbic brain. J. Comp. Neurol. 212, 1–22. https://doi.org/10.1002/cne.902120102

Michael, A.M., Calhoun, V.D., Pearlson, G.D., Baum, S.A., Caprihan, A., 2008. Correlations of diffusion tensor imaging values and symptom scores in patients with schizophrenia. Conf. Proc. Annu. Int. Conf. IEEE Eng. Med. Biol. Soc. IEEE Eng. Med. Biol. Soc. Annu. Conf. 2008, 5494–5497. https://doi.org/10.1109/IEMBS.2008.4650458

Miller, K.L., Alfaro-Almagro, F., Bangerter, N.K., Thomas, D.L., Yacoub, E., Xu, J., Bartsch, A.J., Jbabdi, S., Sotiropoulos, S.N., Andersson, J.L.R., Griffanti, L., Douaud, G., Okell, T.W., Weale, P., Dragonu, I., Garratt, S., Hudson, S., Collins, R., Jenkinson, M., Matthews, P.M., Smith, S.M., 2016. Multimodal population brain imaging in the UK Biobank prospective epidemiological study. Nat. Neurosci. 19, 1523–1536. https://doi.org/10.1038/nn.4393

Minzenberg, M.J., Laird, A.R., Thelen, S., Carter, C.S., Glahn, D.C., 2009. Meta-analysis of 41 functional neuroimaging studies of executive function in schizophrenia. Arch. Gen. Psychiatry 66, 811–822. https://doi.org/10.1001/archgenpsychiatry.2009.91

Mišić, B., Betzel, R.F., de Reus, M.A., van den Heuvel, M.P., Berman, M.G., McIntosh, A.R., Sporns, O., 2016. Network-Level Structure-Function Relationships in Human Neocortex. Cereb. Cortex N. Y. NY 26, 3285–3296. https://doi.org/10.1093/cercor/bhw089

Mitelman, S.A., Torosjan, Y., Newmark, R.E., Schneiderman, J.S., Chu, K.-W., Brickman, A.M., Haznedar, M.M., Hazlett, E.A., Tang, C.Y., Shihabuddin, L., Buchsbaum, M.S., 2007. Internal capsule, corpus callosum and long associative fibers in good and

poor outcome schizophrenia: a diffusion tensor imaging survey. Schizophr. Res. 92, 211–224. https://doi.org/10.1016/j.schres.2006.12.029

Morell, P., Norton, W.T., 1980. Myelin. Sci. Am. 242, 88–90, 92, 96 passim.

Morgan, V.A., McGrath, J.J., Jablensky, A., Badcock, J.C., Waterreus, A., Bush, R., Carr, V., Castle, D., Cohen, M., Galletly, C., Harvey, C., Hocking, B., McGorry, P., Neil, A.L., Saw, S., Shah, S., Stain, H.J., Mackinnon, A., 2014. Psychosis prevalence and physical, metabolic and cognitive co-morbidity: data from the second Australian national survey of psychosis. Psychol. Med. 44, 2163–2176. https://doi.org/10.1017/S0033291713002973

Mori, T., Ohnishi, T., Hashimoto, R., Nemoto, K., Moriguchi, Y., Noguchi, H., Nakabayashi, T., Hori, H., Harada, S., Saitoh, O., Matsuda, H., Kunugi, H., 2007. Progressive changes of white matter integrity in schizophrenia revealed by diffusion tensor imaging. Psychiatry Res. 154, 133–145. https://doi.org/10.1016/j.pscychresns.2006.09.004

Mori, van Zijl, P.C.M., 2002. Fiber tracking: principles and strategies - a technical review. NMR Biomed. 15, 468–480. https://doi.org/10.1002/nbm.781

Morrison, J.H., Hof, P.R., 1997. Life and death of neurons in the aging brain. Science 278, 412–419.

Mukherjee, P., Chung, S.W., Berman, J.I., Hess, C.P., Henry, R.G., 2008. Diffusion Tensor MR Imaging and Fiber Tractography: Technical Considerations. Am. J. Neuroradiol. 29, 843–852. https://doi.org/10.3174/ajnr.A1052

Muñoz Maniega, S., Bastin, M.E., Deary, I.J., Wardlaw, J.M., Clayden, J.D., 2017. Improved Reference Tracts for Unsupervised Brain White Matter Tractography, in: Communications in Computer and Information Science. Presented at the Annual Conference on Medical Image Understanding and Analysis, Springer, Cham, pp. 425–435. https://doi.org/10.1007/978-3-319-60964-5_37

Muñoz Maniega, S., Lymer, G.K.S., Bastin, M.E., Marjoram, D., Job, D.E., Moorhead, T.W.J., Owens, D.G., Johnstone, E.C., McIntosh, A.M., Lawrie, S.M., 2008. A diffusion tensor MRI study of white matter integrity in subjects at high genetic risk of schizophrenia. Schizophr. Res. 106, 132–139. https://doi.org/10.1016/j.schres.2008.09.016

Nakamura, K., Kawasaki, Y., Takahashi, T., Furuichi, A., Noguchi, K., Seto, H., Suzuki, M., 2012. Reduced white matter fractional anisotropy and clinical symptoms in schizophrenia: A voxel-based diffusion tensor imaging study. Psychiatry Res. Neuroimaging 202, 233–238. https://doi.org/10.1016/j.pscychresns.2011.09.006

Nestor, P.G., Kubicki, M., Nakamura, M., Niznikiewicz, M., Levitt, J.J., Shenton, M.E., McCarley, R.W., 2013. Neuropsychological variability, symptoms, and brain imaging in chronic schizophrenia. Brain Imaging Behav. 7, 68–76. https://doi.org/10.1007/s11682-012-9193-0

Nestor, P.G., Kubicki, M., Nakamura, M., Niznikiewicz, M., McCarley, R.W., Shenton, M.E., 2010. Comparing prefrontal gray and white matter contributions to intelligence and decision making in schizophrenia and healthy controls. Neuropsychology 24, 121–129. https://doi.org/10.1037/a0016981

Nestor, P.G., Kubicki, M., Niznikiewicz, M., Gurrera, R.J., McCarley, R.W., Shenton, M.E., 2008. Neuropsychological disturbance in schizophrenia: a diffusion tensor imaging study. Neuropsychology 22, 246–254. https://doi.org/10.1037/0894-4105.22.2.246

Newman, M., 2010. Networks: An Introduction. Oxford University Press, Oxford, New York.

Nieuwenhuys, R., 2012. The insular cortex: a review. Prog. Brain Res. 195, 123–163. https://doi.org/10.1016/B978-0-444-53860-4.00007-6

Niida, A., Niida, R., Kuniyoshi, K., Motomura, M., Uechi, A., 2013. Usefulness of visual evaluation of the anterior thalamic radiation by diffusion tensor tractography for differentiating between Alzheimer's disease and elderly major depressive disorder patients. Int. J. Gen. Med. 6, 189–200. https://doi.org/10.2147/IJGM.S42953

O'Carroll, R., 2000. Cognitive impairment in schizophrenia. Adv. Psychiatr. Treat. 6, 161–168. https://doi.org/10.1192/apt.6.3.161

O'Donoghue, S., Cannon, D.M., Perlini, C., Brambilla, P., McDonald, C., 2015. Applying neuroimaging to detect neuroanatomical dysconnectivity in psychosis. Epidemiol. Psychiatr. Sci. 24, 298–302. https://doi.org/10.1017/S2045796015000074

Oertel-Knöchel, V., Lancaster, T.M., Knöchel, C., Stäblein, M., Storchak, H., Reinke, B., Jurcoane, A., Kniep, J., Prvulovic, D., Mantripragada, K., Tansey, K.E., O'Donovan, M.C., Owen, M.J., Linden, D.E.J., 2015. Schizophrenia risk variants modulate white matter volume across the psychosis spectrum: evidence from two independent cohorts. NeuroImage Clin. 7, 764–770. https://doi.org/10.1016/j.nicl.2015.03.005

Oestreich, L.K.L., Lyall, A.E., Pasternak, O., Kikinis, Z., Newell, D.T., Savadjiev, P., Bouix, S., Shenton, M.E., Kubicki, M., Australian Schizophrenia Research Bank, Whitford, T.J., McCarthy-Jones, S., 2017. Characterizing white matter changes in chronic schizophrenia: A free-water imaging multi-site study. Schizophr. Res. https://doi.org/10.1016/j.schres.2017.02.006

Ohtani, T., Bouix, S., Hosokawa, T., Saito, Y., Eckbo, R., Ballinger, T., Rausch, A., Melonakos, E., Kubicki, M., 2014a. Abnormalities in white matter connections

between orbitofrontal cortex and anterior cingulate cortex and their associations with negative symptoms in schizophrenia: a DTI study. Schizophr. Res. 157, 190–197. https://doi.org/10.1016/j.schres.2014.05.016

Ohtani, T., Bouix, S., Lyall, A.E., Hosokawa, T., Saito, Y., Melonakos, E., Westin, C.-F., Seidman, L.J., Goldstein, J., Mesholam-Gately, R., Petryshen, T., Wojcik, J., Kubicki, M., 2015. Abnormal white matter connections between medial frontal regions predict symptoms in patients with first episode schizophrenia. Cortex J. Devoted Study Nerv. Syst. Behav. 71, 264–276. https://doi.org/10.1016/j.cortex.2015.05.028

Ohtani, T., Nestor, P.G., Bouix, S., Saito, Y., Hosokawa, T., Kubicki, M., 2014b. Medial frontal white and gray matter contributions to general intelligence. PloS One 9, e112691. https://doi.org/10.1371/journal.pone.0112691

Olson, I.R., Heide, R.J.V.D., Alm, K.H., Vyas, G., 2015. Development of the uncinate fasciculus: Implications for theory and developmental disorders. Dev. Cogn. Neurosci. 14, 50–61. https://doi.org/10.1016/j.dcn.2015.06.003

Onnela, J.-P., Saramäki, J., Kertész, J., Kaski, K., 2005. Intensity and coherence of motifs in weighted complex networks. Phys. Rev. E 71. https://doi.org/10.1103/PhysRevE.71.065103

Orliac, F., Naveau, M., Joliot, M., Delcroix, N., Razafimandimby, A., Brazo, P., Dollfus, S., Delamillieure, P., 2013. Links among resting-state default-mode network, salience network, and symptomatology in schizophrenia. Schizophr. Res. 148, 74–80. https://doi.org/10.1016/j.schres.2013.05.007

Ottet, M.-C., Schaer, M., Debbané, M., Cammoun, L., Thiran, J.-P., Eliez, S., 2013. Graph theory reveals dysconnected hubs in 22q11DS and altered nodal efficiency in patients with hallucinations. Front. Hum. Neurosci. 7, 402. https://doi.org/10.3389/fnhum.2013.00402

Padula, M.C., Scariati, E., Schaer, M., Sandini, C., Ottet, M.C., Schneider, M., Van De Ville, D., Eliez, S., 2017. Altered structural network architecture is predictive of the presence of psychotic symptoms in patients with 22q11.2 deletion syndrome. NeuroImage Clin. 16, 142–150. https://doi.org/10.1016/j.nicl.2017.07.023

Palaniyappan, L., Mallikarjun, P., Joseph, V., White, T.P., Liddle, P.F., 2011. Reality distortion is related to the structure of the salience network in schizophrenia. Psychol. Med. 41, 1701–1708. https://doi.org/10.1017/S0033291710002205

Palaniyappan, L., White, T.P., Liddle, P.F., 2012. The concept of salience network dysfunction in schizophrenia: from neuroimaging observations to therapeutic opportunities. Curr. Top. Med. Chem. 12, 2324–2338.

Pardiñas, A.F., Holmans, P., Pocklington, A.J., Escott-Price, V., Ripke, S., Carrera, N., Legge, S.E., Bishop, S., Cameron, D., Hamshere, M.L., Han, J., Hubbard, L., Lynham, A., Mantripragada, K., Rees, E., MacCabe, J.H., McCarroll, S.A., Baune, B.T., Breen, G., Byrne, E.M., Dannlowski, U., Eley, T.C., Hayward, C., Martin, N.G., McIntosh, A.M., Plomin, R., Porteous, D.J., Wray, N.R., Caballero, A., Geschwind, D.H., Huckins, L.M., Ruderfer, D.M., Santiago, E., Sklar, P., Stahl, E.A., Won, H., Agerbo, E., Als, T.D., Andreassen, O.A., Bækvad-Hansen, M., Mortensen, P.B., Pedersen, C.B., Børglum, A.D., Bybjerg-Grauholm, J., Djurovic, S., Durmishi, N., Pedersen, M.G., Golimbet, V., Grove, J., Hougaard, D.M., Mattheisen, M., Molden, E., Mors, O., Nordentoft, M., Pejovic-Milovancevic, M., Sigurdsson, E., Silagadze, T., Hansen, C.S., Stefansson, K., Stefansson, H., Steinberg, S., Tosato, S., Werge, T., GERAD1 Consortium:, CRESTAR Consortium:, Collier, D.A., Rujescu, D., Kirov, G., Owen, M.J., O'Donovan, M.C., Walters, J.T.R., GERAD1 Consortium, CRESTAR Consortium, GERAD1 Consortium, CRESTAR Consortium, 2018. Common schizophrenia alleles are enriched in mutation-intolerant genes and in regions under strong background selection. Nat. Genet. 50, 381–389. https://doi.org/10.1038/s41588-018-0059-2

Park, H.-J., Friston, K., 2013. Structural and Functional Brain Networks: From Connections to Cognition. Science 342, 1238411. https://doi.org/10.1126/science.1238411

Parker, G.J.M., Alexander, D.C., 2005. Probabilistic anatomical connectivity derived from the microscopic persistent angular structure of cerebral tissue. Philos. Trans. R. Soc. Lond. B. Biol. Sci. 360, 893–902. https://doi.org/10.1098/rstb.2005.1639

Paus, T., 2010. Growth of white matter in the adolescent brain: myelin or axon? Brain Cogn. 72, 26–35. https://doi.org/10.1016/j.bandc.2009.06.002

Penke, L., Maniega, S.M., Bastin, M.E., Valdés Hernández, M.C., Murray, C., Royle, N.A., Starr, J.M., Wardlaw, J.M., Deary, I.J., 2012. Brain white matter tract integrity as a neural foundation for general intelligence. Mol. Psychiatry 17, 1026–1030. https://doi.org/10.1038/mp.2012.66

Penke, L., Maniega, S.M., Murray, C., Gow, A.J., Hernández, M.C.V., Clayden, J.D., Starr, J.M., Wardlaw, J.M., Bastin, M.E., Deary, I.J., 2010. A General Factor of Brain White Matter Integrity Predicts Information Processing Speed in Healthy Older People. J. Neurosci. 30, 7569–7574. https://doi.org/10.1523/JNEUROSCI.1553-10.2010

Pérez-Álvarez, M., 2012. [Schizophrenia and modern culture: reasons for insanity]. Psicothema 24, 1–9.

Pérez-Iglesias, R., Tordesillas-Gutiérrez, D., McGuire, P.K., Barker, G.J., Roiz-Santiañez, R., Mata, I., de Lucas, E.M., Rodríguez-Sánchez, J.M., Ayesa-Arriola, R., Vazquez-Barquero, J.L., Crespo-Facorro, B., 2010. White matter integrity and cognitive impairment in first-episode psychosis. Am. J. Psychiatry 167, 451–458. https://doi.org/10.1176/appi.ajp.2009.09050716

Persson, N., Ghisletta, P., Dahle, C.L., Bender, A.R., Yang, Y., Yuan, P., Daugherty, A.M., Raz, N., 2014. Regional brain shrinkage over two years: individual differences and effects of pro-inflammatory genetic polymorphisms. NeuroImage 103, 334–348. https://doi.org/10.1016/j.neuroimage.2014.09.042

Peters, A., 2002. Structural changes in the normally aging cerebral cortex of primates. Prog. Brain Res. 136, 455–465.

Peters, A., Rosene, D.L., 2003. In aging, is it gray or white? J. Comp. Neurol. 462, 139–143. https://doi.org/10.1002/cne.10715

Pettersson-Yeo, W., Allen, P., Benetti, S., McGuire, P., Mechelli, A., 2011. Dysconnectivity in schizophrenia: Where are we now? Neurosci. Biobehav. Rev. 35, 1110–1124. https://doi.org/10.1016/j.neubiorev.2010.11.004

Pfefferbaum, A., Sullivan, E.V., Carmelli, D., 2001. Genetic regulation of regional microstructure of the corpus callosum in late life. Neuroreport 12, 1677–1681.

Pfefferbaum, A., Sullivan, E.V., Hedehus, M., Lim, K.O., Adalsteinsson, E., Moseley, M., 2000. Age-related decline in brain white matter anisotropy measured with spatially corrected echo-planar diffusion tensor imaging. Magn. Reson. Med. 44, 259–268.

Phillips, K.A., Rogers, J., Barrett, E.A., Glahn, D.C., Kochunov, P., 2012. Genetic contributions to the midsagittal area of the corpus callosum. Twin Res. Hum. Genet. Off. J. Int. Soc. Twin Stud. 15, 315–323. https://doi.org/10.1017/thg.2012.10

Pierpaoli, C., Barnett, A., Pajevic, S., Chen, R., Penix, L.R., Virta, A., Basser, P., 2001. Water diffusion changes in Wallerian degeneration and their dependence on white matter architecture. NeuroImage 13, 1174–1185. https://doi.org/10.1006/nimg.2001.0765

Pierpaoli, C., Jezzard, P., Basser, P.J., Barnett, A., Di Chiro, G., 1996. Diffusion tensor MR imaging of the human brain. Radiology 201, 637–648. https://doi.org/10.1148/radiology.201.3.8939209

Pinheiro, J., Bates, D., DebRoy, S., Sarkar, D., R Core Team, 2018. nlme: Linear and Nonlinear Mixed Effects Models. R package version 3.1-137.

Power, R.A., Steinberg, S., Bjornsdottir, G., Rietveld, C.A., Abdellaoui, A., Nivard, M.M., Johannesson, M., Galesloot, T.E., Hottenga, J.J., Willemsen, G., Cesarini, D., Benjamin, D.J., Magnusson, P.K.E., Ullén, F., Tiemeier, H., Hofman, A., van Rooij,

F.J.A., Walters, G.B., Sigurdsson, E., Thorgeirsson, T.E., Ingason, A., Helgason, A., Kong, A., Kiemeney, L.A., Koellinger, P., Boomsma, D.I., Gudbjartsson, D., Stefansson, H., Stefansson, K., 2015. Polygenic risk scores for schizophrenia and bipolar disorder predict creativity. Nat. Neurosci. 18, 953–955. https://doi.org/10.1038/nn.4040

Preacher, K.J., Hayes, A.F., 2008. Asymptotic and resampling strategies for assessing and comparing indirect effects in multiple mediator models. Behav. Res. Methods 40, 879–891. https://doi.org/10.3758/BRM.40.3.879

Preacher, K.J., MacCallum, R.C., 2002. Exploratory factor analysis in behavior genetics research: factor recovery with small sample sizes. Behav. Genet. 32, 153–161.

Qiu, A., Mori, S., Miller, M.I., 2015. Diffusion Tensor Imaging for Understanding Brain Development in Early Life. Annu. Rev. Psychol. 66, 853–876. https://doi.org/10.1146/annurev-psych-010814-015340

Rapoport, J.L., Addington, A.M., Frangou, S., Psych, M.R.C., 2005. The neurodevelopmental model of schizophrenia: update 2005. Mol. Psychiatry 10, 434–449. https://doi.org/10.1038/sj.mp.4001642

Reichenberg, A., Harvey, P.D., Bowie, C.R., Mojtabai, R., Rabinowitz, J., Heaton, R.K., Bromet, E., 2009. Neuropsychological function and dysfunction in schizophrenia and psychotic affective disorders. Schizophr. Bull. 35, 1022–1029. https://doi.org/10.1093/schbul/sbn044

Reijmer, Y.D., Fotiadis, P., Piantoni, G., Boulouis, G., Kelly, K.E., Gurol, M.E., Leemans, A., O'Sullivan, M.J., Greenberg, S.M., Viswanathan, A., 2016. Small vessel disease and cognitive impairment: The relevance of central network connections. Hum. Brain Mapp. 37, 2446–2454. https://doi.org/10.1002/hbm.23186

Reus, L.M., Shen, X., Gibson, J., Wigmore, E., Ligthart, L., Adams, M.J., Davies, G., Cox, S.R., Hagenaars, S.P., Bastin, M.E., Deary, I.J., Whalley, H.C., McIntosh, A.M., 2017. Association of polygenic risk for major psychiatric illness with subcortical volumes and white matter integrity in UK Biobank. Sci. Rep. 7. https://doi.org/10.1038/srep42140

Ribolsi, M., Daskalakis, Z.J., Siracusano, A., Koch, G., 2014. Abnormal Asymmetry of Brain Connectivity in Schizophrenia. Front. Hum. Neurosci. 8. https://doi.org/10.3389/fnhum.2014.01010

Ritchie, S.J., Bastin, M.E., Tucker-Drob, E.M., Maniega, S.M., Engelhardt, L.E., Cox, S.R., Royle, N.A., Gow, A.J., Corley, J., Pattie, A., Taylor, A.M., Valdés Hernández, M.D.C., Starr, J.M., Wardlaw, J.M., Deary, I.J., 2015. Coupled changes in brain white

matter microstructure and fluid intelligence in later life. J. Neurosci. Off. J. Soc. Neurosci. 35, 8672–8682. https://doi.org/10.1523/JNEUROSCI.0862-15.2015

Ritchie, S.J., Tucker-Drob, E.M., Cox, S.R., Dickie, D.A., Hernández, M. del C.V., Corley, J., Royle, N.A., Redmond, P., Maniega, S.M., Pattie, A., Aribisala, B.S., Taylor, A.M., Clarke, T.-K., Gow, A.J., Starr, J.M., Bastin, M.E., Wardlaw, J.M., Deary, I.J., 2017. Risk and protective factors for structural brain ageing in the eighth decade of life. Brain Struct. Funct. 1–14. https://doi.org/10.1007/s00429-017-1414-2

Roalf, D.R., Gur, R.E., Verma, R., Parker, W.A., Quarmley, M., Ruparel, K., Gur, R.C., 2015. White matter microstructure in schizophrenia: associations to neurocognition and clinical symptomatology. Schizophr. Res. 161, 42–49. https://doi.org/10.1016/j.schres.2014.09.026

Roberts, J.A., Perry, A., Roberts, G., Mitchell, P.B., Breakspear, M., 2017. Consistency-based thresholding of the human connectome. NeuroImage 145, 118–129. https://doi.org/10.1016/j.neuroimage.2016.09.053

Rodríguez-Sánchez, J.M., Crespo-Facorro, B., González-Blanch, C., Perez-Iglesias, R., Vázquez-Barquero, J.L., PAFIP Group Study, 2007. Cognitive dysfunction in first-episode psychosis: the processing speed hypothesis. Br. J. Psychiatry. Suppl. 51, s107-110. https://doi.org/10.1192/bjp.191.51.s107

Rosseel, Y., 2012. lavaan: An R Package for Structural Equation Modeling. J. Stat. Softw. 48, 36.

Rotarska-Jagiela, A., Schönmeyer, R., Oertel, V., Haenschel, C., Vogeley, K., Linden, D.E.J., 2008. The corpus callosum in schizophrenia-volume and connectivity changes affect specific regions. NeuroImage 39, 1522–1532. https://doi.org/10.1016/j.neuroimage.2007.10.063

Royle, N.A., Booth, T., Valdés Hernández, M.C., Penke, L., Murray, C., Gow, A.J., Maniega, S.M., Starr, J., Bastin, M.E., Deary, I.J., Wardlaw, J.M., 2013. Estimated maximal and current brain volume predict cognitive ability in old age. Neurobiol. Aging 34, 2726–2733. https://doi.org/10.1016/j.neurobiolaging.2013.05.015

Rubinov, M., Knock, S.A., Stam, C.J., Micheloyannis, S., Harris, A.W.F., Williams, L.M., Breakspear, M., 2009a. Small-world properties of nonlinear brain activity in schizophrenia. Hum. Brain Mapp. 30, 403–416. https://doi.org/10.1002/hbm.20517

Rubinov, M., Sporns, O., 2010. Complex network measures of brain connectivity: uses and interpretations. NeuroImage 52, 1059–1069. https://doi.org/10.1016/j.neuroimage.2009.10.003

Rubinov, M., Sporns, O., van Leeuwen, C., Breakspear, M., 2009b. Symbiotic relationship between brain structure and dynamics. BMC Neurosci. 10, 55. https://doi.org/10.1186/1471-2202-10-55

Saito, J., Hori, M., Nemoto, T., Katagiri, N., Shimoji, K., Ito, S., Tsujino, N., Yamaguchi, T., Shiraga, N., Aoki, S., Mizuno, M., 2017. Longitudinal study examining abnormal white matter integrity using a tract-specific analysis in individuals with a high risk for psychosis. Psychiatry Clin. Neurosci. https://doi.org/10.1111/pcn.12515

Salat, D.H., 2011. The declining infrastructure of the aging brain. Brain Connect. 1, 279–293. https://doi.org/10.1089/brain.2011.0056

Salvador, R., Sarró, S., Gomar, J.J., Ortiz-Gil, J., Vila, F., Capdevila, A., Bullmore, E., McKenna, P.J., Pomarol-Clotet, E., 2010. Overall brain connectivity maps show cortico-subcortical abnormalities in schizophrenia. Hum. Brain Mapp. 31, 2003–2014. https://doi.org/10.1002/hbm.20993

Samartzis, L., Dima, D., Fusar-Poli, P., Kyriakopoulos, M., 2014. White matter alterations in early stages of schizophrenia: a systematic review of diffusion tensor imaging studies. J. Neuroimaging Off. J. Am. Soc. Neuroimaging 24, 101–110. https://doi.org/10.1111/j.1552-6569.2012.00779.x

Schizophrenia Working Group of the Psychiatric Genomics Consortium, 2014. Biological insights from 108 schizophrenia-associated genetic loci. Nature 511, 421–427. https://doi.org/10.1038/nature13595

Schmahmann, J.D.M.D., Pandya, D.N., 2009. Fiber Pathways of the Brain, 1 edition. ed. Oxford University Press, Oxford.

Schmidt, A., Crossley, N.A., Harrisberger, F., Smieskova, R., Lenz, C., Riecher-Rössler, A., Lang, U.E., McGuire, P., Fusar-Poli, P., Borgwardt, S., 2016. Structural Network Disorganization in Subjects at Clinical High Risk for Psychosis. Schizophr. Bull. https://doi.org/10.1093/schbul/sbw110

Schmidt, A., Diwadkar, V.A., Smieskova, R., Harrisberger, F., Lang, U.E., McGuire, P., Fusar-Poli, P., Borgwardt, S., 2015. Approaching a network connectivity-driven classification of the psychosis continuum: a selective review and suggestions for future research. Front. Hum. Neurosci. 8. https://doi.org/10.3389/fnhum.2014.01047

Schmierer, K., Wheeler-Kingshott, C.A.M., Boulby, P.A., Scaravilli, F., Altmann, D.R., Barker, G.J., Tofts, P.S., Miller, D.H., 2007. Diffusion tensor imaging of post mortem multiple sclerosis brain. NeuroImage 35, 467–477. https://doi.org/10.1016/j.neuroimage.2006.12.010

Schmierer, K., Wheeler-Kingshott, C.A.M., Tozer, D.J., Boulby, P.A., Parkes, H.G., Yousry, T.A., Scaravilli, F., Barker, G.J., Tofts, P.S., Miller, D.H., 2008. Quantitative magnetic resonance of postmortem multiple sclerosis brain before and after fixation. Magn. Reson. Med. 59, 268–277. https://doi.org/10.1002/mrm.21487

Schnack, H.G., van Haren, N.E.M., Nieuwenhuis, M., Hulshoff Pol, H.E., Cahn, W., Kahn, R.S., 2016. Accelerated Brain Aging in Schizophrenia: A Longitudinal Pattern Recognition Study. Am. J. Psychiatry 173, 607–616. https://doi.org/10.1176/appi.ajp.2015.15070922

Schneider, K., 1959. Clinical Psychopathology. Grune and Stratton, New York.

Schwartz, J.H., Siegelbaum, S.A., Hudspeth, A.J., 2013. Principles of Neural Science, Fifth Edition. McGraw Hill Professional.

Seeley, W.W., Menon, V., Schatzberg, A.F., Keller, J., Glover, G.H., Kenna, H., Reiss, A.L., Greicius, M.D., 2007. Dissociable intrinsic connectivity networks for salience processing and executive control. J. Neurosci. Off. J. Soc. Neurosci. 27, 2349–2356. https://doi.org/10.1523/JNEUROSCI.5587-06.2007

Seidman, L.J., Giuliano, A.J., Meyer, E.C., Addington, J., Cadenhead, K.S., Cannon, T.D., McGlashan, T.H., Perkins, D.O., Tsuang, M.T., Walker, E.F., Woods, S.W., Bearden, C.E., Christensen, B.K., Hawkins, K., Heaton, R., Keefe, R.S.E., Heinssen, R., Cornblatt, B.A., North American Prodrome Longitudinal Study (NAPLS) Group, 2010. Neuropsychology of the prodrome to psychosis in the NAPLS consortium: relationship to family history and conversion to psychosis. Arch. Gen. Psychiatry 67, 578–588. https://doi.org/10.1001/archgenpsychiatry.2010.66

Seitz, J., Zuo, J.X., Lyall, A.E., Makris, N., Kikinis, Z., Bouix, S., Pasternak, O., Fredman, E., Duskin, J., Goldstein, J.M., Petryshen, T.L., Mesholam-Gately, R.I., Wojcik, J., McCarley, R.W., Seidman, L.J., Shenton, M.E., Koerte, I.K., Kubicki, M., 2016. Tractography Analysis of 5 White Matter Bundles and Their Clinical and Cognitive Correlates in Early-Course Schizophrenia. Schizophr. Bull. 42, 762–771. https://doi.org/10.1093/schbul/sbv171

Selemon, L.D., Goldman-Rakic, P.S., 1999. The reduced neuropil hypothesis: a circuit based model of schizophrenia. Biol. Psychiatry 45, 17–25.

Seok, J.-H., Park, H.-J., Chun, J.-W., Lee, S.-K., Cho, H.S., Kwon, J.S., Kim, J.-J., 2007. White matter abnormalities associated with auditory hallucinations in schizophrenia: a combined study of voxel-based analyses of diffusion tensor imaging and structural magnetic resonance imaging. Psychiatry Res. 156, 93–104. https://doi.org/10.1016/j.pscychresns.2007.02.002

Shafee, R., Nanda, P., Padmanabhan, J.L., Tandon, N., Alliey-Rodriguez, N., Kalapurakkel, S., Weiner, D.J., Gur, R.E., Keefe, R.S.E., Hill, S.K., Bishop, J.R., Clementz, B.A., Tamminga, C.A., Gershon, E.S., Pearlson, G.D., Keshavan, M.S., Sweeney, J.A., McCarroll, S.A., Robinson, E.B., 2018. Polygenic risk for schizophrenia and measured domains of cognition in individuals with psychosis and controls. Transl. Psychiatry 8. https://doi.org/10.1038/s41398-018-0124-8

Shim, M., Kim, D.-W., Lee, S.-H., Im, C.-H., 2014. Disruptions in small-world cortical functional connectivity network during an auditory oddball paradigm task in patients with schizophrenia. Schizophr. Res. 156, 197–203. https://doi.org/10.1016/j.schres.2014.04.012

Skelly, L.R., Calhoun, V., Meda, S.A., Kim, J., Mathalon, D.H., Pearlson, G.D., 2008. Diffusion tensor imaging in schizophrenia: relationship to symptoms. Schizophr. Res. 98, 157–162. https://doi.org/10.1016/j.schres.2007.10.009

Skudlarski, P., Jagannathan, K., Anderson, K., Stevens, M.C., Calhoun, V.D., Skudlarska, B.A., Pearlson, G., 2010. Brain connectivity is not only lower but different in schizophrenia: A combined anatomical and functional approach. Biol. Psychiatry 68, 61–69. https://doi.org/10.1016/j.biopsych.2010.03.035

Skudlarski, P., Schretlen, D.J., Thaker, G.K., Stevens, M.C., Keshavan, M.S., Sweeney, J.A., Tamminga, C.A., Clementz, B.A., O'Neil, K., Pearlson, G.D., 2013. Diffusion tensor imaging white matter endophenotypes in patients with schizophrenia or psychotic bipolar disorder and their relatives. Am. J. Psychiatry 170, 886–898. https://doi.org/10.1176/appi.ajp.2013.12111448

Smith, S.M., 2002. Fast robust automated brain extraction. Hum. Brain Mapp. 17, 143–155. https://doi.org/10.1002/hbm.10062

Smith, S.M., Jenkinson, M., Johansen-Berg, H., Rueckert, D., Nichols, T.E., Mackay, C.E., Watkins, K.E., Ciccarelli, O., Cader, M.Z., Matthews, P.M., Behrens, T.E.J., 2006. Tract-based spatial statistics: voxelwise analysis of multi-subject diffusion data. NeuroImage 31, 1487–1505. https://doi.org/10.1016/j.neuroimage.2006.02.024

Smith, S.M., Johansen-Berg, H., Jenkinson, M., Rueckert, D., Nichols, T.E., Miller, K.L., Robson, M.D., Jones, D.K., Klein, J.C., Bartsch, A.J., Behrens, T.E.J., 2007. Acquisition and voxelwise analysis of multi-subject diffusion data with tract-based spatial statistics. Nat. Protoc. 2, 499–503. https://doi.org/10.1038/nprot.2007.45

Soares, J.M., Marques, P., Alves, V., Sousa, N., 2013. A hitchhiker's guide to diffusion tensor imaging. Front. Neurosci. 7. https://doi.org/10.3389/fnins.2013.00031

Song, S.-K., Sun, S.-W., Ramsbottom, M.J., Chang, C., Russell, J., Cross, A.H., 2002. Dysmyelination revealed through MRI as increased radial (but unchanged axial) diffusion of water. NeuroImage 17, 1429–1436.

Sotiropoulos, S.N., Zalesky, A., 2017. Building connectomes using diffusion MRI: why, how and but. NMR Biomed. https://doi.org/10.1002/nbm.3752

Sporns, O., 2011. The non-random brain: efficiency, economy, and complex dynamics. Front. Comput. Neurosci. 5, 5. https://doi.org/10.3389/fncom.2011.00005

Sporns, O., Tononi, G., Kötter, R., 2005. The human connectome: A structural description of the human brain. PLoS Comput. Biol. 1, e42. https://doi.org/10.1371/journal.pcbi.0010042

Sprooten, E., Sussmann, J.E., Clugston, A., Peel, A., McKirdy, J., Moorhead, T.W.J., Anderson, S., Shand, A.J., Giles, S., Bastin, M.E., Hall, J., Johnstone, E.C., Lawrie, S.M., McIntosh, A.M., 2011. White matter integrity in individuals at high genetic risk of bipolar disorder. Biol. Psychiatry 70, 350–356. https://doi.org/10.1016/j.biopsych.2011.01.021

Sridharan, D., Levitin, D.J., Menon, V., 2008. A critical role for the right fronto-insular cortex in switching between central-executive and default-mode networks. Proc. Natl. Acad. Sci. U. S. A. 105, 12569–12574. https://doi.org/10.1073/pnas.0800005105

Stephan, K.E., Baldeweg, T., Friston, K.J., 2006. Synaptic plasticity and dysconnection in schizophrenia. Biol. Psychiatry 59, 929–939. https://doi.org/10.1016/j.biopsych.2005.10.005

Stephan, K.E., Friston, K.J., Frith, C.D., 2009. Dysconnection in schizophrenia: from abnormal synaptic plasticity to failures of self-monitoring. Schizophr. Bull. 35, 509–527. https://doi.org/10.1093/schbul/sbn176

Sullivan, P.F., 2012. Schizophrenia as a Pathway Disease. Nat. Med. 18, 210–211. https://doi.org/10.1038/nm.2670

Sullivan, P.F., Kendler, K.S., Neale, M.C., 2003. Schizophrenia as a complex trait: evidence from a meta-analysis of twin studies. Arch. Gen. Psychiatry 60, 1187–1192. https://doi.org/10.1001/archpsyc.60.12.1187

Szeszko, P.R., Robinson, D.G., Ashtari, M., Vogel, J., Betensky, J., Sevy, S., Ardekani, B.A., Lencz, T., Malhotra, A.K., McCormack, J., Miller, R., Lim, K.O., Gunduz-Bruce, H., Kane, J.M., Bilder, R.M., 2008. Clinical and neuropsychological correlates of white matter abnormalities in recent onset schizophrenia. Neuropsychopharmacol. Off. Publ. Am. Coll. Neuropsychopharmacol. 33, 976–984. https://doi.org/10.1038/sj.npp.1301480

Szeszko, P.R., Robinson, D.G., Ikuta, T., Peters, B.D., Gallego, J.A., Kane, J., Malhotra, A.K., 2014. White Matter Changes Associated with Antipsychotic Treatment in First-Episode Psychosis. Neuropsychopharmacology 39, 1324–1331. https://doi.org/10.1038/npp.2013.288

Tan, H.-Y., Sust, S., Buckholtz, J.W., Mattay, V.S., Meyer-Lindenberg, A., Egan, M.F., Weinberger, D.R., Callicott, J.H., 2006. Dysfunctional prefrontal regional specialization and compensation in schizophrenia. Am. J. Psychiatry 163, 1969–1977. https://doi.org/10.1176/ajp.2006.163.11.1969

Tandon, R., Keshavan, M.S., Nasrallah, H.A., 2008. Schizophrenia, "Just the Facts" What we know in 2008. 2. Epidemiology and etiology. Schizophr. Res. 102, 1–18. https://doi.org/10.1016/j.schres.2008.04.011

Taylor, A.M., Pattie, A., Deary, I.J., 2018. Cohort Profile Update: The Lothian Birth Cohorts of 1921 and 1936. Int. J. Epidemiol. https://doi.org/10.1093/ije/dyy022

Terwisscha van Scheltinga, A., Bakker, S.C., van Haren, N.E.M., Derks, E.M., Buizer-Voskamp, J.E., Boos, H.B.M., Cahn, W., Hulshoff Pol, H., Ripke, S., Ophoff, R.A., Kahn, R., 2013. Genetic schizophrenia risk variants jointly modulate total brain and white matter volume. Biol. Psychiatry 73, 525–531. https://doi.org/10.1016/j.biopsych.2012.08.017

Thompson, P.M., Ge, T., Glahn, D.C., Jahanshad, N., Nichols, T.E., 2013. Genetics of the Connectome. NeuroImage 80, 475–488. https://doi.org/10.1016/j.neuroimage.2013.05.013

Toulopoulou, T., Picchioni, M., Rijsdijk, F., Hua-Hall, M., Ettinger, U., Sham, P., Murray, R., 2007. Substantial genetic overlap between neurocognition and schizophrenia: genetic modeling in twin samples. Arch. Gen. Psychiatry 64, 1348–1355. https://doi.org/10.1001/archpsyc.64.12.1348

Tournier, J.-D., Calamante, F., Connelly, A., 2007. Robust determination of the fibre orientation distribution in diffusion MRI: Non-negativity constrained super-resolved spherical deconvolution. NeuroImage 35, 1459–1472. https://doi.org/10.1016/j.neuroimage.2007.02.016

Tournier, J.-D., Mori, S., Leemans, A., 2011. Diffusion Tensor Imaging and Beyond. Magn. Reson. Med. 65, 1532–1556. https://doi.org/10.1002/mrm.22924

Tucker-Drob, E.M., 2009. Differentiation of Cognitive Abilities across the Lifespan. Dev. Psychol. 45, 1097–1118. https://doi.org/10.1037/a0015864

Turken, A.U., Whitfield-Gabrieli, S., Bammer, R., Baldo, J., Dronkers, N.F., Gabrieli, J.D.E., 2008. Cognitive processing speed and the structure of white matter pathways:

convergent evidence from normal variation and lesion studies. NeuroImage 42, 1032–1044. https://doi.org/10.1016/j.neuroimage.2008.03.057

Uddin, L.Q., 2015. Salience processing and insular cortical function and dysfunction. Nat. Rev. Neurosci. 16, 55–61. https://doi.org/10.1038/nrn3857

Uddin, L.Q., 2013. Complex relationships between structural and functional brain connectivity. Trends Cogn. Sci. 17, 600–602. https://doi.org/10.1016/j.tics.2013.09.011

Uddin, L.Q., Nomi, J.S., Hebert-Seropian, B., Ghaziri, J., Boucher, O., 2017. Structure and function of the human insula. J. Clin. Neurophysiol. Off. Publ. Am. Electroencephalogr. Soc. 34, 300–306. https://doi.org/10.1097/WNP.0000000000000377

Uddin, L.Q., Supekar, K.S., Ryali, S., Menon, V., 2011. Dynamic reconfiguration of structural and functional connectivity across core neurocognitive brain networks with development. J. Neurosci. Off. J. Soc. Neurosci. 31, 18578–18589. https://doi.org/10.1523/JNEUROSCI.4465-11.2011

Uranova, N.A., Vostrikov, V.M., Orlovskaya, D.D., Rachmanova, V.I., 2004. Oligodendroglial density in the prefrontal cortex in schizophrenia and mood disorders: a study from the Stanley Neuropathology Consortium. Schizophr. Res. 67, 269–275. https://doi.org/10.1016/S0920-9964(03)00181-6

van den Heuvel, M.P., Fornito, A., 2014. Brain networks in schizophrenia. Neuropsychol. Rev. 24, 32–48. https://doi.org/10.1007/s11065-014-9248-7

van den Heuvel, M.P., Mandl, R.C.W., Kahn, R.S., Hulshoff Pol, H.E., 2009a. Functionally linked resting-state networks reflect the underlying structural connectivity architecture of the human brain. Hum. Brain Mapp. 30, 3127–3141. https://doi.org/10.1002/hbm.20737

van den Heuvel, M.P., Mandl, R.C.W., Stam, C.J., Kahn, R.S., Pol, H.E.H., 2010. Aberrant Frontal and Temporal Complex Network Structure in Schizophrenia: A Graph Theoretical Analysis. J. Neurosci. 30, 15915–15926. https://doi.org/10.1523/JNEUROSCI.2874-10.2010

van den Heuvel, M.P., Sporns, O., Scheewe, T., Mandl, R.C.W., Cahn, W., Goñi, J., Hulshoff Pol, H.E., Kahn, R.S., 2013. Abnormal rich club organization and functional brain dynamics in schizophrenia. JAMA Psychiatry 70, 783–792. https://doi.org/10.1001/jamapsychiatry.2013.1328

van den Heuvel, M.P., Stam, C.J., Kahn, R.S., Hulshoff Pol, H.E., 2009b. Efficiency of functional brain networks and intellectual performance. J. Neurosci. Off. J. Soc. Neurosci. 29, 7619–7624. https://doi.org/10.1523/JNEUROSCI.1443-09.2009

Van der Auwera, S., Wittfeld, K., Homuth, G., Teumer, A., Hegenscheid, K., Grabe, H.J., 2015. No association between polygenic risk for schizophrenia and brain volume in the general population. Biol. Psychiatry 78, e41-42. https://doi.org/10.1016/j.biopsych.2015.02.038

Van der Auwera, S., Wittfeld, K., Shumskaya, E., Bralten, J., Zwiers, M.P., Onnink, A.M.H., Usberti, N., Hertel, J., Völzke, H., Völker, U., Hosten, N., Franke, B., Grabe, H.J., 2017. Predicting brain structure in population-based samples with biologically informed genetic scores for schizophrenia. Am. J. Med. Genet. Part B Neuropsychiatr. Genet. Off. Publ. Int. Soc. Psychiatr. Genet. 174, 324–332. https://doi.org/10.1002/ajmg.b.32519

van Erp, T.G.M., Walton, E., Hibar, D.P., Schmaal, L., Jiang, W., Glahn, D.C., Pearlson, G.D., Yao, N., Fukunaga, M., Hashimoto, R., Okada, N., Yamamori, H., Bustillo, J.R., Clark, V.P., Agartz, I., Mueller, B.A., Cahn, W., de Zwarte, S.M.C., Hulshoff Pol, H.E., Kahn, R.S., Ophoff, R.A., van Haren, N.E.M., Andreassen, O.A., Dale, A.M., Doan, N.T., Gurholt, T.P., Hartberg, C.B., Haukvik, U.K., Jørgensen, K.N., Lagerberg, T.V., Melle, I., Westlye, L.T., Gruber, O., Kraemer, B., Richter, A., Zilles, D., Calhoun, V.D., Crespo-Facorro, B., Roiz-Santiañez, R., Tordesillas-Gutiérrez, D., Loughland, C., Carr, V.J., Catts, S., Cropley, V.L., Fullerton, J.M., Green, M.J., Henskens, F.A., Jablensky, A., Lenroot, R.K., Mowry, B.J., Michie, P.T., Pantelis, C., Quidé, Y., Schall, U., Scott, R.J., Cairns, M.J., Seal, M., Tooney, P.A., Rasser, P.E., Cooper, G., Shannon Weickert, C., Weickert, T.W., Morris, D.W., Hong, E., Kochunov, P., Beard, L.M., Gur, R.E., Gur, R.C., Satterthwaite, T.D., Wolf, D.H., Belger, A., Brown, G.G., Ford, J.M., Macciardi, F., Mathalon, D.H., O'Leary, D.S., Potkin, S.G., Preda, A., Voyvodic, J., Lim, K.O., McEwen, S., Yang, F., Tan, Y., Tan, S., Wang, Z., Fan, F., Chen, J., Xiang, H., Tang, S., Guo, H., Wan, P., Wei, D., Bockholt, H.J., Ehrlich, S., Wolthusen, R.P.F., King, M.D., Shoemaker, J.M., Sponheim, S.R., De Haan, L., Koenders, L., Machielsen, M.W., van Amelsvoort, T., Veltman, D.J., Assogna, F., Banaj, N., de Rossi, P., Iorio, M., Piras, F., Spalletta, G., McKenna, P.J., Pomarol-Clotet, E., Salvador, R., Corvin, A., Donohoe, G., Kelly, S., Whelan, C.D., Dickie, E.W., Rotenberg, D., Voineskos, A.N., Ciufolini, S., Radua, J., Dazzan, P., Murray, R., Reis Marques, T., Simmons, A., Borgwardt, S., Egloff, L., Harrisberger, F., Riecher-Rössler, A., Smieskova, R., Alpert, K.I., Wang, L., Jönsson,

E.G., Koops, S., Sommer, I.E.C., Bertolino, A., Bonvino, A., Di Giorgio, A., Neilson, E., Mayer, A.R., Stephen, J.M., Kwon, J.S., Yun, J.-Y., Cannon, D.M., McDonald, C., Lebedeva, I., Tomyshev, A.S., Akhadov, T., Kaleda, V., Fatouros-Bergman, H., Flyckt, L., Farde, L., Flyckt, L., Engberg, G., Erhardt, S., Fatouros-Bergman, H., Cervenka, S., Schwieler, L., Piehl, F., Agartz, I., Collste, K., Victorsson, P., Malmqvist, A., Hedberg, M., Orhan, F., Busatto, G.F., Rosa, P.G.P., Serpa, M.H., Zanetti, M.V., Hoschl, C., Skoch, A., Spaniel, F., Tomecek, D., Hagenaars, S.P., McIntosh, A.M., Whalley, H.C., Lawrie, S.M., Knöchel, C., Oertel-Knöchel, V., Stäblein, M., Howells, F.M., Stein, D.J., Temmingh, H.S., Uhlmann, A., Lopez-Jaramillo, C., Dima, D., McMahon, A., Faskowitz, J.I., Gutman, B.A., Jahanshad, N., Thompson, P.M., Turner, J.A., 2018. Cortical Brain Abnormalities in 4474 Individuals With Schizophrenia and 5098 Control Subjects via the Enhancing Neuro Imaging Genetics Through Meta Analysis (ENIGMA) Consortium. Biol. Psychiatry. https://doi.org/10.1016/j.biopsych.2018.04.023

van Haren, N.E.M., Rijsdijk, F., Schnack, H.G., Picchioni, M.M., Toulopoulou, T., Weisbrod, M., Sauer, H., van Erp, T.G., Cannon, T.D., Huttunen, M.O., Boomsma, D.I., Hulshoff Pol, H.E., Murray, R.M., Kahn, R.S., 2012. The Genetic and Environmental Determinants of the Association Between Brain Abnormalities and Schizophrenia: The Schizophrenia Twins and Relatives Consortium. Biol. Psychiatry 71, 915–921. https://doi.org/10.1016/j.biopsych.2012.01.010

van Os, J., Kenis, G., Rutten, B.P.F., 2010. The environment and schizophrenia. Nature 468, 203–212. https://doi.org/10.1038/nature09563

van Os, J., Rutten, B.P., Poulton, R., 2008. Gene-Environment Interactions in Schizophrenia: Review of Epidemiological Findings and Future Directions. Schizophr. Bull. 34, 1066–1082. https://doi.org/10.1093/schbul/sbn117

Verhaeghen, P., Salthouse, T.A., 1997. Meta-analyses of age-cognition relations in adulthood: estimates of linear and nonlinear age effects and structural models. Psychol. Bull. 122, 231–249.

Verstraete, E., Veldink, J.H., Mandl, R.C.W., van den Berg, L.H., van den Heuvel, M.P., 2011. Impaired structural motor connectome in amyotrophic lateral sclerosis. PloS One 6, e24239. https://doi.org/10.1371/journal.pone.0024239

Viher, P.V., Stegmayer, K., Giezendanner, S., Federspiel, A., Bohlhalter, S., Vanbellingen, T., Wiest, R., Strik, W., Walther, S., 2016. Cerebral white matter structure is associated with DSM-5 schizophrenia symptom dimensions. NeuroImage Clin. 12, 93–99. https://doi.org/10.1016/j.nicl.2016.06.013

Visscher, P.M., Wray, N.R., Zhang, Q., Sklar, P., McCarthy, M.I., Brown, M.A., Yang, J., 2017. 10 Years of GWAS Discovery: Biology, Function, and Translation. Am. J. Hum. Genet. 101, 5–22. https://doi.org/10.1016/j.ajhg.2017.06.005

Voineskos, A.N., 2015. Genetic underpinnings of white matter "connectivity": heritability, risk, and heterogeneity in schizophrenia. Schizophr. Res. 161, 50–60. https://doi.org/10.1016/j.schres.2014.03.034

Voineskos, A.N., Felsky, D., Kovacevic, N., Tiwari, A.K., Zai, C., Chakravarty, M.M., Lobaugh, N.J., Shenton, M.E., Rajji, T.K., Miranda, D., Pollock, B.G., Mulsant, B.H., McIntosh, A.R., Kennedy, J.L., 2013. Oligodendrocyte genes, white matter tract integrity, and cognition in schizophrenia. Cereb. Cortex N. Y. N 1991 23, 2044–2057. https://doi.org/10.1093/cercor/bhs188

Voineskos, A.N., Felsky, D., Wheeler, A.L., Rotenberg, D.J., Levesque, M., Patel, S., Szeszko, P.R., Kennedy, J.L., Lencz, T., Malhotra, A.K., 2016a. Limited Evidence for Association of Genome-Wide Schizophrenia Risk Variants on Cortical Neuroimaging Phenotypes. Schizophr. Bull. 42, 1027–1036. https://doi.org/10.1093/schbul/sbv180

Voineskos, A.N., Felsky, D., Wheeler, A.L., Rotenberg, D.J., Levesque, M., Patel, S., Szeszko, P.R., Kennedy, J.L., Lencz, T., Malhotra, A.K., 2016b. Limited Evidence for Association of Genome-Wide Schizophrenia Risk Variants on Cortical Neuroimaging Phenotypes. Schizophr. Bull. 42, 1027–1036. https://doi.org/10.1093/schbul/sbv180

von Hohenberg, C.C., Pasternak, O., Kubicki, M., Ballinger, T., Vu, M.-A., Swisher, T., Green, K., Giwerc, M., Dahlben, B., Goldstein, J.M., Woo, T.-U.W., Petryshen, T.L., Mesholam-Gately, R.I., Woodberry, K.A., Thermenos, H.W., Mulert, C., McCarley, R.W., Seidman, L.J., Shenton, M.E., 2014. White matter microstructure in individuals at clinical high risk of psychosis: a whole-brain diffusion tensor imaging study. Schizophr. Bull. 40, 895–903. https://doi.org/10.1093/schbul/sbt079

Wang, Q., Cheung, C., Deng, W., Li, M., Huang, C., Ma, X., Wang, Y., Jiang, L., Sham, P.C., Collier, D.A., Gong, Q., Chua, S.E., McAlonan, G.M., Li, T., 2013. White-matter microstructure in previously drug-naive patients with schizophrenia after 6 weeks of treatment. Psychol. Med. 43, 2301–2309. https://doi.org/10.1017/S0033291713000238

Wang, Q., Su, T.-P., Zhou, Y., Chou, K.-H., Chen, I.-Y., Jiang, T., Lin, C.-P., 2012. Anatomical insights into disrupted small-world networks in schizophrenia. NeuroImage 59, 1085–1093. https://doi.org/10.1016/j.neuroimage.2011.09.035

Wardlaw, J.M., Bastin, M.E., Valdés Hernández, M.C., Maniega, S.M., Royle, N.A., Morris, Z., Clayden, J.D., Sandeman, E.M., Eadie, E., Murray, C., Starr, J.M., Deary, I.J., 2011. Brain aging, cognition in youth and old age and vascular disease in the Lothian Birth Cohort 1936: rationale, design and methodology of the imaging protocol. Int. J. Stroke Off. J. Int. Stroke Soc. 6, 547–559. https://doi.org/10.1111/j.1747-4949.2011.00683.x

Ware, E.B., Schmitz, L.L., Faul, J.D., Gard, A., Mitchell, C., Smith, J.A., Zhao, W., Weir, D., Kardia, S.L., 2017. Heterogeneity in polygenic scores for common human traits. bioRxiv 106062. https://doi.org/10.1101/106062

Watts, D.J., Strogatz, S.H., 1998. Collective dynamics of 'small-world' networks. Nature 393, 440–442. https://doi.org/10.1038/30918

Wechsler, D., 1955. Manual for the Wechsler Adult Intelligence Scale. Psychological Corp., Oxford, England.

Weinberger, D.R., 1987. Implications of normal brain development for the pathogenesis of schizophrenia. Arch. Gen. Psychiatry 44, 660–669.

Wernicke, C., 1906. Grundrisse der Psychiatrie. Leipzig, Germany: Thieme.

Westlye, L.T., Walhovd, K.B., Dale, A.M., Bjørnerud, A., Due-Tønnessen, P., Engvig, A., Grydeland, H., Tamnes, C.K., Ostby, Y., Fjell, A.M., 2010. Life-span changes of the human brain white matter: diffusion tensor imaging (DTI) and volumetry. Cereb. Cortex N. Y. N 1991 20, 2055–2068. https://doi.org/10.1093/cercor/bhp280

Wexler, B.E., Zhu, H., Bell, M.D., Nicholls, S.S., Fulbright, R.K., Gore, J.C., Colibazzi, T., Amat, J., Bansal, R., Peterson, B.S., 2009. Neuropsychological near normality and brain structure abnormality in schizophrenia. Am. J. Psychiatry 166, 189–195. https://doi.org/10.1176/appi.ajp.2008.08020258

Whalley, H.C., Dimitrova, R., Sprooten, E., Dauvermann, M.R., Romaniuk, L., Duff, B., Watson, A.R., Moorhead, B., Bastin, M., Semple, S.I., Giles, S., Hall, J., Thomson, P., Roberts, N., Hughes, Z.A., Brandon, N.J., Dunlop, J., Whitcher, B., Blackwood, D.H.R., McIntosh, A.M., Lawrie, S.M., 2015a. Effects of a Balanced Translocation between Chromosomes 1 and 11 Disrupting the DISC1 Locus on White Matter Integrity. PloS One 10, e0130900. https://doi.org/10.1371/journal.pone.0130900

Whalley, H.C., Hall, L., Romaniuk, L., Macdonald, A., Lawrie, S.M., Sussmann, J.E., McIntosh, A.M., 2015b. Impact of cross-disorder polygenic risk on frontal brain activation with specific effect of schizophrenia risk. Schizophr. Res. 161, 484–489. https://doi.org/10.1016/j.schres.2014.10.046

Wheeler, A.L., Voineskos, A.N., 2014. A review of structural neuroimaging in schizophrenia: from connectivity to connectomics. Front. Hum. Neurosci. 8, 653. https://doi.org/10.3389/fnhum.2014.00653

White, T., Ehrlich, S., Ho, B.-C., Manoach, D.S., Caprihan, A., Schulz, S.C., Andreasen, N.C., Gollub, R.L., Calhoun, V.D., Magnotta, V.A., 2013. Spatial characteristics of white matter abnormalities in schizophrenia. Schizophr. Bull. 39, 1077–1086. https://doi.org/10.1093/schbul/sbs106

White, T., Magnotta, V.A., Bockholt, H.J., Williams, S., Wallace, S., Ehrlich, S., Mueller, B.A., Ho, B.-C., Jung, R.E., Clark, V.P., Lauriello, J., Bustillo, J.R., Schulz, S.C., Gollub, R.L., Andreasen, N.C., Calhoun, V.D., Lim, K.O., 2011. Global White Matter Abnormalities in Schizophrenia: A Multisite Diffusion Tensor Imaging Study. Schizophr. Bull. 37, 222–232. https://doi.org/10.1093/schbul/sbp088

White, T., Nelson, M., Lim, K.O., 2008. Diffusion tensor imaging in psychiatric disorders. Top. Magn. Reson. Imaging TMRI 19, 97–109. https://doi.org/10.1097/RMR.0b013e3181809f1e

White, T.P., Joseph, V., Francis, S.T., Liddle, P.F., 2010. Aberrant salience network (bilateral insula and anterior cingulate cortex) connectivity during information processing in schizophrenia. Schizophr. Res. 123, 105–115. https://doi.org/10.1016/j.schres.2010.07.020

Whitfield-Gabrieli, S., Thermenos, H.W., Milanovic, S., Tsuang, M.T., Faraone, S.V., McCarley, R.W., Shenton, M.E., Green, A.I., Nieto-Castanon, A., LaViolette, P., Wojcik, J., Gabrieli, J.D.E., Seidman, L.J., 2009. Hyperactivity and hyperconnectivity of the default network in schizophrenia and in first-degree relatives of persons with schizophrenia. Proc. Natl. Acad. Sci. U. S. A. 106, 1279–1284. https://doi.org/10.1073/pnas.0809141106

Whitford, T.J., Kubicki, M., Schneiderman, J.S., O'Donnell, L.J., King, R., Alvarado, J.L., Khan, U., Markant, D., Nestor, P.G., Niznikiewicz, M., McCarley, R.W., Westin, C.-F., Shenton, M.E., 2010. Corpus callosum abnormalities and their association with psychotic symptoms in patients with schizophrenia. Biol. Psychiatry 68, 70–77. https://doi.org/10.1016/j.biopsych.2010.03.025

WHO, 1994. International Statistical Classification of Diseases and Related Health Problems 10th Revision. Geneva: World Health Organization.

Wijk, B.C.M. van, Stam, C.J., Daffertshofer, A., 2010. Comparing Brain Networks of Different Size and Connectivity Density Using Graph Theory. PLOS ONE 5, e13701. https://doi.org/10.1371/journal.pone.0013701

Wilder, J., 1957. The law of initial value in neurology and psychiatry; facts and problems. J. Nerv. Ment. Dis. 125, 73–86.

Winkler, A.M., Kochunov, P., Blangero, J., Almasy, L., Zilles, K., Fox, P.T., Duggirala, R., Glahn, D.C., 2010. Cortical thickness or grey matter volume? The importance of selecting the phenotype for imaging genetics studies. NeuroImage 53, 1135–1146. https://doi.org/10.1016/j.neuroimage.2009.12.028

Wiseman, S.J., Booth, T., Ritchie, S.J., Cox, S.R., Muñoz Maniega, S., Valdés Hernández, M. del C., Dickie, D.A., Royle, N.A., Starr, J.M., Deary, I.J., Wardlaw, J.M., Bastin, M.E., 2018. Cognitive abilities, brain white matter hyperintensity volume, and structural network connectivity in older age. Hum. Brain Mapp. 39, 622–632. https://doi.org/10.1002/hbm.23857

Wolkin, A., Choi, S.J., Szilagyi, S., Sanfilipo, M., Rotrosen, J.P., Lim, K.O., 2003. Inferior Frontal White Matter Anisotropy and Negative Symptoms of Schizophrenia: A Diffusion Tensor Imaging Study. Am. J. Psychiatry 160, 572–574. https://doi.org/10.1176/appi.ajp.160.3.572

Woodberry, K.A., Giuliano, A.J., Seidman, L.J., 2008. Premorbid IQ in schizophrenia: a meta-analytic review. Am. J. Psychiatry 165, 579–587. https://doi.org/10.1176/appi.ajp.2008.07081242

Woodruff, P.W., McManus, I.C., David, A.S., 1995. Meta-analysis of corpus callosum size in schizophrenia. J. Neurol. Neurosurg. Psychiatry 58, 457–461.

Woods, S.W., 2003. Chlorpromazine equivalent doses for the newer atypical antipsychotics. J. Clin. Psychiatry 64, 663–667.

Wotruba, D., Michels, L., Buechler, R., Metzler, S., Theodoridou, A., Gerstenberg, M., Walitza, S., Kollias, S., Rössler, W., Heekeren, K., 2014. Aberrant coupling within and across the default mode, task-positive, and salience network in subjects at risk for psychosis. Schizophr. Bull. 40, 1095–1104. https://doi.org/10.1093/schbul/sbt161

Wozniak, J.R., Lim, K.O., 2006. Advances in white matter imaging: a review of in vivo magnetic resonance methodologies and their applicability to the study of development and aging. Neurosci. Biobehav. Rev. 30, 762–774. https://doi.org/10.1016/j.neubiorev.2006.06.003

Wright, S.N., Hong, L.E., Winkler, A.M., Chiappelli, J., Nugent, K., Muellerklein, F., Du, X., Rowland, L.M., Wang, D.J.J., Kochunov, P., 2015. Perfusion shift from white to gray matter may account for processing speed deficits in schizophrenia. Hum. Brain Mapp. 36, 3793–3804. https://doi.org/10.1002/hbm.22878

Wright, S.N., Kochunov, P., Chiappelli, J., McMahon, R.P., Muellerklein, F., Wijtenburg, S.A., White, M.G., Rowland, L.M., Hong, L.E., 2014. Accelerated white matter aging in schizophrenia: role of white matter blood perfusion. Neurobiol. Aging 35, 2411–2418. https://doi.org/10.1016/j.neurobiolaging.2014.02.016

Wylie, K.P., Tregellas, J.R., 2010. The role of the insula in schizophrenia. Schizophr. Res. 123, 93–104. https://doi.org/10.1016/j.schres.2010.08.027

Yamawaki, M., Wada-Isoe, K., Yamamoto, M., Nakashita, S., Uemura, Y., Takahashi, Y., Nakayama, T., Nakashima, K., 2015. Association of cerebral white matter lesions with cognitive function and mood in Japanese elderly people: a population-based study. Brain Behav. 5, e00315. https://doi.org/10.1002/brb3.315

Yeo, R.A., Ryman, S.G., van den Heuvel, M.P., de Reus, M.A., Jung, R.E., Pommy, J., Mayer, A.R., Ehrlich, S., Schulz, S.C., Morrow, E.M., Manoach, D., Ho, B.-C., Sponheim, S.R., Calhoun, V.D., 2016. Graph Metrics of Structural Brain Networks in Individuals with Schizophrenia and Healthy Controls: Group Differences, Relationships with Intelligence, and Genetics. J. Int. Neuropsychol. Soc. JINS 22, 240–249. https://doi.org/10.1017/S1355617715000867

Yu, C., Li, J., Liu, Y., Qin, W., Li, Y., Shu, N., Jiang, T., Li, K., 2008. White matter tract integrity and intelligence in patients with mental retardation and healthy adults. NeuroImage 40, 1533–1541. https://doi.org/10.1016/j.neuroimage.2008.01.063

Zalesky, A., 2011. Moderating registration misalignment in voxelwise comparisons of DTI data: a performance evaluation of skeleton projection. Magn. Reson. Imaging 29, 111–125. https://doi.org/10.1016/j.mri.2010.06.027

Zalesky, A., Fornito, A., Cocchi, L., Gollo, L.L., van den Heuvel, M.P., Breakspear, M., 2016. Connectome sensitivity or specificity: which is more important? NeuroImage 142, 407–420. https://doi.org/10.1016/j.neuroimage.2016.06.035

Zalesky, A., Fornito, A., Harding, I.H., Cocchi, L., Yücel, M., Pantelis, C., Bullmore, E.T., 2010. Whole-brain anatomical networks: does the choice of nodes matter? NeuroImage 50, 970–983. https://doi.org/10.1016/j.neuroimage.2009.12.027

Zalesky, A., Fornito, A., Seal, M.L., Cocchi, L., Westin, C.-F., Bullmore, E.T., Egan, G.F., Pantelis, C., 2011. Disrupted axonal fiber connectivity in schizophrenia. Biol. Psychiatry 69, 80–89. https://doi.org/10.1016/j.biopsych.2010.08.022

Zhang, H., Schneider, T., Wheeler-Kingshott, C.A., Alexander, D.C., 2012. NODDI: practical in vivo neurite orientation dispersion and density imaging of the human brain. NeuroImage 61, 1000–1016. https://doi.org/10.1016/j.neuroimage.2012.03.072

Zhang, R., Wei, Q., Kang, Z., Zalesky, A., Li, M., Xu, Y., Li, L., Wang, J., Zheng, L., Wang, B., Zhao, J., Zhang, J., Huang, R., 2015. Disrupted brain anatomical connectivity in medication-naïve patients with first-episode schizophrenia. Brain Struct. Funct. 220, 1145–1159. https://doi.org/10.1007/s00429-014-0706-z

Zhang, Y., Brady, M., Smith, S., 2001. Segmentation of brain MR images through a hidden Markov random field model and the expectation-maximization algorithm. IEEE Trans. Med. Imaging 20, 45–57. https://doi.org/10.1109/42.906424

Zhang, Y., Lin, L., Lin, C.-P., Zhou, Y., Chou, K.-H., Lo, C.-Y., Su, T.-P., Jiang, T., 2012. Abnormal topological organization of structural brain networks in schizophrenia. Schizophr. Res. 141, 109–118. https://doi.org/10.1016/j.schres.2012.08.021

Zhao, T., Cao, M., Niu, H., Zuo, X.-N., Evans, A., He, Y., Dong, Q., Shu, N., 2015. Age-related changes in the topological organization of the white matter structural connectome across the human lifespan. Hum. Brain Mapp. 36, 3777–3792. https://doi.org/10.1002/hbm.22877

Zimmermann, J., Ritter, P., Shen, K., Rothmeier, S., Schirner, M., McIntosh, A.R., 2016. Structural architecture supports functional organization in the human aging brain at a regionwise and network level. Hum. Brain Mapp. 37, 2645–2661. https://doi.org/10.1002/hbm.23200

Zou, G.Y., 2007. Toward using confidence intervals to compare correlations. Psychol. Methods 12, 399–413. https://doi.org/10.1037/1082-989X.12.4.399

Appendices

Appendix I: Chapter 4

Supplementary Table 1. Individual white matter tracts and their corresponding loadings for g_{FA}.

White matter tract	Loadings
GCC	0.751
BCC	0.611
SCC	0.765
FX	0.496
CST-R	0.707
CST-L	0.508
ML-R	0.664
ML-L	0.578
ICP-R	0.728
ICP-L	0.712
SCP-R	0.504
SCP-L	0.525
CP-R	0.643
CP-L	0.530
ALIC-R	0.687
ALIC-L	0.711
PLIC-R	0.705
PLIC-L	0.680
RLIC-R	0.720
RLIC-L	0.750
ACR-R	0.610
ACR-L	0.685
SCR-R	0.863

White matter tract	Loadings
SCR-L	0.764
PCR-R	0.807
PCR-L	0.855
PTR-R	0.771
PTR-L	0.761
SS-R	0.721
SS-L	0.661
EC-R	0.686
EC-L	0.776
CGC-R	0.829
CGC-L	0.768
CGH-R	0.661
CGH-L	0.726
FX/ST-R	0.519
FX/ST-L	0.659
SLF-R	0.858
SLF-L	0.851
SFO-R	0.432
SFO-L	0.556
IFO-R	0.670
IFO-L	0.420
UNC-R	0.553
UNC-L	0.408

Note. A list of abbreviations is provided in Table 3.

Supplementary Table 2. Individual white matter tracts and their corresponding loadings for g_{MD}.

White matter tract	Loadings
GCC	0.652
BCC	0.643
SCC	0.874
FX	0.431
CST-R	0.768
CST-L	0.680
ML-R	0.737
ML-L	0.707
ICP-R	0.828
ICP-L	0.733
SCP-R	0.665
SCP-L	0.595
CP-R	0.679
CP-L	0.557
ALIC-R	0.803
ALIC-L	0.750
PLIC-R	0.817
PLIC-L	0.701
RLIC-R	0.887
RLIC-L	0.864
ACR-R	0.803
ACR-L	0.710
SCR-R	0.918

White matter tract	Loadings
SCR-L	0.902
PCR-R	0.866
PCR-L	0.867
PTR-R	0.816
PTR-L	0.762
SS-R	0.827
SS-L	0.802
EC-R	0.643
EC-L	0.678
CGC-R	0.706
CGC-L	0.630
CGH-R	0.676
CGH-L	0.604
FX/ST-R	0.679
FX/ST-L	0.727
SLF-R	0.893
SLF-L	0.855
SFO-R	0.658
SFO-L	0.351
IFO-R	0.714
IFO-L	0.582
UNC-R	0.604
UNC-L	0.473

Note. A list of abbreviations is provided in Table 3.

Supplementary Table 3. Individual cognitive tests and their corresponding loadings for general intelligence (*g*).

Subtest	Loadings
Digit Sequencing	0.818
Spatial Working Memory	-0.701
Block Design	0.850
Matrix Reasoning	0.877
Vocabulary	0.733

Supplementary Table 4. Individual cognitive tests and their corresponding loadings for information processing speed (g_{speed}).

Subtest	Loadings
Reaction Time Simple	0.752
Reaction Time 5-Choice	0.696
Symbol Coding	-0.815

Supplementary Figure 1. Scree plot obtained from the PCA for g_{FA}.

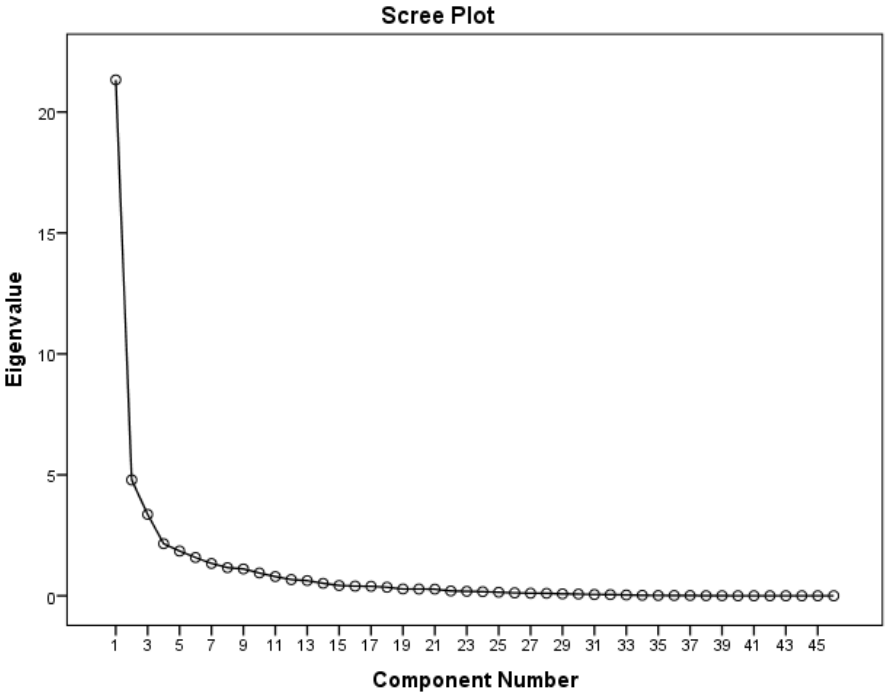

Supplementary Figure 2. Scree plot obtained from the PCA for g_{MD}.

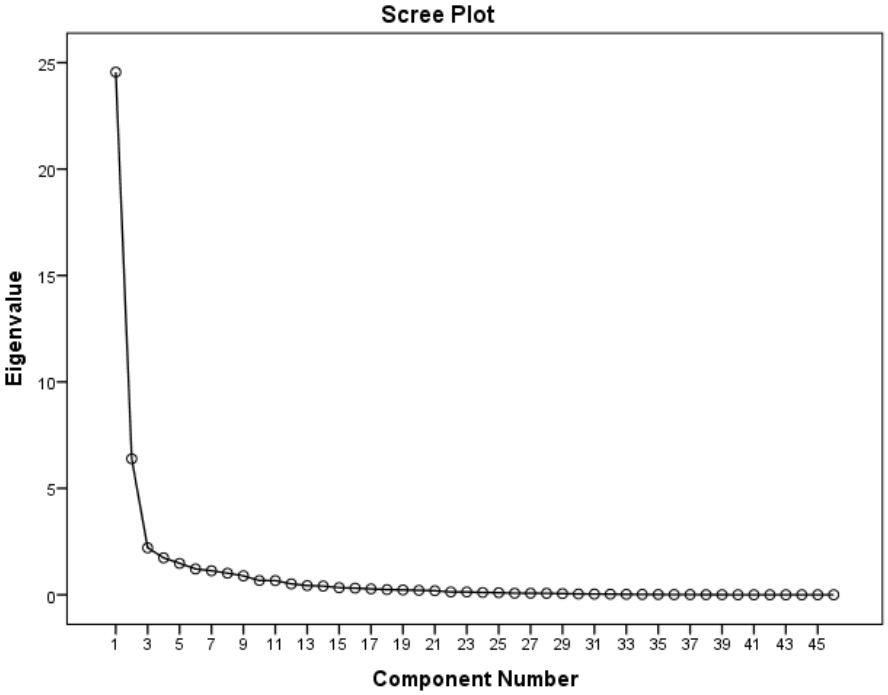

Supplementary Figure 3. Scree plot obtained from the PCA for *g*.

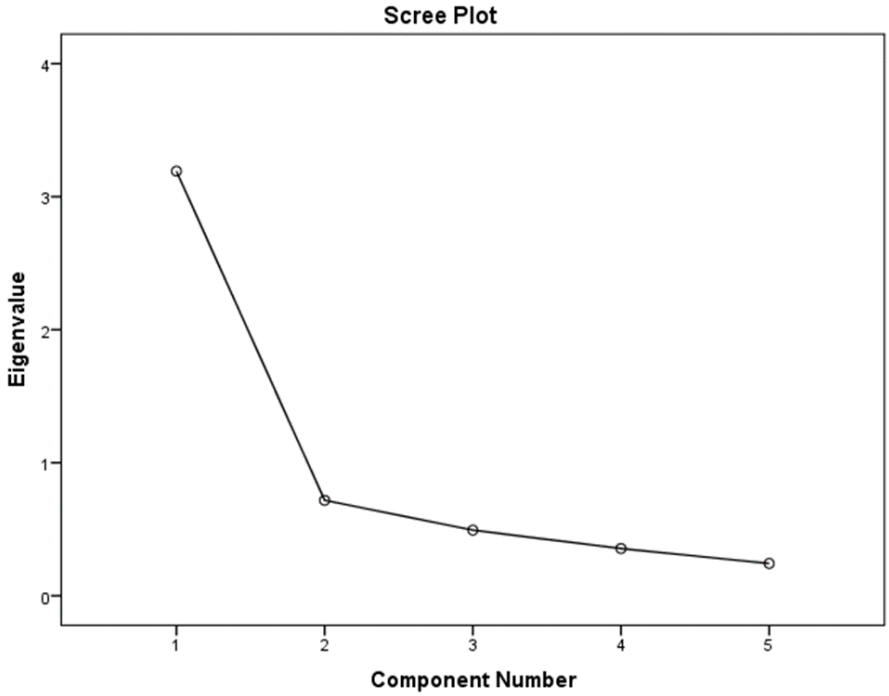

Supplementary Figure 4. Scree plot obtained from the PCA for g_{speed}.

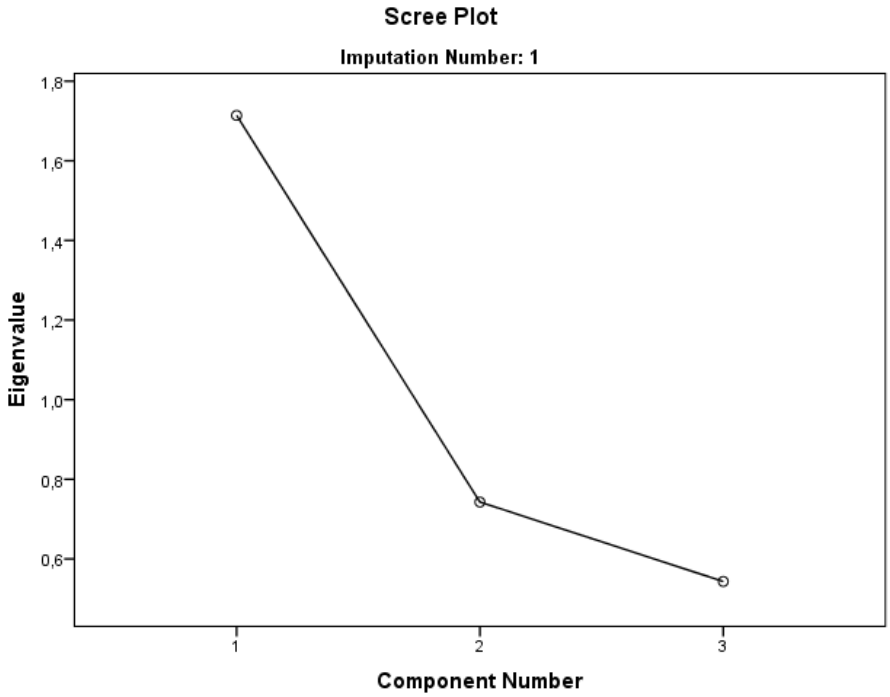

Appendix II: Chapter 5

Supplementary Material Figure 1. Group differences for the average network.

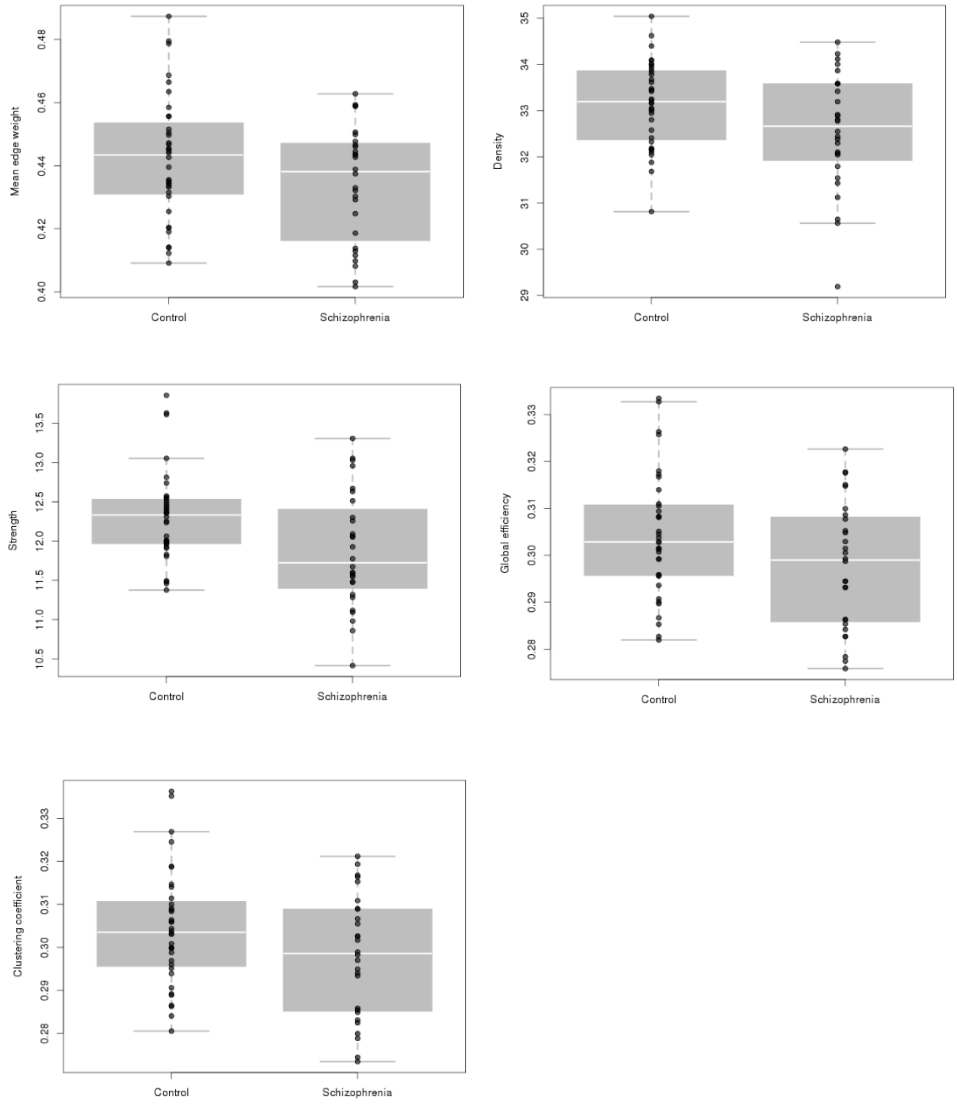

Supplementary Material Figure 2. Scatterplots for associations between central and non-central mean edge weight and IQ. Orange dots represent healthy controls and blue dots patients with schizophrenia.

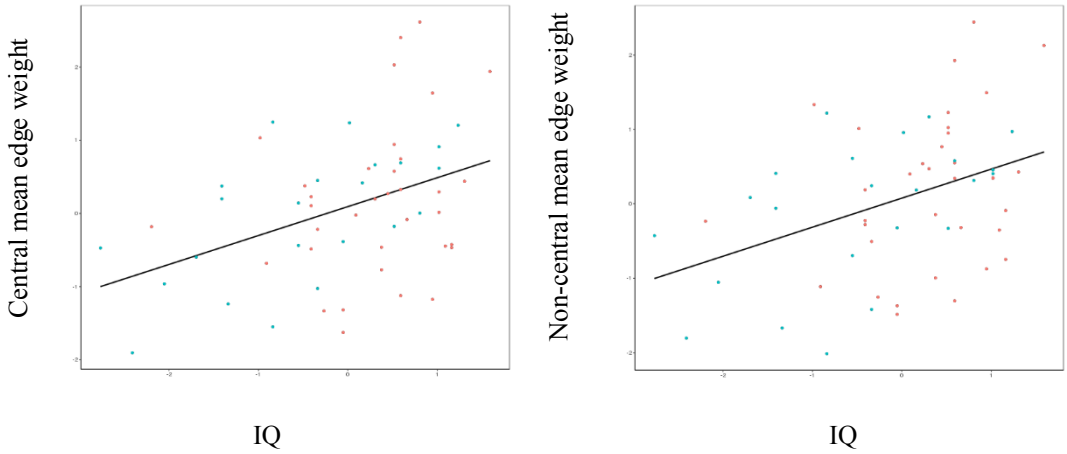

Supplementary Material Figure 3. Scatterplots for associations between metrics of the average network (*y*-axis) and IQ (*x*-axis). Orange dots represent healthy controls and blue dots patients with schizophrenia.

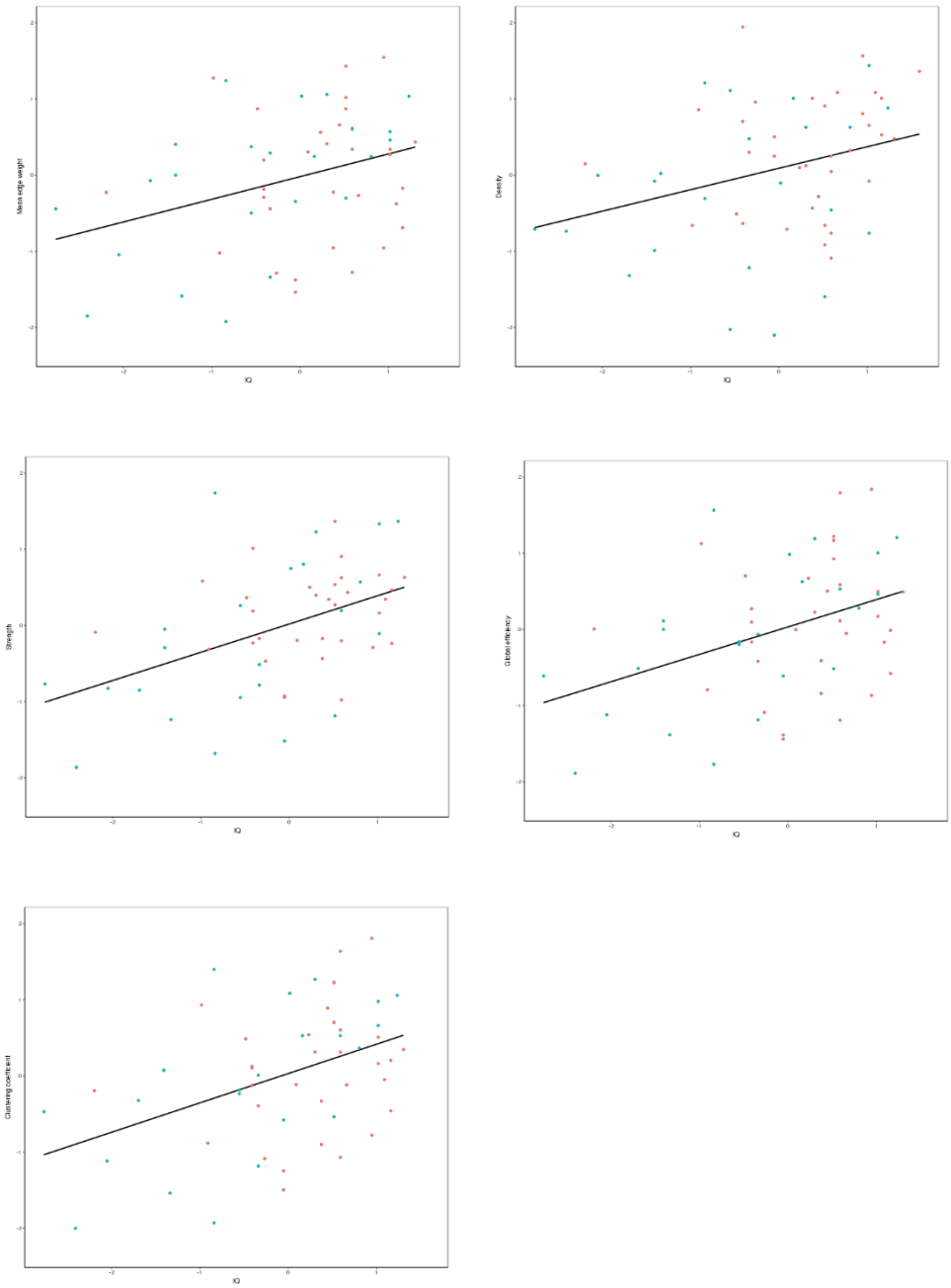

Appendix III: Chapter 6

Supplementary Material Table 1: Descriptive statistics of individual cognitive tests from the Wechsler Adult Scale - III across both waves (age 73 and age 76).

	n	Age 73	*n*	Age 76	*r*	*SE*	p_{FDR}
Wechsler Adult Scale - III							
Matrix reasoning	690	13.37 (4.90)	574	13.16 (5.00)	-0.05	0.019	0.013*
Letter number sequencing	690	10.98 (3.02)	573	10.49 (2.98)	-0.122	0.019	< 0.001*
Block Design	690	34.07 (10.07)	577	32.43 (10.15)	-0.010	0.016	< 0.001*
Symbol search	689	24.63 (6.19)	573	24.53 (6.58)	-0.046	0.018	0.013*
Digit symbol	689	56.24 (12.27)	570	53.73 (12.78)	-0.156	0.013	< 0.001*
Digit span backwards	692	7.84 (2.33)	581	7.76 (2.36)	-0.032	0.018	0.075

Note: SD: Standard deviation, r: standardised estimates from the linear mixed models, SE: standard error. Asterisks represent significance from the linear mixed models ($p_{FDR} < 0.05$).

Supplementary Material Table 2: Percentage of health conditions across both waves (age 73 and age 76).

Health	Age 73	Age 76
Diabetes	10.71%	12.03%
Hypertension	48.81%	54.22%
High cholesterol	41.52%	47.68%
History of cardiovascular disease	27.23%	33.34%

Supplementary Material Figure 1. Scatterplot of the relationship between the percentage of change in MD (mean of left-right values from 73 years to 76 years) and szPGRS at p ≤ 1.0. Standardised linear regression coefficients (β) were derived from the regression between percentage of change in MD and residuals from szPGRS with MDS components and sex. Note that these plots and the accompanying betas (using complete data only) correspond well with the SEM-implied significant associations reported in the main manuscript which account for missingness (FIML) and treat variables and their change as latent (it is inadvisable to extract factor scores directly from the SEM due to issues of factor score indeterminacy, e.g. Grice, 2001). Black line represents linear regression and in grey the 95% confidence interval.

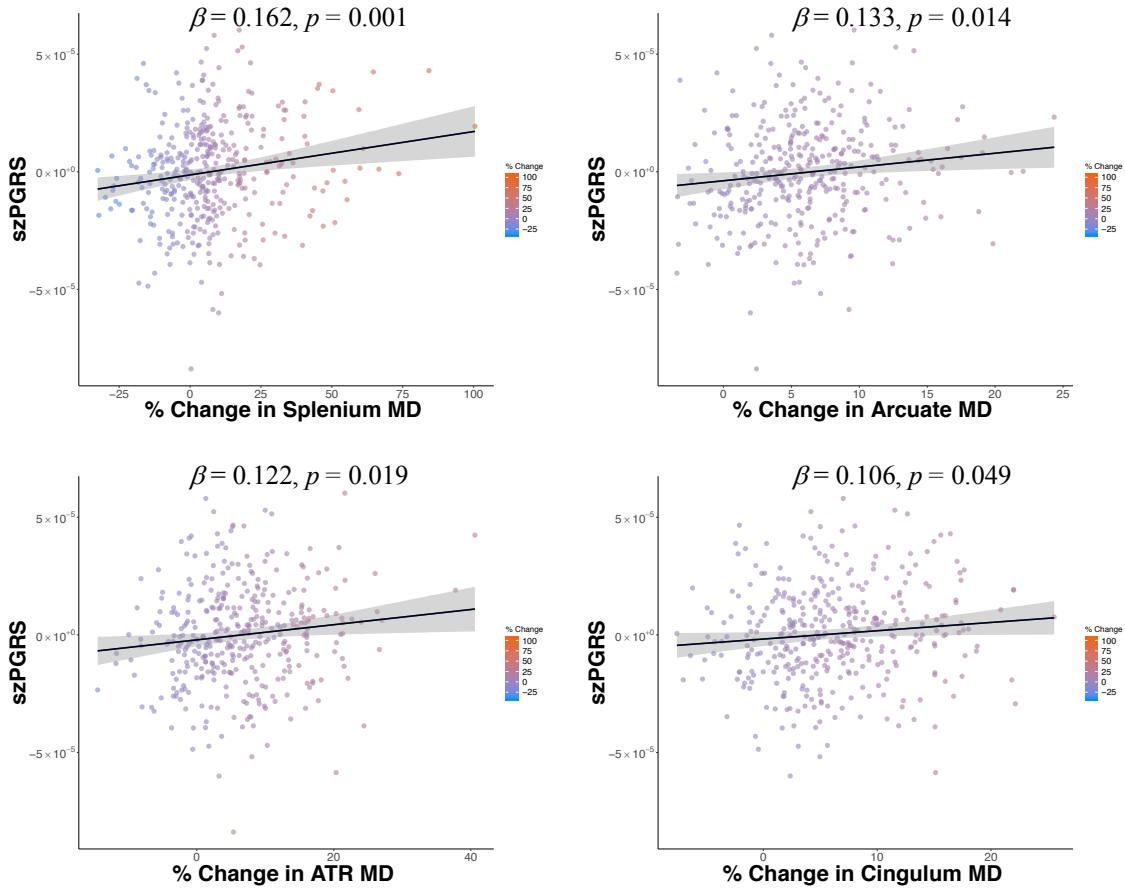

Supplementary Material Table 3. Structural equation modelling results. Standardised estimates from the associations between polygenic risk score for schizophrenia (szPGRS) at a threshold of $P \leq 0.1$ and level and change in connectivity.

	Threshold of $P \leq 0.1$					
	Level (age 73)			Change (age 73 to 76)		
	r	*SE*	p_{FDR}	*r*	*SE*	p_{FDR}
FA						
Genu	0.021	0.153	0.899	-0.037	0.156	0.664
Splenium	-0.004	0.209	0.935	-0.077	0.196	0.458
Arcuate	-0.023	0.011	0.899	-0.046	0.007	0.689
ATR	0.017	0.008	0.899	-0.098	0.008	0.572
Cingulum	0.122	0.014	0.385	-0.230	0.013	0.458
Uncinate	0.063	0.009	0.899	-0.066	0.009	0.664
ILF	-0.048	0.011	0.899	-0.173	0.011	0.689
MD						
Genu	0.045	0.263	0.526	-0.01	0.28	0.847
Splenium	-0.047	0.431	0.526	0.116	0.507	0.079 ·
Arcuate	-0.008	0.001	0.873	0.207	0.001	0.079 ·
ATR	-0.063	0.002	0.526	0.173	0.002	0.115
Cingulum	-0.124	0.001	0.231	0.189	0.001	0.079 ·
Uncinate	-0.094	0.001	0.339	0.025	0.001	0.734
ILF	0.022	0.023	0.873	0.076	0.029	0.734
Connectome						
Mean edge weight	0.035	0.006	0.537	-0.014	0.004	0.862
Strength	0.031	0.132	0.537	-0.010	0.100	0.862
Global efficiency	0.035	0.004	0.537	-0.013	0.003	0.862
Clustering coefficient	0.031	0.004	0.537	-0.012	0.003	0.862

Note: SE: Standard error, FA: fractional anisotropy, MD: mean diffusivity, ATR: anterior thalamic radiations, ILF: inferior longitudinal fasciculus, *p*-values are corrected for multiple comparison using FDR. Dots tendency towards significance.

Supplementary Material Table 4. Structural equation modelling results. Standardised estimates from the associations between polygenic risk score for schizophrenia (szPGRS) at a threshold of P ≤ 0.5 and level and change in connectivity.

	Threshold of P ≤ 0.5					
	Level (age 73)			Change (age 73 to 76)		
	r	*SE*	p_{FDR}	*r*	*SE*	p_{FDR}
FA						
Genu	0.032	0.071	0.868	-0.036	0.072	0.583
Splenium	-0.008	0.097	0.868	-0.97	0.091	0.175
Arcuate	0.010	0.005	0.868	-0.060	0.003	0.596
ATR	0.051	0.004	0.868	-0.150	0.004	0.175
Cingulum	0.110	0.006	0.581	-0.239	0.006	0.175
Uncinate	0.055	0.004	0.868	-0.056	0.004	0.583
ILF	-0.025	0.005	0.868	-0.322	0.005	0.583
MD						
Genu	0.034	0.122	0.583	-0.018	0.129	0.730
Splenium	-0.055	0.200	0.465	0.152	0.235	0.021*
Arcuate	-0.041	0.001	0.583	0.212	< 0.001	0.059 ·
ATR	-0.098	0.001	0.324	0.230	0.001	0.052 ·
Cingulum	-0.115	0.001	0.324	0.160	0.001	0.059 ·
Uncinate	-0.084	0.001	0.324	0.030	0.001	0.581
ILF	0.013	0.011	0.866	0.149	0.013	0.477
Connectome						
Mean edge weight	0.065	0.003	0.233	-0.046	0.002	0.460
Strength	0.060	0.061	0.233	-0.041	0.046	0.460
Global efficiency	0.061	0.002	0.233	-0.042	0.001	0.460
Clustering coefficient	0.063	0.002	0.233	-0.044	0.001	0.460

Note: SE: Standard error, FA: fractional anisotropy, MD: mean diffusivity, ATR: anterior thalamic radiations, ILF: inferior longitudinal fasciculus, *p*-values are corrected for multiple comparison using FDR. Asterisks represent significance ($p_{FDR} < 0.05$) and dots tendency towards significance.

Supplementary Material Table 5. Structural equation modelling results. Standardised estimates from the associations between polygenic risk score for schizophrenia (szPGRS) at a threshold of $P \leq 1.0$ and level and change in white matter microstructure and in general fluid intelligence.

Path type	Path	*r*	*SE*	p_{FDR}
Level - Level	szPGRS- g_f	-0.145	0.029	0.001*
	Splenium MD - g_f	-0.113	0.032	0.020*
	Arcuate MD - g_f	-0.132	0.032	0.012*
	ATR MD - g_f	-0.115	0.028	0.044*
	Cingulum MD - g_f	-0.067	0.030	0.184
Level - Change (Δ)	szPGRS- Δ g_f	0.003	0.015	0.962
	Splenium MD - Δ g_f	-0.129	0.017	0.122
	Arcuate MD - Δ g_f	-0.112	0.018	0.176
	ATR MD - Δ g_f	-0.171	0.016	0.122
	Cingulum MD - Δ g_f	-0.109	0.017	0.183
	g_f - Δ Splenium MD	0.057	0.036	0.264
	g_f - Δ Arcuate MD	-0.130	0.022	0.134
	g_f - Δ ATR MD	-0.261	0.029	0.012*
	g_f - Δ Cingulum MD	-0.090	0.033	0.212
Change (Δ) – Change (Δ)	Δ g_f - Δ Splenium MD	0.026	0.295	0.916
	Δ g_f - Δ Arcuate MD	-0.021	0.186	0.916
	Δ g_f - Δ ATR MD	0.051	0.279	0.916
	Δ g_f - Δ Cingulum MD	-0.010	0.274	0.916

Note: SE: Standard error, g_f: general fluid intelligence, MD: mean diffusivity, ATR: anterior thalamic radiations, *p*-values are corrected for multiple comparison using FDR. Asterisks represent significance ($p_{FDR} < 0.05$).

Appendix IV: Chapter 7

Supplementary Material Table 1. Standardised estimates obtained from the regression models for age and sex and cortical thickness and grey matter volumes of the salience network.

	Age	Sex	Age p_{FDR}	Sex p_{FDR}
Cortical thickness (mm)				
L CAC	0.015	-0.162	< 0.001*	< 0.001*
R CAC	0.018	-0.251	< 0.001*	< 0.001*
L Insula	0.009	0.169	< 0.001*	< 0.001*
R Insula	0.005	0.235	0.109	< 0.001*
Grey matter volume (mm)				
L CAC	-0.005	-0.084	0.122	0.201
R CAC	-0.003	-0.090	0.308	0.201
L Insula	0.007	0.034	< 0.001*	0.566
R Insula	0.004	0.175	0.180	< 0.001*
L Thalamus	-0.026	0.012	< 0.001*	0.756
R Thalamus	-0.027	0.024	< 0.001*	0.568
L Amygdala	0.006	0.204	0.122	< 0.001*
R Amygdala	< 0.001	0.253	0.888	< 0.001*

Note: L: left, R: right, beta: standardised estimates from the regression models, CAC: caudal anterior cingulate. Asterisks represent significance from the linear mixed models (p_{FDR} < 0.05).

Supplementary Material Table 2. Standardised estimates obtained from the regression models for age and sex and fractional anisotropy (FA) of the pathways involved in the salience network.

	Age	Sex	Age p_{FDR}	Sex p_{FDR}
L-Thalamus : L-VDC	-0.011	0.242	0.002*	< 0.001*
L-Thalamus : R-Thalamus	0.012	0.204	< 0.001*	< 0.001*
L-Thalamus : R-VDC	0.009	0.223	0.013*	< 0.001*
L-Thalamus : L-CAC	0.008	0.215	0.018*	< 0.001*
L-Thalamus : L-Insula	-0.009	0.111	0.013*	0.028*
L-Thalamus : R-Insula	0.005	0.139	0.103	0.005*
L-Amygdala : L-VDC	0.006	0.065	0.095	0.170
L-Amygdala : L-Insula	0.005	0.077	0.101	0.115
R-Thalamus : R-VDC	-0.012	0.485	< 0.001*	< 0.001*
R-Thalamus : R-CAC	0.001	0.255	0.865	< 0.001*
R-Thalamus : R-Insula	-0.007	0.185	0.027*	< 0.001*
R-Amygdala : R-VDC	0.006	0.096	0.088	0.056
R-Amygdala : R-Insula	0.016	0.082	< 0.001*	0.095
R-VDC : R-Insula	0.007	-0.156	0.027*	0.002*

Note: L: left, R: right, beta: standardised estimates from the regression models, CAC: caudal anterior cingulate, VDC: ventral diencephalon. Asterisks represent significance from the linear mixed models ($p_{FDR} < 0.05$).

Supplementary Material Table 3. Frequencies and percentages (in parenthesis) of responses to psychotic symptoms.

Question	Yes	No	Preferred not to answer
Did you ever believe that there was an unjust plot going on to harm you or to have people follow you, and which your family and friends did not believe existed?	4 (0.22%)	1300 (72.67%)	485 (27.10%)
Did you ever believe that a strange force was trying to communicate directly with you by sending special signs or signals that you could understand but that no one else could understand (for example through the radio or television)?	3 (0.17%)	1301 (72.67%)	486 (27.16%)
Did you ever hear things that other people said did not exist, like strange voices coming from inside your head talking to you or about you, or voices coming out of the air when there was no one around?	22 (1.23%)	1280 (71.55%)	487 (27.22%)
Did you ever see something that wasn't really there that other people could not see?	20 (1.12%)	1275 (71.27%)	494 (27.61%)

Note: Results based on N=1789 participants.

Appendix V: Methods

Supplementary Material Table 1. Table describing each parameter used in this thesis by chapter.

	Chapter 4	Chapter 5	Chapter 6	Chapter 7
Eddy current correction	eddy_correct (FSL) default parameters			
Brain extraction	FSL's Brain Extraction Tool (BET) default parameters			
Distortions and motion	FDT in FSL by affine registration of all subsequent EP volumes to the first T2-weighted EP volume			
Tensor fit	DTIFIT			
Tractography	Tract-based Spatial Statistics (TBSS; Smith et al., 2006)	-	Probabilistic neighbourhood tractography (PNT), TractoR (Clayden et al., 2011; Muñoz Maniega et al., 2017)	-
White matter atlas	John Hopkins University (JHU) white matter atlas available in FSL	-	-	-
Tissue parcellation	-	Each 3D T1-weighted MPRAGE volume was parcellated into 85 (Desikan-Killiany atlas; Desikan et al., 2006) and 165 (Destrieux atlas) regions-of-interest (FreeSurfer)	Each 3D T1-weighted FSPGR volume was parcellated into 85 (Desikan-Killiany atlas; Desikan et al., 2006) regions-of-interest (FreeSurfer)	
Connectome				
Whole-brain tractography	-	FSL's BedpostX/ProbTrackX algorithm, 100 Markov Chain Monte Carlo iterations with a fixed step size of 0.5 mm between successive points. Tracking was initiated from all white matter voxels.		
Alignment T1 - Diffusion space	-	Cross-modal nonlinear registration		
Thresholding	-	Including connections which occurred in more than 2/3 of the participants (de Reus and van den Heuvel, 2013)		Consistency-based, conserving the top 30% (Roberts et al., 2017)